CARBOHYDRATE COUNT AIDED BY A SIMULATION OF POSTPRANDIAL GLUCOSE DYNAMICS GENERATED BY A MATHEMATICAL MODEL IN PEOPLE WITH TYPE 1 DIABETES MELLITUS.

Doctoral Thesis

Clinical Medicine Doctorate

Student:

Carlos Esteban Builes Montaño, Internal Medicine and Endocrinology specialist, Doctoral student, Clinical Medicine Doctorate.

Director:

Juan Carlos Restrepo Gutierrez, MD, MSc, PhD. Professor of the Faculty of Medicine, University of Antioquia. Liver Transplant Unit, Pablo Tobón Uribe Hospital.

Codirector:

José Fernando García Tirado, MSc, PhD. Assistant Professor, University Clinic of Diabetes, Endocrinology, and Metabolism, Inselspital-University Hospital Bern, University of Bern, Bern, Switzerland.

Faculty of Medicine, University of Antioquia

Medellín, Colombia

2024.

Doctoral Committee

Juan Carlos Restrepo Gutierrez, MD, MSc, PhD. Professor of the Faculty of Medicine, University of Antioquia. Liver Transplant Unit, Pablo Tobón Uribe Hospital.

José Fernando García Tirado, MSc, PhD. Assistant Professor, University Clinic of Diabetes, Endocrinology, and Metabolism, Inselspital-University Hospital Bern, University of Bern, Bern, Switzerland.

Hernán Darío Alvarez Zapata, MSc, PhD. Professor of the Faculty of Mines, National University of Colombia

Laura Lema Pérez. MSc, PhD. Postdoctoral Fellow, Department of Engineering Cybernetics, Norwegian University of Science and Technology, Trondheim, Norway

John Jairo Zuleta Tobón. MD, MSc. Professor of the Faculty of Medicine, University of Antioquia. Research Unit, Pablo Tobón Uribe Hospital.

Alex Humberto Ramírez -Rincón, MD. Internal Medicine and Endocrinology specialist Assistant Professor, Universidad Pontificia Bolivariana.

CONTENTS

INTRODUCTION 8

OBJECTIVES 12

THEORETICAL FRAMEWORK 13

Diabetes Mellitus 13

Diabetes mellitus and its burden 13

Diabetes mellitus treatment 15

Available strategies for insulin subcutaneous application 16

Intestinal glucose absorption, its effect on blood glucose, and implications for insulin dosage 17

Carbohydrate counting in the treatment of diabetes mellitus with insulin 19

Possible limitations of traditional carbohydrate counting 21

Strategies that address some of the limitations of traditional carbohydrate counting 23

Mathematical modeling and diabetes mellitus 25

Mathematical modeling for glycemic control tools 25

Use of mathematical modeling in different areas of interest in diabetes mellitus 26

Mathematical models of glucose physiology and homeostasis 27

EFFICACY AND SAFETY OF CARBOHYDRATE COUNTING VERSUS OTHER FORMS OF DIETARY ADVICE IN PATIENTS WITH TYPE 1 DIABETES MELLITUS: A SYSTEMATIC REVIEW AND META-ANALYSIS OF RANDOMIZED CLINICAL TRIALS. 35

Introduction 35

Methods 37

Types of studies 37

Types of participants 37

Types of interventions 38

Types of outcome measures 38

Search methods for identification of studies 38

Data extraction 39

Risk of bias and quality of evidence 39

Statistical analysis 40

Results 41

Risk of bias 41

Primary outcome 41

Secondary outcomes 48

Publicatrion Bias 50

Sensitivity analysis 51

Discussion 51

Conclusions 52

A PHENOMENOLOGICALLY BASED SEMI-PHYSICAL MODEL OF THE ROLE OF THE GASTROINTESTINAL TRACT IN GLUCOSE HOMEOSTASIS 54

Estimation of glucose rate of appearance in portal vein circulation using a phenomenological-based model 54

Introduction 54

Construction of a PBSM for the role of the stomach and the small intestine in human glucose homeostasis 56

Results and discussion 82

Conclusion 88

Main glucose hepatic fluxes in healthy subjects predicted from a phenomenological-based model 90

Introduction 90

Role of the liver in glucose metabolism 91

Methods 93

Results 109

Discussion 113

Conclusion 116

COUPLING A PHENOMENOLOGICALLY BASED MODEL OF THE GASTROINTESTINAL TRACT TO A PHYSIOLOGICAL MODEL OF GLUCOSE AND DEVELOPMENT OF STUDIA, A MOBILE SOLUTION FOR ITS IMPLEMENTATION 118

STUDIA: An application to support carbohydrate counting by simulating glucose dynamics. 121

Introduction 121

Methods 123

Results 124

Discussion 129

Conclusions 131

Meal-Related Glycemic Trend Information to Assist Bolus Decision-Making in People with Type 1 Diabetes. 132

Introduction 132

Methods 132

Results 136

Discussion 139

Conclusion 140

A NOVEL SIMULATION-BASED DECISION SUPPORT SYSTEM INCREASES THE TIME IN RANGE AND REDUCES HYPOGLYCEMIA IN PEOPLE WITH TYPE 1 DIABETES 142

Introduction 142

Rationale 144

Hypothesis and objectives 147

Hypothesis 147

Objectives 147

Study design 148

Methods 148

Study setting 148

Eligibility criteria 148

Interventions 149

Adherence to the intervention 149

Cointerventions 149

Protocol discontinuation 150

Outcomes 150

Patient chronology 152

Sample size 152

Recruitment 153

Random sequence generation 153

Allocation concealment mechanism 153

Random sequence implementation 153

Blinding 153

Data collection methods 154

Retention 154

Data management 155

Statistical methods 155

Ethical considerations 156

Results 159

Discussion 166

Conclusions 168

CONCLUSIONS AND FUTURE WORK 169

REFERENCES 171
SUPPLEMENTARY MATERIAL 185

FIGURES

Figure 1. Single compartment minimal glucose models. 29
Figure 2. Insulin-independent minimal two-compartment model. 29
Figure 3. Insulin-dependent minimal two-compartment model. 30
Figure 4. Three compartments glucose model. 31
Figure 5. Models of gastric glucose absorption. 33
Figure 6. PRISMA Flow diagram. 42
Figure 7. Risk of bias graph. 45
Figure 8. Risk of bias summary. 45
Figure 9. Carbohydrate counting effect on HbA1c. 46
Figure 10. Effect of carbohydrate counting excluding the three studies contributing to the high heterogeneity. 47
Figure 11. Relationship between trial duration and HbA1c reduction. 48
Figure 12. Modeling hypothesis for the small intestine representing a series of stirred tank reactors with elastic walls and connected by valves. 59
Figure 13. Block diagram of the model. 60
Figure 14. Percentage of basal secretion calculated by the identified fuzzy system. 80
Figure 15. Fit of erfi(x) using an expression of the form $y = a^{bx} + c^{dx}$. 82
Figure 16. Simulated glucose concentration in portal vein following ingestion of the meals reported by [150-152], respectively. 84
Figure 17. Gastric emptying of the mass flow of the chyme through the pyloric valve. 86
Figure 18. Mass contained inside each tank j in the postprandial period. 87
Figure. 19 Representation of a liver sinusoid. 95
Figure 20. Process/Physiology analogy used to build the mathematical model. 96
Figure 21. Block diagram of process systems taken for modeling the liver's role in glucose metabolism. 97
Figure 22. Main biochemical reactions within the liver playing a role in glucose regulation. 100
Figure 23. Estimation made by the model compared with experimental data from (153). 111
Figure 24. Estimation made by the model compared with experimental data from (152). 112
Figure 25. Estimation made by the model compared with experimental data from (151). 113
Figura 26. Graphical representation of the submodels corresponding to insulin. 119
Figure 27. Patients' simulations recorded in STUDIA. 125
Figure 28. Glucose graph from saved data. 126
Figure 29. New register made for a meal in STUDIA. 127
Figure 30. Administrative interface. 128
Figure 31. Comparison between CGM reading and simulation. 129
Figure 32. Smoothed conditional means. 137

Figure 33. Individual glucose simulations. 137
Figure 34. Limits of agreement within 50 mg/dL. 138
Figure 35. Error grid analysis. 139
Figure 36. Participants Flowchart. 160
Figure 37. Change in time in range during the trial. 162
Figure 38. Change in time below range (hypoglycemia) during the trial. 162
Figure 39. Limits of agreement within 50 mg/dL. 164
Figure 40. CGM vs. app glucose simulations. 165
Figure 41. Surveillance Grid analysis. 165

TABLES

Table 1. Studies characteristics. 43
Table 2. Effect of carbohydrate counting in subgroups, change in HbA1c. 46
Table 3. Change in blood lipids. 48
Table 4. Hypoglycemia. 49
Table 5. Substances of interest considered in the gastrointestinal (GI) model. 62
Table 6. Variables, structural parameters, and structural constants of the model. 74
Table 7. Cumulative digestion. 84
Table 8. Cumulative absorption. 85
Table 9. Pancreatic enzymes inactivation. 85
Table 10. Equations of the model's basic structure. 104
Table 11. Model variables, structural parameters, and structural constants. 105
Table 12. Constitutive equations for structural parameters of the model. 106
Table 13. Constitutive equations for structural parameters of the model. 107
Table 14. Assessment equations for functional parameters of the model. 108
Table 15. Degrees of freedom. 109
Table 16. Parameters identified to fit patient data. 134
Table 17. Patients' characteristics. 136
Table 18. Proportions of differences within the proposed values. 138
Table 19. Patients characteristics. 161
Table 20. Primary and secondary outcomes. 161
Table 21. Safety outcomes. 163

INTRODUCTION

Diabetes mellitus (DM) is one of the most common non-communicable chronic diseases. Its prevalence is increasing, and the increase is expected to be more marked in poor and developing countries. For people with type 1 diabetes mellitus (DM1), insulin is the only medication approved for treatment, and for people with type 2 diabetes mellitus (DM2). However, there are new medications; in countries like Colombia, the use of insulin is quite frequent. A treatment based on reducing blood glucose concentration reduces the risk of chronic complications, and carbohydrate counting is the most widely recommended dose calculation technique. Carbohydrate counting is an iterative process for people with DM accompanied by high uncertainty, especially initially. Carbohydrate counting is refined with experience and frequent interventions by doctors and patient support staff.

DM is associated with a higher risk of death, especially of cardiovascular origin, in addition to being accompanied by several micro and macrovascular complications that affect the quality of life of those who suffer from it. Treatment of DM to reduce blood glucose has been shown to reduce the risk of developing these complications. For people with DM1, insulin is the only currently approved form of treatment, and carbohydrate counting is the most recommended technique for dosing insulin doses related to food and prandial insulin.

Carbohydrate counting is a repetitive heuristic process in which, through trial and error, an individual refines his or her ability to predict blood glucose behavior after a meal based on an estimate of the amount of carbohydrates in that meal and the effect that a specific insulin has. Despite being the most recommended dose adjustment technique, some factors, such as lack of precision in estimating the carbohydrate content of a meal, the type of foods in a meal, and the interaction with other nutrients, have been identified as factors. That affects carbohydrate counting.

Strategies have been proposed to refine traditional carbohydrate counting; some take into account not only the amount but the type of carbohydrates consumed (1), others the amount of other macronutrients such as fat and protein (2-4), and others simplify the

calculation of carbohydrate content in food (1). However, the outcomes evaluated in the studies or the difficulty of implementing them outside of a controlled environment limit the use of these strategies.

Decision-making processes that are accompanied by some degree of risk and that are repetitive can be improved using simulations that allow the person to be exposed to the situation without risking it and can be interactive to enable a greater degree of involvement of the individual. Carbohydrate counting is a repetitive process in which a person refines their ability to predict glucose changes after a meal. Carbohydrate counting has a high degree of uncertainty, especially when the person is faced with foods that they have consumed only a few times in the past; the calculation is based on formulas whose parameters have been estimated on a population basis and must be adjusted frequently. This situation exposes patients to decisions that can be made only once and that can have implications for their health immediately in the case of hypoglycemia or the long term with sustained hyperglycemia.

The decision-making process of people who count carbohydrates could be supported by a dynamic simulation that allows them to recreate various “what if” scenarios, where different situations, such as changes in the caloric content of a meal or the dose of insulin, can be evaluated by the individual in a safe environment. Besides safety, the potential benefits in this situation are greater confidence when facing the current situation, improved insulin dose estimates, or adjusted caloric intake. But for a dynamic simulation to make useful predictions, it must reliably recreate the phenomenon, and one of the ways to achieve this is through mathematical modeling.

There are simulators of glucose behavior, but their use has been limited to preclinical research, primarily focused on developing the artificial pancreas. On the other hand, some mathematical models have approached glucose metabolism in a compartmental way, which makes their use difficult outside the purpose for which they were created, and others have focused on specific aspects or organs within glucose metabolism. To the researchers'

knowledge, no mathematical models of glucose metabolism have been proposed that have been used to help patients with DM1 make decisions.

This work aimed to probe whether carbohydrate counting aided by a simulation was better than the traditional technique to estimate insulin dose in people with DM1. To do this, a phenomenological mathematical model of the glucose dynamics in the gastrointestinal system was built to simulate the changes experienced by an individual's blood glucose after a meal. Then, a mobile and simple-to-use solution was developed so that a person could simulate a meal and evaluate the impact of insulin dose estimated by carbohydrate counting. We hypothesized that frequent use of a solution like the one described should result in better glucose control. This hypothesis was tested in a randomized controlled clinical trial.

To facilitate the reading of the document, it has been organized into four self-contained chapters, which allows each of them to be read independently, but they complement each other. Each chapter is written strictly respecting that of the article published on that topic. For this reason, it may sound repetitive or redundant with other text chapters in some parts.

The first chapter presents the results of a systematic literature review that sought to evaluate the effectiveness and safety of carbohydrate counting in different populations and when compared with multiple other educational techniques. The second chapter explains the procedures to obtain a phenomenologically based semi-physical model of the gastrointestinal tract and liver. In Chapter 3, how the gastrointestinal model was coupled with a model adapted from the minimal model, which allows the simulation of glucose changes at the whole body level in addition to including the effect of the application of a dose of insulin in addition to the development of a solution to be used from a mobile device so that people who count carbohydrates could do simulations using the model described in the immediately previous chapter. In the last chapter, the results of a clinical trial are presented in which it was compared whether the form of counting supported by a simulation generated by the model was superior and safer than traditional carbohydrate

counting in people with type 1 diabetes mellitus using as outcome change in time in range and frequency of hypoglycemic episodes.

OBJECTIVES

1. Identify and synthesize the available evidence about the effectiveness and safety of using carbohydrate counting in people with type 1 diabetes mellitus.

2. Develop a phenomenologically based mathematical model that reproduces the role of the gastrointestinal tract in glucose metabolism.

3. Couple the gastrointestinal tract models with a whole-body model to generate simulations of post-meal glucose changes in people with type 1 diabetes mellitus and implement the model solution on a mobile device that allows a person to simulate multiple scenarios when eating.

4. Determine if a strategy based on carbohydrate counting supported by a simulation of postprandial glucose behavior improves glycemic control in people with type 1 diabetes mellitus.

THEORETICAL FRAMEWORK

Diabetes Mellitus

Diabetes mellitus and its burden

Diabetes mellitus (DM) is one of the most prevalent non-communicable chronic diseases in the world. In 2019, it was estimated that 463 million people lived with DM worldwide; by 2045, that number is expected to rise to 700 million. The prevalence of DM in adults in Colombia is estimated at 8.4% (95%CI 6.0-11.3), which in 2017 represented a little less than 3 million people affected, being the second country in the region (South America and the Caribbean - SACA) with the most significant number of people with DM (2). Etiologically, three different types of DM are distinguished: type 1 DM (DM1), which is characterized by progressive destruction of pancreatic beta cells leading to absolute insulin deficiency; type 2 DM (DM2), which results from a combination of different degrees of insulin resistance and deficiency, and monogenic DM in which hyperglycemia is the consequence of a specific genetic defect. There are other types, such as gestational DM, drug-induced or hyperglycemia resulting from other endocrine disorders, diseases of the exocrine pancreas, or strange immunological forms (3).

Elevated blood glucose levels have been associated with microvascular complications (4, 5) and macrovascular (6, 7). Stratton and colleagues (8) Stratton and colleagues evaluated the relationship between elevated blood glucose levels and the likelihood of developing either macrovascular complications (acute myocardial infarction, angina, ischemic stroke, and peripheral arterial disease) or microvascular complications (diabetic kidney disease, diabetic retinopathy, or diabetic neuropathy) associated with type 2 diabetes (DM) in an observational analysis of individuals included in the UK Prospective Diabetes Study (UKPDS). This study assigned patients to the intervention group with an intensive treatment strategy and a target fasting glucose of 108 mg/dL. In comparison, the control group followed a usual treatment strategy with a target fasting glucose of 270 mg/dL. Participants were monitored using glycated hemoglobin (HbA1c) to assess their degree of exposure to hyperglycemia over the observation period, and 3005 individuals with an average follow-up time of 10

years were included in the exposure analysis. The age-, sex-, ethnicity-, and diabetes duration-adjusted incidence rate for any diabetes-related complication increased with rising HbA1c levels, with a more significant increase observed for microvascular complications than macrovascular complications. In a different model that also considered treatment type (strict vs. conventional), the relationship between HbA1c and complications remained unchanged, suggesting that treatment alone does not influence the risk of complications. The analysis did not reveal a threshold below which the risk ceased to decrease or above which the risk stopped increasing.

Not only is hyperglycemia associated with an increased risk of chronic complications, but it is also strongly linked to the manifestation of acute forms of disease decompensation, diabetic ketoacidosis (DKA), and hyperosmolar hyperglycemic state (HHS). In a descriptive study reviewing 2233 hospital admissions and 44 episodes of DKA or HHS at a university hospital in Medellin (9), it was reported that poor adherence or inadequate prescription of therapy for DM is the second leading cause of decompensation. In addition, A1c values suggest that individuals adherent to therapy mostly had poor metabolic control before decompensation.

The economic burden of DM in Colombia is estimated to represent 8% of public health expenditure. The cost per person for the disease is expected to double by 2030 (10). In a cost-of-illness study based on an incidence model, incorporating both societal and Ministry of Health perspectives as payers and simulating direct and indirect costs, a lifetime cost per patient was determined to be COP 57,565,000 from a societal standpoint and COP 19,576,000 from the Ministry's perspective. Forty-seven percent of the expenditure is attributed to treating the disease (11). In addition to economic costs, diabetes mellitus (DM) ranks among the leading causes of death and disability. Based on preliminary data published by the National Administrative Department of Statistics (DANE), DM is the ninth leading cause of death in Colombia (12), and on average, adults in Colombia lose 0.24 years of life due to the disease (13).

Diabetes mellitus treatment

A treatment strategy based on stricter glucose control with a goal that seeks to reduce HbA1c values close to those of a person without diabetes has been shown to reduce mortality, as well as the appearance of micro and macrovascular complications in both people with DM1 (14, 15) and DM2 (16, 17). HbA1c has become the preferred method for monitoring the treatment of individuals with diabetes mellitus (DM), and its reduction is associated with a lower risk of complications. There is consensus that an HbA1c target should guide the treatment strategy, and this target should be individualized (18, 19). Although regulatory bodies delineate stringent criteria for endorsing pharmaceutical interventions in diabetes (20), b., the landscape for non-pharmacological strategies awaits more defined parameters, with some authors advocating for a threshold of at least 0.3% reduction in A1c values as a potential clinical benchmark (21, 22).

Over the past two decades, pharmacological options for individuals with DM2 have evolved alongside a deeper comprehension of the disease and its mechanisms. This evolution has facilitated the development of a patient-centered treatment strategy. However, for individuals with type 1 diabetes DM1, insulin remains the sole treatment option available to date (3). Insulin stands among the most frequently prescribed medications for treating adults with DM in Colombia. A cross-sectional study analyzing data from 2001 to 2003 across nine centers in Medellín and encompassing information from 3,583 patients—95% of whom had type 2 diabetes DM2—revealed an insulin usage frequency of 19.6% (23). In another study aimed at assessing the prescription patterns of diabetes medications within the national healthcare system, utilizing medication dispensing records with a prescription period of no less than three months, data from 1,836,777 individuals were analyzed. Among them, 7,308 patients across 19 cities were receiving diabetes treatment. Insulin emerged as the third most prescribed medication, being formulated for 21.8% of the patients (24). The authors reported exclusive insulin use in 10% of the patients and assumed that these individuals were likely diagnosed with DM1. While the prescription landscape has evolved, incorporating new medications for the treatment of type 2 diabetes DM2, insulin remains a frequently employed form of therapy. In 2014, Barengo and colleagues assessed

prescription patterns in 5 cities of Colombia through an electronic survey, gathering information from 5,098 patients with DM2. Once again, insulin emerged as the third most prescribed medication, with the usage of long-acting (or basal) insulin reported in 22% of individuals and fast-acting (or prandial) insulin in 7% (25). More recently, at the Pablo Tobon Uribe Hospital, among patients intended to initiate treatment with a glucagon-like peptide-1 receptor agonist, with an average disease duration of 10.3 years (SD 8.7), 71% of patients were on long-acting insulin, and 40% were on short-acting insulin. These findings consistently suggest that the use of insulin in individuals with DM2 appears to remain stable. It can be inferred that approximately 20 to 30% of DM2 patients, and 100% of those with type 1 diabetes DM1, are users of long-acting insulin. Additionally, about 30 to 50% of individuals with DM2 use at least one dose of fast-acting insulin, while nearly all DM1 patients rely on it. In the short term, no shift in this trend is anticipated, attributed to the high cost of new diabetes medications, the efficacy of insulin, and its relatively low cost in Colombia.

Available strategies for insulin subcutaneous application

Insulin can be administered through multiple daily injections of the preparations as mentioned earlier or insulin pumps, devices for continuous subcutaneous infusion. Insulin pump therapy can be used alone or with a constant glucose monitor (sensor-augmented insulin pump therapy). Most patients have an insulin dose based on estimates made by their physicians empirically or through population-based approximations (26). In patients using multiple-dose regimens, the initial dose of basal insulin can be defined by a standard dose, a weight-based dose, or computed through different formulas, and it is adjusted considering fasting glucose with dosing schemes based on dose proportions or fixed adjustments. The initial estimation of prandial insulin dose can also be made as a standard dose, but this assumes that food intake at all meals or meals with the same schedule will always be similar. This assumption poses a challenge addressed by dietary restriction. It can also be calculated based on weight. Still, this approach overlooks certain aspects, such as variability in insulin sensitivity among individuals, and again assumes relatively constant food consumption with meals. The prandial insulin dose is often adjusted as a proportion

of the insulin dose, taking into account post-meal blood glucose or using the carbohydrate counting technique, the latter being proposed as the ideal method for dose adjustment (3, 27).

Carbohydrate counting is a meal planning technique developed in the early 20th century in which the insulin dose administered with each meal is based on the amount of carbohydrates. The assumption behind this strategy is that the quantity rather than the type of carbohydrates impacts blood glucose levels after a meal. While carbohydrate counting is not a new technique, it gained popularity with the results of the study designed by "The Diabetes Control and Complications Trial Research Group (DCCT)." This study assigned a group of adolescents and adults to a strict management treatment strategy guided by glucose targets at 3 am, before meals, and at night. A daily insulin dose adjustment based on glucose levels and diet through carbohydrate counting documented a reduction in the risk of developing retinopathy, diabetic kidney disease, diabetic neuropathy, or any progression of these conditions. (15). Additionally, within the intensive control group, patients who utilized carbohydrate counting experienced a 0.5% reduction in A1c levels compared to those on fixed insulin doses.

Intestinal glucose absorption, its effect on blood glucose, and implications for insulin dosage

Glucose is not an abundant component in the human diet; however, the carbohydrates we ingest in sucrose, lactose, or starches are rich in glucose. Carbohydrates, during digestion, require the action of different enzymes to be hydrolyzed and subsequently absorbed, and this occurs slightly differently with each.

Sucrose is hydrolyzed at the intestinal brush border by sucrase, and the resulting glucose is absorbed more efficiently by enterocytes than fructose, which tends to accumulate in the intestinal lumen. However, the absorption mechanism does not seem to limit sucrose absorption and is proportional to the quantity entering the intestine. (28). Carbohydrates more complex or derived from a food source with a higher fiber content exhibit a different

absorption mechanism characterized by incomplete absorption, facilitating their passage to the colon (29). Additionally, their absorption rate is influenced by numerous factors such as the rate of digestion, particle size, food preparation, transit time, and the content of other macronutrients such as fat and proteins (30). Complex carbohydrates undergo hydrolysis into simpler components such as maltose and maltotriose, subsequently converting to glucose, fructose, or galactose. Once enzymatically cleaved by brush-border enzymes (maltase, isomaltase, lactase, trehalase, saccharase), simple carbohydrates are swiftly transported into enterocytes through transporters located proximally to the enzyme action sites.

Glucose and galactose are transported via the sodium-glucose cotransporter type 1 (SGLT1), primarily in the duodenum and jejunum. This transporter facilitates the absorption of two sodium ions and one glucose molecule, leveraging the gradient established in the basolateral membrane by the sodium-potassium ATPase pump. In the intestinal lumen, sodium ion binding precedes, inducing a conformational change and allowing glucose molecule binding. At this juncture, the transporter rotates, aligning the binding sites for sodium and glucose with the enterocyte cytosol. Post uncoupling, glucose is transported into the portal circulation through facilitated diffusion via the glucose transporter GLUT 2, with subsequent rotation of SGLT1. This event may occur up to a thousand times per minute. Approximately 10% of the glucose entering enterocyte cytosol is utilized for energy production.

Fructose is transported via facilitated diffusion through GLUT5 transporters in both apical and basolateral membranes, allowing fructose to enter the portal circulation. Fructose does not transform within the enterocyte. Lactose is enzymatically converted into glucose and galactose by lactase, a non-inducible disaccharidase whose concentration is genetically determined. In most humans, its levels decline around 3 to 5 years of age. In specific populations worldwide, lactase levels persist at infantile quantities (31).

The impact of various types of carbohydrates in the diet on postprandial glucose was assessed in individuals with type 1 diabetes (DM1) using meals with different glycemic indices but the same carbohydrate quantity in a euglycemic clamp protocol and labeled glucose (U-13C glucose) (32). Meals with a low glycemic index resulted in a slow but sustained elevation of plasma glucose that extended beyond 8 hours, in contrast to the high glycemic index meal, which induced a faster and 50% higher absorption peak with a much more rapid decline and complete absorption within 6 hours. Both groups were treated with the same insulin dose and infusion rate, and tracer absorption was identical.

Carbohydrate counting in the treatment of diabetes mellitus with insulin

Under the widely accepted assumptions that DM1 is characterized by an inability to produce insulin, that carbohydrates are the primary macronutrients responsible for the increase in blood glucose concentration after a meal, and that treatment should be based on an insulin dose adjusted to the meal rather than restricting food to fit the insulin dose, carbohydrate counting has been regarded as the ideal form of prandial insulin dosing in individuals with DM1 (33). The effectiveness and safety of carbohydrate counting have been assessed in only a few clinical trials, and some systematic reviews have been published, synthesizing part of the available evidence.

In a systematic review (34) that included seven clinical trials (35-41) with a total of 703 patients, 599 of whom were adults, the study compared carbohydrate counting (CCHO) with what was described as standard treatment or low glycemic index diets. The result of this systematic review suggests that CCHO does not significantly reduce HbA1c by -0.35% (95% CI -0.75 to 0.06), and the effect was heterogeneous (X2) among the studies (32%, $p< 0.001$). The authors used their tool for assessing the risk of bias and determined that the primary risk of bias for all studies was related to the fact that despite using random assignment for the intervention, none employed any concealment mechanism, and due to the nature of the intervention, proper blinding was challenging. Visual analysis of the funnel plot indicated asymmetry in two studies (36, 37) that favors the comparator, and these differ

from the rest in various aspects. The authors reported a second analysis that excluded only adults and experiments with parallel groups, showing an effect on A1c reduction of -0.64% (95% CI -0.91 to -0.37). For other outcomes, meta-analysis was impossible due to a lack of comparative data within the studies or a highly heterogeneous reporting method that did not allow for meaningful comparisons.

In another systematic review (42), which included three additional studies (43-45), the ten studies included data from 773 patients, including 422 adults. Carbohydrate counting was compared with standard treatment, low glycemic index diets, or nutritional interventions with some education but not carbohydrate counting. The risk of bias analysis showed that in most studies (7/10), the authors found it unclear how the random sequence was generated and in (7/10) how it had been kept concealed. However, due to the difficulty in blinding the intervention, studies were considered to have a low risk of bias if they were low risk in all domains except blinding. The final assessment classified two studies as low risk, five as having an indeterminate risk, and three as high risk of bias. Half of the included studies (5/10) compared CCHO with standard education for type 1 diabetes treatment.

The overall effect on HbA1c reduction was -0.35% (95% CI -0.65 to -0.05) with substantial heterogeneity (I^2=71.2%, p<0.001), based on moderate-quality evidence due to the risk of bias and inconsistency among studies. In subgroup analysis, the authors reported a significant reduction in A1c of -0.68% (95% CI -0.98 to -0.38) when carbohydrate counting was compared with standard treatment and not with other forms of treatment, with a change in HbA1c of 0.02% (95% CI -0.34 to 0.39). They also reported a significant reduction in A1c in studies conducted in adults, -0.40% (95% CI -0.78 to -0.02), and not in those conducted in children and adolescents, -0.29 (95% CI -0.82 to 0.24). Four studies were included to analyze secondary outcomes to evaluate the effect on insulin dose, and three to assess hypoglycemia events and changes in body mass index. No differences were found for any of the outcomes.

Another meta-analysis of clinical experiments evaluated the effectiveness of carbohydrate counting only in adults with DM1, excluding pregnant women or people with chronic kidney

disease. (43). Five studies meeting the proposed inclusion criteria were included in the analysis. These five studies (35, 38-41) were part of previous meta-analyses and comprised 572 patients. The overall effect on HbA1c reduction was -0.45% (95% CI -0.85 to -0.13) with high heterogeneity (I^2=72%). The authors mentioned an intention to conduct a sensitivity analysis and review primary studies to explain the heterogeneity, but this is not reported in the article's final version. For the analysis of secondary outcomes, four studies were included to evaluate the effect on the risk of hypoglycemia, three for assessing quality of life, and two for lipid profile. No differences were found for any of the outcomes. In the meta-analysis by Fu et al. and Vaz et al., the quality of evidence was graded according to the GRADE system (Grading of Recommendations Assessment, Development, and Evaluation). The quality was considered moderate for the primary outcome in both, and for the secondary outcomes, it was low.

Other outcomes not included in these systematic reviews have been assessed in individual studies with a limited number of patients and in surveys. In these studies, carbohydrate counting has been associated with the possibility of greater variety in food intake and increased dietary flexibility, both in patients using multiple injections and those using insulin pumps (44-46).

Possible limitations of traditional carbohydrate counting

One of the concerns raised with carbohydrate counting, and suggested by some authors that it could limit its effectiveness, is the lack of precision in estimating the number of carbohydrates. Overestimating the quantity of carbohydrates could lead to hypoglycemic episodes and the need to consume more carbohydrates. At the same time, underestimating could result in administering an insufficient insulin dose, increasing the risk of hyperglycemia. Meade and colleagues (47), in the "Carbohydrate Test Study," assessed the accuracy of carbohydrate counting through a survey in a group of adults from a center dedicated to caring for individuals with DM1 and DM2. The study does not clearly outline how the sample was selected, and a simple instrument designed by the researchers was

used, intended to be applied during a consultation, and based on meal models. The researchers did not find an association between carbohydrate counting training and changes in HbA1c. However, those with higher scores on the test reported lower HbA1c values. Carbohydrate overestimation was common (82% of participants overestimated to some degree), while underestimation was minimal (12%). On average, study subjects tended to overestimate carbohydrate content by 40%. An interesting finding from the study was that a significant proportion of patients (36%) were not interested in retraining.

The accuracy in carbohydrate counting could be influenced by numerous factors, such as the experience of the counter, the type of training received, and the frequency of practice, and the type of food and its preparation may have an impact. In a study in Japan, Kawamura et al (48) presented life-sized photographs of cooked meals to various groups of individuals, including patients (both children and adults), parents of patients, and medical and paramedical staff involved in caring for individuals with diabetes. The photographs were categorized into three groups based on their carbohydrate content, and individuals were grouped based on their experience in carbohydrate counting.

In the high-carbohydrate content group, as the amount of carbohydrates decreased, overestimation increased, and as the content increased, underestimation also rose. Foods with a high caloric content favored overestimation of carbohydrate content. In low-carbohydrate meals, the quantity always seemed to be overestimated. The third group of foods, consisting of fruits and desserts, produced the highest level of overestimation. Estimation errors appear to be common among both those counting carbohydrates and those teaching the technique.

Not only carbohydrates but also the amount of fat in a meal affects postprandial glucose. In a group of 7 patients with type 1 diabetes (DM1), the impact of a meal with 60g of fat was evaluated compared to a meal with 10g. A closed-loop system was employed for insulin delivery, and macronutrient content was controlled to ensure equal amounts of carbohydrates and protein in both meals. Patients were assessed in a controlled

environment for 48 hours. Eventually, researchers obtained seven studies from patients with adequate matching between open-loop and closed-loop periods.

The meal with a higher fat content was associated with a higher postprandial glucose value (Area Under the Curve [AUC] >120 mg/dL = 16,967 ± 2,778 vs. 8,350 ± 1,907 mg/dL) and an average 42% higher insulin dose (49).

However, not only fat affects postprandial glucose in individuals with type 1 diabetes (DM1). The impact of other macronutrients was evaluated by García-López et al (50) comparing the effect of two meals with a known but different amount of macronutrients (fat and protein) and identical carbohydrate content using a continuous glucose monitoring system in a 3-hour observation period after meals. With both meals, patients mostly remained within the target range (70 to 180 mg/dL), 84.5% vs. 93.1%. However, the resulting glucose pattern for both meals was different, with the low-fat and low-protein meal reaching pre-prandial levels within the observation time, while with meal 2, it never returned to the initial values.

Strategies that address some of the limitations of traditional carbohydrate counting

Strategies have been proposed to complement carbohydrate counting, either by considering the type of carbohydrates consumed, the content of other macronutrients, or by modifying the way carbohydrate content is estimated in the meal. One proposed strategy involves incorporating not only the quantity but also the quality of carbohydrates into the calculation. Glycemic Load (GL) is obtained as the product of the carbohydrate content in grams and the glycemic index of the foods. This approach was tested in a cross-over pilot experiment with 9 patients who were randomly assigned to 1-week periods of insulin dose estimation based on carbohydrate counting or GL. Continuous glucose monitoring systems were used during this study (51). As a measure of glycemic variability, the authors used the maximum amplitude of glucose 3 hours after the meal. The amplitude was lower in the intervention group (75.9 ± 1 mg/dL) compared to the control group (98.4 ± 1.77 mg/dL). The intervention was also associated with a greater variation in insulin dose

despite the meals being identical in both periods. There were no differences in the time spent with glucose below 70 mg/dL or in the number of hypoglycemic episodes.

The addition of protein counting was assessed in an experiment with a standardized meal containing 14g of carbohydrates, 2.4g of fat, and 40g of protein (52). The insulin-to-carbohydrate ratio was higher (2.2 vs. 4.6) when protein was incorporated into carbohydrate counting. The mean postprandial glucose was lower with protein counting -32.4 mg/dL (95% CI -52.2 to -12.6), and the time in range without hyperglycemia (with the upper limit defined as 140 mg/dL) was also lower with protein counting, incidence ratio (IR) 0.75 (95% CI 0.62 to 0.89), without increasing the risk of hypoglycemia IR 1.97 (0.90 to 4.27).

Another alternative is the Food Insulin Index (FII), developed as a physiological approach to classifying foods based on how they induce insulin release or "insulin demand." This strategy considers not only the quantity of carbohydrates in foods but also the potential insulinotropic effect of other foods. In summary, the FII compares the insulin response to isoenergetic food portions. A 1000 kJ (239 Kcal) portion is used as the basis for comparison, and subsequently, an index for mixed meals is developed based on the response to the white bread (=100) standard (53). Compared to carbohydrate counting, the Food Insulin Index (FII) correlates better with insulin demand in healthy individuals. In individuals with type 1 diabetes using an insulin pump, the FII was compared to carbohydrate counting in a clinical experiment, incorporating it into what the authors termed Food Insulin Demand (FID). To compute FID, knowledge of the FII of the consumed food and the energy content of the meal is required (FID = FII × kJ per portion/1000). The insulin-to-FID ratio was established by multiplying the insulin-to-carbohydrate ratio by a factor of 1.7. Continuous glucose monitoring was employed to assess outcomes related to glucose levels (54). After 12 weeks of intervention, the reduction in A1c was not different in the two groups -0.1 ± 0.1% vs. -0.3 ± 0.2%. In most glucose-related outcomes, no differences were found between the groups (fasting glucose, standard deviation around the mean glucose, area under the curve for glucose 120 minutes after breakfast, time in range 70 to 140 mg/dL, time out of range >140mg/dL or <70 mg/dL). The only outcome where the intervention was superior was the mean amplitude of glucose excursions (MAGE) -110 ± 18 mg/dL vs. -23.4±18 mg/dL.

In both groups, patients reported feeling comfortable with the intervention. The study was stopped before completing the planned sample (26 out of 32) because the interim analysis did not report a difference in the primary outcome (A1c). FID has some disadvantages, such as the need to create food tables, making cross-cultural generalization difficult, and it is subject to a learning curve for patients.

A novel strategy is the semi-quantitative estimation of carbohydrates known as the Simplified Bolus strategy, which places less emphasis on the accuracy of carbohydrate counting (CCHO). In a cross-over pilot clinical trial involving patients using a closed-loop bihormonal insulin pump (1), the effectiveness endpoint was the average glucose over 15 hours (study period), and other outcomes such as time in range, insulin dose, and glucagon were evaluated. Ten patients completed the protocol, and a difference in average glucose was documented: 126 vs. 156.6 mg/dL. Additionally, there was less time spent above 180 mg/dL (14.9% vs. 30.7%) and more time below 70 mg/dL (8.1 vs. 2.5%).

Mathematical modeling and diabetes mellitus

Mathematical modeling for glycemic control tools

The key allostatic processes for maintaining glucose homeostasis include its absorption, production, transport, and consumption. Like any biological process in the body, glucose homeostasis is tightly regulated by various mechanisms with continuous feedback through complex and ever-changing phenomena.

Computational mathematical models enable the solution of a large number of equations that can represent complex biological phenomena. These models can aid in studying specific elements such as the response of these systems to internal or external signals or disturbances. Additionally, models allow for simulations, and these simulations are not bound by the traditional constraints of biological experiments, such as ethical, economic, and technological limitations. Moreover, simulations can provide measurements that might be challenging or unfeasible in experimental subjects. Finally, unlike biological experiments,

simulations can be repeated numerous times with as many variations as the scientist desires, allowing for the design and guidance of future experiments (55).

Use of mathematical modeling in different areas of interest in diabetes mellitus

The homeostasis of glucose and the condition resulting from its alteration, DM, has been of interest to modelers. Ajmera and colleagues (56) provide an excellent review of the models available up to 2012 and propose a classification into categories based on the information used for their construction. Clinical Models, which are structurally simple and usually contain only essential biological descriptions, aim to emulate available clinical information. On the other hand, there are Knowledge-Based or Physiological Models. Unlike the former, these are mostly mechanistic or first-principle models that attempt to describe different biological phenomena related to glucose control. They typically incorporate more physiological knowledge about the processes. Subsequently, these models may also have clinical utility. Models can also be classified according to their purpose (57, 58). There are those used to evaluate diagnostic tests, to build controllers used in artificial pancreas systems, for predicting the behavior of a condition, such as DM and its complications, to assess pharmacological characteristics of medications like insulin, or to describe glucose behavior in different organs or the entire body, including hypothetical scenarios. There are also models for the costs associated with DM treatment. Building on these considerations, Frietzen and colleagues propose classifying models as Metabolic and Measurement Models and Development Models (58).

One of the mathematical models in diabetes that has yielded excellent results in predicting glucose behavior is the UVa/Padova mode (59). This model currently has approval from the United States Food and Drug Administration (FDA) as a substitute for preclinical trials of certain insulin treatments, thus avoiding experimentation on animals as dictated by protocols for introducing new treatments/medications in humans. Despite the significant theoretical progress achieved through the construction of the UVa/Padova model, which has primarily modeled the effects of insulin and glucagon, there are still unanswered

questions regarding unmodeled interaction mechanisms that have indications of playing a significant role in the glucose homeostatic mechanism.

Mathematical models of glucose physiology and homeostasis

From the point of view of the way it is constructed, a mathematical model can be empirical or mechanistic (60). In empirical models, very little or none of the real object exists in the model. The mathematical structures are adjusted to existing mathematical templates based on collected observations (data). In contrast, mechanistic models incorporate knowledge of the fundamental mechanisms of the object. The variability among individuals and perturbations such as food and exercise to blood glucose pose a challenge for any modeling technique that aims to represent this phenomenon. A review of the literature reveals that different groups have addressed this problem with both empirical and mechanistic models. Hereinafter, we will refer to mechanistic models as physiological or mechanistic models. Some of the most important ones are summarized below.

Physiological mathematical models of glucose homeostasis

One of the most significant challenges in developing a physiological model is the validation of its results against experiments of the phenomenon it aims to model. Glucose is a ubiquitous energy source in all mammals, and abundant data are available in animals. The animal models commonly studied to model glucose behavior and diabetes mellitus, with an attempt to generalize these results to humans, have been rats and dogs. The latter appear to be a better model since dogs share some mechanisms related to insulin resistance, and it is technically simpler to obtain certain samples useful in experiments (61).

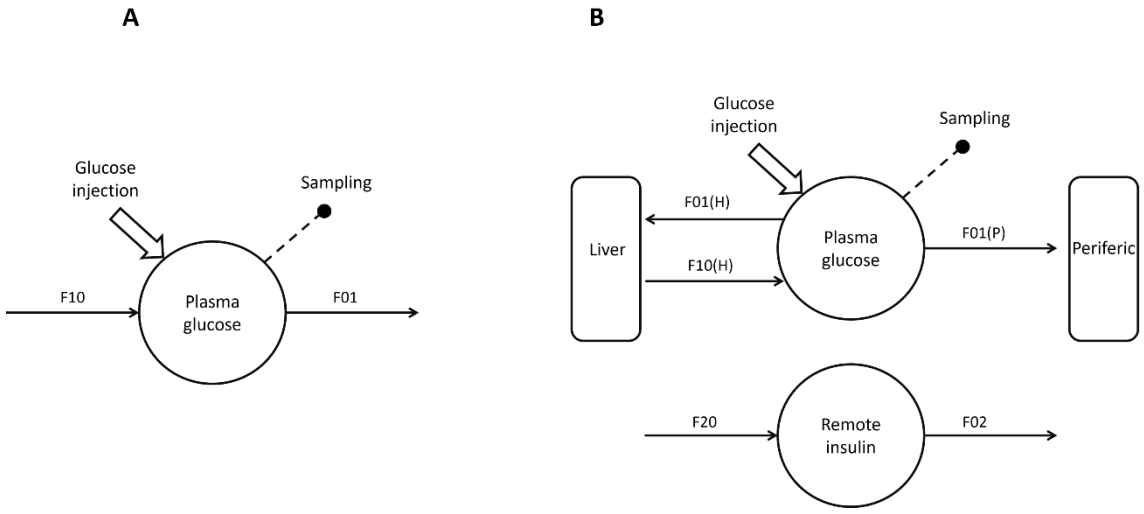
The use of radioactive isotopes as tracers to assess the passage of glucose from one compartment to another at the whole-body level has allowed significant advances in modeling glucose homeostasis. Labeling with isotopes of hydrogen and carbon enables the evaluation of different processes. For instance, hydrogen labeled at position 2 or 3 is lost during glycolysis, while hydrogen labeled at position 6 is lost in gluconeogenesis, allowing its use to study these phenomena. On the other hand, carbon labeled at position 14 is lost in the process of energy formation from glucose (62).

The kinetics of isotopes throughout the body can be evaluated using techniques involving injections (bolus) or infusions. The intravenous glucose tolerance test (IVGTT), an injection technique, allows the observation of the tracer's increase in blood concentration and its decrease over time. This enables the calculation of glucose uptake stimulated by glucose itself, usually referred to as "glucose effectiveness," and insulin action sensitivity. Continuous infusion methods are commonly used in glucose clamp experiments. In these experiments, the glucose infusion rate is used as an index of insulin sensitivity, allowing not only the assessment of glucose effectiveness and insulin sensitivity but also the evaluation of glucose kinetics in non-steady states (such as during feeding or exercise). It is common to combine continuous infusion with tracer priming by injecting the tracer to reduce the time to reach the steady state of the isotope.

Single compartment glucose models: Single-compartment models can be divided into two groups, as illustrated in Figure 1: those that are insulin-independent, where a single "pool" or "reservoir" of venous glucose is considered, with an input (glucose appearance) and an output (glucose disappearance). Insulin-dependent models have two compartments, one for plasma glucose and the other for remote insulin. The glucose compartment has one input and two outputs, representing the rate of glucose disappearance to the liver and peripheral tissues. The peripheral insulin compartment has an input from plasma insulin and an output to the plasma. Both models were proposed by Bergman (63) from Bolie's work (64) and, for the study of peripheral insulin sensitivity, the insulin-dependent model was expanded by Cobelli (65). This minimal model assumes a constant rate of glucose appearance and allows for the calculation of glucose effectiveness and sensitivity to glucose, making it suitable for interpreting the IVGTT. Due to its simplicity, this is the most widely used model for estimating insulin sensitivity.

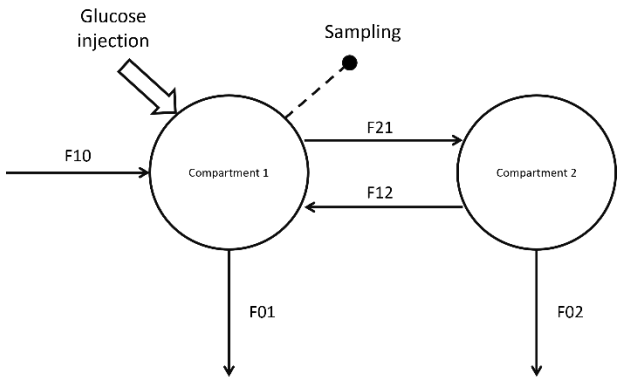
Figure 1. Single compartment minimal glucose models.

A. Insulin independent, B. Insulin Dependent.



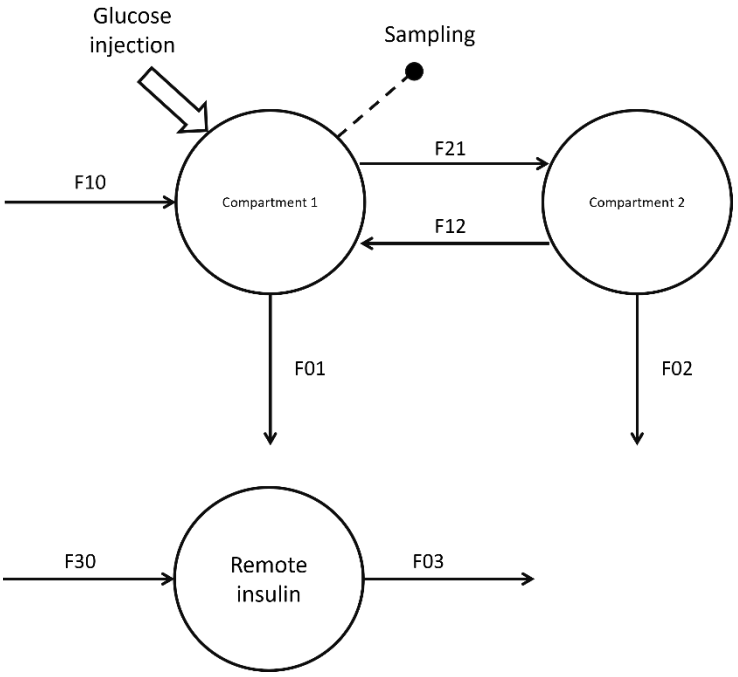
Two compartments glucose models: Single-compartment models simplify glucose kinetics to a uniform distribution outside the cells. Two-compartment models attempt to address this by adding an additional compartment for interstitial fluid glucose. In the insulin-independent model, glucose moves into compartment 1 from the liver (hepatic glucose production), and both compartments have bidirectional communication. From compartment 1, there is irreversible loss due to tissue uptake independent of insulin action, and irreversible loss from compartment 2 represents glucose uptake stimulated by glucose itself (66) (Figure 2).

Figure 2. Insulin-independent minimal two-compartment model.



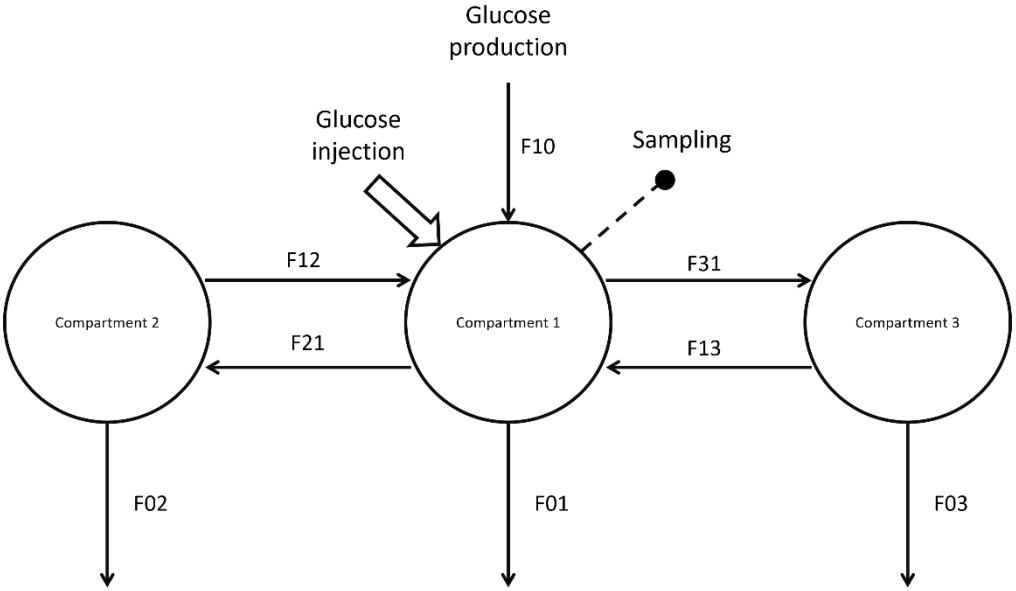
The insulin-dependent version proposed by Caumo and Cobelli (67) to assess hepatic glucose production contains two compartments for glucose and one remote compartment for insulin. All insulin-dependent extraction occurs from compartment 1, and all insulin-independent extraction occurs from compartment 2 with slow exchange. Insulin reaches the remote compartment from plasma insulin, as shown in Figure 3.

Figure 3. Insulin-dependent minimal two-compartment model.



Three compartments glucose models: Cobelli proposed a three-compartment model to describe the transition between the initial and final stages of a hyperinsulinemic euglycemic clamp experiment (68). Compartment 1 entry represents glucose production, compartment 2 represents peripheral tissues that reach a rapid equilibrium of glucose, and compartment 3 represents those with a slow equilibrium. Compartment 2 is related to tissues such as the liver, kidneys, and brain, while compartment 3 includes muscles and adipose tissue. Losses from compartment 1 represent insulin-independent peripheral glucose utilization, and losses from compartment 3 represent insulin-dependent utilization (see Figure 4).

Figure 4. Three compartments glucose model.

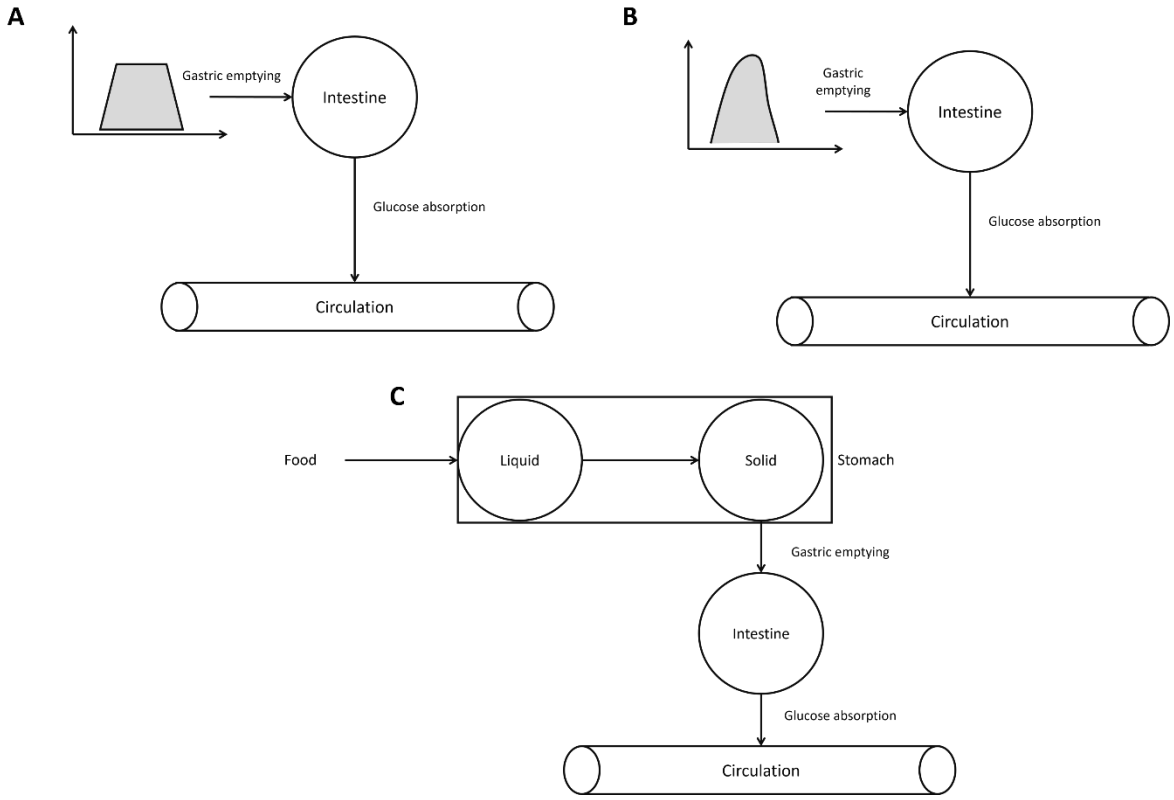


Other modeling techniques: Other modeling techniques have been proposed. Ghosh and colleagues (69) proposed a nonlinear autoregressive model in which the current glucose value depends on the immediately preceding and insulin values. This model was developed for use within a control algorithm. Another nonlinear mixed-effects model was developed to estimate insulin sensitivity using only plasma glucose data, eliminating the need to measure insulin levels, and its performance is deemed acceptable for this purpose (70).

Extensions to the minimal model to include an oral stimulus: The minimal model and its extensions were primarily designed to analyze venous stimuli, either as a bolus or continuous infusion. However, experiments needed to provide data for these models are cumbersome, time-consuming, expose subjects to uncomfortable situations, and have a high cost. Some of these difficulties can be alleviated if a stimulus originating from food is used instead of an injection. Additionally, having models that adequately represent the gastrointestinal kinetics of glucose can be useful when helpfuling control algorithms for use in everyday situations by patients.

An important barrier that had to be overcome in the development of these models was the technique for measuring the rate of appearance (Ra) of glucose in the splanchnic bed, to prevent the overcompensation that might occur in a whole-body model when plasma glucose is measured. The Cobelli and Dalla Man group tested various gastrointestinal models with a novel multi-tracer technique and oral protocols, allowing Ra estimation to compare the estimates made by the models (71) Several models were compared. The first describes gastric emptying as a trapezoid function and linear absorption kinetics in the intestine (72), the second describes gastric absorption as an exponential function (73), and two in-house models, both represented as a linear chain of three compartments. The first two represent the stomach with its liquid and solid phases, and the third represents the intestine. The second model changes the kinetics of gastric emptying and glucose absorption in the intestine to a nonlinear model, where gastric emptying is determined by the gastric glucose content (74). The models were compared using the sum of the squared residuals from the comparison between predictions and models, and the lowest value was obtained with the second proposed model. This second model seems to better describe intestinal glucose absorption. Figure 5 provides a graphical representation of the models. This model was later incorporated into the minimal model to provide a gastrointestinal glucose input for use with the oral glucose tolerance test (OGTT) (75).

Figure 5. Models of gastric glucose absorption.



Empirical mathematical models of glucose homeostasis

Empirical models or those entirely derived from data typically require large datasets. This has been one of the significant limitations in the expansion of this type of model, which is primarily based on machine learning. However, with the increase in the use of continuous or intermittent glucose sensors, the availability of such data has risen, along with the number of empirical models, especially in the field of prediction.

A recent systematic literature review synthesizing available evidence on empirical models (data-driven) (76) found that the majority of these models have been developed after 2010. The most commonly used techniques include feedforward neural networks, hybrid models that combine a physiological model with some form of machine learning, and recurrent neural networks. Most models have a prediction horizon of less than 30 minutes, although times as long as 2 hours have been reported. These models have used data from approximately 288 daily measurements for 2 to 1400 days, and the metrics used to evaluate

the model's predictive ability are so varied that they do not allow for a comprehensive assessment of the results.

Phenomenological-based semi-physical mathematical models: In between mechanistic and empirical models, there are semi-physical models, which incorporate elements of both forms of modeling. Semi-physical models can be based on empirical structures or phenomena. Phenomenology-based semi-physical models (PBSM) belong to the subfamily of gray-box models and share with white-box models the mechanistic approach to their construction. These phenomenology-based models get their name because the development of their basic structure is similar to that of a first-principles model, using the principles of conservation of mass, energy, motion, and chemical reaction. They are semi-physical because empirical formulations are used for at least one of their parameters. This modeling technique has been used in the field of engineering and has several characteristics that make it attractive for modeling dynamic biological phenomena, as listed below.

To obtain a PBSM, a proposed procedure facilitates not only its implementation but also the reproducibility of the technique (77). The development involves using descriptions of the phenomenon of interest with a level of detail defined by the modeler, and the basic structure of the model comes from the phenomenon, providing interpretability to the parameters (78). This is crucial because understanding the meaning of the parameters allows for adjustments to the peculiarities of a patient or situation. Moreover, with interpretable parameters, valuable information about the phenomenon can be derived. The model construction can be hierarchical, allowing different levels of detail in each partition that can be adjusted to the specific needs and future applications. This modular structure enables the creation of various models that interact to explain a complete and complex phenomenon.

EFFICACY AND SAFETY OF CARBOHYDRATE COUNTING VERSUS OTHER FORMS OF DIETARY ADVICE IN PATIENTS WITH TYPE 1 DIABETES MELLITUS: A SYSTEMATIC REVIEW AND META-ANALYSIS OF RANDOMIZED CLINICAL TRIALS.

In this chapter, a systematic review and meta-analysis are presented, summarizing the efficacy and safety of carbohydrate counting as a nutritional education technique in individuals with type 1 diabetes mellitus. Some of the limitations of previously reported systematic reviews were addressed, new references were included, and new questions were explored, such as the impact of time on the effectiveness of the technique. It is presented as it was published (79).

Introduction

Diabetes mellitus (DM) is one of the most prevalent chronic conditions globally. In 2019, 463 million people lived with DM worldwide, and by 2045 that number is expected to rise to 700 million (80). But, not only is DM common, but it is also a costly disease, and the cost per person probably will double by 2030 (10), with most of this cost arising from treatment (11).

High blood glucose levels in people with diabetes relate to microvascular (4, 5) and macrovascular (6, 7) complications and also to hyperglycemic crises (81). Therefore, glycemic control remains the cornerstone of DM treatment. Glycated hemoglobin (HbA1c) levels close to normal relate to a lower risk of chronic complications and mortality in people with booth DM1 and DM2 (14, 82). Insulin remains the only approved treatment for people with DM1.

Among the different ways of estimating insulin dose, carbohydrate counting is regarded as the ideal way to calculate meal-related insulin doses since it allows greater flexibility in diet and could, in some people, reduce the burden of the disease (3, 27, 44).

Carbohydrate counting efficacy has been summarized in some systematic reviews (SR); however, the results are inconclusive. The effects differ in the SR, including adults (21) and adults and children (16, 19). On the other hand, all these SR found significant heterogeneity in the results that require further analysis. Additionally, new evidence has been available since the publication of this SR (22, 23). We believed that a systematic review that includes all age groups, accounting for different sources of heterogeneity such as diverse comparators, and carbohydrate counting and insulin application technic and also with a formal assessment of the evidence's risk of bias and quality could contribute to the existing knowledge of carbohydrate counting's efficacy and safety.

Carbohydrate counting is a meal planning technique developed in the first half of the 20th century in which the dose of insulin with each meal is based on the total amount of carbohydrates. There are three carbohydrate counting levels; basic carbohydrate counting or level 1, in which the subject is conscious of foods that contain any carbohydrate. Intermediate or level 2 introduces the concept of glucose patterns and how to change the insulin dose accordingly. And level 3 or advanced carbohydrate counting allows counting through an exchange list of usually 15 grams equivalents, 10 grams portions, or the grams of carbohydrate eaten and coupling with the insulin dose (83).

Insulin dose calculation in carbohydrate counting requires an equation with two main components: The meal dose, computed from a ratio of insulin to carbohydrate usually estimated by a physician using a population approach. And a correction fraction derived from the current blood glucose value, the blood glucose target, and an insulin sensitivity factor, i.e., the amount of rapid-acting insulin necessary to reduce blood glucose level in a certain amount.

Carbohydrate counting was popularized with the Diabetes Control and Complications Trial Research Group trial (DCCT). A group of adolescents and adults was randomized to either a strict treatment strategy with insulin dose adjustment based on the glucose value and diet using several techniques, including carbohydrate counting or usual diabetes care. As a result, the intensive care group experienced a reduction in the risk of new-onset or

progression of retinopathy, diabetic kidney disease, or neuropathy (82). Additionally, the carbohydrate counting patients reduced an additional 0.5% in HbA_{1c} compared to fixed insulin doses within the intensive control group.

This SR's primary objective was to assess carbohydrate counting's effect in reducing HbA1c without increasing the risk of hypoglycemia, promoting weight gain, or a higher daily insulin dose. Also, evaluate the impact of carbohydrate counting on blood lipid profile and quality of life.

Methods

This systematic review was conducted following the Cochrane Review methods and the Cochrane Handbook for Systematic Reviews of Interventions (84) and registered in PROSPERO under code: CRD42020218499.

Types of studies

We included randomized controlled clinical trials with a parallel-group design comparing any form of carbohydrate counting with standard care or other forms of dietary advice or insulin dose calculation in people with DM1. These trials had to assess any outcome of interest for this review with a follow-up period of at least three months. Blinding the intervention was not a selection criterion because the primary outcome is objective, and blinding an educational intervention like carbohydrate counting is nearly impossible. Quasi-experiments, cluster-randomized trials, and observational studies were excluded. Also, cross-over clinical trials were excluded because the carryover effect is likely to occur in an educational intervention such as carbohydrate counting.

Types of participants

We included studies with patients of any age with DM1 defined according to the American Diabetes Association (ADA) standards valid at the beginning of the trial. Ideally, diagnostic criteria should have been described and the time since the diagnosis made explicit, in order to minimize the risk of including patients in the honeymoon period. There were no restrictions based on the setting.

Types of interventions

All trials included any form of carbohydrate counting training with an exchange list, grams portions, or grams count in one of the comparing groups. And any form of nutritional advice, standard diabetes nutrition advice, fixed insulin dose diet, low carbohydrate diets, or any other dietary intervention in the other group. Studies with patients treated with any other diabetes medication different from insulin therapy, either as multiple daily doses or continuous subcutaneous infusion (insulin pump therapy), were excluded.

Types of outcome measures

Many of the critical health outcomes in DM1 take many years to develop and are not usually measured in educational interventions in diabetes clinical trials. However, HbA1c is a surrogate outcome that correlates very well with the blood glucose level and the risk of developing chronic diabetes complications (4-7). Therefore, as the primary outcome, we consider the variation of HbA1c. And as secondary outcomes, the number of hypoglycemia events, changes in body weight, blood lipids levels, and the total daily dose of insulin. We also evaluated changes in health-related quality of life using diabetes treatment satisfaction questionnaires.

Search methods for identification of studies

The following databases were searched from inception to October 2020: MEDLINE (Pubmed), Embase, Cochrane Central Register of Controlled Trials (CENTRAL), ClinicalTrials.gov (www.clinicaltrials.gov). The World Health Organization International Clinical Trials Registry Platform (ICTRP) (http://apps.who.int/trialsearch) was not available at the moment of this SR due to heavy traffic generated by the COVID-19 outbreak. To identify grey literature, we included the following databases: Open Grey, Lens, Directory of Open Access Journals (DOAJ), and Biblioteca Virtual en Salud. Studies in any language, from any country and any date, were included. For detailed search strategies, see Supplementary Table 1.

We screened reference lists from relevant published studies, including trials, systematic reviews, meta-analyses, and narrative reviews, and contacted corresponding authors of

published clinical trials to ask whether they were willing to provide any missing data or information.

Data extraction

Two authors (CEBM, NARH) independently scanned the title and abstract of every record retrieved in the search to determine the studies to be included. All potentially relevant articles were read in full. Differences were resolved by a third author (NAOC) and justified in a group meeting. Following the PRISMA statement (85), the selection process is shown in Figure 6.

Studies were selected based on the following criteria: 1. The study was a randomized controlled trial. 2. The target population included patients with DM1. 3. The study intervention or comparator was any form of CARBOHYDRATE COUNTING. 4. Outcome measures of interest to the review were recorded as part of the study.

Two authors (CEBM, NARH) independently extracted all the relevant data corresponding to population characteristics, intervention, comparison, co-interventions, and outcomes using standard data extraction templates for studies that fulfill the inclusion criteria. Disagreements were resolved by discussion or, if required, by a third author (NAOC).

Risk of bias and quality of evidence

The risk of bias (ROB) was assessed by two authors (CEBM, NARH) independently using the Cochrane Collaboration tool (86), and disagreements were resolved in discussion with a third author (NAOC). Every study's risk was judged as low, some concerns, or high, according to the tool's recommendations. The criteria for each domain can be found in Supplementary Table 1. In addition, ROB is presented in a full ROB graph (Figure 7) and a summary of ROB judgments (Figure 8).

The overall quality of evidence for each outcome was assessed using the Grading of Recommendations Assessment, Development, and Evaluation (GRADE) working group approach (84, 87).

Statistical analysis

A standardized mean difference (SMD) was pooled with its 95% coefficient interval for all continuous data using a random-effects model. Only the level at which randomization occurred was considered. We expected clinical heterogeneity from the following characteristics: Age (adults and children), carbohydrate counting technic (exchange list, grams portions, or grams count), type of comparator (standard diabetes nutrition advice, fixed insulin dose diet, low carbohydrate diets, or any other form of dietary intervention), and the form of insulin therapy (multiple injections and insulin pump therapy) and planned subgroup analyses for each of them using a fixed-effects (plural) model that contains both random effects (within subgroups) and fixed effects (subgroups are assumed to be fixed).

The duration of the trial could also be related to the primary outcome. For example, as an educational technique, carbohydrate counting may improve over time, but as with any other repetitive activity, a person may lose interest and adherence over time. In this respect, a meta-regression was performed to check whether the trial duration relates to any effect size differences.

We explored heterogeneity by visual inspection of the forest plots and using the I^2 statistic to examine inconsistency across studies to assess the impact of heterogeneity on the meta-analysis. The threshold for substantial heterogeneity was considered to be 50% or more, as suggested in (84), and in such a case, a prediction interval is presented.

To assess small-study effects, we used a funnel plot, plotted as a contour-enhanced funnel plot, to distinguish publication bias from other causes of asymmetry. We used the Egger test of the intercept to quantify the funnel plot asymmetry (88), and when significant ($p<0.05$), Duval & Tweedie's trim-and-fill procedure (89) was implemented to estimate the actual effect size.

A sensitivity analysis restricted to low bias risk studies was used to explore their influence on the effect size. All statistical analyses were conducted using R statistical programming language and environment (90) and the functions available in (91).

Results

The database and other resource searches resulted in 801 records. After removing duplicates, 333 were screened and 301 were excluded after the title and abstract evaluation. Following the full-text article assessment, 20 studies were excluded, seven because both the intervention and comparator included CARBOHYDRATE COUNTING, five were systematic reviews, three were non-randomized clinical trials, two were single-arm clinical trials, one had no relevant outcomes, one was a partial report of another clinical trial, and one was a protocol of an ongoing clinical trial. Finally, 11 studies (35, 36, 38, 39, 41, 54, 92-96) were included in the qualitative and quantitative synthesis (Figure 6).

Data from 899 patients were available from the eleven studies included; six evaluated carbohydrate counting efficacy in adults (n= 598). Advanced carbohydrate counting was used in eight of these. In seven studies, carbohydrate counting was compared to standard diabetes education, and the most frequent form of insulin therapy was multiple daily doses. The patients were followed for 52 ± 35.5 weeks. Table 1 presents the characteristics of the participants and outcomes of the 11 studies.

Risk of bias

Only one study was judged as having a low risk of bias (54), six fell into the some concern category (35, 36, 38, 41, 95, 96), and four showed a high bias risk (39, 92-94). The more frequent concerns were related to bias in the randomization process or missing outcome data. Figures 7 and 8 present the risk of bias assessment. Table 2 show the overall quality of evidence for each outcome.

Primary outcome

The change in HbA1c was reported in all the studies. In the entire population (adults and children), carbohydrate counting does not reduce HbA1c compared to standard diabetes education and other forms of dietary advice, SMD – 0.24% (95%CI -0.68 to 0.21). A result with significant heterogeneity (I^2 = 80%, $p < 0.01$) Figure 9.

Figure 6. PRISMA Flow diagram.

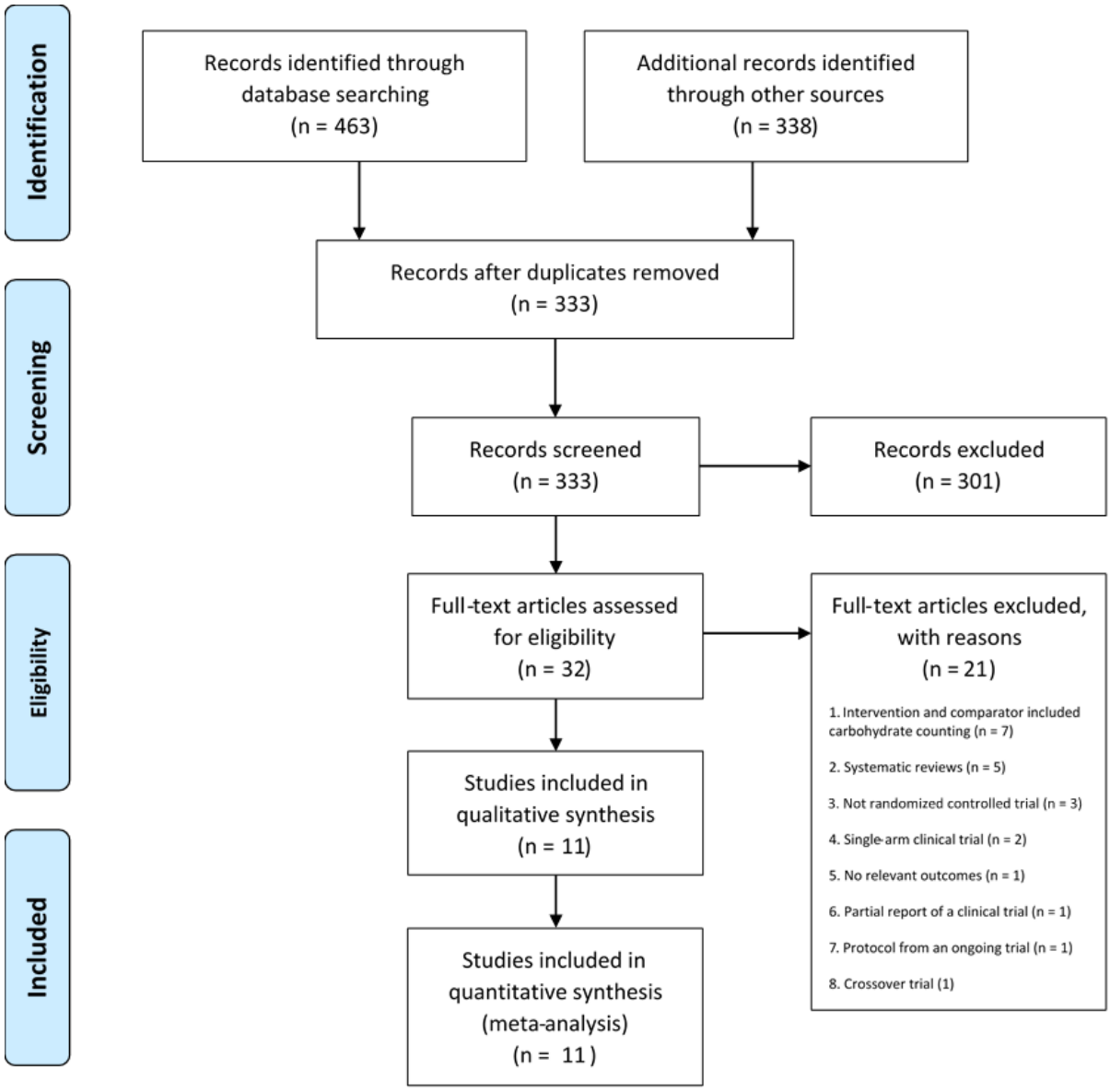


Table 1. Studies characteristics.

Study	Country	Follow up (weeks)	Population	n	Carbohydrate counting technic	Comparison	Insulin administration technic	Initial HbA1c	Intention to treat analysis
Gilbertson, 2001	Australia	52	Children	104 G1: 49 G2: 55	Portions	Low glycemic		G1: 8.6 (1.4) G2: 8.3 (1.3)	Yes
Bell, 2016	Australia	12	Adults	26 G1: 13 G2: 13	index diet	Multiple daily doses		G1: 8.6 (0.3) G2: 8.1 (0.2)	Yes
DeAlbuquerque, 2014	Brasil	52	Children	28 G1: 14 G2: 14	Exchange list	Food		G1: 10.6 (3.4) G2: 8.4 (2.1)	No
Scavone, 2010	Rome	38	Adult	256 G1: 100 G2: 156	Insulin Index	Continuous subcutaneous infusion		G1: 7.8 (1.3) G2: 7.5(0.8)	Yes
Trento, 2011	Italy	120	Adult	56 G1: 27 G2: 29	Advanced	Standard education	Multiple daily doses	G1: 7.6 (1.3) G2: 7.7 (1.2)	No
Laurenzi 2011	Italy	24	Adult	61 G1: 28 G2: 28	Advanced	Standard education	Multiple daily doses	G1: 7.9 (0.9) G2: 8.1 (1.5)	Yes
Enander, 2012	Sweden	48	Children	45 G1: 15 G2: 30	Advanced	Standard education	Multiple daily doses	G1: 7.2 (0.6) G2: 7.7 (1.0)	No
Schmidt, 2012	Denmark	16	Adult	51 G1: 22 G2: 21 G3: 8	Advanced	Standard education	Continuous subcutaneous infusion	G1: 8.8 (0.7) G3: 9.1 (0.7)	Yes

DAFNE, 2002	England	24	Children	169 G1: 84 G2: 85	Advanced	Standard education	Continuous subcutaneous infusion	G1: 9.4 (1.2) G2: 9.3 (1.1)	No
Goksen, 2014	Turkey	110	Adults	84 G1: 27 G2: 30	Advanced	Standard education	Multiple daily doses	G1: 8.1 (1.0) G2: 8.4 (1.5)	No
Donzeau, 2020	France	52	Children	57 G1: 55 G2: 55	Advanced	Standard education	Multiple daily doses		Yes

Figure 7. Risk of bias graph.

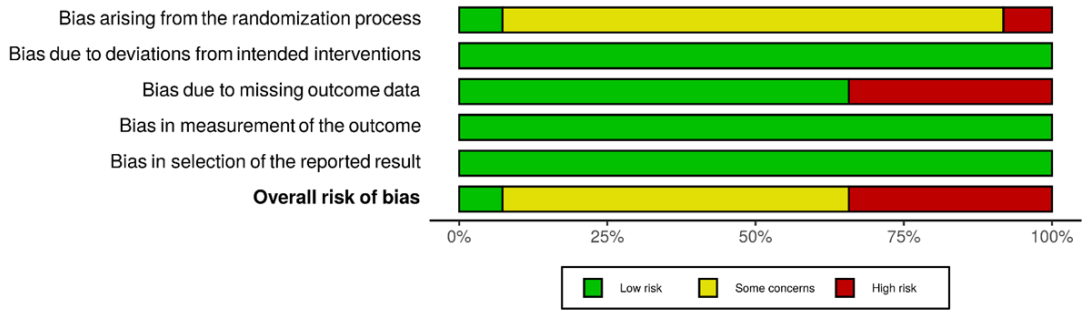


Figure 8. Risk of bias summary.

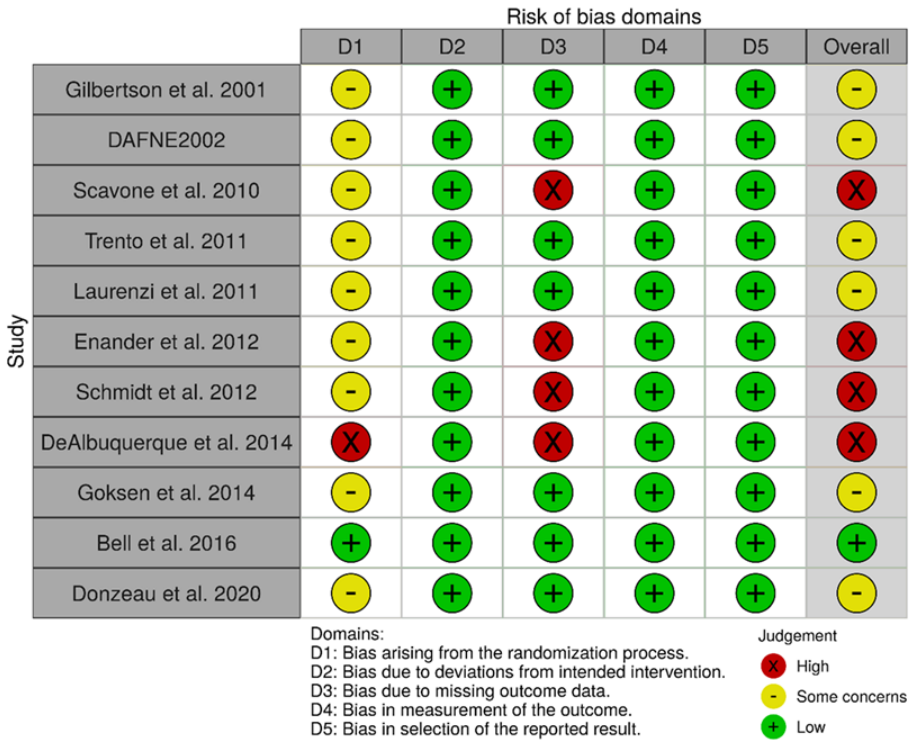
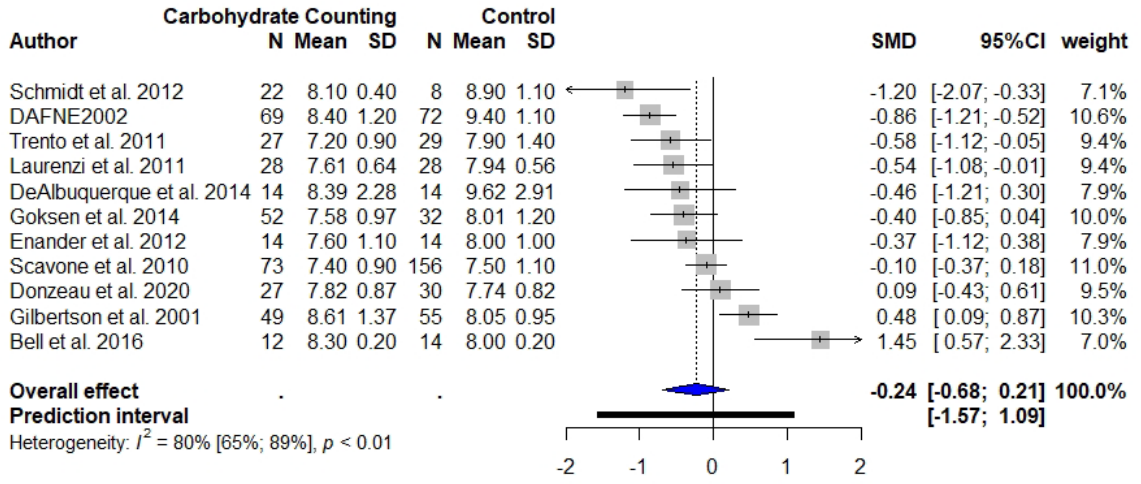


Figure 9. Carbohydrate counting effect on HbA1c.



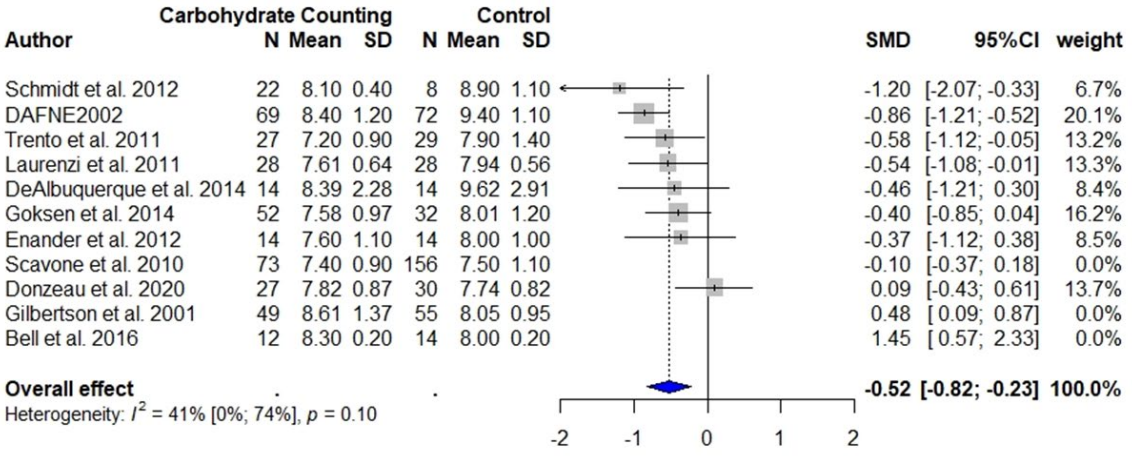
The prespecified subgroup analysis of the primary outcome revealed no difference in HbA1c reduction in the different age groups (children and adults) (p 0.53). Advanced carbohydrate counting significantly reduces HbA1c SMD -0.44% (95%CI -0.76 to -0.11), but other carbohydrate counting technics (gram lists or grams portions) don't, SMD -0.58% (95%CI -2.08 to 2.89). The comparison group's analysis revealed that compared to the usual diabetes education, carbohydrate counting significantly reduces HbA1c, SMD -0.51% (95%CI -0.83 to -0.19) but not compared to other diet methods SMD 0.31% (95%CI -0.99 to 1.61). Table 2. shows all the subgroup analysis results.

Table 2. Effect of carbohydrate counting in subgroups, change in HbA1c.

Subgroup	SMD (95%CI)	I^2	$p_{subgroup}$
Population			0.53
Child	-0.08% (-0.60 to 0.45)	64.7%	
Adult	-0.24% (-0.68 to 0.21)	84.6%	
Carbohydrate counting technic			0.16
Advanced	-0.44% (-0.76 to -0.11)	62%	
Exchange list or gram portions	-0.41% (-2.08 to 2.89)	89%	
Insulin injection technic			0.29
Multiple daily doses	-0.40% (-0.89 to 0.10)	82%	
Continuous subcutaneous infusion	0.12% (-1.57 to 1.51)	80%	
Comparison group			0.06
Usual diabetes education	-0.51% (-0.83 to -0.19)	59%	
Other diet methods	0.31% (-0.99 to 1.61)	83%	

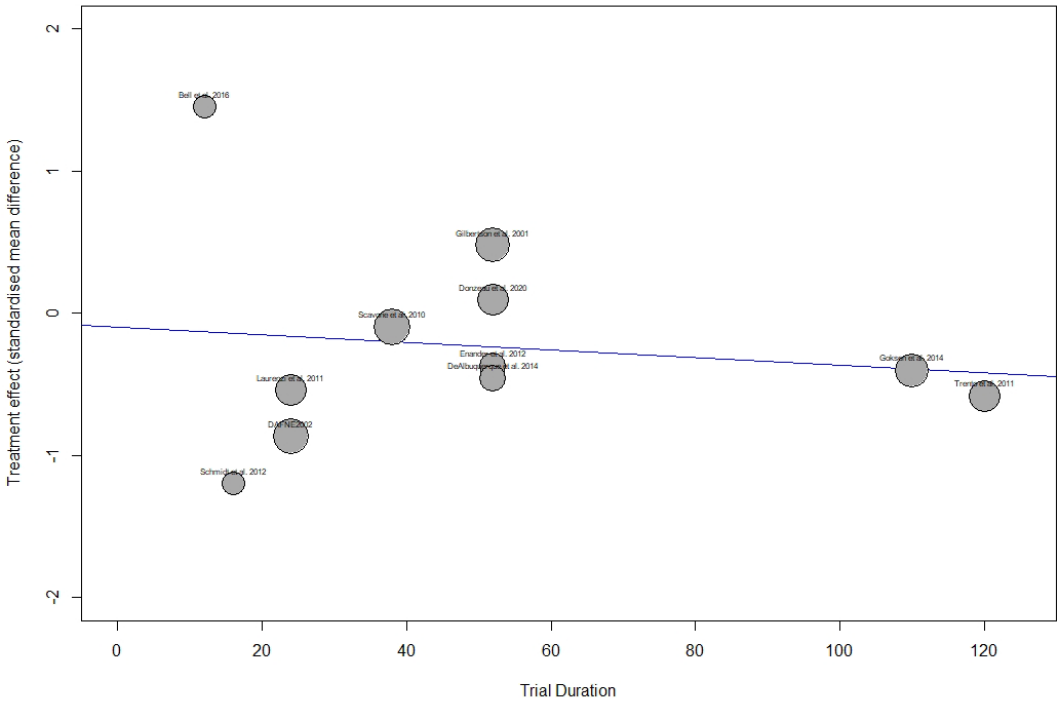
Both the I^2 and the visual inspection of the forest plot suggest a high heterogenicity. Furthermore, the apriori subgroup analysis confirms that this heterogeneity comes from the carbohydrate counting technic or trial comparator. So using Graphic Display of Heterogeneity (GOSH) plots (Supplementary Figure 1), (97) and three clustering algorithms k-means (98), density reachability and connectivity clustering (DBSCAN) (99), and Gaussian Mixture Models (100) (Supplementary Figure 2), we identify three studies (36, 39, 54) responsible for more than one population effect size. Hence, as an additional result, we present a second analysis excluding these three studies from the analysis showing a significant reduction with carbohydrate counting in HbA1c, SMD – 0.52% (95%CI -0.82 to -0.23) with no significant heterogeneity (I^2 = 42%, p < 0.10), figure 10.

Figure 10. Effect of carbohydrate counting excluding the three studies contributing to the high heterogeneity.



To assess the effect of trial duration (time) in the size effect, we performed a meta-regression with the studies' duration in weeks as a continuous predictor. The trial duration didn't account for any change in the size effect, R^2=0.0%, p=0.67, Figure 11.

Figure 11. Relationship between trial duration and HbA1c reduction.



Secondary outcomes

Blood lipids: Five studies reported changes in blood lipids (35, 41, 54, 94, 95). Carbohydrate counting did not significantly increase total cholesterol, HDL-Cholesterol, LDL-Cholesterol, or triglycerides (Table 3).

Table 3. Change in blood lipids.

	SMD (CI95%)	I^2 (*p* value)
Total cholesterol change, mg/dL	0.71 (-2.07 to 3.48)	95% (<0.01)
HDL-Cholesterol, change, mg/dL	0.59 (-0.24 to 1.42)	68% (0.01)
LDL-Cholesterol, change, mg/dL	-0.02 (-0.23 to 0.18)	0% (0.77)
Triglycerides, change, mg/dL	-0.47 (-1.8 to 0.87)	95% (0.01)

Daily insulin dose: Change in the daily amount of insulin was reported in three studies (41, 92, 95), and carbohydrate counting was not related to a significant change in the insulin dose SMD -0.21units (95%CI -0.75 to 0.32), I^2 = 0% p<0.54.

Bodyweight: Three studies reported the changes in body composition as the difference in body mass index (BMI) (41, 94, 95) and carbohydrate counting didn't produce a significant change in BMI SMD -0.05 Kg/m² (95%CI -0.97 to 0.87), I^2 = 34% p<0.22.

Hypoglycemia: Hypoglycemia reports were very heterogeneous in how reported, and the studies' definitions prevented formal meta-analysis. Some studies described it qualitatively (35, 92), others reported the mean of episodes (36), other the proportion of patients presenting at least one event at the beginning and end (39) and ones as the time below range in continuous glucose monitoring (54). In table 4, we summarize the reports.

Table 4. Hypoglycemia.

Study	Definition	Baseline	End of study
Gilbertson. 2001	Mean episodes per month	Carbohydrate counting 7.3 ± 5.7 Comparator 6.9 ± 6.2	Carbohydrate counting 5.8 ± 5.5 Comparator 6.9 ± 6.8
DAFNE study group. 2002	The proportion of participants experiencing severe hypoglycemia	Carbohydrate counting 22% Comparator 11%	Carbohydrate counting 18% Comparator 15%
Scavone. 2010	End of the study hypoglycemia events	Not reported	Carbohydrate counting 4% Comparator 7%
Enander. 2012	Frequency of hypoglycemia, defined as PG <63 mg/dL	Significantly reduced for the whole study group (p=0.011) when comparing the start and the end of the study. Still, there were no significant differences between the groups.	
Bell. 2016	Time below range (70 to 180 mg/dL) as a proportion	Carbohydrate counting 8.5 ± 1.8% Comparator 7.1 ± 1.4%	Carbohydrate counting 9.4 ± 2.1% Comparator 3.1 1.4 %

Quality of life and satisfaction questionaries: Several questionaries and different ways of reporting quality of life (QoL) and treatment satisfaction were used in six studies (35, 38, 41, 54, 93, 96), so we decided that a qualitative synthesis was more appropriate to report this outcome. One study used the diabetes quality-of-life measure (DQOL) (41), and both

groups experience and improve in their quality of life (QoL) carbohydrate counting (88.7±9.2 vs. 78.0±9.9) and control group (88.7±12.5 vs. 80.4±11.7).

Two studies used the Diabetes-Specific Quality-of-Life Scale (DSQOLS) questionnaire (38, 96). One of them only reported the changes in the questionnaire's different domains with no significant difference among groups (38). Donzeau and collaborators (23) applied the DSQOLS to both the parents and the patients and found an improvement in QoL related to carbohydrate counting.

Two studies used the Audit of diabetes dependent quality of life tool (ADDQoL) to evaluate the QoL and explore the treatment satisfaction with the diabetes treatment satisfaction questionnaire (DTSQ) (35, 93). The DAFNE Study Group (35) reported a change in QoL with a mean difference of 2.2 (95%CI 1.3 to 3.1) and in treatment satisfaction with a mean difference of 8.75 (95%CI 7.02 to 10.48) after six months of using carbohydrate counting. On the other hand, Schmidt and collaborators (93) didn't find any change in the ADDQoL questionary among groups. Still, they did report a significant shift in DTSQ with a within-group difference at the end of the follow-up of 9.1 (6.0–12.2).

Finally, one study didn't use any tool but directly asks all the patients for their overall experience (54). All the patients agreed that their method (carbohydrate counting or comparator) was easy to use and that they could enjoy a wide range of foods. Around half of the participants in both groups felt their blood glucose levels were better managed during the study, 54% vs. 55%, and the remainder felt there had been no change. None of the subjects felt their glycemic control had deteriorated while they were involved in the study.

Publicatrion Bias

Both contour-enhanced funnel plot (101) and Eggers test suggests that publication bias is unlikely (Supplementary Figure 4) (Egger's test, Intercept: - 0.0241, p=0.99).

Sensitivity analysis

The prespecified sensitivity analysis restricting to low bias risk studies was impossible because only one study was judged as having low bias risk (54).

Discussion

This systematic review synthesizes the information available on carbohydrate counting efficacy and safety. When compared to standard diabetes education, advanced carbohydrate counting is more efficient at reducing HbA1c without changing the concentration of blood lipids, patients's body-wight, daily insulin dose, or increasing the risk of hypoglycemia. It also appears that patients trained in carbohydrate counting positively impact their QoL and diabetes treatment satisfaction.

Both graphical and statistical analyses revealed high heterogenicity in the HbA1c change seen with carbohydrate counting. The subgroup analysis suggested that the carbohydrate counting technique and the trial comparator may explain most of this heterogeneity. Using the graphic display of heterogeneity and clustering algorithms, we were able to find three very influential studies that account for most of the heterogeneity and behave like a completely different population. First, Bell and colleagues (54) compare The Food Insulin Demand (FID). This formula transforms the Food Insulin Index (FII), a ranking food algorithm based on the insulin response, into a prandial insulin dose. One study showed that FII predicts insulin requirements more precisely than carbohydrate counting in healthy individuals (102). Besides the innovative technique, the small sample size for this study was very small (n:26). Although we found that it has a low bias risk arising from the randomization process, the HbA1c at the beginning of the trial was substantially different (table 1). The change after 12 weeks was no different between groups ($p = 0.3$). Finally, in (36), Gilbertson and colleagues compared carbohydrate counting to a low glycemic index (GI) diet. GI accounts for the change in glucose instead of insulin after a meal and restricts food such as ordinary bread, potatoes, and rice. This study also had a high risk of bias due to missing data given a 14% dropout rate, 73% of this occurring in the carbohydrate counting group with a per-protocol analysis. As proposed in a previous meta-analysis, one

source of heterogeneity is the comparison group (42). However, we found that the carbohydrate counting technique is another critical source of heterogeneity and it must be taken into account when analyzing carbohydrate counting data.

Carbohydrate counting is essentially a repetitive decision-making technique with the patient or the caregiver trained to pair an insulin dose to a specific meal content. Repetitive decision-making can be improved by practice, it can have a considerable burden, and its precision can change over time. This is why we hypothesize that the studies' follow-up time may influence the effect on HbA1c. Although the metaregression analysis suggests a trend towards lesser HbA1c, this was not statistically significant over time.

Hypoglycemia events are one of the main concerns for people with DM1 and parents of children with DM1 (103), reflecting poorly on QoL (104). Insulin therapy is one of the leading risk factors for severe hypoglycemia (105). Still, less than half of the studies included reported hypoglycemia events as their outcomes, and all of them had a different definition for it (Table 4). The need for standardized reporting has been long recognized, and the American Diabetes Association Workgroup on Hypoglycemia proposed, in 2005, a standardized convention for reporting hypoglycemia frequency and severity among studies (106). Although the available data suggest that carbohydrate counting does not relate to a higher hypoglycemia risk, it is of paramount importance that clinical researchers incorporate the proposed definition into the outcomes of future clinical trials.

Finally, other important safety outcomes such as changes in body weight, blood lipids, and daily insulin dose seem unaffected by carbohydrate counting. But some reports suggest that it allows more food choices for people with DM1 (17), and only a minority of trials included these outcomes.

Conclusions

Evidence suggests that carbohydrate counting is an effective and safe insulin dose calculation technique. However, there is a high degree of uncertainty regarding the effect of carbohydrate counting, and it may not be better than other insulin matching techniques

such as GI and FII. Of the three levels of carbohydrate counting, clinicians should aim for patients to learn advanced carbohydrate counting as it seems to be more efficient in reducing HbA1c.

Future research in carbohydrate counting should include long-term critical clinical outcomes such as the risk of micro and macrovascular complications. Also, researchers should use a standardized hypoglycemia definition that allows a better assessment of safety.

A PHENOMENOLOGICALLY BASED SEMI-PHYSICAL MODEL OF THE ROLE OF THE GASTROINTESTINAL TRACT IN GLUCOSE HOMEOSTASIS

In this chapter, the construction of a series of phenomenological mathematical models of the stomach, intestine, and liver function in glucose homeostasis is presented. Together, these models represent the effects these organs have on glucose metabolism in both fasting and postprandial states. The results are presented as they were published (107, 108).

Estimation of glucose rate of appearance in portal vein circulation using a phenomenological-based model

Introduction

Glucose homeostasis is a process by which glucose levels remain stable overall, even though glucose molecules constantly appear and disappear from the bloodstream as they are absorbed, generated, and consumed in different tissues. The gastrointestinal system plays a significant role in such equilibrium since it processes ingested food, leading to the absorption of new glucose molecules and a concurrent energetic expenditure by the mechanical work of the muscles responsible for the peristalsis. In such a process, the ingestion of carbohydrates, fats, protein, and fiber plays a significant role in the rate of glucose appearance in the portal system circulation. The presence of these nutrients changes both the caloric content and the rheological properties of the food mixture, and therefore has a direct impact on the gastric emptying and the glucose absorption rates. Hence, developing a mathematical model to describe how the gastrointestinal system is involved in the postprandial changes in blood glucose concentration becomes an essential task in the management and treatment of diabetes mellitus.

Most physiological models describing blood glucose changes are based on the minimal model. The minimal model and extensions were developed to analyze a venous stimulus delivered as a bolus or continuous infusion (63, 109, 110). However, the experiments

required to provide data for these models are cumbersome, take time, expose experimental subjects to uncomfortable situations, and are expensive. Part of these difficulties can be solved if a food stimulus is used instead of an injection. In addition, models that adequately represent the gastrointestinal kinetics of glucose can be helpful when designing control algorithms used in everyday situations by patients. Some of the available gastrointestinal glucose absorption models use a compartment structure to describe gastric emptying using mathematical functions and linear kinetics to describe intestinal absorption (72, 73). Others had changed the kinetics of gastric emptying and glucose absorption in the intestine to a non-linear model in which gastric emptying is determined by gastric glucose content (74, 75, 111). Finally, some of the most recent models include the dynamics of the effects of insulin and incretin (112) by using a multi-level model that merges both whole body and cellular levels, as well as exogenous insulin (113).

There is a clear need for a mathematical model that considers the physiological aspects involved in human gastrointestinal digestion and nutrient absorption. This chapter presents an integrated phenomenological-based model for the role of the stomach (114) and small intestine (115) in human glucose homeostasis, constructed by unifying two existing but independent models for the roles of each one of these organs separately. Both models were slightly modified to be coupled, additional physiological aspects were considered in each one, thus obtaining the model of the gastrointestinal tract presented here. However, the model considers the energy expenditure required for peristaltic movements and the effect of water, fats, proteins, and fiber on digestion. Furthermore, a calorie-constant emptying rate is proposed for the stomach, and a new modeling hypothesis is presented for the small intestine portrayed as a series of elastic tanks. The model also includes changes in the volume of the stomach through the digestive process, as well as new kinetic expressions for intestinal absorption and the digestion of nutrients. It is based on first principles such as mass and energy balances. However, it was adjusted using experimental data reported in the literature, rendering a not entirely physiological model while guaranteeing parameter interpretability (116).

Construction of a PBSM for the role of the stomach and the small intestine in human glucose homeostasis

A phenomenological-based semi-physical model (PBSM) is a specific type of gray-box model in which the basic structure arises from first principles, such as mass and energy balances, and at least one parameter is adjusted using experimental data. Because of its nature, this kind of model has a modular structure and parameter interpretability. This section presents a PBSM to represent the role of the gastrointestinal tract in glucose homeostasis in humans. The model was constructed following a ten-step methodology proposed in (117, 118).

Pre-construction of the model

The pre-construction of the model consists of all the steps that precede the establishment of the model structure from mass and energy balances.

Process description and objective of the model.

As ingested food reaches the stomach through the esophagus, the stomach walls start to widen, which leads to the release of gastric juices, mainly composed of water, hydrochloric acid, and pepsin. Mechanical digestion begins in the stomach, and food is propelled against the stomach walls to be mixed. These movements are caused by peristalsis, which implies mechanical work and energy expenditure. Simultaneously, enzymatic digestion of about 5% of the ingested proteins, and 10–30% of the lipids takes place, and lingual enzymes progressively turn these into amino acids, peptides, free fatty acids, and acylglycerols (119).

As the digestive process progresses, more gastric acid is added to the mixture, which, coupled with the appearance of the products of the enzymatic digestion, leads to changes in the viscosity and particle size of the mix, also called chyme. During the lag phase of gastric emptying, chyme is processed without emptying until it reaches the appropriate rheological properties to pass to the small intestine. The duration of this stage depends highly on the caloric content, and the amount of lipids and liquids in the meal (120, 121). Food passes to the small intestine through the pylorus, in a controlled process in which the rate of calories entering the small intestine is kept approximately constant at 1–4 kcal/min (122). As food

begins to leave the stomach, it progressively shrinks and eventually collapses when left empty.

The small intestine is a tubular organ with a length of approximately 6 m, composed of three sub-sections: Duodenum, jejunum, and ileum. Its inner radial layer, the mucosa, is made of epithelial tissue that mediates the transport of substances from the intestinal lumen to the blood and lymph. As chyme enters the small intestine, it is mixed with pancreatic secretions and bile from the liver. Pancreatic secretions contain the enzymes to degrade carbohydrates, proteins and lipids into monomers and oligomers that can be absorbed through the intestinal wall. In contrast, the bile contains the salts needed to emulsify the lipids. Food travels along the intestine due to peristaltic movements, and simultaneously, nutrients are digested and absorbed together with water and electrolytes. Dietary fiber is neither digested nor absorbed in the small intestine, but it affects the properties of the mixture and, therefore, the absorption rate of glucose.

The model objective is to estimate the glucose absorption into the portal system from a mixed meal. In this regard, the question to be solved by the proposed model is: What is the rate of glucose appearance in the bloodstream due to food digestion and absorption in the stomach and small intestine?

Modeling hypothesis and level of detail: The model's level of detail is considered to be macroscopic, since the stomach and the small intestine are independently seen as a whole. A diagram for the modelling hypothesis used for the stomach can be found in (114). Since the food mixing in the stomach implies energy expenditure, it is modeled using an analogy with the energy losses by friction when a heterogeneous mixture flows through a closed assembly of circular pipe. The procedure followed to determine the length of each pipeline section is broadly described in (114). The fluid is considered to be driven through the pipe circuit by a pump, which represents the work done by the stomach wall. Thus, the amount of energy that is effectively transferred to the fluid is taken as 50% of the total power of the pump, assuming that half of the energy provided is used by the cells of the stomach wall for peristalsis. As an additional assumption, the pipe circuit is considered to be full of chyme,

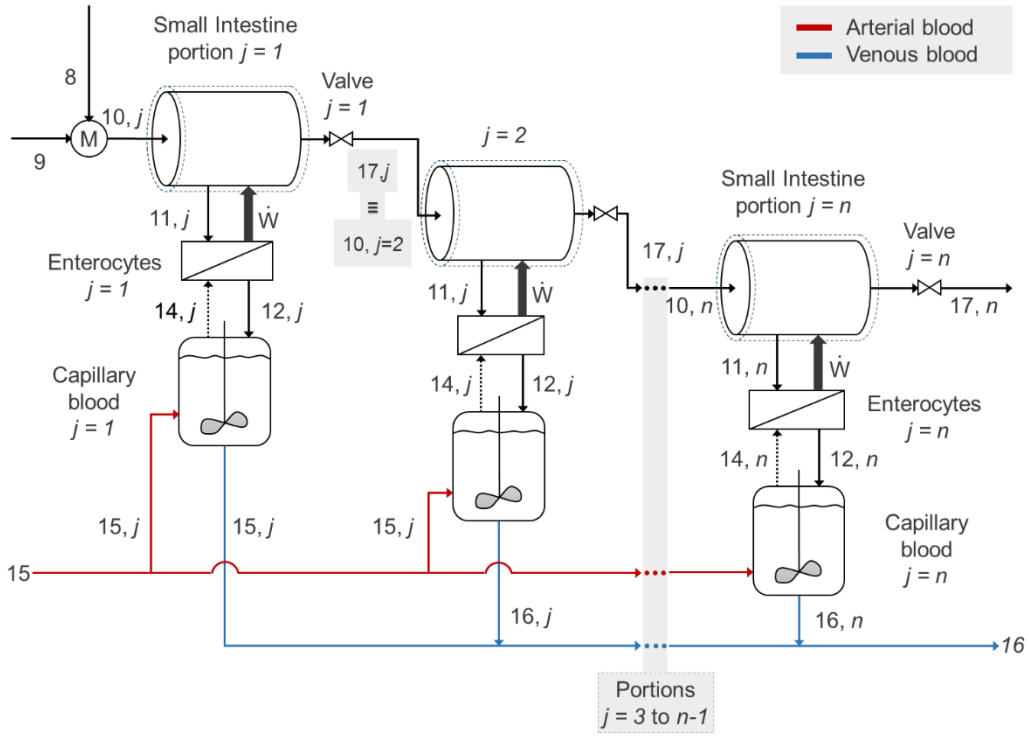
even though the real scenario is that both chyme and air are inside the stomach. To compensate for this assumption, the friction factor is adjusted from data, and the speed of the meal inside the pipe circuit is considered to be constant, although the cross-sectional area is accordingly widened and reduced to represent gastric dilution and emptying, respectively. It is assumed that the tissue forming the stomach wall does not retain or lose mass.

As the process begins, there is an inflow of gastric juice to the stomach. Since the distension of the stomach walls is directly related to the release of gastric juices, this flow is considered proportional to the stomach volume at every moment. The small intestine's neural and hormonal mechanisms provoke feedback control over gastric emptying, and as chyme reaches the duodenum, gastric secretions are inhibited (123, 124). Thus, this model assumes that gastric juices are only added until the beginning of the emptying. The amount of gastric juices produced in response to a given meal is still not entirely known, but for this model, it is taken to be twice the volume of the ingested meal, as reported in (125). Once emptying begins, there is no more dilution with gastric juices, so the process is seen, at both times, as a semi-batch process. The time needed to charge the stomach is considered negligible, as it is too short (15–20 min) compared to the total digestive time (approximately 3 h). Also, since the output of the stomach is too small during the lag phase, it is assumed to be negligible and, therefore, the pylorus is considered an on-off valve. The process is deemed to occur at constant temperature due to the thermal regulation of the human body.

The small intestine is modeled as a set of stirred tanks, each with an elastic, semipermeable wall (126), connected to the adjacent tank through a valve that regulates the outflow according to the pressure drop between the two tanks. A detailed diagram for the modeling hypothesis of the small intestine is shown in Figure 12. Considering the elasticity of the wall of the tanks, a relationship between deformation and the normal force applied against the wall is established. Hence, such force determines the pressure of the fluid contained in the tank. Even though the cross-sectional area would initially be calculated using the diameter of the intestinal lumen, the pressure increase is related to muscle contractions, which, in

contrast, diminishes the cross-sectional area. This effect is considered in the function that describes the opening of the valves. It is assumed that 10% of the absorbed glucose is invested in the peristaltic movements of the small intestine (75).

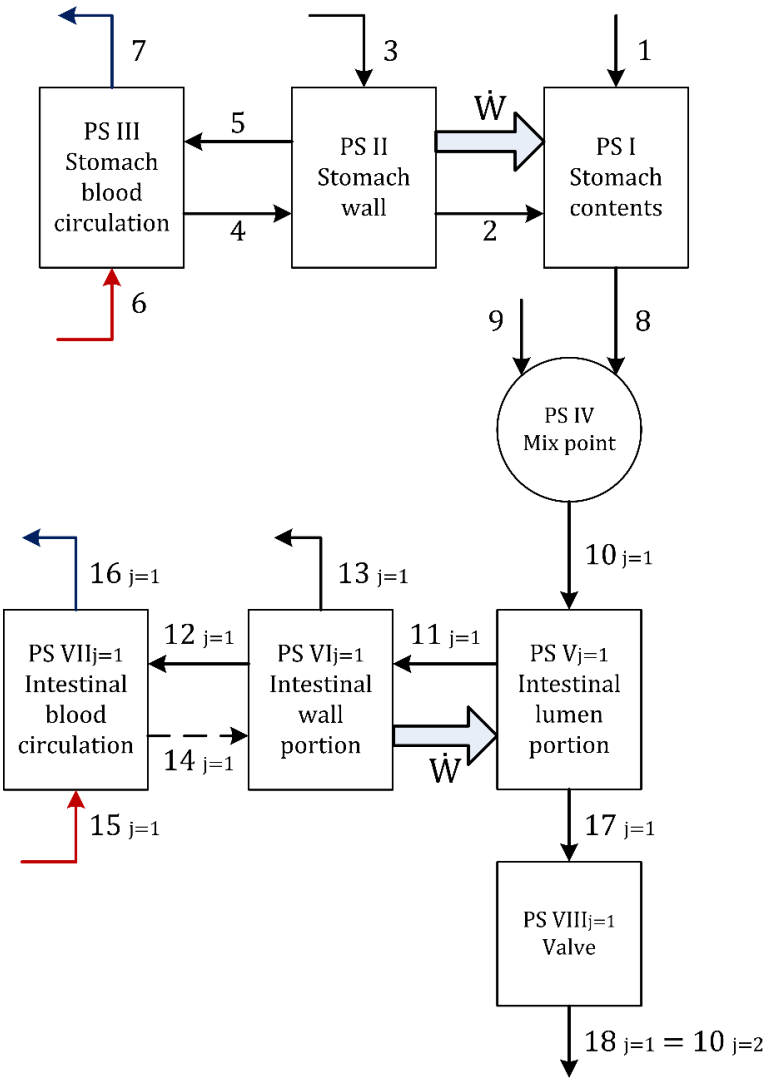
Figure 12. Modeling hypothesis for the small intestine representing a series of stirred tank reactors with elastic walls and connected by valves.



Additional considerations of the modeling hypothesis are as follows: i) all the polysaccharides, proteins and lipids are taken as a standard molecule, formed by 1000 units of glucose, 154 amino acids, and 3 esterified oleic acid units, respectively; ii) Even though water and some drugs can be absorbed in the stomach, nutrient absorption is negligible. Therefore, absorption is considered to happen exclusively in the small intestine.

Process systems definition: The process systems (PS) are defined according to the exchange of the substances of interest. Eight PS are defined for the current process as explained below, and they are all illustrated in Figure 13.

Figure 13. Block diagram of the model.



PSI correspond to the gastric mass contained in the stomach. Ingested food coming from the esophagus is represented by stream 1, gastric juices correspond to stream 2, and the chyme coming out of the stomach is stream 8.

PSII corresponds to the stomach wall. Stream 3 carries the reactants needed to produce gastric juices. Stream 4 represents the reactants required to carry out glucose oxidation in the stomach wall, while the sub-products of that reaction (carbon dioxide and water) are delivered to the venous bloodstream in stream 5. The energy resulting from glucose oxidation is transferred to the **PSI** (thick arrow). The blood that supplies the stomach wall is **PSIII**, which receives arterial blood from the arterial celiac trunk through stream 6 and drains venous blood through stream 7.

PSIV corresponds to a hypothetical mixing point where chyme emptied from the stomach is perfectly mixed with the pancreatic juices and bile entering through stream 9. Stream 10 represents the homogeneous mixture entering the small intestine.

PSV represents the content of an intestinal lumen partition. Stream 11 represents the nutrients absorbed through the intestinal wall, and stream 17 represents the chyme flow passing from the current intestinal partition j to the next one j+1. The system's energy input is given by peristalsis (thick arrow).

PSVI represents a partition of the intestinal wall. A portion of the absorbed glucose is assumed to be used by this system to carry out peristaltic contractions, expressed as an energy expenditure with a thick arrow. Stream 13 represents a portion of the absorbed water, along with fatty acids and glycerol. In contrast, absorbed glucose, amino acids, electrolytes and remaining water pass to capillary blood through stream 12. If there is no absorption, the intestinal wall uses glucose from the capillary blood, represented by stream 14 as a dashed line.

PSVII represents the intestinal blood irrigation. Here, arterial blood represented by stream 15 is mixed with glucose, amino acids, water, and electrolytes absorbed in stream 12. Stream 16 represents the venous capillary blood.

PSVIII corresponds to the valve connecting the tank that represents the j intestinal partition to the j+1 tank. Stream 18 represents the chyme outflow of the first tank, which corresponds to the inflow to the second one.

Model construction

Application of the conservation principle: Mass balances are applied over the process systems to get the basic structure of the PBSM. These balances are presented in molar units for the systems in which chemical reactions take place, and in mass units otherwise. PSII is the exception as balances are presented in mass units, as a consumption expression giving the reaction rate for glucose combustion instead of a kinetic expression. Not all of the mass and energy balances are presented here, only those that provide non redundant information regarding the process. Abbreviations of the substances of interest considered in the different process systems are detailed in Table 5.

Table 5. Substances of interest considered in the gastrointestinal (GI) model.

Abbreviation	Substance
AA	Amino acids
G	Glucose
FA	Fatty acids
W	Water
Gli	Glycerol
CHO	Carbohydrates
Pro	Proteins
Lip	Lipids
CHO*	Shortened carbohydrates
Pro*	Shortened proteins
AP	Pancreatic amylase

PP	Pancreatic protease
LP	Pancreatic lipase
AP – In	Inactive pancreatic amylase
PP – In	Inactive pancreatic protease
LP – In	Inactive pancreatic lipase

PSI—Stomach content: As explained earlier, this process system is always seen as a semi-batch process with no absorption taking place through the stomach walls.

Total mass balance

$$\frac{dN_I}{dt} = \dot{n}_2 - \dot{n}_8 + \sum_s \left(\sigma_{s,I} \cdot r_{s,I}\right) \quad (1)$$

where N_I represents the moles in the process system I, $\dot{n}_2$ indicates the molar flow entering the stomach through the stomach walls, $\dot{n}_8$ is the molar flow leaving the stomach due to gastric emptying. Moreover, $\sigma_{s,I}$ y $r_{s,I}$, indicate the stoichiometric coefficient and the reaction rate for the substance s, respectively. The substances of interest s considered for this PS are CHO, G, Lip, FA, Pro, AA, F, GL, GP, GJ, and W. Finally, Equation 1 represents the variation over time of the moles present in the stomach due to dilution, gastric emptying, and enzymatic reactions.

Component mass balance: The following expression is obtained, after applying a mass balance for every substance s in the stomach.

$$\frac{dN_{s,I}}{dt} = x_{s,2}\,\dot{n}_2 - x_{s,8}\,\dot{n}_8 + \sigma_{s,I} \cdot r_{s,I} \quad (2)$$

where $N_{s,I}$ represents the moles of s present in the PSI, and $x_{s,2}$ is the molar fraction of each substance in the stream containing gastric juices (it has a value of 1 for gastric juices and 0 for all of the other substances). Finally, $x_{s,8}$ is the molar fraction of each substance in the stomach outflow, which under the assumption of perfect mixing, is equal to the molar fraction inside the stomach at every instant.

Total energy balance: An energy balance is developed for a stationary state between the departure and arrival points of the gastric mass through the assumed piping system (114). The continuity of the mass flow in the pipe circuit means that pressures, densities, flow regime factors, velocities, and heights do not change between the two considered points. Therefore, the energy balance can be reduced to the following expression:

$$\dot{W} = \frac{1}{\eta}\left(\dot{m}_I \, h_f\right) \tag{3}$$

where $\dot{W}$ represents the energetic supply from the stomach walls, η is the efficiency to perform the mechanical work, $\dot{m}_I$ is the mass flow inside the stomach, and h_f represents the friction losses that the mass flow experiences while moving from the departure point to the arrival point of the assumed pipe circuit. This term was determined by using a mathematical expression for each of the pipes from the circuit, and it is broadly described in (114).

PSII—Stomach Wall: The process occurring in this PS is seen as continuous. The only reaction considered is glucose combustion, which represents the thermodynamic state change resulting from the glucose oxidation pathway occurring in live tissues.

Total mass balance: The total mass balance for the PSII is developed assuming that the stomach wall neither loses nor gains mass over the process. Enzymatic secretions from the stomach wall are not considered and enzymes are assumed to already be in the stomach from the beginning of the process. Finally, the mass flow of stream 3, which carries the reagents necessary to produce gastric juices, is assumed to be equal to the mass flow of stream 2, which corresponds to gastric juices. The balance is therefore written as:

$$\dot{m}_5 = \dot{m}_4 \tag{4}$$

Component mass balance: Even though this PS receives and processes multiple substances (glucose, oxygen, carbon dioxide, and water), the only mass balance for glucose that brings useful information to the model is the following:

$$\dot{m}_4 = \frac{\hat{r}_{G,II}}{w_{G,4}} \tag{5}$$

where $r_{G,II}$ represents the reaction rate for glucose combustion in mass units, and w_G is the mass fraction of glucose in the stream containing the required reactants.

Total energy balance: The mechanical work performed by the system can be determined using the balance of thermal energy while considering the mechanical effects $\dot{W}$. For this balance, it was assumed, as mentioned above, that the human body has a perfect control system for temperature regulation. Therefore, the total energy change in this system is considered to be 0. As mass flows $\dot{m}_2$ and $\dot{m}_3$ are considered equal in both magnitude and composition, their enthalpies are also equivalent. Finally, the mass flow for the streams $\dot{m}_4$ and $\dot{m}_5$ and is equal, and, after evaluating the enthalpy of each stream, it was concluded that their energetic content is roughly equal. Under these assumptions, the energy balance can be written as:

$$\hat{r}_{G,II} = \frac{1}{\overline{\Delta H}_{r_{G,II}}} \dot{W} \tag{6}$$

where $\dot{W}$ represents the mechanical power of the work done by the stomach wall, and $\overline{\Delta H}_{r_{G,II}}$ represents the specific molar heat of reaction for glucose combustion.

PSIII—Stomach Blood Irrigation: No reactions occur in this PS, therefore, balances are developed in mass units.

Total mass balance

Considering no accumulation within this PS, and bearing in mind that mass flows $\dot{m}_4$ and $\dot{m}_5$ are equal, means that mass flows $\dot{m}_6$ y $\dot{m}_7$ are equal as well. Thus, the total mass balance is given by:

$$\frac{dM_{III}}{dt} = 0 \Rightarrow M_{III} = Constant \tag{7}$$

where M_{III} is the total blood mass in the vessels irrigating the stomach, which, as evinced, has a constant value. This value was estimated based on the literature (127).

Component mass balance: As with PSII, the substance of greatest interest on this PS is also glucose. For the development of said balance, perfect mixing is assumed, which means that $M_{G_{III}} = M_{III}\frac{dw_{G,7}}{dt}$, and the resulting balance:

$$\frac{dw_{G,7}}{dt} = \frac{1}{M_{III}}\left(w_{G,6}\,\dot{m}_6 - w_{G,4}\,\dot{m}_4 - w_{G,7}\,\dot{m}_7\right) \tag{8}$$

where $\dot{m}_k$ represents the mass flow of the stream k and $w_{G,k}$ represents the mass fraction of glucose in the same stream.

PSIV—Mixing point: The mixing of ingested food with bile and pancreatic juices in PSIV is analyzed as a continuous process. Since no chemical reactions are considered here, the mass balances can be expressed in mass units.

Total mass balance: The total mass balance over PSIV gives information on the mass flow resulting from mixing the ingested food emptied from the stomach $\dot{m}_8$ with pancreatic juices and bile $\dot{m}_9$, a process taking place in the first portion of the duodenum. Since no mass is accumulated in the hypothetical mixing volume within the duodenum, then $\frac{dM_{IV}}{dt} = 0$, The resulting expression, solving for the mixture mass flow entering the duodenum $\dot{m}_{10,1}$ is the following algebraic equation:

$$\dot{m}_{10,1} = \dot{m}_8 + \dot{m}_9 \tag{9}$$

Component mass balance: Given that pancreatic juices and bile dilute the ingested food and add new substances to it, it is important to determine the composition of the mass flow starting to pass into the small intestine to calculate the digestion and absorption rates in the following PSs. The mass fraction of each component $w_{s_{10,1}}$ exiting the PSIV is determined by:

$$w_{s_{10,1}} = \frac{w_{s_8}\dot{m}_8 + w_{s_9}\dot{m}_9}{\dot{m}_{10,1}} \tag{10}$$

where w_{s_8} is the mass fraction of components of the ingested food and w_{s_9} is the pancreatic juices and bile emptied into the duodenum.

Balances for the PSV—Intestinal lumen portion: Gastric mass flow is relatively slow compared to the length of the small intestine. Therefore, each portion j is assumed to be short enough to consider uniform properties throughout the contained gastric mass. Building the model makes it possible to account for the axial change of properties such as concentration, density, and pressure over time, all influenced by digestion, absorption, and mass flow velocity rates.

Thus, the analysis of the portions or instances j of this PS is performed by considering them as individual continuously-stirred tank reactors with two distinctive characteristics: i) the walls of the tanks are elastic, and thus their volumes are variable, and ii) there can be either positive or negative accumulation of gastric mass.

Total mass balance: The balance is expressed in terms of the change of the total mass contained in an elastic tank $\mathrm{M_{V,j}}$ as:

$$\frac{dM_{V,j}}{dt} = \dot{m}_{10,j} - \dot{m}_{11,j} - \dot{m}_{17,j} \qquad (11)$$

where $\dot{\mathrm{m}}_{10,j}$ is the mass flow of gastric mass entering a tank *j*, $\dot{\mathrm{m}}_{11,j}$, j the rate of mass absorption in each portion j towards the portal system, and $\dot{\mathrm{m}}_{17,j}$, j the mass flow of chyme moving on to the next portion of the intestine. In turn, a total volume balance is applied to each tank, assuming that only radial deformation is significant for the intestinal wall. Consequently, the length of each cylindrical tank remains constant. While this may not be true locally for a single portion, contraction and relaxation of muscles along the small intestine cause simultaneous shortening and elongation, altogether assumed to cancel each other out (128). Applying the chain rule over the total mass balance gives:

$$\frac{dM_{V,j}}{dt} = \frac{d\left(\rho_{V,j}V_{V,j}\right)}{dt} = V_{V,j}\frac{d\rho_{V,j}}{dt} + \rho_{V,j}\frac{dV_{V,j}}{dt}$$

where ρV,j is the density of chyme and VV,j is the volume of a tank. Subsequently, after replacing in Equation 11, the change in the volume of a tank is expressed as follows:

$$\frac{dV_{V,j}}{dt} = \frac{1}{\rho_{V,j}}\left(\dot{m}_{10,j} - \dot{m}_{11,j} - \dot{m}_{17,j} - V_{V,j}\rho_{V,j}\right) \qquad (12)$$

which successively gives place to an expression for the change of the radius of a transverse section of PSV: rj, shown in Equation 13. Assuming each portion of PSV as a cylinder, the differential change can be written as:

$$\frac{dV_{V,j}}{dt} = \frac{d\left(\pi r_j^2 L_V\right)}{dt} = 2\pi L_{Vrj}\frac{dr_j}{dt}$$

where LV is the length of an elastic tank. By replacing $d\left(\pi r_j^2 L_V\right)$ in the total volume balance, the resulting expression for a change in the radius of a cylindrical intestinal portion is

$$\frac{dr_j}{dt} = \frac{1}{2\pi L_{Vrj}\rho_{V,j}}\left(\dot{m}_{10,j} - \dot{m}_{11,j} - \dot{m}_{17,j} - V_{V,j}\rho_{V,j}\right) \qquad (13)$$

This expression, in particular, allows flow and hydrodynamic pressure calculations, further detailed for PSV and PSVIII in the section where constitutive and assessment equations are presented.

Lastly, since chyme composition changes during gastric emptying digestion and absorption processes, the density of the multi-component, homogeneous chyme is determined by clearing:

$$\frac{d\rho_{V,j}}{dt} = \frac{1}{V_{V,j}}\left(\frac{dM_{V,j}}{dt} - \rho_{V,j}\frac{dV_{V,j}}{dt}\right)$$

from the previously defined chain rule, which after being replaced in Equation 11 gives:

$$\frac{d\rho_{V,j}}{dt} = \frac{1}{V_{V,j}}\left(\dot{m}_{10,j} - \dot{m}_{11,j} - \dot{m}_{17,j} - \rho_{V,j}V_{V,j}\right) \qquad (14)$$

Note that on the right-side of Equations 12 and 14, the terms $\frac{dV_{V,j}}{dt}$ and $\frac{d\rho_{V,j}}{dt}$ were re-written as $V_{V,j}$ and $\rho_{V,j}$ respectively, as they are parameters for the model.

Component mass balance: In this PS, the component mass balances, and their derived molar concentration and mass fraction balances are described for the substances s: AA, G, FA, W, Gly, CHO, Pro, Lip, CHO*, Pro*, PA, PP, PL, PA-In, PP-In, PL-In. Firstly, a general s component mass balance over PSV, including the mass flow of input and output streams, chemical reactions, and absorption terms, is expressed as

$$\frac{dM_{s_{V,j}}}{dt} = w_{s_{10,j}}\dot{m}_{10,j} - \dot{n}_{s_{11,j}}\mathfrak{M}_s - w_{s_{17j}}\dot{m}_{17,j} + V_{v,j}\mathfrak{M}_s\sum_i r_{s_{I,j}} \qquad (15)$$

where $M_{s_{VI,j}}$, is the mass of the component s in a portion j of the PSV. $w_{s_{10,j}}$ the mass fraction of s in the stream 10 entering the j–th tank, $\mathfrak{M}_s$ is the is the molar mass of s, $w_{s_{17j}}$ is the mass fraction of s in the stream 17 exiting the j–th tank, and is the molar rate of reaction of the component s in the reaction i = 1…6, which refer to the digestion and enzyme deactivation reactions, taking place in the chyme within the tank j. Chemical reaction and absorption rate terms for each component are further explained in the section where constitutive and assessment equations are presented.

The general balance of mass components is then expressed in terms of molar concentration $C_{sv,j}$ and mass fraction $w_{sv,j}$to allow the calculation of mass flows, reaction, and absorption rates. To express it in terms of the molar concentration, $M_{s_{V,j}}$ is replaced by $\mathfrak{M}_s C_{sv,j} V_{V,j}$ in the differential. By applying the chain rule and solving the differential for the molar concentration of *s* and writing $\frac{dV_{V,j}}{dt}$ as $\dot{V}_{V,j}$

$$\frac{dC_{svj}}{dt} = \frac{1}{\mathfrak{M}_s V_{v,j}} \left(\frac{dC_{svj}}{dt} - \mathfrak{M}_s C_{sv,j} \dot{V}_{V,j}\right)$$

Finally, by replacing Equation 15 in the latter, the general expression of the change of molar concentration of s is obtained as:

$$\frac{dC_{svj}}{dt} = \frac{1}{\mathfrak{M}_s V_{v,j}} \text{ x } (w_{s_{10,j}} \dot{m}_{10,j} - \dot{n}_{s_{11,j}} \mathfrak{M}_s - w_{s_{17j}} \dot{m}_{17,j} + V_{v,j} \mathfrak{M}_s \textstyle\sum_i r_{s_{I,j}} - \mathfrak{M}_s C_{sv,j} \dot{V}_{V,j}) \quad (16)$$

Similarly, to express the general balance of mass components in terms of mass fraction, it suffices to define $M_{sv,j} = M_{v,j} W_{SV,j}$ and apply the chain rule, the differential is solved for the mass fraction of *s*. Replacing $\frac{dM_{v,j}}{dt} = \dot{M}_{v,j}$ yields:

$$\frac{dw_{SV,j}}{dt} = \frac{1}{M_{V,j}} \left(\frac{dw_{sv,j}}{dt} - w_{SV,j} \dot{M}_{v,j}\right)$$

Lastly, if Equation 15 is replaced for the $\frac{dM_{s_{V,j}}}{dt}$ term in the last expression, the change in the mass fraction is defined as:

$$\frac{dw_{svj}}{dt} = \frac{1}{M_{V,j}} \text{ x } (w_{s_{10,j}} \dot{m}_{10,j} - \dot{n}_{s_{11,j}} \mathfrak{M}_s - w_{s_{17j}} \dot{m}_{17,j} + V_{v,j} \mathfrak{M}_s \textstyle\sum_i r_{s_{I,j}} - w_{SV,j} \dot{M}_{v,j}) \quad (17)$$

PSVI—Intestinal wall portion: This PS is analyzed as a continuous filtration process, in which several substances of the chyme that flow along the intestinal lumen (PSV,j) are selectively transferred through a semipermeable membrane to cells of the intestinal wall and to the interstitium.

Total mass balance: Since the cells that are part of the intestinal wall consume nutrients to carry out their metabolic functions, mainly during the postprandial state (129), , two

additional terms were included in the input and output mass flows of this PS in the following total mass balance.

$$\frac{dM_{VI,j}}{dt} = \dot{m}_{11,j} + \dot{m}_{14,j} - \dot{m}_{12,j} - \dot{m}_{13,j} - r_{s_{VI,j}}$$

where $\dot{m}_{12,j}$ is the mass flow of components that pass into the bloodstream (assumed to be glucose, amino acids, and water), $\dot{m}_{13,j}$ is the mass flow of components drained by the lymph (assumed to be glycerol and fatty acids), $\dot{m}_{14,j}$ the mass flow of glucose for cell uptake, and the rate of consumption of s by each portion j of the small intestine wall. Even though the energy expenditure of the small intestine implies the consumption of different nutrients, the primary purpose of the model is to determine the rate of glucose absorption. Therefore, only glucose consumption is considered in this PS with no mass accumulation occurring within this PS, the equation can be rewritten as presented in Equation 18, which is further solved for $\dot{m}_{12,j}$, the stream that carries the substances (AA, G and W) absorbed into the bloodstream.

$$\dot{m}_{12,j} = \dot{m}_{11,j} + \dot{m}_{14,j} - \dot{m}_{13,j} - r_{s_{VI,j}} \qquad (18)$$

Component mass balance: Similarly, the component mass balance is now performed for the absorbed components (glucose, amino acids, fatty acids, water, and glycerol), considering there is no mass accumulation,

$$\dot{m}_{s12j} = \dot{n}_{s_{11,j}} \mathfrak{M}_s + w_{s_{14,j}} \dot{m}_{14,j} - w_{s_{13,j}} \dot{m}_{13,j} - r_{s_{VI,j}} \qquad (19)$$

where $\dot{m}_{s12j} = w_{s_{12,j}} \dot{m}_{12,j}$, j is the mass flow of the component s in the stream k = 12, and $w_{s_{k,j}}$ are the mass fractions of s in the streams k = 13, 14. It is important to note that for s ≠ G, the mass fractions $w_{s_{14,j}} = 0$ and $w_{G_{14,j}} = 1$ as cell uptake of nutrients in this PS was only considered for glucose.

PSVII—Intestinal blood circulation: In this PS, a continuous mixing process in the blood that supplies the intestine is considered.

Total mass balance: No mass is accumulated inside the mixing tanks and no chemical reactions are taken into consideration, therefore $\frac{dM_{VII,j}}{dt} = 0$. Since mass flows $\dot{m}_{12,j}$, $\dot{m}_{14,j}$ y $\dot{m}_{15,j}$ are known, the total mass balance in PSVII is expressed in terms of the mass flow of blood draining the small intestine.

$$\dot{m}_{16,j} = \dot{m}_{12,j} + \dot{m}_{15,j} - \dot{m}_{14,j} \tag{20}$$

Moreover, the sum of all the $\dot{m}_{16,j}$ mass flows along the small intestine represents the mass flow of the superior mesenteric vein $\dot{m}_{16}$, which in turn transports glucose into the portal vein.

$$\dot{m}_{16} = \sum_{j} \dot{m}_{16,j} \tag{21}$$

Component mass balance: The component mass balance for glucose is of particular interest as it is directly linked to answering the question posed for the model. Given that no mass is accumulated, $\frac{dM_{G_{VII,j}}}{dt} = 0$, the balance gives rise to an algebraic equation. The dynamic change of glucose mass in the stream 16, j is then defined as:

$$w_{G_{16,j}}\dot{m}_{16,j} = \dot{m}_{16,j} = w_{G_{12,j}}\dot{m}_{12,j} + w_{G_{15,j}}\dot{m}_{15,j} - w_{G_{14,j}}\dot{m}_{14,j} \tag{22}$$

As mentioned above, $w_{G_{14,j}} = 1$ because only glucose is being considered for cell nutrient uptake in the mathematical model. Also, the product $w_{G_{16,j}}\dot{m}_{16,j}$ is the mass flow of glucose in the stream 16, which can be simply written as $\dot{m}_{G16,j}$ and the mass fraction$w_{G_{16,j}}$ derives from the systemic glucose concentration, as explained in the section where constitutive and assessment equations are presented.

Before determining glucose concentration in the stream 16, the individual mass flows of glucose from each portion j must be added up:

$$\dot{m}_{G16} = \sum_j \dot{m}_{G16j} \tag{23}$$

Finally, the mass fraction of glucose in stream 16 is expressed as

$$w_{G16} = \frac{\dot{m}_{G16}}{\dot{m}_{16}} \tag{24}$$

Given the widespread acceptance of mg/dL concentration units to measure glucose levels in the blood, the last expression is posed as

$$C_{G16} = \frac{1}{10}\rho 16 w_{G16} = mg/dL \tag{25}$$

Moreover, the current model can include expressions for other components such as amino acids, glycerol, and water absorbed in the bloodstream. This task would imply the definition

of more specific rates of amino acid absorption, and a particular partition coefficient between blood and lymph for water, glycerol, and low-weight fatty acids.

PSVIII—Valve: The muscles in the intestinal wall regulate mass flow between portions of the small intestine. One way to account for the regulation of chyme flow, as well as other factors that slow down the flow of chyme, such as friction, is to model the flow through a static valve as a continuous process.

Total mass balance: Since this PS represents a flow area, there is no mass accumulation, rendering $\frac{\mathrm{dM_{VIII,j}}}{\mathrm{dt}} = 0$, thus $\dot{m}_{17,j} = \dot{m}_{18,j}$ However, stream $\dot{m}_{18,j}$ is only considered for the last portion j, then, the stream exiting the valve of slice j immediately enters the next portion of small intestine j + 1. Thus $\dot{m}_{18,j} = \dot{m}_{10,j}$ and

$$\dot{m}_{17,j} = \dot{m}_{10,j} + 1 \tag{26}$$

Component mass balance: Similarly, compositions remain unchanged while the stream flows across the flow area, rendering:

$$w_{s_{17,j}} = w_{s_{10,j+1}} \tag{27}$$

Total energy balance. Repeated contraction and relaxation of the smooth muscle tissue in the small intestine propagates caudally as a peristaltic wave, which facilitates chyme digestion and absorption by generating flow patterns and exerting stress that aids breakdown, mixing, and transport (128). This movement favors churning and mixing food particles in chyme rather than its transport to maximize nutrient absorption throughout the segments of the small intestine. For this reason, the chyme flow velocity is low, and the flow regime is primarily laminar, although contractions lead to fluid circulation and the production of vortices.

For this PS, peristaltic muscle contractions are assumed to produce both a pressure difference and a variation in flow area, resembling a fluid flow through a static valve. Thus, an energy balance would provide insights into the calculation of the chyme flow from one portion of the small intestine to another, due to peristalsis. For this purpose, thermal effects were neglected, given that body temperature is regulated within a narrow interval.

However, a mechanical energy balance provides information regarding friction effects and hydrodynamic pressure on chyme flow. Since no mass is accumulated in the valve, a mechanical energy balance for steady flow using Bernoulli's principle is applied, setting departure and arrival points right before and after the valve, respectively. The area of valve connections is equal for both ends, therefore, $\mathrm{v}_{17,\mathrm{j}} = \mathrm{v}_{10,\mathrm{j}+1}$. Assuming a uniform and steady flow, negligible height changes, and replacing the definition of flow coefficient further explained in (130), the mechanical energy balance (MEB) renders:

$$\dot{m}_{10,j+1} = c_{v_j}\, \rho_{V,j} \sqrt{P_{V,j} - P_{V,j+1}} \qquad (28)$$

Basic structure of the model: The basic structure of the model is obtained by choosing those equations that bring up the most relevant, non-redundant information. For the current model, these are: (1), (2) and (3), taking into account that Equation (2) generates 11 equations, one for every substance s. Also, Equations (5), (6), (7), (8), (9) and (10), where the latter generates 17 equations, one for every component s entering the first portion j of the intestinal lumen. Equations (11), (12), (13), (14), (15), (16) and (17), where the last three equations generate 20 equations each, one for every component s considered for Eq (10), but adding inactive components PA-In, PP-In, PL-In. In addition, Equation (19), which generates 5 equations, one for each component *s* absorbed into the portal system. Likewise, Equations (20), (21), (22), (23), (24) and (25), all of them representing the appearance of glucose in the portal system, and Equations (26), (27) and (28), where the second expression generates 20 more, one for every component s that is not digested or absorbed, and passes to the colon. The whole set of equations are presented in the Supplementary table 3.

Determining variables, structural parameters, and structural constants: In this step, the model's variables, structural parameters, and structural constants are established and described in Table 6**.**

Table 6. Variables, structural parameters, and structural constants of the model.

PS	Variables	Structural parameters	Constants
I	N_I, $N_{s,I}$, $\dot{W}$	$\dot{m}_2$, $\dot{m}_8$, $x_{s,8}$, $r_{s,I}$, $\dot{m}_1$, h_F	$x_{S,2}$, $\sigma_{s,I}$, η
II	$\dot{m}_4$, $\hat{r}_{G,II}$	-	$w_{G,4}$, $\Delta\bar{H}r_{G,II}$
III	$w_{G,7}$	$\dot{m}_6$, $\dot{m}_7$, $w_{G,6}$	M_{III}, $w_{G,4}$
IV	$\dot{m}_{10,1}$, $w_{s_{10,1}}$	$\dot{m}_{10,j}$, $w_{s_{10,j}}$	$\mathfrak{M}_s$
V	$M_{V,j}$, $V_{V,j}$, r_j, $\rho_{V,j}$, $M_{s_{V,j}}$, $C_{s_{V,j}}$, $w_{s_{V,j}}$	$\dot{m}_{11,j}$, L_V, $\dot{n}_{s_{11,j}}$, $r_{s_{i,j}}$, $w_{s_{14,j}}$	-
VI	$M_{VI,j}$, $M_{s_{VI,j}}$	$\dot{m}_{12,j}$, $\dot{m}_{13,j}$, $r_{s_{VI,j}}$, $w_{s_{12,j}}$, $w_{s_{13,j}}$	-
VII	$\dot{m}_{16,j}$, $\dot{m}_{16}$, $\dot{m}_{G_{16,j}}$, $\dot{m}_{G_{16}}$, $w_{G_{16}}$	$\dot{m}_{14,j}$, $\dot{m}_{15}$, $w_{s_{14,j}}$, $w_{G_{15,j}}$	-
VIII	$\dot{m}_{17,j}$, $w_{s_{17,j}}$, $\dot{m}_{10,j+1}$	$c_{v_j} w_{s_{10,j+1}} P_{V,j} P_{V,j+1}$	-

s substance: *CHO*, *G*, *Lip*, *FA*, *Pro*, *AA*, *Fib*, *GL*, *GP*, *GJ*, *W*, *B*, O_2, CO_2. *k* current: 1...17.

Constitutive and assessment equations for structural and functional parameters: Generally, constitutive and assessment equations are algebraic equations of diverse origins, formulated and added to the conservation balances to include specific knowledge such as mass transfer and reaction rates, leading to a model with a deeper level of detail (60). Every structural parameter may be defined with a constitutive or assessment equation. In turn, each parameter derived from these expressions is called a functional parameter and may be further defined by another constitutive equation, by a constant value from data from literature, or may be identified from real data.

The parametric identification procedure comprised testing parameter values to reduce model prediction error in contrast to experimental data. The resulting extended structure of the model arises from the underlying phenomena, available knowledge of the process, and the skill of the modeler. The selection of the most relevant constitutive and assessment equations is discussed below. Constitutive and assessment equations for defining the model's structural parameters are reported in the Supplementary Table 4. Constitutive equations for defining functional parameters are provided in Supplementary Table 5, while

Supplementary Table 6 introduces assessment equations and the model's constants. Notations A and I used in the tables refer to if the parameters were assumed and their value was fixed under different conditions for the entire simulation, or identified, respectively. From the model (M) means that the parameter is calculated by an equation that represents the dynamics of the system itself.

As mentioned in the modeling hypothesis, a set of stirred tanks with elastic walls was used as an analogy to represent the movement of chyme through the intestinal lumen. A link between the deformation of the small intestine wall and the hydrodynamic pressure (PV,j) of the fluid flowing from tank to tank can be established by relating a constitutive model of the strain energy density with the equilibrium of forces along the wall. The small intestine wall is well characterized by the Fung hyperelastic model (131, 132). The hydrodynamic pressure can be calculated, in cylindrical coordinates, as detailed in (133).

As previously described, complete digestion of macronutrients and inactivation of digestive enzymes occur in PSV, setting the pace at which several bio-available nutrients are released. For reasons of simplification, a general expression for reaction rates is further detailed to determine the concentration of substances of interest for glucose homeostasis, such as glucose and gluconeogenic precursors (e.g., glycerol, alanine, glutamine). Reaction rates are calculated at a temperature of T = 310.

Reaction i = 1: Carbohydrate digestion. In this model, carbohydrates (CHO) are assumed to be simple amylose chains with an average molar mass equal to 180000kg/kmol. The hydrolysis reaction releases a glucose molecule from one end of the amylose chain per water molecule, shortening its length progressively (producing CHO*). For reasons of simplification, the molar mass of the amylose chain is considered constant. In turn, a mass balance calculates the remaining equivalent moles of a hypothetical complete amylose chain. The expression for the reaction rate is adapted to take the form of first-order reaction kinetics, depending solely on the concentration of the pancreatic amylase enzyme. The underlying assumption is that enzyme concentration is limiting and much lower than that of the substrates, so the reaction order is zero for CHO concentration.

$$CHO + H2O \rightarrow CHO* + G \quad (19)$$

Reaction i = 2: Pancreatic amylase inactivation. Digestive enzymes in chyme are gradually inactivated along the small intestine predominantly due to pH changes, interactions with many substances in the chyme, and the presence of proteases, which partly degrade peptide bonds and alter structural integrity, comprising catalytic activity. The higher resistance of the pancreatic amylase against proteases makes it more stable than lipases and proteases (134). A simplified description of the inactivation of pancreatic amylase (PA) is presented in the equation.

$$AP \rightarrow inactive\ AP \quad (30)$$

Reaction i = 3: Protein digestion. Proteins are digested through a hydrolysis reaction, which is simplified by assuming that reaction with one molecule of water releases one average amino acids and produces a shortened protein (Pro*), described in Equation 31. All the ingested proteins are assumed to be myosin, the most abundant of proteins found in meat (135) with an average molar mass equal to 493000kg/kmol (136). Since the protein chain is continuously shortened, a mass balance is proposed to obtain a rate expression in terms of an equivalent, intact myosin molecule.

$$Pro + H2O \rightarrow Pro* + AA \quad (31)$$

Reaction i = 4: Protease inactivation. Many proteases released along the gastrointestinal tract digest proteins in the small intestine. Trypsin was set as the equivalent average pancreatic protease for this model. Rate expression for the inactivation reaction depends solely on protease concentration.

$$PP \rightarrow inactive\ PP \quad (32)$$

Reaction i = 5: Lipid digestion. For this reaction, all lipids are considered to be triglycerides, more specifically triolein, which produces three units of oleic acid (FA, for fatty acid) and one of glycerol (Gly) upon its hydrolysis, catalyzed by pancreatic lipases. This reaction is shown in Equation 33, and the reaction rate is described with a first-order expression,

depending on the concentration of pancreatic lipase, assuming enzyme concentration to be significantly much lower than that of the substrates.

$$Lip \ + \ 3\,H_2O \ \rightarrow \ 3\,FA \ + \ Gly \tag{33}$$

Reaction i = 6: Pancreatic lipase inactivation. Inactivation of pancreatic lipase, presented in Equation 34, is caused both by proteases and the interaction of these enzymes with other substances in the chyme. For this reason, the expression for the reaction rate depends on the concentration of both PL and PP, as shown in Equation 34.

$$PL \ \rightarrow \ PL - In \tag{34}$$

Regarding the absorption of nutrients into the bloodstream, glucose, amino acids, fatty acids, and water all pass through the wall of the small intestine in different ways. Luminal glucose is mainly absorbed across the brush membrane border through the Na+-glucose cotransporter SGLT1 and the GLUT2 carrier protein. The latter mechanism of glucose absorption is known as facilitated diffusive transport and is increasingly prevalent at higher glucose concentrations. The hydrophobicity of the membranes prevents strict passive or diffusive transport of glucose and tight junctions between enterocytes, leaving molecules no space to passively diffuse into the interstitium (137). While the exclusive protein-mediated and Na+-codependent glucose transport could be deemed as a saturable transport mechanism, the increasing presence of GLUT2 proteins in the brush border membrane with higher glucose concentrations bypasses saturation. For instance, this could be mathematically represented by adding a passive transport term to a Michaelis-Menten absorption kinetics expression (138, 139). Prior data from glucose absorption experiments in the human jejunum has been successfully fitted to glucose uptake expressions with both active and passive components (140). Accordingly, this type of glucose uptake expression was included as a constitutive equation of this model, as shown in Equation 22 in the Supplementary Table 4. It is now known that the passive absorption term in this constitutive equation accounts for the effect of increasing GLUT2 proteins at the brush membrane border with higher glucose levels. Thus, this term refers to a facilitated diffusive transport

mechanism rather than a passive one. Since glucose absorption rates differ along the small intestine, parameters were identified separately for the duodenum, jejunum, and ileum.

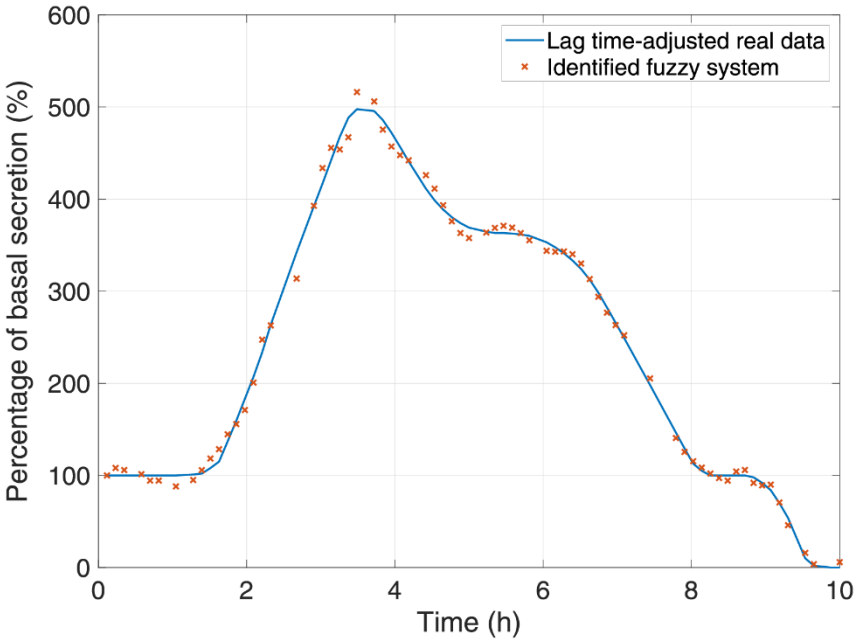
Although many amino acid transporters are present in the brush border membrane, the real scenario involves the absorption of di- and tri-peptides into enterocytes through oligopeptide transporters, succeeded by their break down into amino acids by peptidases (141). Since hydrolysis of oligopeptides is very rapid and geared toward a more straightforward mathematical expression, only the absorption of an average, equivalent amino acid is being considered. Moreover, bearing in mind that the absorption of amino acids and peptides mainly occurs via an active, saturable transport mechanism, it would be sufficient for the goal of the model to use a simple Michaelis-Menten kinetic expression, to which L-alanine and glycine absorption data in human jejunum has been successfully fitted (141), as shown in Supplementary Table 4. Once again, the values of functional parameters arising from the absorption expression were independently identified for the duodenum, jejunum, and ileum.

Lipids and bile acids form mixed micelles within the intestinal lumen, facilitating transport across the unstirred diffusion barrier at the lumen-membrane interface, ensuring a sufficient concentration gradient for lipid uptake. Unlike absorption of more polar substances, transport of lipids across the brush border membrane does not exclusively rely on transporter proteins. Transport of short-chain fatty acids across the membrane may occur via simple passive diffusion, while the uptake of medium-chain, large-chain fatty acids, and other lipids takes place by active and facilitated transport mechanisms [46]. Despite the diversity of transfer mechanisms, types and sizes of lipids, the model is intended to produce a lower level of detail regarding lipid absorption. Thus, a more straightforward mass transfer expression following Fick's first law of diffusion is proposed for oleic acid, the only fatty acid assumed to make part of the ingested meal (esterified in the form of triolein). The expression, further detailed in Supplementary Table 4, includes an assumed equilibrium concentration to set the concentration gradient that drives the uptake of fatty acids, considering that the chemical complexity within the cell renders such value indeterminable over time.

Water is absorbed throughout the three structural parts of the small intestine. This physiological process is heavily influenced by the osmolality of chyme (142), blood volume, and gastric emptying rate and therefore depends on a wide range of mechanical and neurohormonal stimuli occurring before, during and after the ingestion of a meal (124). The osmolality of chyme is not considered as a variable to reduce the complexity of the constitutive equation that integrates water absorption with the model. The simulated scenario implies that its value is such that it produces a positive net water absorption from the lumen into the systemic circulation. Thus, this model does not account for the effect of altered intestinal motility due to the composition of the ingested meal, drinks, or drugs, nor any neuromuscular disorders. On average, water absorption in the small intestine of healthy humans ranges from 9 to 15 mL · cm−1 · h−1, following ingestion of various carbohydrate solutions (143). From these data, water absorption percentages in the small intestine (144), and assuming that: i) the flow of chyme and other secretions in the small intestine ranges between 0 and 20 ·−1 and ii) the duodenal mass flow is a significant mechanical stimulus that is linearly related to the water absorption rate, the water absorption coefficients of the duodenum, jejunum, and ileum were identified and are presented in Supplementary Table 4.

The values of the total gastric mass emptied from the stomach and the mass fraction of each component are obtained by solving equations of the PSI−IV, described earlier and further detailed in (114). This gastric mass flow is mixed in the duodenum with bile and pancreatic juices arriving through the hepatopancreatic duct to aid the digestion of partially digested chyme. Secretions of pancreatic enzymes and bile are estimated from a Takagi-Sugeno fuzzy model, identified based on data reported in [50], and obtained using the methodology described by (145). This fuzzy model is set with thirteen rules and determines the percentage of secretions over the postprandial state with an interdigestive or basal secretion, which serves as the reference. For the meal previously detailed and its corresponding gastric emptying lag time, the percentages of basal secretion calculated based on the fuzzy model are shown in Figure 14.

Figure 14. Percentage of basal secretion calculated by the identified fuzzy system.



Pancreatic and bile secretions are influenced by the concentration of nutrients in the duodenum and several neurohormonal signals stimulated by the sight and taste of food, the distension of both stomach and duodenum, and other factors such as stress or depression. Generally, these produce a pronounced peak in the rate of hepatopancreatic secretions, followed by a sustained, moderate secretion rate before transitioning into the interdigestive period, where secretions are minimum, or basal (146, 147). In the fuzzy model, both the appearance of the peak over the postprandial period and the subsequent plateau can be slightly anticipated or delayed according to the lag time of gastric emptying.

The resulting percentage of basal secretion is then transformed into a mass flow by using a conversion factor, considering that, on average: i) interdigestive and maximum postprandial pancreatic juice flows are 0.25 and 4 mL · min^{-1}, respectively [52], and ii) interdigestive and maximum postprandial flows of bile are 0.75 and 2.5 mL · min−1, sequentially (148, 149).

On the other hand, the concentration of pancreatic enzymes in the mixed bile and pancreatic juice is yet to be determined. The products of lipid digestion have been shown to be major stimulants of pancreatic enzyme secretions (150). Thus, a relationship between the concentration of fatty acids and enzyme activity of pancreatic amylase was established.

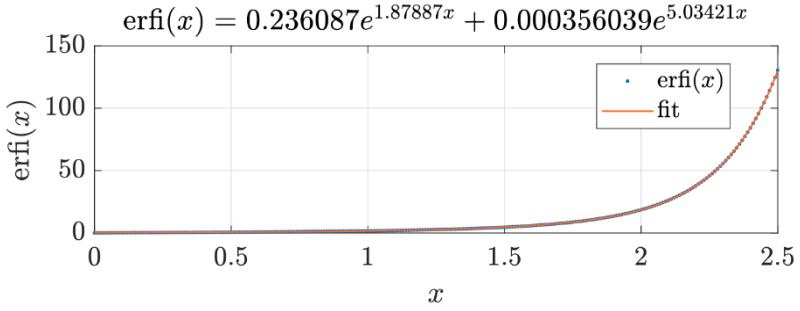
This relationship (Equation 16 in Supplementary Table 5) was formulated using a Michaelis-Menten-like expression, which assumes that cell receptors sensing fatty acids are saturable, with an added constant term representing the enzyme activity due to stimuli other than the presence of fatty acids in the duodenum. The expression was fitted using data on enzyme activity of secreted pancreatic amylase with various oleic acid concentrations (150), and it was converted into activities of equivalent pancreatic protease and lipase using amylase to lipase to trypsin ratios (146), all according to the current concentration of fatty acids in the first portion of the small intestine.

The cell glucose uptake rate which depends on the energetic expenditure of the small intestine wall was assumed as a 10% of absorbed glucose $\dot{n}_{GII,J}$ (75). However, when no enteral glucose is present in the lumen, the intestinal wall sources glucose from the systemic circulation via $\dot{m}_{14,j}$, which was adjusted at a fixed consumption rate. Since arterial blood flow of the superior mesenteric artery is divided into smaller branches that locally irrigate all the portions of the small intestine, the mass fraction (and therefore, the molar concentration) of glucose remains unchanged, rendering $w_{G15} = w_{G15,j}$. This value is deemed the systemic glucose concentration, which will accordingly change in response to the glucose absorption rate into the blood of capillaries. Blood in the capillaries drains the small intestine, converging in the superior mesenteric vein, which delivers enteral glucose into the portal vein, with a glucose mass fraction equal to w_{G16}. The glucose concentration data used to obtain W_{G16} were retrieved from (151) and, in turn, identified another fuzzy model (following the methodology described by (145), which allows a sampling of the systemic glucose concentration at any given time.

The portal vein raises from gastric, splenic, superior mesenteric and inferior mesenteric veins, so that determining each mass flow and composition would considerably increase the model's complexity. A more convenient and still realistic scenario is to assume the magnitude of the volume flow irrigating the small intestine equal to that of the portal vein, so the flow of the components being absorbed from the small intestine has a weighted impact on the composition due to the higher dilution that a larger volume flow produces. Thus, arterial flow $\dot{m}_{15}$ is calculated using the volume flow in the portal vein.

Simulation of the computational model: Programming and simulation of the model were performed using MaTLab®. To significantly reduce computation time, the imaginary error function, erfi(x), was simplified by fitting within the interval x ∈ [0, 2], obtaining the expression erfi(x) = $0.236^{1.88x}$ + $0.000356^{5.034x}$, shown in Fig 15. The maximum absolute error and root-mean-square error are 0.21 and 0.0181, respectively. For x > 2, the former solver for erfi(x) in MaTLab® is used. The computational model is free (interested readers can obtain it from the corresponding author) and can be used to generate the simulations presented in the paper.

Figure 15. Fit of erfi(x) using an expression of the form y = a^{bx}+ c^{dx}.



The mathematical model responses were contrasted with data available in the literature. Experimental data from three studies (151-153) were used to compare the rate of glucose appearance in the portal system, and the inactivation percentage of pancreatic enzymes was fitted with data taken from (146). Percentages for the digestion of macro-nutrients and the absorption of glucose, fatty acids, amino acids, and water in the three structural parts of the small intestine were adjusted following data available in (144, 154-157). Further details of data comparison are discussed extensively in the next section.

Results and discussion

The gastrointestinal tract is an organ system that has been studied with greater interest in the last two decades to determine the rate of glucose appearance in plasma after a meal. Most of the existing models that calculate the absorption rate of glucose in plasma are compartmental models that only consider the transit of glucose through the stomach and intestine and do not consider some physiological aspects of the digestion and absorption

processes, including proteins and fats involved in glucose absorption. This section presents the results of the proposed phenomenological-based semi-physical model of the gastrointestinal tract. The simulation was carried out for the digestion, through the stomach and small intestine, of three different meals to assess the model's prediction and description ability when compared to experimental data available in the literature (151-153). In all three cases, the mathematical model fits the experimental data with a mean absolute error of 0.4%. Few parameters were manually calibrated due to their interpretability and the model's basic structure based on the underlying phenomena. Additionally, the model considers many physiological aspects of the digestion and absorption of other nutrients in both the stomach and the intestine, which affect the rate of glucose appearance in plasma.

Figure 16 shows the results of the glucose appearance rate in the portal system for the model compared with data found in the literature and their particular conditions. These data from the literature were only used to compare and evaluate the responses of the model and not to make parametric adjustments. Parametric adjustments were made with population data of percentages of digestion and absorption of nutrients in the small intestine are reported in Table 7 and 8, and in table 9 the pancreatic enzymatic inactivation is shown. In [56], a novel natural tracer method is proposed to measure complex carbohydrate turnover in the postprandial state in healthy subjects. Meal content considered in this case is 52.2g of carbohydrates, 35.5g of protein, 27.1g of lipids, and 600.1kcal of the total energy content of the food. On the other hand, a reconstructed rate of glucose appearance by employing a tracer two-step method [57] is used to validate the model response following a triple-tracer mixed meal containing 10kcal/kg, 45% carbohydrates, 15% protein, and 40% fat. The rate of glucose appearance after an ingestion of glucose load in healthy subjects is also used to contrast the model response. In this case, the subjects of the study [58] ingested 1g of glucose per kg of body weight (as a 45% aqueous solution) for 5 minutes. In all three cases, the mathematical model fits the experimental data with few parameters to calibrate due to their interpretability and the model's basic structure based on the underlying phenomena.

Figure 16. Simulated glucose concentration in portal vein following ingestion of the meals reported by [150-152], respectively.

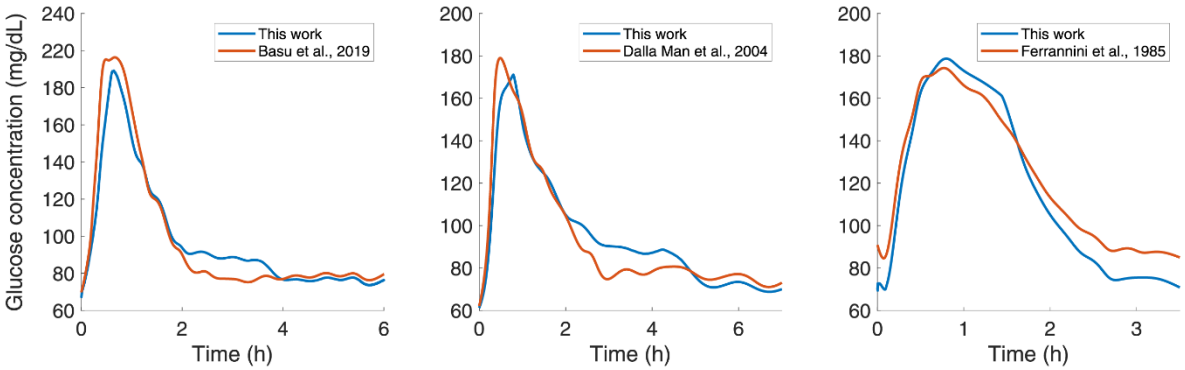


Table 7. Cumulative digestion.

Percentage of cumulative digestion of nutrients in the intestine							
	Duodenum		Jejunum		Ileum		
Nutrient	**Ref**	**Sim**	**Ref**	**Sim**	**Ref**	**Sim**	**Reference**
Carbohydrates	–	63.5%	75%	75.5%	84.2 – 89.5%	89.9%	(146)
Protein	33%	31.1%	60%	65.4%	89.5 – 94.7%	92.1%	(154, 155)
Lipids	–	32.0%	–	44.4%	68.7 – 75%	72.5%	(154, 158)

Table 8. Cumulative absorption.

Percentage of cumulative absorption of nutrients in the intestine							
	Duodenum		Jejunum		Ileum		
Nutrient	**Ref**	**Sim**	**Ref**	**Sim**	**Ref**	**Sim**	**Reference**
Carbohydrates	25%	25.5%	75%	75.0%	84.2-89.5%	89.9%	(156)
Protein	33%	31.1%	80%	80.0%	89.5-94.7%	92.1%	(154)
Lipids	-	32%	-	44%	68.7-75%	72.5%	(157)

Table 9. Pancreatic enzymes inactivation.

Rate of inactivation of pancreatic enzymes in the intestine				
	Jejunum		Ileum	
Enzyme	**Reference**	**Simulation**	**Reference**	**Simulation**
Amilase	15%	15.6%	26%	26.6%
Protease	36%	37.1%	78%	74.8%
Lipase	–	29.6%	75 – 80%	80.0%

Figure 17 shows the gastric mass flow passing from the stomach to the first portion of the duodenum through the pylorus valve over time. Initially, until the chyme reaches specific rheological properties in the stomach to be emptied into the duodenum, the mass flow through the pylorus increases until it reaches a maximum point. Then, the flow remains constant for the next 2 hours, which is the duration of digestion in the stomach for the considered mixed meal, where proteins and fats are partially digested before mass flow decreases until complete emptying (159). Digestion then continues in the small intestine, where some components are absorbed into the portal system. It is worth clarifying that the gastric emptying rate is mainly a function of the caloric density of the ingested meal and

that the relationship between these variables is linear. Furthermore, the nature of the calories seems to play a minor role in determining the rate of gastric emptying in humans.

Figure 17. Gastric emptying of the mass flow of the chyme through the pyloric valve.

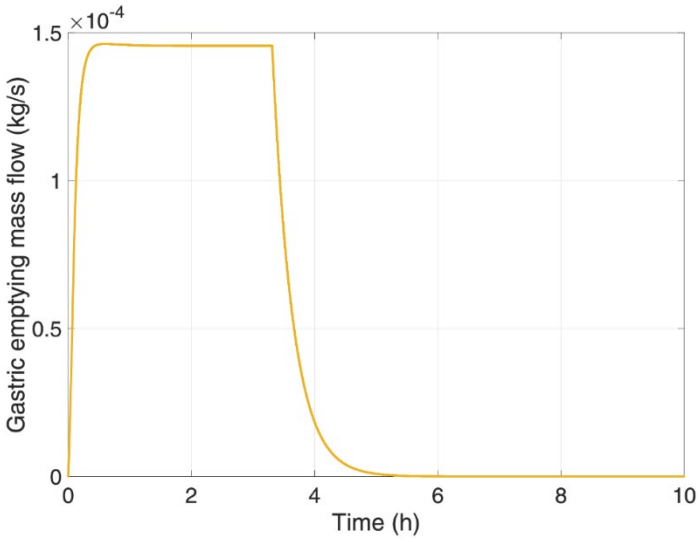
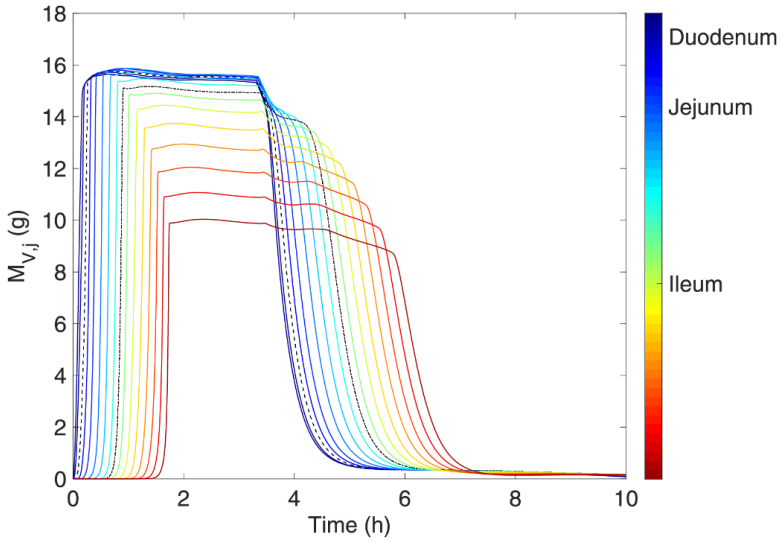


Figure 18 displays the accumulation of gastric mass on each portion of the small intestine in time. As can be noted, the duodenum contains the highest content of chyme. As the gastric mass is digested, nutrients are absorbed into the bloodstream, which causes a decrease in lumen food content as it moves towards the ileum until being almost completely emptied after 7 hours of digestion. This considering that there is no more ingestion during that time interval. The percentages of digestion and absorption in each part of the small intestine were obtained by adjusting the parameters for reaction kinetics and absorption rates as in the data reported in the literature.

Figure 18. Mass contained inside each tank j in the postprandial period.



Tables 7, 8 and 9 compares data collected from the literature (Ref column) with simulation data (Sim column) for the digestion of macronutrients, the absorption of nutrients and water, and the accumulated inactivation percentages of the considered pancreatic enzymes up to the duodenum, jejunum, and ileum. Macronutrients and their simplest, digested forms (glucose, amino acids, and fatty acids) are mostly digested and absorbed in the ileum. Undigested and non-absorbed nutrients continue to the large intestine to be fermented and converted into shorter peptides, amino acids, and fatty acids. The activities of pancreatic enzymes do not decrease in the first portion of the gut because that is where digestion begins, where pancreatic juice and bile are first mixed with the chyme. Later, activities begin decreasing during their passage from the duodenum to the terminal ileum, although the degradation rates of the individual enzymes are different (134). While the activity of pancreatic lipase is lost more rapidly and at a higher percentage, proteases and amylase are more stable, with the activity of pancreatic amylase being the least-decreasing during intestinal digestion. Simulation data is close to the data found in the literature, indicating that the model can reliably reproduce the digestion and absorption of the nutrients in the gastrointestinal tract. Moreover, the literature has unclear percentages of digestion for carbohydrates and lipids in the duodenum and lipids in the mid-jejunum, and data available from experiments are missing. In this regard, the proposed model can provide this missing

information accurately due to the high coupling of the mathematical model, the inclusion of available physiological knowledge, and the representation of the digestion and absorption processes in the human body that are as close to physiology as possible.

Conclusion

The gastrointestinal tract is a complex organ system with many interactions between different parts, tissues, and cells. In the control of blood glucose levels, physiological aspects such as early detection of meals and rate of glucose appearance have challenged the controller's performance in maintaining normal glucose levels and, consequently, an appropriate treatment of people with diabetes mellitus. Several studies have tried calculating the glucose appearance rate by using different techniques and mathematical modelling methodologies, commonly by compartmental models. In this study, a novel technique was used to develop a phenomenological-based semi-physical model to represent the role of the gastrointestinal tract in glucose metabolism in healthy humans. The proposed physiological model has many parameters, but their estimation was not a difficult task thanks to their interpretability. Additionally, the model is modular, meaning that, it can be used in algorithms developed to improve glucose control in people with diabetes mellitus, for other diagnostic purposes, or it can be combined with mathematical models of other organs to obtain a complete mathematical model of glucose metabolism in humans. Actually, the presented model is integrated with a liver model (160) and a model representing insulin pharmacokinetics and runs on a mobile app to predict glucose dynamics after consuming a mixed meal and assess whether carbohydrate counting improves in people who live with diabetes (108). The model could be extended for future work by adding several functionalities such as duodenal feedback control of gastric emptying, which relies on the concentration of carbohydrate, lipid and protein digestion products, pH, osmolarity, distension and hormonal effects such as the incretin effect. Also, the chemical composition of meals and the physical nature of food remain crucial in regulating the emptying rate, affecting intestinal transit time. Consequently, modeling

these phenomena is essential for understanding the relationships between the physical and chemical properties of food and digestion and absorption rates.

Main glucose hepatic fluxes in healthy subjects predicted from a phenomenological-based model

Introduction

In healthy subjects, blood glucose levels are maintained within a narrow range of around 70–110 md/dL thanks to a sophisticated natural closed feedback loop involving mainly the gastrointestinal (GI) tract, pancreas, kidneys, liver, and peripheral tissues, despite complex disturbances caused mainly by glucose-containing meals and a lack of physical activity. In this complex orchestration, the liver plays a key role, acting as a buffer in all fasting, postprandial, and post-absorptive states through hepatic glucose production and utilization (glycogenolysis, glycolysis, glycogenesis, and gluconeogenesis) (161, 162). In this complex and intertwined metabolic process, insulin and glucagon (viz. the glucose-lowering hormone and its antagonist) are used and degraded.

Insulin and glucagon are the main regulatory hormones in glucose homeostasis. In what seems an indirect process, insulin acts on adipose tissue lipolysis by suppressing free fatty acids, which in turn modulate (suppress) hepatic glucose production (161). Glucagon, on the other hand, promotes hepatic glycolysis as a response to hypoglycemia. Moreover, major insulin and glucagon clearance takes place in the liver (163, 164), being the latter process less known and quantified in humans than the former (163).

Understanding hepatic glucose metabolism is key in explaining the main mechanisms of glucose regulation and to provide useful and actionable insight to treat impaired glucose conditions such as DM1 and DM2. Although DM1 (a.k.a. insulin-dependent diabetes) is a widespread autoimmune disease, the prevalence of DM2 is increasing at alarming rates due mainly to the modern lifestyle, among other well studied causes (165). According to the International Diabetes Federation (IDF) as of 2019, 463 million people had diabetes with a 51% estimated increase in 2045 (∼ 700 million) (165).

Digital therapeutics have emerged in recent years as a promising alternative for diabetes care (166, 167) This encompasses a variety of tools including apps for decision support systems and automatic insulin delivery (a.k.a. the artificial pancreas) and the widespread

use of the Internet to provide specific targeted treatment. Behind-the-scenes, mathematical models of (or related to) glucose homeostasis play a key role in the design, testing, and implementation of these technologies. Specifically, computer simulation has, undoubtedly, accelerated the development of such technologies and has, for the specific case of the artificial pancreas, replaced the animal trials in the preclinical testing phase (168, 169).

The mathematical representation of glucose homeostasis either in healthy subjects or in DM1/DM2 has been a subject of intense research for over 40 years now (168, 170). Although numerous investigations have contributed to building the body of knowledge regarding such a complex mechanism, there is still some important that remains unknown/not thoroughly understood; e.g., the effect of different types of physical activities in endogenous glucose production and glucose utilization, glucagon metabolism, and accurate dynamical representations of insulin and glucagon secretion, among others.

Despite the key role of the liver in glucose homeostasis, there is, as yet, no accurate simulation model of the glucose-related hepatic metabolism, representing known physiological aspects and with the possibility of being individualized (identified) with specific field data. In this work, we propose a novel physiologic mathematical model of the glucose hepatic metabolism developed by a well established modeling methodology (114, 171). Key aspects such as Endogenous Glucose Production (EGP), hepatic glucose utilization, and insulin and glucagon clearance are integrated into this mathematical model together with metabolic and hormonal regulation. We show the prediction ability of the model by replicating in the simulation the results from three different experimental setups available in the literature (151-153) for a median hypothetical subject with minimal parameter calibration.

Role of the liver in glucose metabolism

The liver receives the mainstream of nutrients, including carbohydrates, right after reaching the bloodstream from the intestine. As such, it dampens both carbohydrate and several hormone fluxes through different pathways (172). Specifically, glucose enters hepatocytes via Glucose transporter 2 (GLUT2), a bidirectional transporter that allows passive entry and

exit by concentration difference rather than by insulin action, a common mechanism elsewhere (173).

Once inside the hepatocytes, glucose can be stored as glycogen, used to produce energy or fatty acid synthesis (174). The first step in hepatic glucose metabolism is its phosphorylation to Glucose 6 phosphate (G6P) by Glucokinase (GK), a low molecular weight enzyme that is not inhibited by its product, G6P, and has a lower affinity for glucose compared to other hexokinases (175). G6P can then undergo isomerization to Glucose 1 phosphate (G1P) or Fructose 6 phosphate (F6P) or oxidation to gluconolactone. In the postprandial period, about 50% of the ingested glucose will be converted to glycogen through the G1P pathway (direct route) (176), but the storage capacity of glycogen in the liver is limited and excess glucose from the diet goes in part to fatty acid synthesis (177). Also, in the postprandial period, the liver is not predominantly oxidative, which causes the amount of glucose to be metabolized through the F6P pathway to be very small (178).

GK is a widely regulated enzyme in the liver; whole activation occurs by Fructose 1 phosphate (F1P) and its gene transcription is subject to hormonal regulation (insulin and glucagon). Direct and indirect inhibition are mediated by Glucokinase regulatory protein (GKRP) and Fructose 1–6 biphosphate (FBP), respectively. In the presence of F6P, GKRP binds to form an inhibitory complex, which separates in the presence of F1P losing its activity. During the postprandial period, F1P levels are high, facilitating the flow of glucose into the cell by concentration difference (179). Also, GK concentration is higher in the cytoplasm, where high levels of insulin increase its transcription (180). In contrast, in the post absorptive period, GK remains inside the nucleus from which it cannot exert its action on glucose (181), where high levels of glucagon repress its transcription.

After an oral carbohydrate intake, the activity of Glucose 6 phosphatase (G6Pase) is partially suppressed by insulin (182), but glucose stimulates G6Pase and, paradoxically, this seems to be necessary to maintain high levels of G6P, which in turn, is needed to switch from glycogenolysis to glycogenogenesis (183). The mechanism used by the liver to transition from being a glucose-producing organ to a glucose storing organ is similar to that of a

switch; it is a matter of debate whether the effector is glucose or insulin. However, the action is parallel to glucose concentration. In spite of this, insulin is necessary to achieve the maximum glycogen concentration in the presence of glucose (184). Although glycogen's main route comes directly from the metabolism of ingested carbohydrates, glucose produced via gluconeogenesis may represent up to 25% of the total amount of glycogen production in fed and fasting states (176).

Methods

In this section, we discuss the steps taken to build a phenomenological-based semi-physical model (PBSM) accounting for the role of the liver in glucose homeostasis. We used a three-phase methodology to build the model (117). In the pre-construction phase, we described the process to be modeled and the model's objective, proposed a modeling hypothesis, stated the level of detail, and defined the process systems. In the construction phase, we applied the conservation principle, obtaining the model's basic structure. We then classified the symbols forming the equations selected for the basic structure as variables, structural parameters, and constants. We used constitutive and assessment equations to define the unknown parameters of every process system. A constitutive equation approximates the response of a physical quantity to external stimuli using a law or principle. An assessment equation is a mathematical relation to assess a parameter's numerical value. In the final step of the construction phase, the model's degrees of freedom are verified. In the final phase, we constructed a computational model and contrasted its results against experimental data available in the literature. Examples of previous models following this methodology are available elsewhere (114, 118, 171, 185, 186). This methodology makes it possible to build a mathematical model based on the current knowledge of physiology, with interpretable parameters and a unique and modular basic structure. This enables the model to be used for different purposes.

Model pre-construction

Process description and model aim: Unlike any other organ, the liver receives blood from two sources, the portal vein and the hepatic artery. The blood from the portal vein flows from the splanchnic bed. In the post-absorptive state, the species concentrations resemble the ones in the systemic circulation. After a carbohydrate-containing meal, portal vein blood contains a high concentration of glucose, fatty acids, or amino acids, depending on the type of food. Oxygen-rich blood from the peripheral circulation enters via the hepatic artery with a more or less constant glucose concentration. The hepatic artery's terminal branches and the portal vein (portal triad) empties its blood content into small channels called sinusoids. These low-pressure vascular tunnels carry blood from the portal triads toward the central hepatic vein. One hepatic lobule contains millions of sinusoids lined by highly fenestrated endothelial cells and surrounded by hepatocytes, as depicted in Figure 19. This configuration allows the exchange of nutrients, metabolism-related substances, and oxygen to flow between blood and the hepatocytes.

In healthy individuals, a blood glucose concentration of around 90 mg/dL (~ 72–180 mg/dL) is maintained, in part, due to the liver's ability to store and produce glucose. As described earlier, the glucose storage process is mainly active in the postprandial period where 50% of the ingested glucose is converted to glycogen (176). But most glucose (both ingested and circulating) is used in other metabolic routes such as fat production. In fasting, the liver breaks down glycogen to supply glucose and can produce glucose from non-hexose precursors such as lactate (187). Part of that circulating glucose is used by the liver to supply its energy requirements.

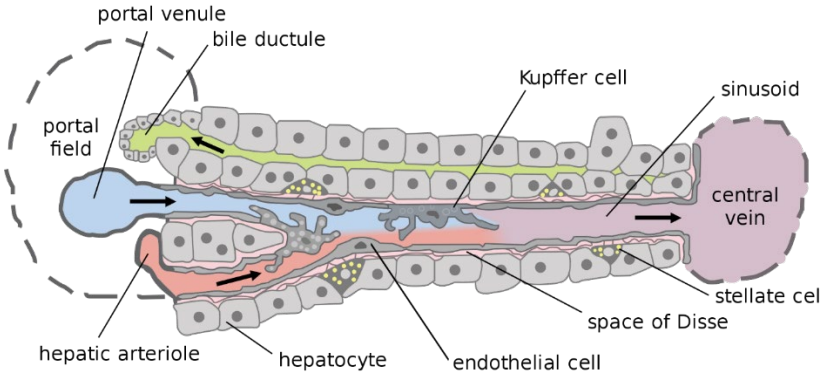
All the physiologic phenomena of glucose metabolism in the liver, e.g., glycolysis (energy production), glycogenesis (glycogen storage), glycogenolysis (glycogen breakdown to produce glucose), and gluconeogenesis (glucose production from non-hexose precursors) coexist and are regulated by the intermediated products of different reactions such as G6P and by hormones secreted by the pancreas (insulin and glucagon). In the postprandial period, high levels of insulin and glucose promote glucose storage and decrease glucose

production. During fasting, low circulating glucose concentration, decreasing/increasing insulin/glucagon production from the pancreas, blocks glucose storage and facilitates endogenous glucose production (EGP).

In our model, all four described physiological phenomena as well as the regulatory influence of insulin and glucagon on the liver are considered in both postprandial and fasting states.

Figure. 19 Representation of a liver sinusoid.

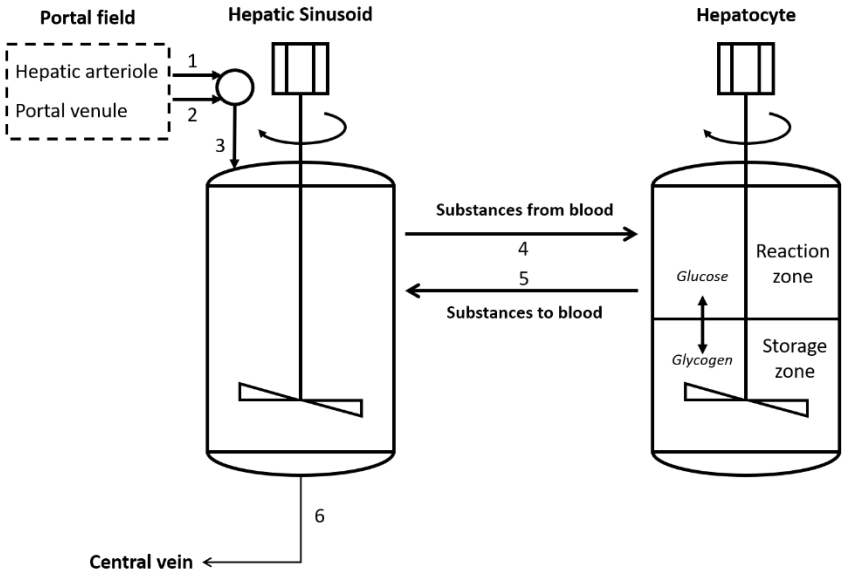
Figure reproduced from Frevert, U. et al. (188), in line with Creative Commons Attribution License - CC BY 4.0.



Model hypothesis and level of detail: All glucose metabolism within the liver occurs in the hepatocytes, in a dynamic process that involves an exchange of substances between blood and cells. The hepatocyte is considered here as the elemental brick forming the sinusoid, therefore allowing the scaling-up of millions of sinusoids to represent the entire liver. The process/physiology analogy to develop the model is shown in Figure 20. Blood entering the hepatic sinusoid gathers flows 1 and 2 (hepatic artery and portal vein, respectively). Here, blood volume and density are assumed to be constant due to the circulation's regulatory mechanisms that in usual conditions maintain strict control in human blood pressure, temperature, and density (189). The hepatic sinusoid is considered a continuously stirred tank, and it is where the exchange of model's substances of interest takes place. The total amount of hepatocytes in a sinusoid is regarded as a two-zone continuous stirred tank

reactor. In the upper part, it behaves like a regular continuously stirred reactor where all chemical reactions take place. In the lower part, it maintains perfect agitation and acts as a glycogen reservoir. The metabolic zonation of hepatic glucose metabolism (190) is not considered here since we aim at a net effect of the entire liver rather than a specific contribution from a given hepatocyte.

Figure 20. Process/Physiology analogy used to build the mathematical model.

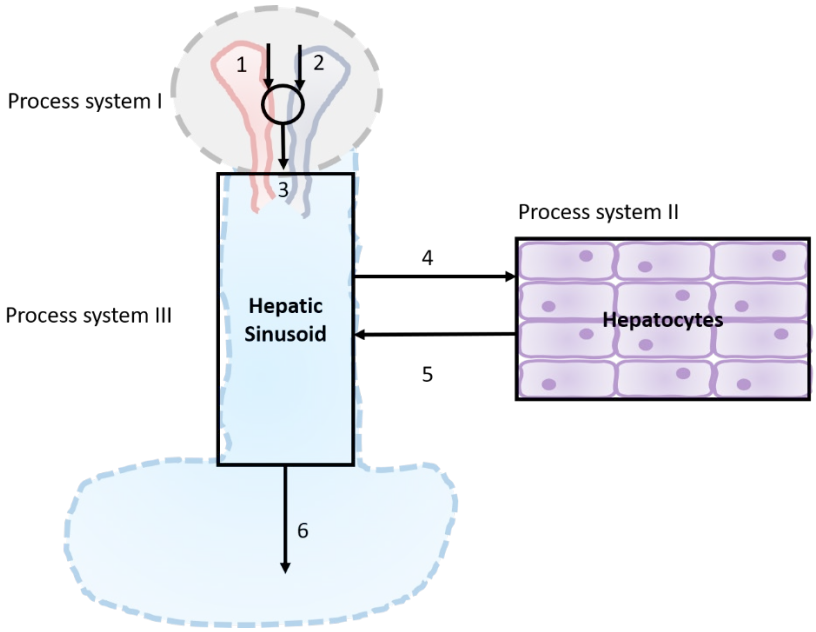


Definition of process systems (PS): A Process System (PS) is an engineering abstraction of the real object allowing for the statement of a set of differential equations laying out the model's basic structure. Every PS is naturally a part of the modeled process, a volume where the properties of the substances of interest change (191). Regarding the liver, three PSs were defined, see Figure 21. PSI is a mixing point merging the two blood streams entering the liver, the hepatic artery (stream 1) and portal vein (stream 2). The blood inflow to the hepatic sinusoids (PSIII) is hypothesized as a single flow represented by flow 3. We assume that all substances of interest, i.e., all substances playing a role in the glucose metabolism, diffuse across the blood vessels' walls irrigating the liver tissue to reach the hepatocytes (PSII). This transport is represented with stream 4. Once in the hepatocytes, the necessary biochemical reactions take place and the products generated in these reactions return to

the sinusoids via the mass flow 5, to be later discharged from PSIII to the bloodstream via stream 6.

Figure 21. Block diagram of process systems taken for modeling the liver's role in glucose metabolism.

1: Blood from the hepatic artery, 2: Blood from the portal vein, 3: Blood entering hepatic sinusoid, 4: Substances entering hepatocytes, 5: Substances leaving hepatocytes, 6: Blood to central hepatic vein



Model construction

The conservation principle: Mass balances were applied in mass units to PSI and PSIII for simplicity. We resorted to molar units in PSII to handle all biochemical reactions of interest. Total mass balance and mass balance for each substance of interest were also formulated as shown below.

Hepatic sinusoid inlet (PSI): All mass flows will be represented by $\dot{m}_k$ with k as the number or stream as in Figure 21.

Total mass balance: The total mass balance of PSI is given by:

$$\frac{dM_I}{dt} = \dot{m}_1 + \dot{m}_2 - \dot{m}_3 \quad (1)$$

with M_I the total mass of substances contained in PSI, $\dot{m}_1$ the oxygen-rich blood flow supply from the hepatic artery from the systemic circulation, and $\dot{m}_2$ the blood flow from the portal vein coming from the intestine with the absorbed nutrients. $\frac{dM_I}{dt} = 0$ the constant blood volume and density. In this way, the total mass balance for the PSI yields:

$$\dot{m}_3 = \dot{m}_1 + \dot{m}_2 \quad (2)$$

Component mass balance: Glucose concentration from the splanchnic bed changes dynamically as per the mixing of the meal-related carbohydrate absorption and bloodstream coming from the systemic circulation. Essential hormones from the pancreas such as insulin and glucagon as well as non-carbohydrate gluconeogenesis precursors (i.e., lactate, glutamine, alanine, glycerol) are also included into the balances and generalized as:

$$\frac{dM_{j,I}}{dt} = \dot{m}_1 w_{j,1} + \dot{m}_2 w_{j,2} - \dot{m}_3 w_{j,3} \quad (3)$$

where $w_{j,k}$ is the mass fraction of component *j* in the stream *k*, with *j*: glucose (G), insulin (Ins), glucagon (Gluca), lactate (Lac), glutamine (Glut), alanine (Ala) y glycerol (Gly). Only amino acids from the systemic circulation are taken into account because amino acids from diet had little or no effect on hepatic glucose production [38]. Total mass of component j can be expressed as $M_{j,I} = w_{j,I} M_I$. Obtaining the derivative on this expression, considering perfect agitation ($w_{j,I} = w_{j,3}$) y $\frac{dM_I}{dt} = 0$ Equation (3) becomes:

$$\frac{dw_{j,3}}{dt} = \left(\dot{m}_1 w_{j,1} + \dot{m}_2 w_{j,2} - \dot{m}_3 w_{j,3}\right) \frac{1}{M_I} \quad (4)$$

Hepatocytes (PSII): In this PS, we consider the main biochemical reactions within the liver playing a role in glucose regulation. The liver keeps a similar EGP ratio from non-carbohydrate precursors in both postprandial and post-absorptive states. The stoichiometric balance for this glucose production is somehow equivalent to that occurring in the kidneys (171). The remaining biochemical reactions present the following stoichiometric balances:

a. Glycogenesis (i = 1). The moles of glucose are phosphorylated to form moles of glycogen in the hepatocytes, with conversion of adenosine triphosphate (ATP) to adenosine diphosphate (ADP)

   Glucose - 1 - P + ATP + $Glycogen_n$ + H_2O -> $Glycogen_{n+1}$ + ADP + 2Pi

b. Glycogenolysis (i = 2). Glycogen dephosphorylates to form glucose:

   Glycogenn + Pi → Glycogenn−1 + Glucose - 1 – P

c. Gluconeogenesis (i = 3). Stoichiometric balances via every non-carbohydrate precursor are reported elsewhere (171).

d. Insulin clearance and glucagon degradation (i = 4 and i = 5, respectively). These are equimolar reactions as follows:

   Insulin → Insulin*Glucagon → Glucagon*

   where Insulin* and Glucagon* are inactivated insulin and glucagon molecules, respectively.

e. Glycolysis (i = 6). Hepatocytes consume glucose at a constant rate during the postprandial state.

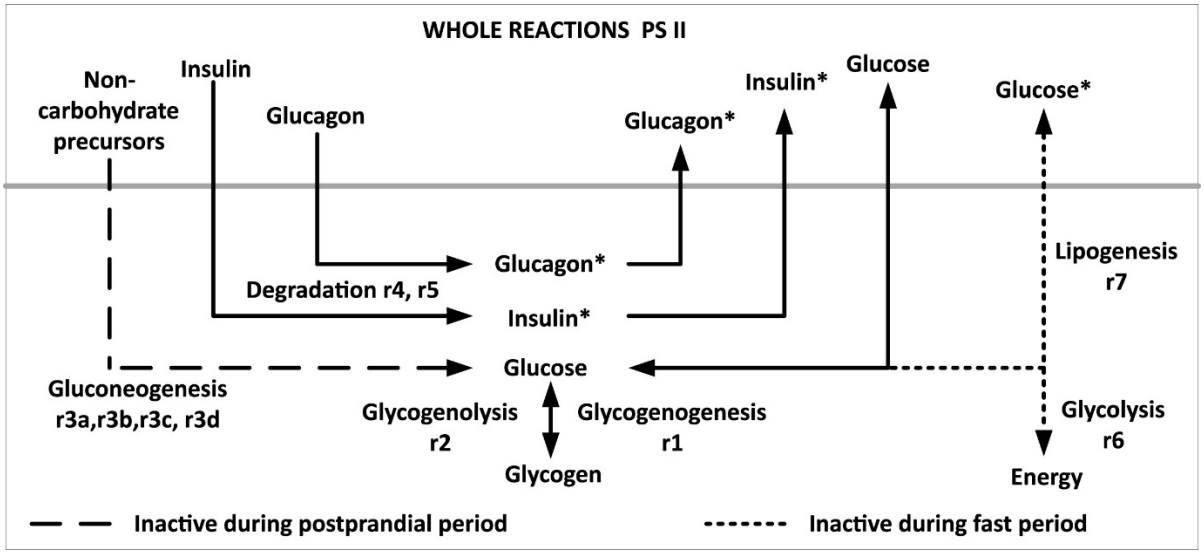
f. Lipogenesis (i = 7). Once glycogen stores in the liver reach their maximum capacity in the postprandial state, glucose is synthesized by an alternate metabolic pathway to form fat. This reaction also occurs during fasting when the hepatocytes catch half of the amount of glucose entering the sinusoid to form nicotine adenine dinucleotide phosphoric acid (NADPH). In both states, we consider an equimolar reaction as

   Glucose → G*

   With G* being the fatty acids produced from glucose.

Figure 22 summarizes the reactions taking into account in the model.

Figure 22. Main biochemical reactions within the liver playing a role in glucose regulation.



Total mass balance: the total mass balance of the PSII is written generically as:

$$\frac{dN_{II}}{dt} = \dot{n}_4 - \dot{n}_5 + \sum\left(r_i \sigma_{i,j}\right) \quad (5)$$

where N_{II} is the total mass of the substance in *Kg/mol*. $\dot{n}_4$ is the molar flow of substance entering the hepatocytes in corresponding units. The amount of glucose from the blood in the sinusoids entering to the hepatocytes varies from around 50% in the fasting state to 30% after a meal (178). In the fasting state, the liver prioritizes glucose consumption for energy production (178). Most of the glucagon and insulin metabolism occurs in the liver; around 80% of the insulin and 58% of glucagon entering the liver undergo clearance in the hepatocytes (164, 192, 193). All the non-carbohydrate precursors for gluconeogenesis enter the reactor on. The products of the reactions in the hepatocytes are represented by $\dot{n}_5$. r_i is the reaction rate for glycolysis, glycogenesis, glycogenolysis, and gluconeogenesis, and also for insulin and glucagon inactivation. $\sigma_{i,j}$ represents the stoichiometric coefficients, with (+) sign for products and (−) sign for reactants. Subindices *i* and *j* represent the chemical reactions and reaction products, respectively. All insulin and glucagon that enters into the hepatocytes undergo proteolysis. Instead of including unnecessary additional balances, the model replaces the same amount of insulin and glucagon that enters through $\dot{n}_4$ into

inactive products in $\dot{n}_5$, so there is no accumulation. Also, the model describes the liver clearance for both hormones with a positive sign (+) for products and a negative sign (−) for reactants.

Component mass balance: In this PS, glycogen also enters into play. Component mass balances for all species of interest in this PS can be written as:

$$\frac{dN_{j,II}}{dt} = \dot{n}_4\, x_{j,4} - \dot{n}_5\, x_{j,5} + \sum\left(\sigma_{i,j} r_i\right) \tag{6}$$

with $N_{j,II}$ the total moles of every component of interest and $x_{j,5}$ the molar fraction of component j leaving the hepatocytes. For the sake of simplicity, the terms are written in molar flows of specific substance instead of molar fractions and total flows yielding:

$$\frac{dN_{j,II}}{dt} = \dot{n}_{j,4} - \dot{n}_{j,5} + \sum\left(\sigma_{i,j} r_i\right) \tag{7}$$

where inactive glucose (*G**) produced via lipogenesis and *Ins** and *Gluca** do not enter the hepatocytes since they are reaction products, therefore $\dot{n}_4 = 0$. The balance for G*, Ins*, and Gluca* might be rewritten as:

$$\frac{dN_{j,II}}{dt} = -\dot{n}_{j,5} + \sum\left(\sigma_{i,j} r_i\right) \tag{8}$$

Once insulin, glucagon, and non-carbohydrates precursors enter the hepatocytes, they react and are converted into other substances not considered here. In this sense, $\dot{n}_5 = 0$ and the mass balance for j = Ins, Gluca, Glut, Lac, Ala, and Gly becomes:

$$\frac{dN_{j,II}}{dt} = \dot{n}_{j,4} + \sum\left(\sigma_{i,j} r_i\right) \tag{9}$$

Glycogen is phosphorylated and dephosphorylated only within the hepatocytes. Henceforth, there is no glycogen input/output. In this regard, the mass balance for glycogen is written as:

$$\frac{\mathrm{dN_{j,II}}}{\mathrm{dt}} = \sum\left(\sigma_{\mathrm{i,j}} \mathrm{r_i}\right) \tag{10}$$

Hepatic sinusoid (PSIII): As mentioned earlier, for this PS balances are performed in mass units for simplicity.

Total mass balance: Following the nomenclature in Figure 21, the total mass balance for PSIII can be written as:

$$\frac{dM_{III}}{dt} = \dot{m}_3 + \dot{m}_5 - \dot{m}_4 - \dot{m}_6 \tag{11}$$

In this PS there is no mass accumulation (blood density and volume remain constant), therefore $\frac{dM_{III}}{dt} = 0$ and:

$$\dot{m}_6 = \dot{m}_3 + \dot{m}_5 - \dot{m}_4 \tag{12}$$

Component mass balance: In this PS, the focus is on in the species leaving the sinusoids via the hepatic vein. The component mass balances can be written in a general form as:

$$\frac{dM_{j,III}}{dt} = \dot{m}_3\, w_{j,3} + \dot{m}_5\, w_{j,5} - \dot{m}_4\, w_{j,4} - \dot{m}_6\, w_{j,6} \tag{13}$$

with $M_{j,III}$ being the mass of component of interest *j* in the hepatic sinusoid. Using the perfect mixing condition of all substances into the hepatic sinusoid, the equivalence $w_{j,6}$ and $M_{j,III} = w_{j,III} M_{III}$ can be applied to solve the derivative of $M_{j,III}$ with M_{III} constant. Replacing this derivative solution in Equation (13), the component mass balance in the PSIII becomes

$$\frac{dw_{j,6}}{dt} = (\dot{m}_3 w_{j,3} + \dot{m}_5 w_{j,5} - \dot{m}_4 w_{j,4} - \dot{m}_6 w_{j,6}) \frac{1}{\rho_b V_b} \tag{14}$$

in case *j = G*. With the above in mind, the mass balance for insulin, glucagon, and non-carbohydrates precursors yields:

$$\frac{dw_{j,6}}{dt} = (\dot{m}_3 w_{j,3} - \dot{m}_4 w_{j,4} - \dot{m}_6 w_{j,6}) \frac{1}{\rho_b V_b} \tag{15}$$

For inactive insulin *(Ins*)* and glucagon *(Gluca*)* and fatty acids produced via lipogenesis (*G**), the balance reads as:

$$\frac{dw_{j,6}}{dt} = (\dot{m}_5 w_{j,5} - \dot{m}_6 w_{j,6}) \frac{1}{\rho_b V_b} \quad (16)$$

The basic structure of the model: The basic structure of the model comes from the active balances detailed in the previous section. The equations with relevant information for each PS are described as follows.

PSI: Equations. (3), (5). The latter generates seven equations, one for every component *j:* glucose, insulin, glucagon, lactate, glutamine, alanine, and glycerol.

PSII: Equationss. (5), (7) (for glucose), (8) (one for every inactive component *j* = G*, Ins*, and Gluca*), (9) (for j = Ins, Gluca, Glut, Lac, Ala, and Gly), and (10) for glycogen.

PSIII: Equations. (12), (14), (15) (for *j* = Ins, Gluca, Glut, Lac, Ala, Gly), (16) (one for every inactive component *j* = Ins*, Gluca*, and G*).

In this sense, the basic structure of the model is composed of 31 equations as summarized in table 10.

Table 10. Equations of the model's basic structure.

Process system	Equations	Component
PS_I	$\dot{m}_3 = \dot{m}_1 + \dot{m}_2$	
	$\frac{dw_{j,3}}{dt} = (\dot{m}_1 w_{j,1} + \dot{m}_2 w_{j,2} - \dot{m}_3 w_{j,3}) \frac{1}{\rho_b V_b}$	j = G, Ins, Gluca, Glut, Lac, Ala, Gly
PS_{II}	$\frac{dN_{II}}{dt} = \dot{n}_4 - \dot{n}_5 + \sum(r_i \sigma_{j,i})$	
	$\frac{dN_{j,II}}{dt} = \dot{n}_{j,4} - \dot{n}_5 x_{j,5} + \sum(r_i \sigma_{j,i})$	j = G
	$\frac{dN_{j,II}}{dt} = -\dot{n}_5 x_{j,5} + \sum(r_i \sigma_{j,i})$	j = *G**, *Ins**, *Gluca**
	$\frac{dN_{j,II}}{dt} = \dot{n}_{j,4} + \sum(r_i \sigma_{j,i})$	j = Ins, Gluca, Glut, Lac, Ala, Gly
	$\frac{dN_{j,II}}{dt} = \sum(r_i \sigma_{j,i})$	j = Glycogen
PS_{III}	$\dot{m}_6 = \dot{m}_3 + \dot{m}_5 - \dot{m}_4$	
	$\frac{dw_{j,6}}{dt} = (\dot{m}_3 w_{j,3} + \dot{m}_5 w_{j,5} - \dot{m}_4 w_{j,4} - \dot{m}_6 w_{j,6}) \frac{1}{\rho_b V_b}$	j = G
	$\frac{dw_{j,6}}{dt} = (\dot{m}_3 w_{j,3} - \dot{m}_4 w_{j,4} - \dot{m}_6 w_{j,6}) \frac{1}{\rho_b V_b}$	j = Ins, Gluca, Glut, Lac, Ala, Gly
	$\frac{dw_{j,6}}{dt} = (\dot{m}_5 w_{j,5} - \dot{m}_6 w_{j,6}) \frac{1}{\rho_b V_b}$	j = *G**, *Ins**, *Gluca**

The indexes are j = G, Ins, Gluca, Gluta, Lac, Ala, Gly, G*, Ins*, Gluca*, Glycogen; i (hepatic biochemical reactions): 1 = Glycogenesis, 2 = Glycogenolysis, 3 = Gluconeogenesis, 4 = Insulin clearance, 5 = Glucagon clearance, 6 = Glycolisis, 7 = Lipogenesis.

Variables, structural parameters, and structural constants: As detailed in Ref. (171), PBSMs is composed of variables, structural parameters, and constants. The structural parameters can be opened further to obtain a deeper level of detail. In the methodology used in this study (77), the parameters and constants that emerged from the application of the conservation principle are deemed as structural. While those that appear once the structural parameters have been defined are deemed as functional parameters. The classification of the model components are reported in Table 11.

Table 11. Model variables, structural parameters, and structural constants.

	PS_I	PS_{II}	PS_{III}	Total
Variables	$\dot{m}_3, w_{j,3}$	N_{II}, $N_{j,II}$	$\dot{m}_6, w_{j,6}$	31
Structural Parameters	$\dot{m}_1, \dot{m}_2, w_{j,1}, w_{j,2}, \rho_b$, V_b	$\dot{n}_4, \dot{n}_5, \dot{n}_{j,4}, x_{j,5}$, r_i	$\dot{m}_4, \dot{m}_5, w_{j,4}$, $w_{j,5}$	42
Structural Constants	–	$\sigma_{j,i}$	–	26

The indexes are j = G, Ins, Gluca, Gluta, Lac, Ala, Gly, G*, Ins*, Gluca*, Glycogen; i (hepatic biochemical reactions): 1 = Glycogenesis, 2 = Glycogenolysis, 3 = Gluconeogenesis, 4 = Insulin clearance, 5 = Glucagon clearance, 6 = Glycolisis, 7 = Lipogenesis.

Constitutive and assessment equations for structural and functional parameters. Definition of constants: As mentioned earlier, functional parameters show up once structural parameters are defined. The set of new equations proposed here to complete the whole structure of the model is labeled as an extended structure of the model. Mathematical expressions used to define a parameter in terms of new parameters are often known as constitutive equations. We use the term assessment equation to the assign a functional parameter with a given value either from the literature or from an assumption. Table 12 reports the set of constitutive equations used to define the structural parameters. In this table,"instances" refers to the number of equations generated given the different components of interest in that particular stream. Functional parameters can in turn be re-defined in terms of new constitutive equations when deemed necessary. Table 13 details which functional parameters are re-defined. Finally, Table 14 summarizes all parameters with a fixed numerical value or defined by using an assessment equation as well as all model constants.

Table 12. Constitutive equations for structural parameters of the model.

#	Description	Constitutive/Assessment Equation	Instances	Ref.
1	Mass flow rate of blood entering in the liver from the hepatic artery (stream 1).	$\dot{m}_1 = \rho_b \dot{V}_{ab}$	1	[42]
2	Mass flow rate of blood entering in the liver from the portal vein (stream 2).	$\dot{m}_2 = \rho_b \dot{V}_{vb}$	1	[42]
3	Mass fraction of components of interest entering in the liver via the hepatic artery.	$w_{j,1} = C_{j,1} \frac{1}{\rho_b} \mathfrak{M}_j$	7	UC
4	Mass fraction of components of interest entering in the liver via the portal vein.	$w_{j,2} = C_{j,2} \frac{1}{\rho_b} \mathfrak{M}_j$	7	UC
5	Density of the blood.	$\rho_b = 1060\ \mathrm{kg/m^3}$	1	[43]
6	Volume of blood irrigating the liver.	$V_b = 0.25\ vol$	1	
7	Molar flow of substances of interest involved in glucose metabolism entering hepatocytes from sinusoids.	$\dot{n}_4 = \sum \dot{n}_{j,4}$	1	[42]
8	Molar flow of substances of interest out of the hepatocytes towards the sinusoids	$\dot{n}_5 = \dot{V}_5 \overline{\rho}_5$	1	[42]
9	Reaction velocity of insulin and glucagon clearance, and gluconeogenesis occurring in the liver.	$r_i = k_{0,i} N_{j,II}\, e^{\frac{-Ea_i}{RT}}$	3	[42]
10	Rate of glycogenogenesis reaction occurring in the liver in both postprandial and postabsorptive states.	$r_1 =$	1	[44, 45]
11	Rate of glucose production from glycogen stored in the liver.	$\begin{cases} 0 & \text{if } C_{G,2} \le C_{G,1} \wedge N_{Glgn,II} > 500\ mol \\ k_{0,1} x_{G,4} e^{\frac{-Ea_1}{RT}} & \text{if } C_{G,2} > C_{G,1} \end{cases}$	1	[44, 45]
12	Rate of glucose consumption by hepatocytes (glycolysis).	$r_2 = \begin{cases} k_{0,2} N_{Glgn,II}\, e^{\frac{-Ea_2}{RT}} & \text{if } C_{G,2} \le C_{G,1} \wedge C_{Gluca} > 77\ pmol/L \wedge N_{Glgn,II} > N_{Glgn,II_{min}} \\ 0 & \text{if } C_{G,2} > C_{G,1} \vee N_{Glgn,II} \le N_{Glgn,II_{min}} \wedge C_{Gluca} > 77\ pmol/L \wedge C_{G,2} \le C_{G,1} \end{cases}$	1	[46]
13	Fat production rate by lipogenesis due to excess glucose in the liver.	$r_6 = \begin{cases} 0 & \text{if } C_{G,2} \le C_{G,1} \\ k_{0,6} x_{G,4} e^{\frac{-Ea_6}{RT}} & \text{if } C_{G,2} > C_{G,1} \end{cases}$	1	[44, 45]
14	Molar flow of glucose entering the hepatocytes.	$r_7 = \begin{cases} k_{0,7} x_{G,4} e^{\frac{-Ea_7}{RT}} & \text{if } C_{G,2} \le C_{G,1} \\ 0 & \text{if } C_{G,2} > C_{G,1} \wedge N_{Glgn,II} \le 500\ \mu mol \\ k_{0,7} N_{G,II} e^{\frac{-Ea_7}{RT}} & \text{if } C_{G,2} > C_{G,1} \wedge N_{Glgn,II} > 500\ \mu mol \end{cases}$	1	A
15	Molar flow of insulin entering the hepatocytes.	$\dot{n}_{G,4} = \begin{cases} PU_{G_{pa}} \dot{n}_{G,3} & \text{if } C_{G,2} \le C_{G,1} \\ PU_{G_{pp}} \dot{n}_{G,3} & \text{if } C_{G,2} > C_{G,1} \end{cases}$	1	[47]
16	Molar flow of glucagon entering the hepatocytes.	$\dot{n}_{Ins,4} = PC_{Ins} \dot{n}_{Ins,3}$	1	A
17	Molar flow of non-carbohydrate precursor entering the hepatocytes.	$\dot{n}_{Gluca,4} = PC_{Gluca} \dot{n}_{Gluca,3}$	1	[44]
18	Molar fraction of glucose (G), inactive glucose (G^*), inactive insulin (Ins^*), and inactive glucagon ($Gluca^*$) leaving the hepatocytes.	$\dot{n}_{j,4} = C_{j,3} \dot{V}_{hep} PC_j$	4	[42]
19	Mass flow rate of substances of interest entering the hepatocytes.	$x_{j,5} = \frac{N_{j,II}}{N_{II}}$	4	[42]
20	Mass flow rate of the reaction products returning to the bloodstream from the hepatocytes.	$\dot{m}_4 = \sum (\dot{n}_4 \mathfrak{M}_j)$	1	UC
21	Mass fraction of component j entering the hepatocytes by stream 4.	$\dot{m}_5 = \dot{n}_5 \mathfrak{M}_5$	1	UC
22	Mass fraction of component j leaving the hepatocytes by stream 5.	$w_{j,4} = \dot{n}_{j,4} \mathfrak{M}_j \frac{1}{\dot{m}_4}$	7	UC
		$w_{j,5} = x_{j,5} \frac{\mathfrak{M}_j}{\mathfrak{M}_5}$	10	UC

Abbreviations. UC: Unit conversion, A: Assumed. Indexes j = G, Ins, Gluca, Gluta, Lac, Ala, Gly, G^*, Ins^*, $Gluca^*$, Glgn. Indexes i (biochemical reactions): 1 = Glucogenogenesis, 2 = glycogenolysis, 3 = Gluconeogenesis, 4 = Insulin clearance, 5 = Glucagon clearance, 6 = Glycolysis, 7 = Lipogenesis.

Table 13. Constitutive equations for structural parameters of the model.

#	Description	Constit. Equation	Instances	Ref.
1	Volumetric flow rate of blood entering the liver from the hepatic artery.	$\dot{V}_{ab} = 10\ \frac{mL}{kg - min}$	1	[48]
2	Volumetric flow rate of blood entering the liver from the portal system.	$\dot{V}_{vb} = 20\ \frac{mL}{kg - min}$	1	[48]
3	Circulating blood volume.	$Vol = 80\ BW$	1	[48]
4	Volumetric flow rate out of hepatocytes.	$\dot{V}_5 = \sum(\dot{V}_{r_i}) + \sum(\dot{V}_4)$	1	O
5	Average molar density of flow out of hepatocytes (stream 5).	$\overline{\rho}_5 = \frac{1}{\sum \frac{x_{j,5}}{\overline{\rho}_j}}$	1	O
6	Molar fraction of component j entering the hepatocytes.	$x_{j,4} = \frac{\dot{n}_{j,4}}{\dot{n}_4}$	3	UC
7	Molar flow of $j = G$, *Ins*, and *Gluca* entering the hepatic sinusoids via stream 3.	$\dot{n}_{j,3} = w_{j,3}\ \frac{1}{\mathfrak{M}_j}\ \dot{m}_3$	3	UC
8	Molar-volumetric concentration of component $j = G$, *Ins*, and *Gluca* entering the hepatic sinusoids.	$C_{j,3} = w_{j,3}\ \rho_b\ \frac{1}{\mathfrak{M}_j}$	3	UC
9	Volumetric flow entering the hepatocytes.	$\dot{V}_{hep} = 0.6\ \dot{V}_b$	1	[48]
10	Total molar mass of components leaving liver and returning the hepatic sinusoids via stream 5	$\mathfrak{M}_5 = \sum (x_{j,5}\ \mathfrak{M}_j)$	1	[42]
11	Volumetric flow due to reaction i.	$\dot{V}_{r_i} = \sigma_{G,i}\ r_i\ \frac{1}{\overline{\rho}_G}$	3	A
12	Volumetric flow in the stream 4.	$\dot{V}_4 = \dot{n}_4\ \frac{1}{\overline{\rho}_4}$	1	A
13	Total volumetric flow of blood entering the liver.	$\dot{V}_b = \dot{V}_{ab} + \dot{V}_{vb}$	1	O
14	Average molar density of stream 4 that enters the hepatocytes.	$\overline{\rho}_4 = \frac{1}{\sum(\frac{x_{j,4}}{\overline{\rho}_j})}$	1	O
15	Molar flow of stream 4.	$\dot{n}_4 = \sum(\dot{n}_{j,4})$	1	[42]

Abbreviations. O: Own equation. UC: Unit conversion, A: Assumed. Indexes j = G, Ins, Gluca, Gluta, Lac, Ala, Gly, *G**, *Ins**, *Gluca**, Glgn. Indexes i (biochemical reactions): 1 = Glucogenogenesis, 2 = glycogenolysis, 3 = Gluconeogenesis, 4 = Insulin clearance, 5 = Glucagon clearance, 6 = Glycolysis, 7 = Lipogenesis.

Table 14. Assessment equations for functional parameters of the model.

The numerical values are fixed parameters in the model. Constants of the model are also reported in this table shown in the "value" column.

Symbol	Description	Value	Instances	Ref.
$C_{Gluta,1}$	Molar-volumetric concentration of glutamine in systemic circulation entering the liver via stream 1.	0.6 mmol/L	1	[49]
$C_{Lac,1}$	Molar-volumetric concentration of lactate in systemic circulation entering the liver via stream 1.	0.8 mmol/L	1	[49]
$C_{Ala,1}$	Molar-volumetric concentration of alanine in systemic circulation entering the liver via stream 1.	0.3 mmol/L	1	[49]
$C_{Gly,1}$	Molar-volumetric concentration of gly in systemic circulation entering the liver via stream 1.	0.1 mmol/L	1	[49]
$C_{j,2}$	Molar-volumetric concentration of component j in portal venous system entering the liver via stream 2.	Experimental data was considered for j=G, *Ins*, and *Gluca*. For j=precursors, concentrations are considered the same values of $C_{j,1}$	3	[13,14,15]
$\mathfrak{M}_j$	Molar mass of component j (known value).		7	A
$k_{0,i}$	Theconstant rate of glucose production and consumption due to biochemical reactions involved in glucose metabolism and that take place in the liver.		7	I
Ea_i	Activation energy for glucose production and consumption via biochemical reactions involved in glucose metabolism and taking place in the liver.		7	I
$PU_{G,pa}$	Percentage of glucose uptake in the liver in post-absorptive state.	50%	1	[20]
$PU_{G,pp}$	Percentage of glucose uptake in the liver in postprandial state.	21%	1	[20]
PC_{Ins}	Percentage of insulin clearance in the liver.	71%. Range reported in the literature 20–80%	1	I
PC_{Gluca}	Percentage of glucagon clearance in the liver.	58%	1	A
PC_j	Uptake percentage of non-carbohydrate precursors in the liver.		4	I
BW	Body weight.	70 kg	1	A
$\tilde{\rho}_j$	Molar density of component j.		4	A
R	Universal constant for ideal gas.	8.314 J/molK	1	[42]
T	Blood temperature.	37 °C	1	[50]
$\sigma_{j,i}$	Stoichiometric coefficient for component j in the reaction i where is consumed.	−1	6	[51,52,52]
$\sigma_{j,i}$	Stoichiometric coefficient for component j in the reaction i where is produced.	1	5	[51,52,52]

Abbreviations. A: Assumed. I: Identified. Indexes j=G, Ins, Gluca, Gluta, Lac, Ala, Gly, G^*, Ins^*, $Gluca^*$, Glgn. Indexes i (biochemical reactions): 1=Glucogenogenesis, 2=glycogenolysis, 3=Gluconeogenesis, 4=Insulin clearance, 5=Glucagon clearance, 6=Glycolysis, 7=Lipogenesis.

Degrees of freedom analysis: The analysis of degrees of freedom in the model helps to establish the model closure in terms its computational solution. In this regard, our goal is to find whether the number of unknowns is equivalent to the number of equations (including variables and model parameters). For the purpose of the present model, we present the analysis of the degrees of freedom in Table 15, where a final 0 DoF is obtained. It is worth clarifying that the sole purpose of this analysis is to evaluate whether the model can be implemented in simulation. For identifiability purposes, the model can be parameterized with only twelve parameters. These tunable parameters must be defined by a numerical value that must be identified to provide a specific dynamic behavior.

Table 15. Degrees of freedom.

	V	SP	FP	Net	DoF
Equations	31	23	57	111	0
Unknowns	31	23	57	111	

Abbreviations. V: variables, SP: structural parameters, FP: functional parameters, Net: sum of *SP+FP+V*, and DoF: degrees of freedom (difference between unknowns and equations).

Simulation of the computational model: The model was programmed and solved using MatLab@ version 9.8.0 - R2020a (Natick, Massachusetts: The MathWorks Inc.).

Results

We presented a detailed Phenomenological-Based Semi-physical Models (PBSM) of the human hepatic glucose metabolism for healthy subjects accounting for the two major hormones involved in glucose regulation, insulin and glucagon. Results from three different experiments available in the literature were used to assess the prediction ability of the proposed model (151-153). It is worth mentioning that since the three experimental conditions are different, the types of stimuli and observations also differ from one another.

In this case, since we are interested in assessing the physiological coherence of the model, we replicated at replicating the median traces of the experimental outputs by considering a hypothetical “median” virtual subject.".

Figure 23 shows the results of our model in reconstructing the experimental results presented in Ref. (153), where 11 subjects underwent an Oral Glucose Tolerance Test (OGTT) following an overnight fast. The purpose of the experiment was to measure the rate of oral glucose appearance, splanchnic glucose uptake, suppression of hepatic glucose production, and peripheral glucose uptake using hepatic vein catheterization and a double-tracer technique. For the considered scenario, absolute errors of (mean ± std) 5.4 ± 5.2 mg/dL, 38.7 ± 28.4 pmol/L, and 41.1 ± 101.6 µmol were obtained for systemic glucose, systemic insulin, and glycogen, respectively, when comparing the model output with respect to the available experimental data.

Figure 24 shows the results of the developed model in reproducing the experimental setup in Ref. (152), where 88 healthy subjects (46 male - 42 female) underwent an OGTT. The rate of glucose appearance was estimated from a two-tracer protocol. For the considered scenario, absolute errors of (mean ± std) 7.5 ± 6.8 mg/dL and 15.3 ± 15.4 pmol/L were obtained for systemic glucose and systemic insulin, respectively, when comparing the model output with respect to the available experimental data.

A more realistic setup where 16 healthy subjects were challenged with a mixed meal after overnight fasting was considered by Basu et al. in Ref. (151). This experiment provided information following a more conventional meal and reports useful information such as the rate of glucose appearance (Ra) and C-peptide concentration, estimated by means of a triple-tracer technique, allowing the estimation of pancreatic insulin within the portal vein after the meals. Figure 25 shows the performance of our model in reproducing such results. Absolute errors of (mean ± std) 7.5 ± 7.5 mg/dL, 30.9 ± 48.5 pmol/L, and 0.49 ± 0.45 pmol/L were obtained for systemic glucose, systemic insulin, and systemic glucagon, respectively, when comparing the model output with respect to the available experimental data.

Figure 23. Estimation made by the model compared with experimental data from (153).

Panels A–C represent the inputs: (A) arterial glucose concentration (aG), (B) venous glucose concentration (vG), and (C) venous insulin concentration (vI). Panels D–F depict the model outputs: (D) systemic glucose (sysG), (E) systemic insulin (sysI), and (F) Glycogen

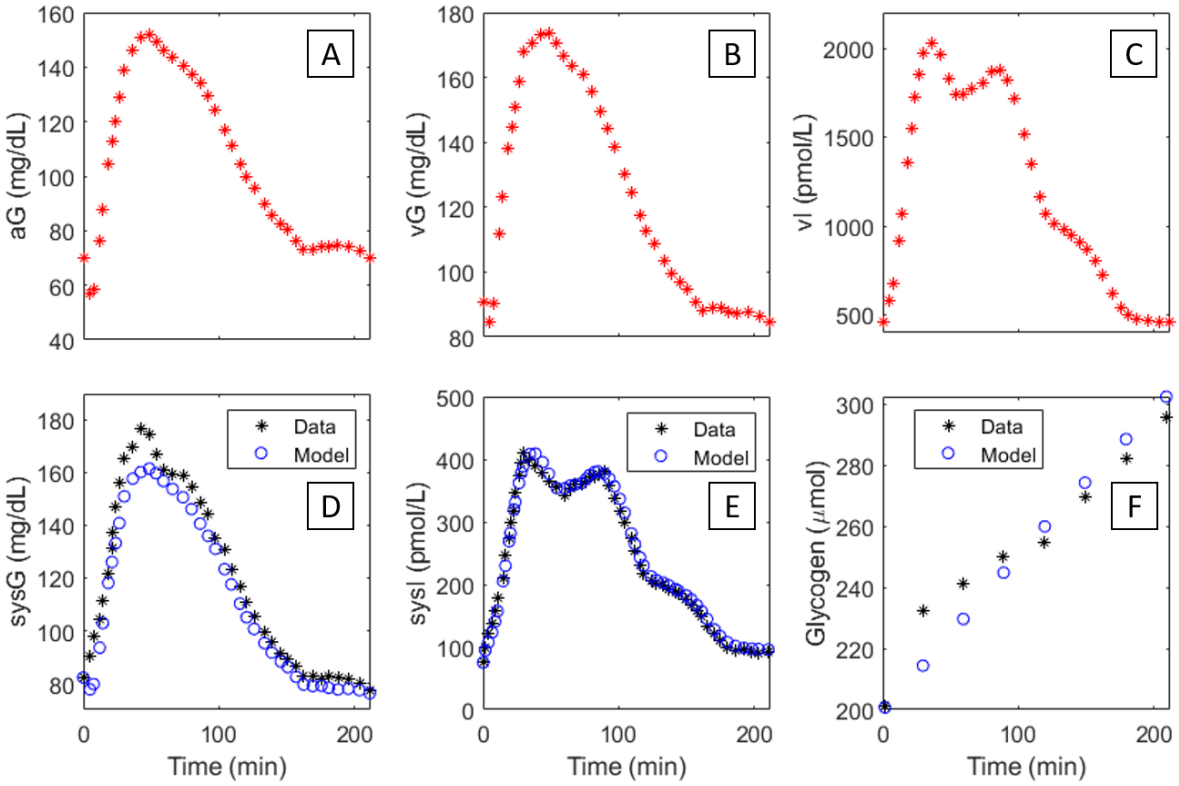


Figure 24. Estimation made by the model compared with experimental data from (152).

Panels A–D represent the inputs: (A) arterial glucose concentration (aG), (B) venous glucose concentration (vG), (C), arterial insulin concentration (aI) and (D) venous insulin concentration (vI). Panels E–F depict the model outputs: (E) systemic glucose (sysG) and (F) systemic insulin (sysI)

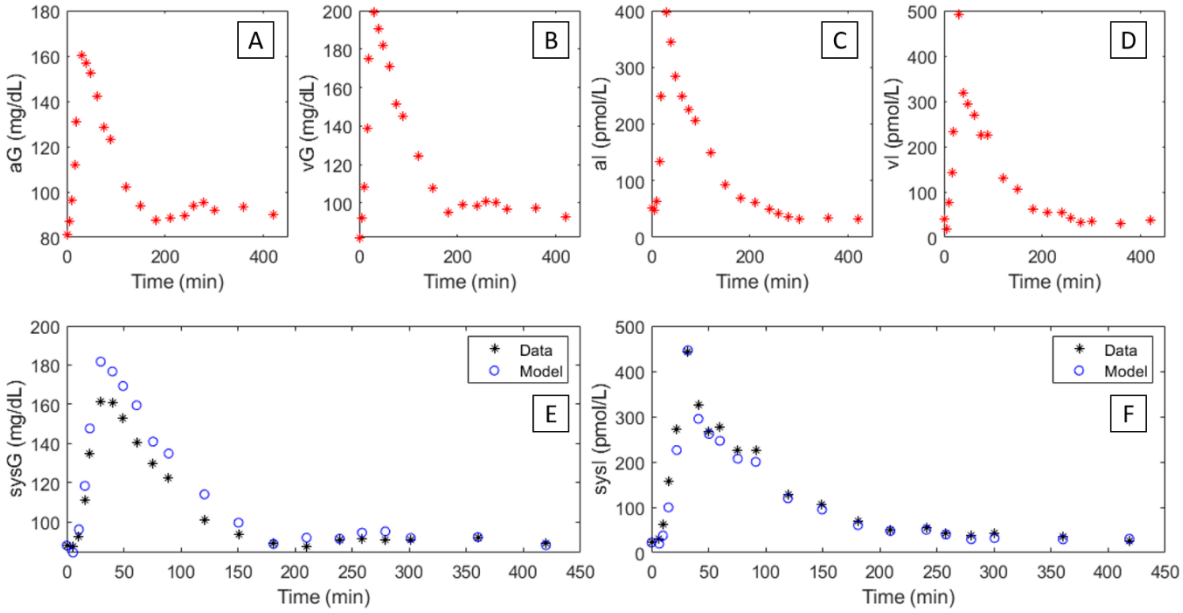
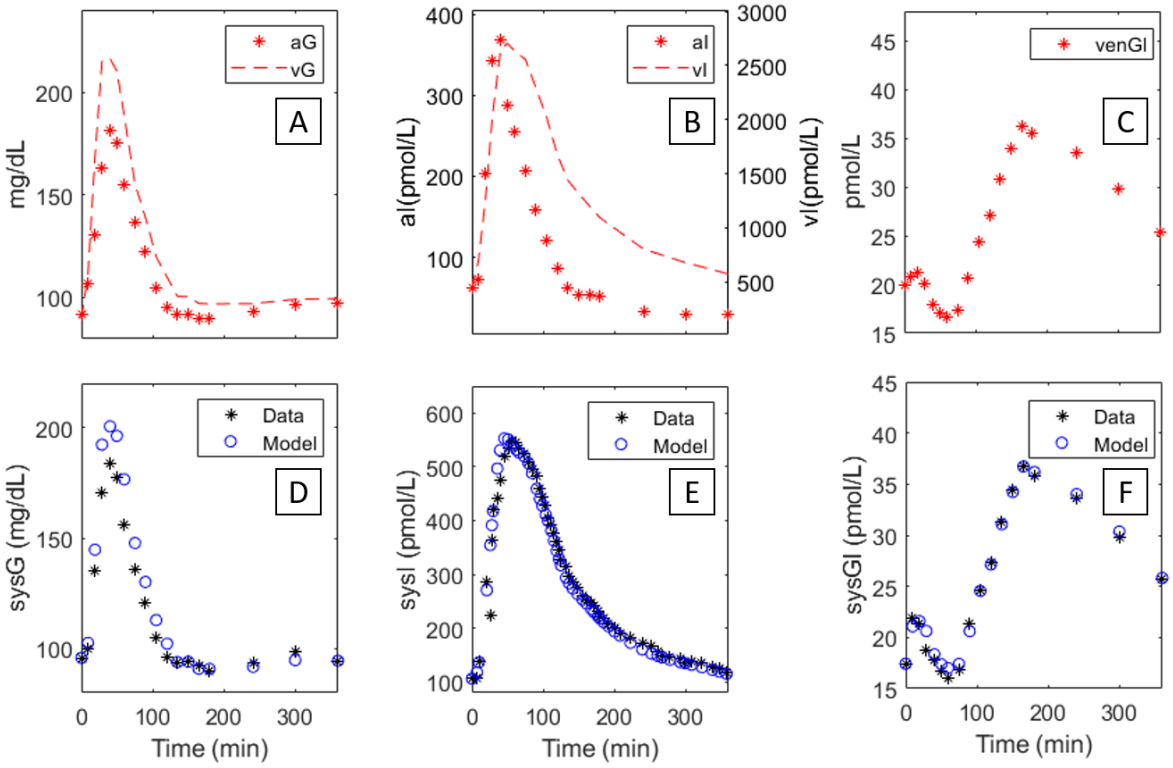


Figure 25. Estimation made by the model compared with experimental data from (151).

Panels A–C represent the inputs: (A) arterial and venous glucose concentration (aG, vG), (B) arterial and venous insulin concentration (aI, vI), and (C) arterial glucagon concentration (aGl). Panels D–F depict the model outputs: (D) systemic glucose (sysG) and (E) systemic insulin (sysI), and (F) systemic Glucagon.



Discussion

This work presents a phenomenological-based model describing the flows of glucose, insulin, and glucagon in both fasting and postprandial states in non-diabetic individuals and the changes in liver glycogen concentrations. The simulation results showed the model's ability in reproducing results from several experimental setups involving different measurement methods, stimuli, and measured variables. Despite the crucial role that the liver plays in glucose metabolism, most mathematical models available in the literature have typically described parts of that role through compartmental models (either minimal or maximal).

Single-compartment models have shown limitations in recreating hepatic glucose production, especially in the non-steady state. Two-compartment models were developed to describe this dynamic during an intravenous glucose tolerance test (IVGTT) (67). Although minimal models are parsimonious, the simplistic mathematical structure makes them prone to averaging the data instead of providing an actual explanation for the experiment. Moreover, in spite of the involvement of certain physiological knowledge (arguably, compartmental modeling is usually built upon strong assumptions to keep the model structure simple), its extension to slightly different conditions is usually not straightforward. The Sorensen model (194) is one of the most complex physiological compartmental models used to describe whole body glucose homeostasis. In the model, two different compartments represent glucose and insulin metabolism. However, the liver's role is simplified to a mass balance equation preventing the model from obtaining estimations of other hepatic processes such as hepatic glucose production.

In (75), the authors developed a maximal compartmental model to describe the so-called glucose-insulin system after a glucose load in both healthy subjects and those with DM2. This model version, which later gave way to the well-known UVA-Padova simulator did not include the glucagon action. In this model, the glucose liver's glucose production is presented in terms of glucose and insulin signals. Several parameters need to be identified from multiple tracer experiments, such as the effectiveness of liver glucose effectiveness, amplitude of the action of insulin on the liver, amplitude of the action of the portal insulin on the liver, and the delay between insulin signal and insulin action. Hepatic insulin metabolism is also incorporated through two clearance terms involving the portal insulin secreted by the pancreas and a more difficult to interpret “delayed” insulin signal Id. The role of glucagon and the use of the simulation model in subjects with DM1 is included in Ref. (195).

In spite of the considerable effort to obtain a model of first principles, we ended up with a highly descriptive model with parameter interpretability and few parameters to calibrate (individualize). As shown in Figures 23, 24 and 25, the predictions made for a virtual

averaged subject coincide with the observed behavior in three different, unrelated experiments.

Other compartmental models involving different aspects of the hepatic glucose metabolism can be found elsewhere (196), or using data related to pharmacokinetics/pharmacodynamics rather than experiments made under physiological conditions (197). Chalhoub et al. proposed a model for the key reactions of carbohydrates metabolism and transport in the liver (196). This model was built with information from previous models and intended to explain carbohydrate metabolism changes related to high-intensity exercise. In addition, this model recreates hepatocytes zonation, a characteristic not included in our model as we were interested in the net effect of the entire liver. The ability of our model to reproduce data from an experiment that measured glucose concentration in the hepatic vein (153) suggests that liver metabolic zonation can be simplified if the modeling objective is the contribution of the entire organ in the glucose metabolism.

Mathematical models can also be used to explain the kinetics of the reactions that take place in glucose metabolism. Glycogen synthesis and degradation are essential for gluconeogenesis. El-Refai (198) and collaborators proposed a detailed six-compartmental model to explain glycogen formation from glucose and vice-versa using plasma glucose concentration, liver glycogen level, and a chemical reaction rate. The model made it possible to describe different liver-related insulin actions to glucose metabolism and carbon incorporation to the glycogen formation cycle via simulation. Figure 23 shows how our model can recreate the liver's glycogen formation after a meal using stoichiometric balances. This information can determine the glucose production rate via glycogenolysis during the fasting state, allowing more extended simulations to be performed.

Mechanistic detailed models like the proposed here can be used to obtain clinically meaningful information. One of the most detailed models for the role played by the liver in glucose metabolism was proposed by König and collaborators. It made it possible to simulate liver carbohydrate metabolism at the molecular level with hormonal regulation

(199). This “stand-alone” liver model was then used to explain the possible mechanisms behind the augmented hypoglycemia risk seen in patients with type 2 diabetes mellitus under insulin treatment (200). As with König's model, our model agrees with the experimental data from the liver's internal process, including the hepatic glucose production, hepatic glucose utilization, and hormonal control, and it recreates both postprandial and fasting states. Unfortunately, to the best of the authors knowledge, a detailed explanation of the set of differential equations is currently unavailable which hampers further comparisons.

Extended models can theoretically have a better predictive ability as they incorporate more physiological information. The proposed model can be integrated with additional models via the circulation to form a digital copy of the human glucose metabolism. Further investigation will be needed to reach the level of progress of currently available simulation models (75, 195, 201, 202). However, in these models, the role of the liver in glucose homeostasis has been simplified to the main functions of glucose uptake and production with less consideration to hormonal and metabolic modulation of these processes; some of these models even consider a constant rate of glucose production. Our model incorporates both hormonal and metabolic modulation in glucose production and uptake, leading to a more precise recreation of the liver's role in glucose homeostasis.

Conclusion

The liver plays an important role in glucose regulation in the human body, but its physiological aspects have been reduced in the existing mathematical models for simplicity. A phenomenological-based model able to reproduce not only the key metabolic pathways but also the complex hormonal regulation can have several applications, for example, in the study the physiology in healthy and non-healthy subjects, as well as in the development of therapeutic interventions for people with diabetes. The methodological approach proposed in this work allows having parameters interpretability resulting in an easy way to adjust the kinetics parameters of the model. It is also versatile due to its basic structure allowing its adaptation to different conditions. Perhaps the only limitation of the model is the large

number of parameters, which makes it difficult to implement in some practices. Finally, this model could be combined with other models to form a whole-body glucose metabolism model.

COUPLING A PHENOMENOLOGICALLY BASED MODEL OF THE GASTROINTESTINAL TRACT TO A PHYSIOLOGICAL MODEL OF GLUCOSE AND DEVELOPMENT OF STUDIA, A MOBILE SOLUTION FOR ITS IMPLEMENTATION

This chapter describes the coupling of the stomach and intestine models and the liver model with an extended version of the minimal glucose model called the Double Triangular Minimum Model (DTMM) (203). This coupled model was implemented in a mobile solution called STUDIA, the STUDIA development process is presented as published (160). STUDIA was subsequently tested in a controlled environment with historical data from people with DM1.

The equations that describe the DTMM are the following:

$$\dot{G} = -S_g G + S g G_b - X S_I G + \frac{f \cdot R_a}{V_g \cdot BW} \quad (1)$$

$$\dot{X} = -p_2 X + p_2 (I - I_b) \quad (2)$$

$$\dot{Q}_1 = -(k_{m1} + k_{md}) Q_1 + m(t) \quad (3)$$

$$\dot{Q}_2 = -k_{m2} Q_2 + k_{md} Q_1 \quad (4)$$

$$\dot{I}_{sc1} = -(k_1 + k_d) I_{sc1} + J(t) \quad (5)$$

$$\dot{I}_{sc2} = -k_2 I_{sc2} + k_d I_{sc1} \quad (6)$$

$$\dot{I} = -nI + \frac{IR_a}{V_I \cdot BW} \quad (7)$$

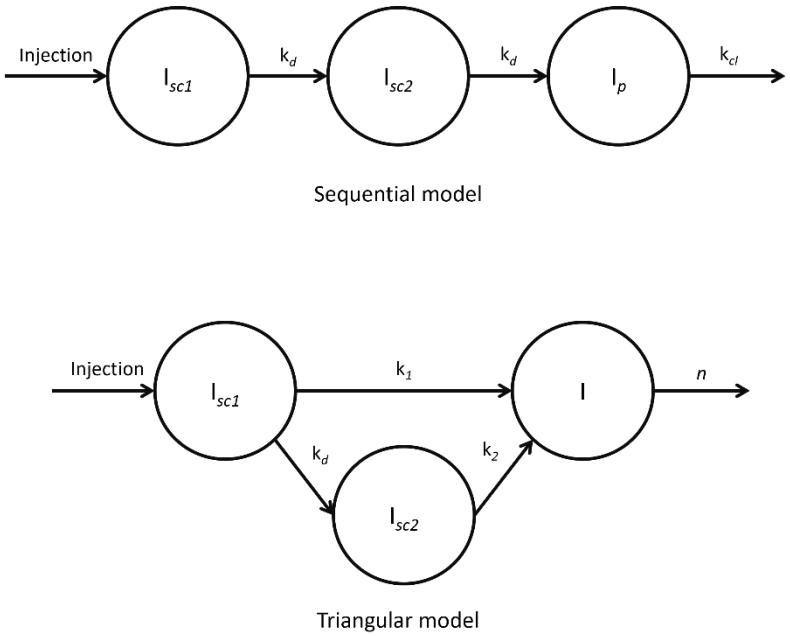
where:

$$IR_a = k_1 I_{sc1} + k_2 I_{sc2}$$
$$R_a = k_{m1} Q_1 + k_{m2} Q_2$$

and G is the concentration of plasma glucose in mg/dL, X is the proportion of insulin in the remote compartment in L/minute, $Q1$ y $Q2$ are the glucose masses in the stomach and intestine in milligrams, respectively, I_{sc1} e, I_{sc2} are the amounts of non-monomeric and monomeric insulin in the subcutaneous tissue in milli Units, respectively. I_p is the amount of insulin in the plasma in insulin milli Units, m is the rate of carbohydrate absorption from a meal (mg/min), J represents the entry of exogenous insulin (mU/min) and BW is the subject's weight. The model parameters can be found in (203).

This model was selected as it is a simple physiological model that improves the physiological representation of insulin injections by modifying the linear arrangement reported in (204) to a triangular arrangement, Figure 26 . Additionally, this model has been used both in experiments with simulated subjects (203) and with prediction strategies in patients with DM1 (205).

Figure 26. Graphical representation of the submodels corresponding to insulin.



The coupling of the models is achieved by replacing two terms of the model with the outputs of the gastrointestinal (107) and hepatic (108) models.

The oral component of the model is given by:

$$R_a = k_{m1}Q_1 + k_{m2}Q_2$$

And from the gastrointestinal model as previously mentioned, this rate of glucose appearance in the splanchnic bed can be obtained as shown in Figure 18, the term f represents the fraction of carbohydrates absorbed by the intestine. R_a that our gastrointestinal model estimates already incorporates this term, as well as the volume of glucose distribution V_g and has been adjusted for the weight of the individual BW.

The DTMM model assumes a constant hepatic glucose production represented by the term SgG_b of the equation, this term can be replaced by the EGP estimated by the liver model. This EGP is the result of the modulation made by insulin, as well as all the processes of glucose utilization and production mentioned above.

The equation for the coupled model is as follows:

$$\dot{G} = -S_g G + EGP - XS_I G + R_a$$

STUDIA: An application to support carbohydrate counting by simulating glucose dynamics

Introduction

Diabetes mellitus (DM) is one of the most common chronic conditions found in Colombia, which ranks second in the region (South America and the Caribbean - SACA) (2). Indeed, its prevalence in adults has been estimated at 8.4% (CI95% 6.0-11.3), which is equivalent to a little less than 3 million people affected in 2017. Chronic hyperglycemia has been linked to the development of microvascular (4, 5) and macrovascular complications (6, 7). Also, high blood glucose is related to acute forms of DM decompensation, diabetic ketoacidosis (DKA), and hyperglycemic hyperosmolar state (HHS) (9). A treatment strategy based on stricter glucose control intended to reduce glycated hemoglobin (HbA1c) to values closer to those of a person without diabetes has been proven to reduce mortality as well as the appearance of micro and macrovascular complications in people with type DM1 (14, 15) and those with DM2 (16, 17).

In the last 20 years, the treatment has also evolved for people with DM2. A better understanding of the disease and its mechanisms allowed for more treatment options and an individualized treatment strategy. However, for people with DM1, the only currently available treatment is still insulin (3). In Colombia, insulin is among the most widely used therapies for adults with DM (23-25), possibly due to drug price regulation policies.

Most patients use insulin based on dose estimates made by their physicians empirically or based on population approximations (26). However, carbohydrate counting is regarded as the ideal way to calculate meal-related insulin doses. It allows greater flexibility in diet and could, in some people, reduce the burden of the disease (3, 27, 44).

The efficacy and safety of carbohydrate counting have recently been reported in a systematic review, in which carbohydrate counting was associated with a significant reduction in HbA1c in both adults and children, standardized mean difference (SMD) -0.52% (95% CI -0.82 to -0.23). Advanced carbohydrate counting, but not the other forms of

carbohydrate counting, significantly reduces the HbA1c, SMD -0.44% (CI95% -0.76 to -0.11), and is higher when compared to standard nutritional education, SMD -0.51% (CI95% -0.83 to -0.19). Carbohydrate counting was not associated with an increase in the risk of hypoglycemia, blood lipid concentration, or weight changes. And it seems to improve quality of life, specifically, in the domains related to the disease or its treatment. And despite being an iterative educational technique, its effectiveness is not affected by its use for up to two years (206).

Several strategies have been proposed to complement carbohydrate counting. For example, some take into account not only the amount but the type of carbohydrates that are consumed (51); others, the macronutrients content of a meal such as fat and protein (53, 54, 207); and others still, simplify the estimation of the carbohydrate content in food (1).

We propose a different approach to complement carbohydrate counting. Carbohydrate counting is a repetitive heuristic process in which, through trial and error, individuals refine their ability to predict blood glucose behavior after a meal based on an estimate of the carbohydrates contained in that meal and the effect that a specific insulin dose has on their body. A dynamic simulation will allow individuals to recreate various "what if?" scenarios where different situations, such as changes in the caloric content or the insulin dose, can be evaluated by an individual in a safe environment. The potential benefits in this specific situation, apart from safety, include greater confidence in dealing with the present case, modifying insulin dose estimates, or modifying caloric intake.

In this paper, we present the development of STUDIA. A mobile app that allows individuals to simulate four-hour postprandial period glucose changes related to a specific meal and insulin dose based on carbohydrate counting and the user’s current glycemic condition.

Methods

Glucose simulation

Using the phenomenological-based mathematical modeling technique, we developed a mathematical model of the role of the gastrointestinal tract in glucose metabolism (208). The model has three submodels: a stomach submodel, which simulates food transformation and rate-limiting for the passage of ingested food to the intestine (114); a second submodel of the small intestine which computes the intestinal glucose absorption rate (115); and a third submodel of the liver calculating the endogenous glucose production (EGP) and regulation of glucose ingested from food (108). This model was coupled with the minimal glucose model, which has been extensively used to study the physiology of glucose metabolism (203). This coupling allows a simulation of the whole body and includes the effect of exogenous insulin that people with DM1 must use.

Requirements engineering for the App

A requirements gathering process was carried out in which the necessary and desired functionalities of the application were initially defined. Next, a person-based approach with potential users' profiles was created using expert knowledge, and this information was then used to identify non-functional requirements. Finally, the possible roles of patients and researchers in the application were defined and, based on these roles, the functionalities described were complemented, and the user stories organized.

Software architecture and design

Initially, the mobile application's most essential needs and functionalities were identified, and possible technological stacks that went hand in hand with the requirements were evaluated. Among those selected were Flutter®, React Native®, Kivy®, and Android studio®. Next, the advantages and disadvantages of using each were identified and evaluated under the criteria of user experience (UX) /user interface (UI), learning curve, flexibility, and the possibility of executing mathematical models with a resolution of differential equations. This last criterion was the one with the greatest weight. Finally, the application's views, colors, and elements were also defined.

Stepper (Step by step) was used to create a mockup of the user inputs before the simulation. A series of views were defined that accompany the operation of the application, including the start view, historical preferences, and favorites. The data from one patient with DM1 who uses an insulin pump was used to generate simulations to show STUDIA results. Continuous glucose monitor (CGM) readings were used for comparison.

Results

The chosen architecture for the mobile app was Android Studio® with support for Android® devices from 5.1 onwards, connected to AWS® for the connection with the databases and the subsequent results analysis. A custom Java method for solving differential equations was also developed.

User interface

STUDIA's user interface consisted of four main features, a login, a previous data search and display, a new record, and a saving simulation feature. The login uses a custom-generated code to guarantee patient anonymity for ethical, legal, and clinical research purposes. STUDIA complies with Colombian law 1581 of 2012 on personal data protection. The login requires a password, which is only needed the first time the application is accessed. After successful login, the user has two options, to review previously stored data or create a new record. For example, if the user chooses to check their historical data, a list of all the user's simulations listed by date and meal is displayed, as shown in Figure 27. In addition, a glucose graph for the specific stored data will be displayed by selecting one of the previous simulations, as shown in Figure 28.

Figure 27. Patients' simulations recorded in STUDIA.

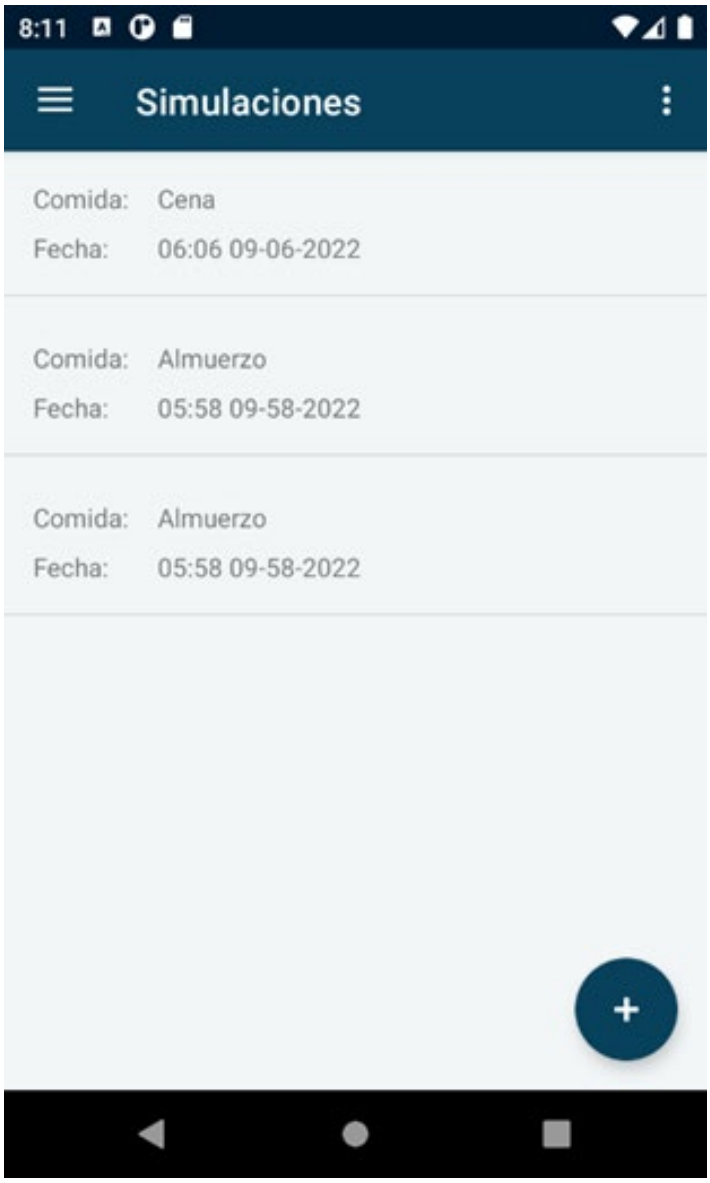
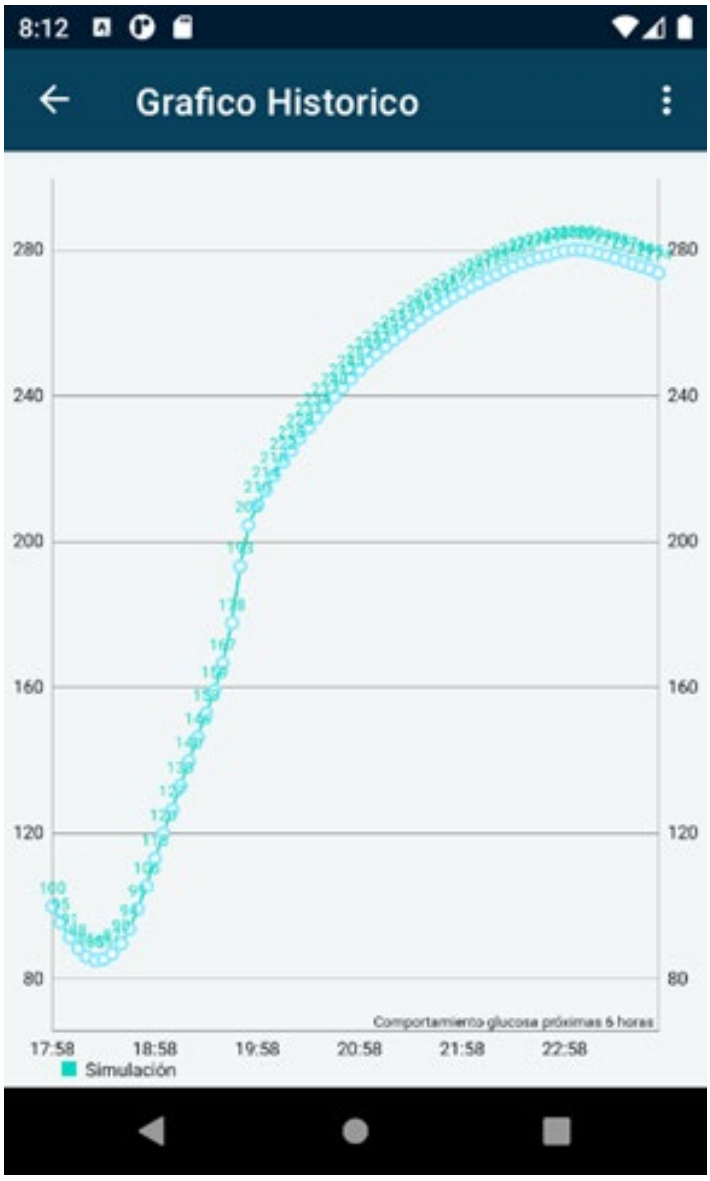


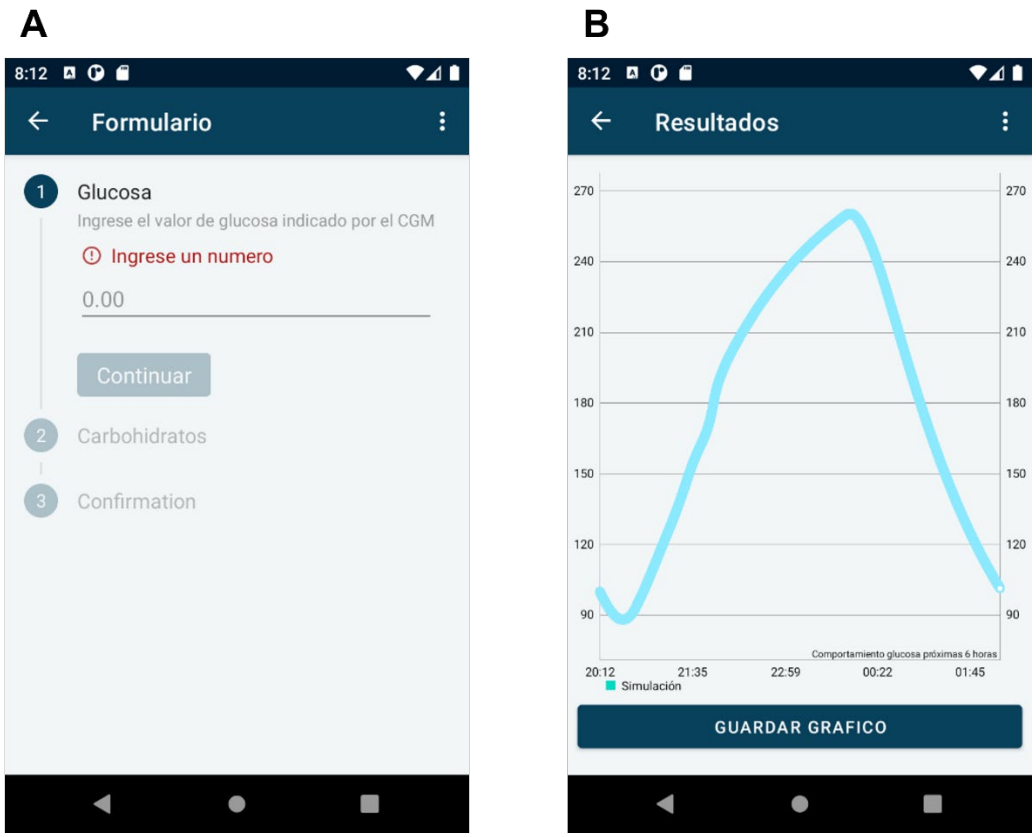
Figure 28. Glucose graph from saved data.



If the user decides to add a new record, STUDIA will ask for the current blood glucose concentration and estimated carbohydrate content of the meal. Then STUDIA will compute the insulin dose based on the individual insulin-sensitive factor and insulin to carbohydrate ratio and simulate the glucose change related to that meal. Finally, the user may choose to save the most satisfying simulation based on the actual insulin dose and meal content, as shown in Figure 29.

Figure 29. New register made for a meal in STUDIA.

A. Input data module. B. Simulation made by STUDIA and saving feature



Administrative interface

The administrative interface has three views where administrators can manage the simulation input variables for each patient and consult, filter, and download the simulation data. The interface is controlled by two different roles: the general administrator who can add patients, and the researcher who can view individual patients and simulation data stored. The Angular® frontend developer was used, as it guarantees good role management, data protection, and interaction with users. The backend connects with the AWS® service, developed with Node js®. Figure 30 shows the administrative interface.

Figure 30. Administrative interface.

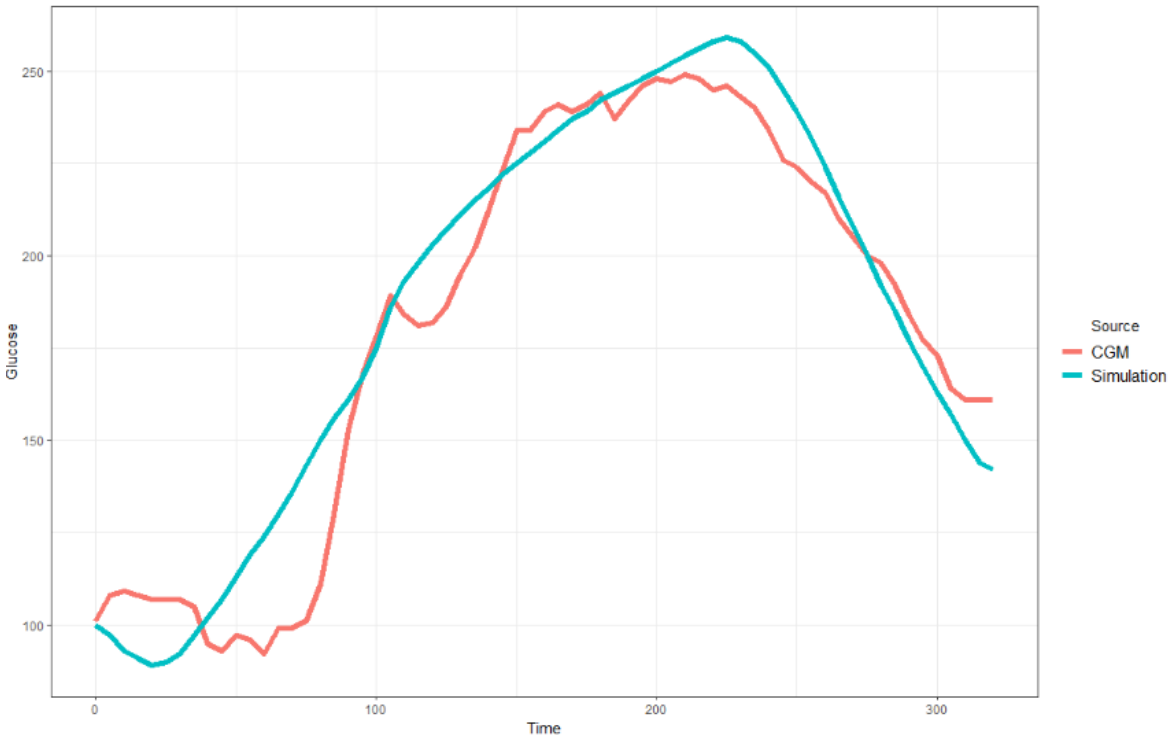


Simulation results

The simulation is generated as shown in Figure 29-B. The layout emulates readings traditionally obtained from a continuous glucose monitor, and we believe that this makes it easier for patients to understand. The patient can simulate several scenarios for the same meal and save these for future analysis. The patient can change either the meal's insulin dose or carbohydrate content in each simulation, allowing for different "what if" simulated situations.

Compared to data from CGM, the App can reproduce the postprandial glucose excursions very precisely. An example of simulated glucose dynamics for patient meal data is shown in Figure 31.

Figure 31. Comparison between CGM reading and simulation.



Discussion

Carbohydrate counting should be the preferred insulin dose estimation technique for most patients with DM1 using prandial insulin. However, one of the concerns associated with this technique that could limit its effectiveness is the lack of precision in estimating the number of carbohydrates in a meal. An overestimation could lead to hypoglycemia and the need to eat or drink fast-acting carbohydrates, while an underestimation leads to lower insulin doses and a risk of hyperglycemia (47). The lack of precision could result from many factors such as the person's experience, the type of training they receive, the frequency with which they practice, and the kind of food they consume and how it is prepared (48). Also, other macronutrients like fat (49) and protein (50), which are not considered in traditional carbohydrate counting, can affect postprandial glucose.

Carbohydrate counting can be seen as a decision-making process. Solving a problem detected in the desired situation requires one or more decisions to be made, which in turn requires knowledge transformation (209). Thus, successful counting will depend on individuals' ability to anticipate glucose change based on an estimate of a meal's

carbohydrate content and insulin needs. But apart from retraining patients in carbohydrate counting, there are not many tools with which patients can safely refine their abilities.

As has been proven in different fields such as administration and management, sports (210), military (211), emergency responders, aviation, among others, decision-making processes can be refined by using simulations. While the above scenarios are not similar to the one experienced by a patient calculating an insulin dose, refinement by repetition is. However, in DM, simulation has been limited but successful in improving physicians' performance in treatment (212, 213), but has not been used by patients themselves.

STUDIA is a tool that can help patients refine their carbohydrate counting and provide a platform for clinical research. STUDIA simulates glucose changes using some of the person's characteristics, meal content, and insulin dose as inputs. But for a dynamic simulation to make useful predictions, it must reliably recreate the phenomenon. In STUDIA, simulations are created using a mathematical model.

Diabetes mellitus has been a subject of interest to mathematical modelers for decades. Ajmera and collaborators (56) offer an excellent review of the models available until 2012 and propose a classification into categories according to the information they use for their construction. *Clinical Models*, which are structurally simple and usually contain only essential biological descriptions, are intended to emulate available clinical data. *Knowledge-Based or Physiological Models*, unlike the former, are primarily mechanistic or first principles. They are designed to describe different biological phenomena related to glucose control, and they usually have a more significant amount of information based on physiological knowledge of the processes. These models could potentially be clinically useful. Models can also be classified according to their purpose (57, 58). Some are used to evaluate diagnostic tests, and others to construct controllers used in artificial pancreas systems. Models can be used to predict the behavior of a condition, for example, diabetes mellitus and its complications, or to evaluate the pharmacological characteristics of drugs such as insulin, or to describe the behavior of glucose in different organs or in the whole body, including hypothetical scenarios. Finally, some models predict the costs associated

with treating diabetes. Based on this, Frietzen and collaborators propose that the models be classified either as *Metabolic and Measurement Models* or *Development Models* (58).

STUDIA would serve as a clinical application of a mechanistic or first-principle model to aid patients in treating diabetes. The only other approach similar to using simulation in such a matter is a pilot study in which patients used a Web-Based Simulation Tool to generate personalized models of glucose metabolism, and it did not bring about a significant change in time in range. Nevertheless, the authors conclude that it could be used to empower people with DM1 (214). We plan to test STUDIA's capability to predict glucose excursions using data for multiple meals from patients with DM1. We also intend to compare the continuous use of STUDIA during four weeks to traditional carbohydrate counting in a clinical trial with a prespecified change in time in range as the primary outcome (ClinicalTrials.gov Identifier: NCT05181917).

Conclusions

We present the first of a kind glucose simulation app based on a phenomenological mathematical model for patients and clinical research use: STUDIA. Simulation may potentially be used to improve carbohydrate counting in people with diabetes mellitus. Complex phenomenological models can have clinical applications. Future work will reveal whether simulation is more efficacious than traditional carbohydrate counting in people with diabetes.

Meal-Related Glycemic Trend Information to Assist Bolus Decision-Making in People with Type 1 Diabetes.

Introduction

Carbohydrate counting is the more recommended meal planning technique to control glucose in people with type 1 diabetes (DM1) (215). Carbohydrate counting not only safely reduces HbA1c in adults and children (206) but also allows a more varied diet (44-46) and reduces the risk of developing microvascular complications (15).

Carbohydrate counting is a decision-making process. One or more decisions must be made to solve a problem detected in the desired situation, which requires transforming knowledge (209). Thus, successful carbohydrate counting will depend on individuals' ability to anticipate glucose changes based on an estimate of a meal's carbohydrate content and insulin needs.

Most decision-making processes can be refined by using model-based simulations. This has been proven in different fields such as administration and management, sports (210), military (211), emergency responders, aviation, and others. While these scenarios are not like the one experienced by a patient calculating an insulin dose, refinement by repetition is.

We present an analysis of the accuracy of a decision support system that uses mathematical models to predict postprandial glucose based on carbohydrate counting and patient parameters.

Methods

Participants

We used the data from five patients with DM1 who participated were enrolled on clinical trial (205), wearing a continuous glucose monitor (Dexcom G6; Dexcom, San Diego, CA) and recorded the estimated carbohydrate content of each meal to compare the prediction capability of a decision support system (DSS).

Decision Support System

A phenomenological-based semi-physical model (PBSM) representing the role of the human gastrointestinal tract, including the stomach (114), the small intestine (107), and the liver (108), in glucose regulation in healthy was developed and then coupled with a compartmental minimal model (160) representing the dynamic relationships between oral carbohydrate ingestion and the transport and action of glucose and insulin in some compartments of the body.

The PBSM of the gastrointestinal tract was constructed following a three-phase methodology presented in (77), in which the process of interest is described, and the objective of the model and hypotheses are proposed. Process systems (PS) were defined by following physical separations within the process, distinguishable phase changes, or characteristics that mark spatial differences, i.e., abstracting the natural partitions of the organs. As the initial division, the entire gastrointestinal system was split into three separate PSs, one for each organ. Additional internal process systems were considered depending on the organ's anatomy and physiology. Still, the fundamental partition was to separate the blood that irrigates the organ from the tissue that makes it up. Over every PS, mass balances are applied to get the model's basic structure, which is extended when constitutive and assessment equations are chosen for defining the model's parameters (116). The mathematical model has 208 differential equations, corresponding to 19 for the stomach, 158 for the small intestine, and 31 for the liver.

The Subcutaneous Oral Glucose Minimal Model has seven differential equations. Interactions between glucose and insulin are captured in a two-state compartmental model; Two compartments represent the gastrointestinal tract, where the oral glucose transport occurs; The last three compartments express the transport of insulin from subcutaneous infusion with an insulin pump to plasma (203). The coupling with the PBSM of the gastrointestinal tract previously introduced consisted of replacing in the minimal model the term $S_G \cdot G_b$ with the hepatic glucose production calculated by the liver model and using the small intestine model to estimate the rate of glucose appearance in the portal

system. This eliminates the need for the submodel representing the gastrointestinal tract in the original minimal model, which reduces it to 5 equations, keeping the original insulin-related equations and changing the dynamics of plasma glucose, as shown in the following equation.

$$\dot{G}(t) = -S_G \cdot G + \frac{HGP}{\Delta t} - X \cdot S_I \cdot G + \frac{Ra_{new}}{V_g \cdot BW}$$

Where G is the plasma glucose concentration in mg/dL, S_g is the fractional glucose effectiveness in L/min. HGP is the hepatic glucose production in mg/dL, X is the proportion of insulin in the remote compartment (L/min), S_I is the insulin sensitive in L/min/mU/L, Ra_{new} is the rate of glucose appearance in the portal system from the intestine in L/min, $V_g$is the distribution volume of glucose in dl/Kg and BW is the body weight in Kg.

Even though the mathematical model has a significant number of parameters (for further details about the equations and parameters of the models, refer to (107, 108, 114), most of them are interpretable and have a physical meaning within the model's context. This simplifies the identification process, leading to only four parameters that require tuning, as shown in Table 16.

Table 16. Parameters identified to fit patient data.

Symbol	Description	Range	Units	Model
S_g	Fractional glucose effectivness.	0.0001-0.02	$\frac{1}{min}$	Minimal model.
S_I	Insulin sensitivity.	0.00001-0.01	$\frac{1}{min}\ per\ \frac{mU}{L}$	Minimal model.
t_{lag}	Lag time for dilution to stop.	0-100	*min*	Stomach model.
$\dot{E}_{8_{iso}}$	Energy flow out of the stomach.	0-4	$kcal \cdot \frac{1}{m}$	Stomach model.

min: minutes, *mU*: miliunits, *L*: liters

Data Background

Data from the CGM four hours after a mixed meal ingestion containing more than 20 grams of carbohydrates and a reported dose of fast-acting insulin was retrieved from the available dataset. Meals are considered if four hours apart from each other. A glucose simulation for each meal was made based on the insulin dose, the carbohydrate content, and the participant's weight. Four model parameters were adjusted for each patient, making these parameters specific for each physiology.

Data Analytics

The graphical patterns of the CGM and decision support system are displayed using smoothed conditional means. A generalized additive model with integrated smoothness estimation was selected due to the number of observations. This graphical representation was selected due to its effectiveness allowing plotting patterns without overplotting. The mean absolute error (MAE) and mean fundamental relative difference (MARD) were computed.

Although the simulation is not an actual glucose measurement, its agreement with the actual glucose trace should be assessed if it aims to assist this sensitive decision-making. As the differences between methods did not follow a normal distribution, a non-parametric approach was used to estimate the limits of agreement (216). There is no reported reference value for the difference between a glucose prediction and the blood glucose, so we present the percentage of observations within a difference of 20, 30, and 50 mg/dL. Considering that the model estimates blood glucose and the comparison is made with interstitial glucose from a CGM, a difference between 15 and 30% could be expected (217-219).

To incorporate the clinical significance of a possible glucose measurement error, a consensus has recommended an error grid to evaluate the clinical risk associated with a glucose measurement method (220). This same principle can be used to estimate the clinical risk associated with a simulation if it is used to aid decision-making. Therefore, the

potential clinical risk derived from the measurement and prediction disagreement was evaluated using the glucose error grids (220).

Ethical considerations

Ethics approval for this research is not required. No personal identification data was collected during the investigation. Each participant was identified using only a code. No member of this research had access to the code's identity.

Results

Individual data from the participants are presented in Table 17. A total of 67 meals with 3158 glucose measurements were simulated. The simulated meals contained 37.88 ± 14.96 grams of carbohydrates.

Table 17. Patients' characteristics.

	Subject 1	Subject 2	Subject 3	Subject 4	Subject 5
Age, years	31	24	51	55	27
Weight, kilograms	83	68.5	77.2	56.85	84.2
Height, centimeters	168.2	161.5	181	168.5	167.2
HbA1c, %	6.3	8.6	6.7	6.6	6.8
Total daily insulin dose, units	48.67	38.5	27	30	39.8

The MAE between the two methods was 15.32 ± 23.02 mg/dL, and the MARD was 10.12%. In Figure 32, the smoothed conditional means are shown; in Figure 33, each individual's selected meals are presented.

Figure 32. Smoothed conditional means.

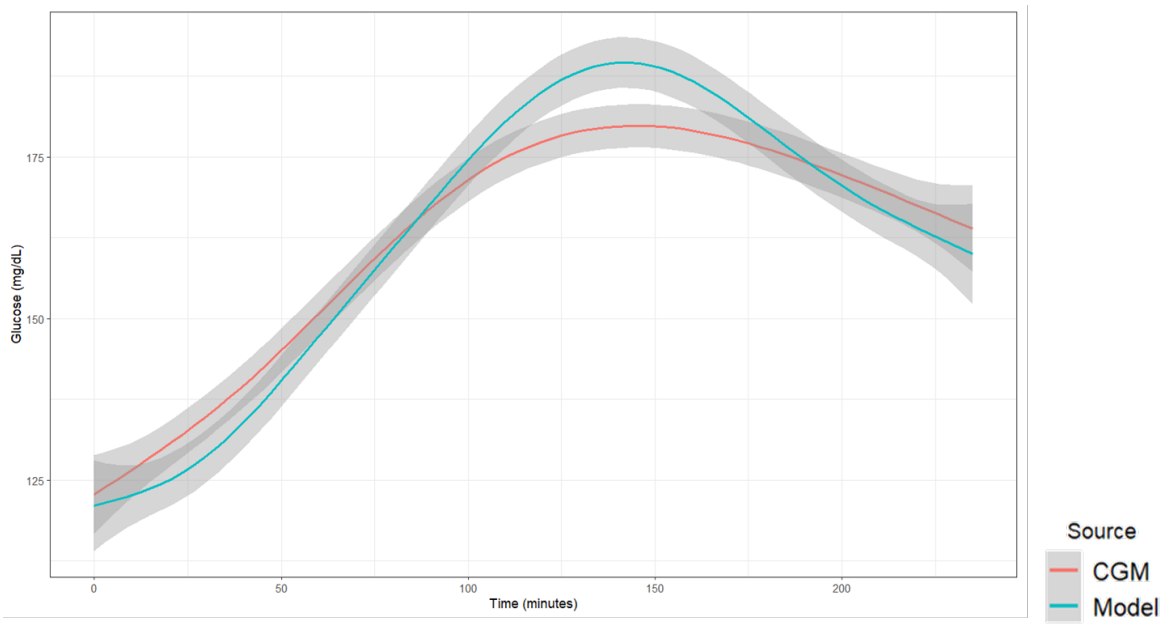
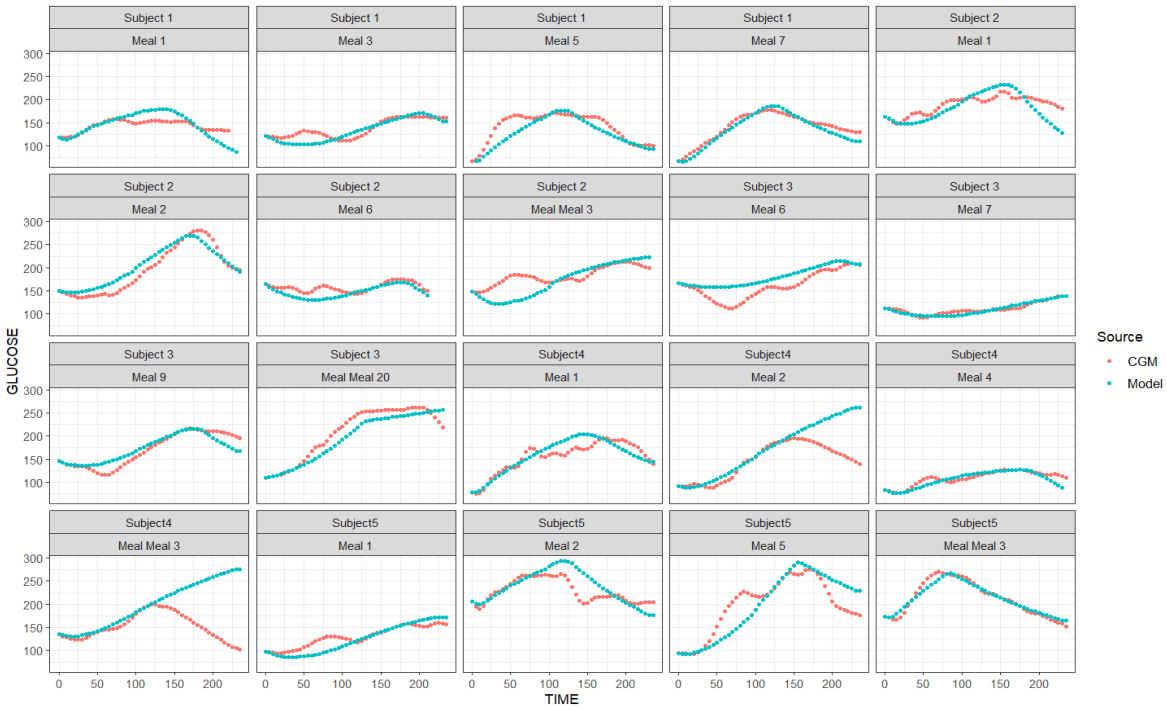


Figure 33. Individual glucose simulations.



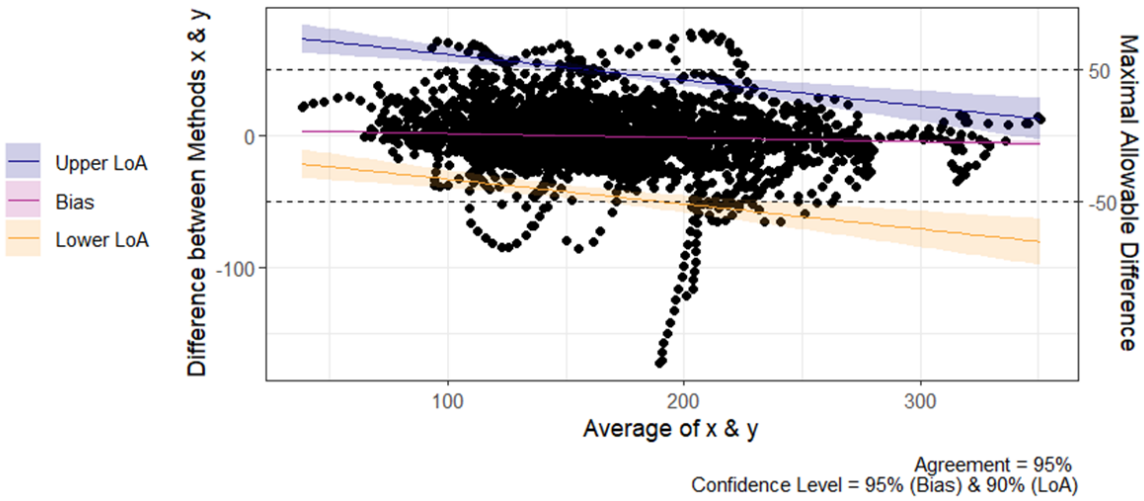
Agreement

A total of 3158 differences between both methods were evaluated; 95% (CI95%, 94% to 96%) of the differences were lower than 50 mg/dL. Table 18 summarizes the observation within a difference of 20, 30, and 50 mg/dL. The limits of agreement for a 50 mg/dL difference are presented in Figure 34.

Table 18. Proportions of differences within the proposed values.

	20 mg/dl (95%CI)	30 mg/dl (95%CI)	50 mg/dl (95%CI)
Differences	0.74 (0.72 - 0.75)	0.87 (0.86 a 0.88)	0.95 (0.94 a 0.96)

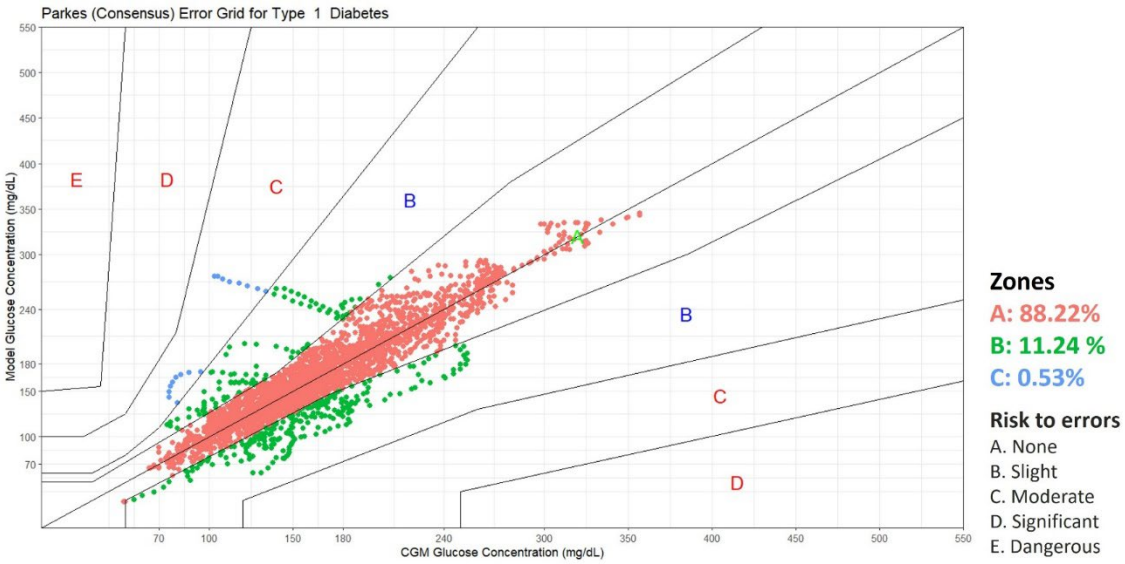
Figure 34. Limits of agreement within 50 mg/dL.



Error grid analysis

The error grid analysis is presented in Figure 35. 99.46% of the measurements fell within zones A and B. No measurement fell on zones D or E.

Figure 35. Error grid analysis.



Discussion

A decision-making support system based on mathematical physiologic models accurately predicts the glucose trend for a specific meal with minimal parameter adjustments. Simulations allow recreating risky scenarios in a safe environment to refine a given process; CC errors are directly related to postprandial hyper or hypoglycemia in people with DM who count carbohydrates for insulin dose estimation. In DM, simulations have been extensively used to design technology, educate medical doctors, but very rarely to educate patients. To the best of the author's knowledge, the only reported experience relates to a pilot study where a web-based simulation tool was used for model personalization. However, no significant results were achieved. Still, the results suggest that it could be used to empower people with DM1 (214).

A glucose metabolism physiological model can serve several purposes, so there is no single method for comparison with the actual glucose concentration. The MAE provides a straightforward, simple-to-understand measurement of the model "mistakes" and has been extensively used to compare models in different fields. As it is expressed in mg/dL, it is easy to comprehend and gives a lineal score for the prediction error. The decision-making support system has a low MAE. However, there is no consensus on an acceptable error margin for a glucose model to predict glucose trends after a mixed meal for a four-hour prediction horizon.

The MARD has been used to assess the accuracy of several blood glucose monitoring systems, including continuous glucose monitoring (221-224). Although it is also a lineal score, a lower MARD has been associated with a lower insulin dose error (221).

The results from the error grid analysis suggest that this decision support system may safely aid in the decision-making process of carbohydrate counting in people with diabetes. The decision support system will be tested on a clinical trial (ClinicalTrials.gov Identifier: NCT05181917) where an app will be used to generate the simulations (STUDIA) as a persuasive tool, allowing the patients to change either their insulin dose or meal content.

This study has some limitations. First, although the model parameters were easily adjusted, this was done for each patient, and some changes were made between the meals for some parameters, given that not the macronutrient from the meal were available, only carbohydrate amount. Also, the small sample size limits the results' generalization. Finally, simulating only postprandial meals prevents the analysis of hypoglycemia events, a critical glucose simulation outcome.

Conclusion

Improve carbohydrate counting in people with DM1 may be possible using a decision support system based on carbohydrate counting. Accurate predictions may help people make better choices, but this must be proven in a clinical trial. The adjustment of model parameters for each patient was not a difficult task due the interpretability of model

parameters to be adjusted. The possible time evolution of some of these parameters could be captured by using an adaptive on-line technique.

A NOVEL SIMULATION-BASED DECISION SUPPORT SYSTEM INCREASES THE TIME IN RANGE AND REDUCES HYPOGLYCEMIA IN PEOPLE WITH TYPE 1 DIABETES

This chapter presents the results of a clinical trial that compares carbohydrate counting using STUDIA decision support system to traditional carbohydrate counting in people with type 1 diabetes (ClinicalTrials.gov Identifier: NCT05181917). The protocol of this clinical trials is available at (225).

Introduction

Diabetes mellitus (DM) is one of the most prevalent chronic non-communicable diseases globally. In 2019, it was estimated that 463 million people lived with DM worldwide; by 2045, that number is expected to rise to 700 million. The prevalence of DM in adults in Colombia is estimated at 8.4% (CI95% 6.0-11.3), a little less than 3 million people affected in 2017, ranking second in the region (South America and the Caribbean - SACA) (2).

High blood glucose concentrations characterize DM, and chronic hyperglycemia has been linked to the development of microvascular (4, 5) and macrovascular complications (6, 7). Also, high blood glucose is related to acute forms of DM decompensation, diabetic ketoacidosis (DKA), and hyperglycemic hyperosmolar state (HHS) (9).

A treatment strategy based on stricter glucose control intended to reduce glycated hemoglobin (HbA1c) has been shown to reduce mortality and the risk of micro and macrovascular complications in people with type 1 DM (DM1) (14, 15) and type 2 DM (DM2) (16, 17). Therefore, HbA1c has become the preferred method to monitor the treatment of people with DM, and its reduction is associated with a lower risk of complications. There is consensus that an HbA1c goal should guide the treatment strategy and be individualized (18).

Drug Regulatory agencies recommend determining the minimum expected reduction in HbA1c to consider approval of new therapies for treating DM(20). Still, for non-pharmacological interventions, there is no formal recommendation. However, some authors have proposed that at least 0.3% reductions in the HbA1c value could be clinically significant (21, 22).

Carbohydrate counting is a meal planning technique developed in the early 1900s in which the dose of insulin given with each meal is based on the amount of carbohydrates. It became popular with the Diabetes Control and Complications Trial (DCCT) results. Individuals assigned to a strict treatment strategy and insulin dose adjustments guided by carbohydrate counting experienced a significant reduction in the risk of developing microvascular complications and an additional 0.5% reduction in HbA1c (15).

A systematic review has recently reported the efficacy and safety of carbohydrate counting. Carbohydrate counting was associated with significantly reducing HbA1c in adults and children, DMS - 0.52% (95% CI -0.82 to -0.23) without increasing the risk of hypoglycemia or significant changes in blood lipids concentration or weight. It also seems to improve the quality of life, specifically in the disease or treatment domains. Despite being an iterative education technique, its effectiveness is not affected by its use for up to two years (206).

However, carbohydrate counting is not perfect, and lack of precision could result from factors such as the person's experience, the type of training they receive, the frequency with which they practice, the kind of food they consume, and how it is prepared (48). Also, other macronutrients like fat (49) and protein (50), not considered in the traditional technique, can affect postprandial glucose. Therefore, several strategies have been proposed to complement CCHO. For example, some take into account not only the amount but also the type of carbohydrates that are consumed (51), others the amount of other macronutrients such as fat and protein (53, 54, 207), and others simplify the estimation of the carbohydrate content in food (1).

Carbohydrate counting is a repetitive heuristic process in which, through trial and error, individuals refine their ability to predict blood glucose behavior after a meal based on an

estimate of the amount of carbohydrates in that meal and the effect that a specific insulin dose has on their body. A dynamic simulation allows individuals to recreate various "what if?" scenarios where different situations, such as changes in the caloric content or the insulin dose, can be evaluated by an individual in a safe environment. Besides safety, the potential benefits in this situation include greater confidence in dealing with the present case, modifying insulin dose estimates, or modifying caloric intake. But for a dynamic simulation to make useful predictions, it must reliably recreate the phenomenon, and one way to do so is through mathematical modeling.

Using a mathematical modeling technique proposed in (77), this research team developed a phenomenological-based semiphysical model (PBSM) of the gastrointestinal tract's role in glucose metabolism (107, 114). Furthermore, this model was coupled to the minimal glucose model with a triangular subcutaneous insulin model (108), allowing for simulating glucose changes and the effect of exogenous insulin that people with DM1 must use.

Rationale

One of the main goals of diabetes treatment is to reduce the risk of micro and macrovascular complications, and reasonable control of blood sugar levels is the best strategy currently available to achieve this. Therefore, patients with DM1 need to calculate the correct doses of insulin. Carbohydrate counting is the most widely recommended strategy for that calculation because it significantly reduces HbA1c (42, 43, 226) and allows patients to eat a more varied diet (44-46).

Carbohydrate counting can be seen as a decision-making process. One or more decisions must be made to solve a problem detected in the desired situation, which requires transforming knowledge (209). Thus, successful carbohydrate counting will depend on individuals' ability to anticipate glucose change based on an estimate of a meal's carbohydrate content and insulin needs.

Human decision-making processes can be refined by using simulations. This has been proven in different fields such as administration and management, sports (210), military (211), emergency responders, aviation, and others. While these scenarios are not like the

one experienced by a patient calculating an insulin dose, refinement by repetition is. Nevertheless, in the context of diabetes mellitus, simulation has shown limited yet successful outcomes in enhancing physicians' treatment proficiency (212, 213) ; however, its impact when used by patients remains to be fully realized.

Intervention choice: The intervention, a Simulation-Based Decision Support System named STUDIA, supports carbohydrate counting by predicting blood glucose levels after a meal using a phenomenologically based semi-physical mathematical model. STUDIA has several advantages over traditional carbohydrate counting. First, it considers the effects of other macronutrients, such as fat or protein, on blood glucose concentration. Adding the protein/insulin ratio and carbohydrates show to improved postprandial glucose control (52). Also, fat has an essential effect on postprandial glucose dynamics, making it more challenging to estimate the insulin dose and timing in people who count carbohydrates (227). STUDIA incorporates a fixed fat and protein ratio based on the reported ratios of mixed meals used in experiments (151). Having this information allows for better-informed decisions about insulin doses. In addition, STUDIA provides information on changes in blood glucose before insulin administration or food intake, acting as a behavior-persuasive tool for diet or insulin dose variations at each meal. Finally, STDUIA is easy to use (160).

Comparator choice: The comparator for this study is carbohydrate counting, as it is the most widely recommended technique for calculating the prandial insulin dose in patients with DM. In addition, carbohydrate counting efficacy and safety profile are well known (34, 42, 43). They have also been the comparator for alternative prandial insulin dose adjustment strategies such as Glycemic Load (GL) (51) and Food Insulin Index (FID) (54), among others (1, 52).

Techniques inferior to carbohydrate counting were not chosen as the effect of the intervention would be magnified. On the other hand, several methods have similar or superior results to those obtained with carbohydrate counting, but these are not widely used.

Outcome choice: The primary outcome of this study is time in range (TIR) derived from continuous glucose monitoring (CGM). Today, CGM is more widely available through real-time or intermittent scanning, allowing for almost instantaneous data on glucose changes in patients. This results in a very efficient way of monitoring blood glucose-related changes in DM therapy. In the past, one of the difficulties of using CGM was the lack of standardization in its interpretation. However, an international group of experts recently proposed the ten measures of clinical utility that should be recorded in the evaluation of CGM, including TIR, which has the most significant clinical utility (228). TIR can be expressed as a percentage of time or the number of hours or minutes that a patient remains in a given range of glucose values for the duration of the CGM measurement. By consensus, TIR has been adopted as the time that an individual remains with blood glucose concentrations between 70 to 180 mg / dL (228). This definition of TIR was used during this clinical trial. The patient's time outside this range is called "time out of range" for glucose concentrations higher than 180 mg/dL time out of range in hyperglycemia and values below 70 mg/dL time out of range in hypoglycemia.

TIR has several characteristics that make it attractive. First, changes can be observed in short periods. Second, its relationship with HbA1c has been well established. Even in periods as short as seven days, it correlates very well with HbA1c values. Third, there is a linear relationship between TIR and HbA1c. Changes of 0.8% in HbA1c correspond to changes of 10% in TIR (229). And like HbA1c, improvement in TIR is associated with a lower risk of microvascular complications (230). Based on the acceptance that a strategy that reduces HbA1c could reduce the risk of complications related to DM, that changes in TIR have a linear relationship with changes in HbA1c, and that TIR correlates with the risk of developing microvascular outcomes, this glycemic control metric was selected as the outcome.

There is a lack of consensus around what should be a minimal clinically significant change in TIR. Drug regulatory agencies have recommended determining the minimum expected reduction in HbA1c to consider approval of new therapies for treating DM (20). Still, for non-pharmacological interventions, there is no formal recommendation. However, some

authors have proposed that at least 0.3% reductions in the HbA1c value could be clinically significant (21, 22). Based on the correlation between HbA1c and TIR, a change in TIR of 3.75% will relate to a change in HbA1c of 0.3%.

Hypothesis and objectives

Hypothesis

A strategy based on carbohydrate counting supported by a simulation of postprandial glucose behavior is superior to traditional carbohydrate counting to induce an increase of at least 3.75% in the TIR of glucose in 4 weeks in adults with Type 1 diabetes mellitus receiving multiple-dose insulin therapy or continuous insulin infusion therapy with an insulin pump.

Objectives

Primary objective

To determine whether a strategy based on carbohydrate counting supported by a simulation of postprandial glucose behavior for four weeks increases the glucose range (70 to 180 mg/dL) in people with DM1 compared to a strategy based only on carbohydrate counting.

Secondary glucose control objectives

Determine whether carbohydrate counting supported by a simulation compared to traditional carbohydrate decreases the average time above range (TAR), time below range (TBR), and glucose variability.

Safety objectives

Determine whether carbohydrate counting supported by a simulation compared to traditional carbohydrates relates to an increased risk of DKA, HSS or hypoglycemia events.

STUDIA agreement with the CGM readings objectives

Determine the agreement between the phenomenological-based model and the postprandial glucose measured by continuous glucose monitoring. And the potential clinical risk from using STUDIA.

STUDIA usability and patients reported objectives

Describe the adherence to STUDIA and its usability. Also, the decisions made by individuals assigned to the STUDIA group related to food choices and insulin dose. Finally, describe the diabetes-related treatment satisfaction.

Study design

This study evaluates the carbohydrate counting supported by a simulation strategy in a superiority randomized, parallel-group, open-label clinical trial with a change in TIR at 28 days (4 weeks) as the primary outcome and 1-1 allocation.

Methods

Study setting

Patients with DM1 previously trained in carbohydrate counting whose follow-up was feasible were recruited from university hospitals and clinics dedicated to treating people with DM in Medellín, Colombia.

Eligibility criteria

Inclusion criteria

The following were the inclusion criteria for the clinical trial:

- Age: Adults 18 years old or older.
- DM1 with at least one year since diagnosis.
- Treatment with a multiple daily injection scheme or insulin pump.
- Trained in advance carbohydrate counting.
- Have an HbA1c below 10% three months before the randomization.
- Deemed fit to used STUDIA.

Exclusion criteria

Patients with one of the following criteria will be excluded from the trial:

- Confirmed or possible diabetic gastroparesis.
- Chronic renal disease and an estimated filtration rate of 65 ml/min/1.73m2 or less using the CKD-EPI (Chronic Kidney Disease Epidemiology Collaboration) equation.
- Patients treated with any other medication different from insulin for DM.
- Pregnant women.

Interventions

Intervention description

The intervention, the STUDIA decision support system, is based on advanced carbohydrate counting aided by a simulation of the possible changes in blood glucose in response to the intake of three main daily meals, a smartphone app developed by the research team that incorporates the model, and a carbohydrate counter. STUDIA allows for a more informed decision-making process using a graphical display of glucose changes like a CGM system. Details on how the system is parametrized and the simulations are generated can be found in (160).

Carbohydrate counting supported by a simulation: Patients assigned to the intervention group had the STUDIA app installed on their mobile devices. As STUDIA was developed for the Android® operating system (OS), those participants without an Android® phone were provided with one with STUDIA preinstalled for the duration of the trial. STUDIA has two functions: an insulin bolus calculator and a graphical interface displaying a glucose tendency curve four hours after a meal. This graph is built using the estimations made by the model (107, 108, 160).

Carbohydrate counting: The patients assigned to the control group also had installed the STUDIA app on their mobile devices, but the graphical interface was disabled, receiving only the insulin dose information.

Adherence to the intervention

During the study, adherence to the intervention was actively evaluated. At each visit, the researchers had access to the frequency of use of the application and were instructed to reinforce its use by participants. Patients were advised to use the app to simulate daily meals.

Cointerventions

Since only patients with DM1 were recruited, no treatment for DM different from insulin, either with a multiple injection scheme or an insulin pump, was allowed. Patients continued their usual care during the study with the visits that their physician considered pertinent.

Protocol discontinuation

Clinical trial participation was planned to be discontinued for reasons related to safety or participants' preferences; details can be found in the published version of the protocol (225).

Outcomes

Primary outcome

Primary outcome

Time in range (TIR) is expressed as the ratio between the number of hours a patient spends between 70 and 180 mg / dL glucose range and the total number of hours of monitoring (50). Data was taken for four weeks. This follow-up time was selected because, although the 14-day data correlate very well with the glycemic control of approximately three months and with the average glucose and hyperglycemia metrics, it would appear that four weeks is the time deemed necessary to adequately evaluate the time in hypoglycemia (231, 232).

Secondary glucose control outcomes

Time above range (TAR) (> 180 mg / dL) and time below range (TBR) (<70 mg / dL) were calculated as the TIR. As a measure of glycemic variability, the change in the coefficient of variation of glycemia in the 28 days of measurements is described in both groups.

Safety outcomes

For the safety outcomes, the following definitions were used.

Hyperglycemic crisis: To define an episode of DKA or HSS, the definition proposed by the American Diabetes Association was followed (233). Criteria for the definitions are presented in the supplementary Table 1.

Hypoglycemia: Hypoglycemia was defined according to the recommendations made by the American Diabetes Association, the European Association for the Study of Diabetes (234), and the International Consensus for the use of the CGM (235) as episodes longer than 15 minutes as follows:

Grade 1 hypoglycemia: A glucose value of less than 70 mg/dL.

Grade 2 hypoglycemia: A glucose value of less than 54 mg / dL.

Grade 3 hypoglycemia: Any glucose value that produces sufficient cognitive impairment to require the assistance of a third party.

STUDIA agreement with the CGM readings

To assess the agreement between the prediction made by STUDIA and the CGM readings, the difference between each glucose measurement for each simulation of the control group patients was used to estimate the limits of agreement as proposed by Bland and Altman, the proportion of difference that fell below a meaningful difference and the potential clinical impact of the differences. Also, the model's mean relative difference and mean absolute relative difference compared to the CGM were calculated.

STUDIA usability and patients reported outcomes

Participants in both groups were instructed to use STUDIA to simulate glucose changes with the three main meals of the day. To measure the actions conducted by users of the application, it contains a survey of 4 questions to be answered after each calculation: changes in insulin dose, planned meal amount, or neither.

A System Usability Scale was applied at the end of the study to evaluate STUDIA usability. This scale consists of 10 questions, each of which can be scored from 1 to 5, where one is total disagreement and five is complete agreement. Despite its simplicity, the scale has been widely used to measure systems, applications, and objects' usability and has been adapted to Spanish (236).

Finally, Patient-reported outcomes were measured using the Spanish version of The Diabetes Treatment Satisfaction Questionnaire (DTSQ) (237). Patients completed the questionnaire during their first and final visits. The DTSQ comprises eight questions, of which 6 assess different domains of treatment satisfaction. Each question is scored on a 7-point Likert scale from 0 (very dissatisfied) to 6 (very satisfied). Two additional items,

perceived hyperglycemia and perceived hypoglycemia, are assessed through 2 questions using a 7-point scale from 0 (none of the time) to 6 (most of the time) (238).

Patient chronology

The primary outcome, TIR, was computed based on the continuous glucose monitoring (CGM) data (228). All patients considered eligible to be randomized by their physicians were invited to participate in the study. All the information and informed consent was sent to them digitally. Those who decided to participate received an electronic eligibility questionnaire based on the inclusion and exclusion criteria. The chosen patients were invited to an initial visit to receive training in the STUDIA app. Data from the CGM and patient characteristics were used to adjust the model. Then, patients were randomized to the intervention or the control group. The patients had a telephone follow-up every week for four weeks by one of the researchers. During the follow-ups, the researcher obtained continuous glucose monitoring data, questioned the patient about adherence, and asked about possible outcomes of interest. During the study, their physicians adjusted the patients' insulin therapy if necessary, following local or international clinical practice guidelines on treating people with DM1|. On the first and last visit, all patients completed the DTSQ. On the previous follow-up, the application's patients completed the Usability Scale.

Sample size

The sample size was calculated based on the primary outcome, i.e., the expected difference in the TIR. No studies have been conducted to evaluate the effect of a simulation on the TIR in patients using continuous glucose monitoring. However, in clinical trials of adult patients with DM1, differences in the TIR have been reported as being between 4.5% (95% CI 4.25 to 4.91)(239)and 9.6% (IC95% 8.0 to 11.2%) (240)with the use of CGM over 16 weeks.

Twenty-eight patients, 14 per group, were required to estimate the difference in the TIR using a mixed-effects model assuming a standard deviation of 4%, a statistical power of 90%, a type I error rate of 0.05%, and intra-subject variability of 5%, and inter-subject variability of 9% (240). Experiments evaluating carbohydrate counting have reported 0 to 46% withdrawal rates, higher as follow-up time increases (38, 51, 54, 207, 241-243). The

sample size was adjusted to 15 patients per group to admit a withdrawal rate of 10% in the intervention group, assuming that no patients in the control group could access the intervention. To maintain statistical power sample size was adjusted by the factor obtained using the formula $(1-\rho_t)^2$ were $\rho_t$represents the retirement ratio, as proposed in (244).

Recruitment

Participants were recruited from University Hospitals and clinics specializing in the treatment of DM1, to which patients are referred for treatment with an insulin pump or CGM support in Medellín, Colombia. Participants were invited to the study by their treating physicians or diabetes coaches at each site.

Random sequence generation

Using the Sealed Envelope Ltd. web application, participants were randomly assigned to the intervention or control group in a 1-1 ratio by a sequence of computer-generated random numbers using the Sealed Envelope Ltd. web-based central randomization system.

Allocation concealment mechanism

Allocation concealment was maintained using the Sealed Envelope Ltd. web-based central randomization system. This system used an allocation code known only by the study coordinator. It was revealed after the last evaluation visit, preventing the researcher from knowing the group to which the patient was assigned.

Random sequence implementation

The Pablo Tobón Uribe hospital research unit implemented randomization during the study. The study coordinator accessed the Sealed Envelope Ltd. web page and generated a code for each participant on their first visit. Within the web page, the codes (A and B) and the assignment of each code to one of the arms of the study (A for the STUDIA group and B for the control group) were prerecorded. Doing so ensured the independence of the researchers and those responsible for data analysis.

Blinding

Due to the nature of the intervention, participants and investigators were not blinded. Instead, those responsible for data analysis were unaware of the assigned group until the last patient's final follow-up.

Data collection methods

The data was collected using the code assigned to each patient during the generation of the randomization sequence, and the databases were built weekly with the following information:

Time in and out of range: The time in and out of range was obtained using the manufactured CGM system platform (Freestyle Libre; Abbott, Alameda, CA). Data was obtained each week by one of the investigators.

Glycemic variability: The glycemic variability was calculated based on the data obtained from the CGM.

Hypoglycemic and hyperglycemic crisis episodes: At each follow-up, one of the investigators inquired and recorded the hypoglycemic and hyperglycemic crisis episodes from the past week.

STUDIA agreement with the CGM readings: The data to compute the differences used to estimate the deal was the CGM readings that were stored on the CGM system platform and were retrieved for each participant at the end of the study and the glucose estimations that STUDIA made were stored on a server (160) and also retrieved at the end of the trial. These data were then matched by date and time.

Actions carried out by the participants: The patient's decision was reported in the STUDIA app and stored on a server (160).

Usability of the application and treatment satisfaction: The participants completed the usability scale during the last visit. And they completed the DTSQ on the first and last visit. This data was stored on a server and subsequently analyzed (160).

Retention

Given the short follow-up time, no losses were expected. However, all reasonable efforts were made to ensure follow-ups. The next visit was scheduled at each follow-up visit, and the participants were reimbursed for transportation costs when required to attend the visits.

Participants were allowed to leave the study at any time and for any reason. In addition, researchers were instructed to withdraw participants if they considered any danger to the participant continuing in the research or if the competent authority decided to do so.

Data management

All data was recorded electronically in forms stored on a virtual server during the study. Access to these forms was restricted, and only authorized personnel for the Pablo Tobón Uribe Hospital research unit had access.

The data obtained from the CGM was stored in its original format on a virtual server once the patient had been de-identified. It can be accessed for data quality verification reasons.

Pablo Tobón Uribe Hospital's research unit and the principal investigator will store all data indefinitely, but any information that could identify the patients has been deleted.

Statistical methods

The normality analysis used a Q-Q (quantile-quantile) graph and the Shapiro-Wilk test for continuous variables. Data distribution presents continuous variables as mean, standard deviation, medians, and interquartile ranges. Qualitative variables are presented as absolute frequencies and proportions.

Analysis population:

Complete analysis set (intention to treat): The full analysis includes all randomized individuals.

The per-protocol analysis set: The per-protocol analysis set comprises individuals who performed at least 80% of the suggested simulations. This proportion of the use of the simulation was proposed based on previous results that show that CGM sensor wear time is associated with more significant reductions in glucose levels (245).

Objectives analysis plan

Statistical analyses were performed on the complete set analysis, and all patients were included in the primary and secondary analyses. A mixed model analysis was used for the primary analysis to evaluate the time-in-range difference. The TIR was included as the

dependent variable in the mixed-effects model analysis—the study group was included as the independent variable. The initial TIR, HbA1c, and type of treatment were planned to be included as adjustment variables to the model (225). Given the high correlation between the HbA1c and TIR (229), only initial TIR was included to avoid model overfitting.

The episodes of hypoglycemia and the number of DKA or HSS were compared using a ratio of incidence rates, calculated using a Poisson regression (246, 247).

For the agreement analysis, as the differences between methods did not follow a normal distribution, a non-parametric approach was used to estimate the limits of agreement (216). There is no reported minimal significant difference (70, 71) for glucose prediction and blood glucose reading in an insulin dose decision-making process. A threshold of 50 mg/dL was selected. This threshold was selected based on an ideal 180 mg/dL postprandial glucose (248). Considering that the model estimates blood glucose and the comparison is made with interstitial glucose from a CGM, a difference between 15 and 30% could be expected (217, 218). The potential clinical impact of the differences between both methods is that a surveillance grid analysis was performed like the one described in (249). Finally, the mean relative difference and mean absolute relative difference for the model compared to the CGM were calculated.

Protocol changes: After the COVID-19 pandemic, the recruitment strategy was changed to include a virtual invitation strategy for potential candidates. At the beginning of the trial, a request to include people with HbA1c lower than 7.5 was made due to better glycemic control of the patients using a CGM system in the centers than expected. The Pablo Tobón Uribe hospital research and ethical committee approved both changes.

Ethical considerations

The ethical considerations of this protocol are based on the amendment made in 2013 during the general assembly in Fortaleza, Brazil, of the World Medical Association to the Declaration of Helsinki, Ethical Principles for Medical Research on Human Beings, and on the Fourth Version of the Ethical Guidelines for Health-Related Research with Human Beings

prepared by the Council for International Organizations of Medical Sciences (CIOMS) in collaboration with the World Health Organization (WHO). The ethical considerations of this protocol comply with Resolution 8430 from the Ministry of Health of Colombia. Furthermore, this protocol was approved by Pablo Tobon Uribe Hospital's ethics committee on 28/January/2021.

The researchers conducted the informed consent process. This was obtained in writing with the participant's signature. For this purpose, an instrument was designed and signed by the participant and two witnesses not related to the investigation, and the purpose, methods, possible benefits, risks, and the freedom of both to participate and to leave the research at any time were stipulated. In addition, researchers were available throughout the investigation to answer participants' questions and ensure they fully understood.

The individuals selected to participate could all provide consent, so subrogation was not anticipated. All the changes to the protocol that affected the participants' rights, risks, or benefits were submitted to the ethics committee of the Pablo Tobón Uribe Hospital, and the consent was renewed.

Personal identification data and clinical variables were collected during the investigation. All personal information obtained from the participants during the research has been treated following the provisions stipulated in Colombian Law 1581 of 2012 on personal data protection. This information is only accessible to personnel involved in the investigation who require it for their work or those in charge of preparing and curating the database. The clinical variables are stored in another database. Each participant was identified using only code. Access to the code's identity is only available to those treating the central database. This information will be made public for no reason other than those stipulated in the law.

The expected benefit for the research participants assigned to the intervention group was the possible increase in the time in the established glucose range during the postprandial period. This change should not modify the risk of developing a disease complication in the short term. However, the intervention was expected to produce changes in individual

conduct, especially in food selection. This increase in time range could also be associated with a better perception of the disease.

The risk that was anticipated with the intervention is hypoglycemia, a risk related to the use of insulin. However, one of the expected behavioral changes in the participants was a change in the insulin dose. Therefore, participants were retrained in treating hypoglycemia as a mitigation measure. In addition, patients at high risk of presenting an episode of hypoglycemia or high risk associated with hypoglycemia were excluded from the investigation.

This research was considered research with a risk greater than the minimum. Thus, the following was guaranteed: 1) the possibility that the participants could withdraw voluntarily without this giving rise to discrimination or altering the care of their disease. 2) Health care coverage through an insurance policy for adverse events related to the participation in the investigation. 3) A safety data surveillance committee was assembled to define the suspension of the investigation in case the intervention put the health or life of any participants at risk.

Any health needs other than those associated with the trial during the research identified during the trial were communicated to the participant and referred for care within the health system.

Some of the data obtained during the investigation could be useful for later studies. The Pablo Tobón Uribe Hospital will store these data and, if necessary, share them anonymously with the researchers only in minimal risk investigations and with prior authorization from the ethics committee. Participants were informed of this as part of the informed consent process. Participants may withdraw their consent so that their data cannot be used in future research. Compensation was planned to cover travel costs for each of the visits.

The inclusion of people belonging to vulnerable groups such as children, pregnant or breastfeeding women, people in dependency relationships with researchers, or adults without the capacity to consent was not foreseen for this research.

The inclusion of people belonging to vulnerable groups such as children, pregnant or breastfeeding women, people in dependency relationships with researchers, or adults without the capacity to consent was not foreseen for this research. The informed consent instrument is available in the supplementary material.

Results

Randomization and Participant Characteristics

Between May 2023 and November 2023, 68 persons with DM1 were assessed for eligibility; 28 participants underwent randomization; 14 patients were assigned to the intervention group and 14 to the control group. All participants completed the planned follow-up, and none withdrew consent (Figure 36).

The median age of the participants was 32.5 years 50% were women, and 90% had been counting carbohydrates for more than one year. Three patients were on treatment with an insulin pump. Table 19 summarizes the participant's main characteristics.

Primary and secondary outcomes

Results for the primary and secondary outcomes are summarized in Table 20. During the four weeks of the trial, TIR in the participants using the STUDIA app increased from a mean of 59.2±21.9 to 67.1±16.3 while in the control group, it decreased from a mean of 64.1± 23.2 to 60.4±24.4. The crude mean difference between groups was 7.44% (95%CI 3.20 to 12.61), and the adjusted mean difference was 6.95% (CI 95% 3.51 to 10.39). Most of the change occurred during the first follow-up weeks (Figure 37).

Similarly, the use of STUDIA favors a reduction in the TBR with a mean crude difference between groups of -1.53% (95%CI -2.59 to -0.47) and an adjusted difference of -1.11 (95% CI -2.2 to -0.20). Unlike what happened with the change in the TIR, most of the change difference in the TBR occurred during the final period of the follow-up (Figure 38). There was no difference in the TAR or glucose variability between groups during the treatment period (Table 20).

Figure 36. Participants Flowchart.

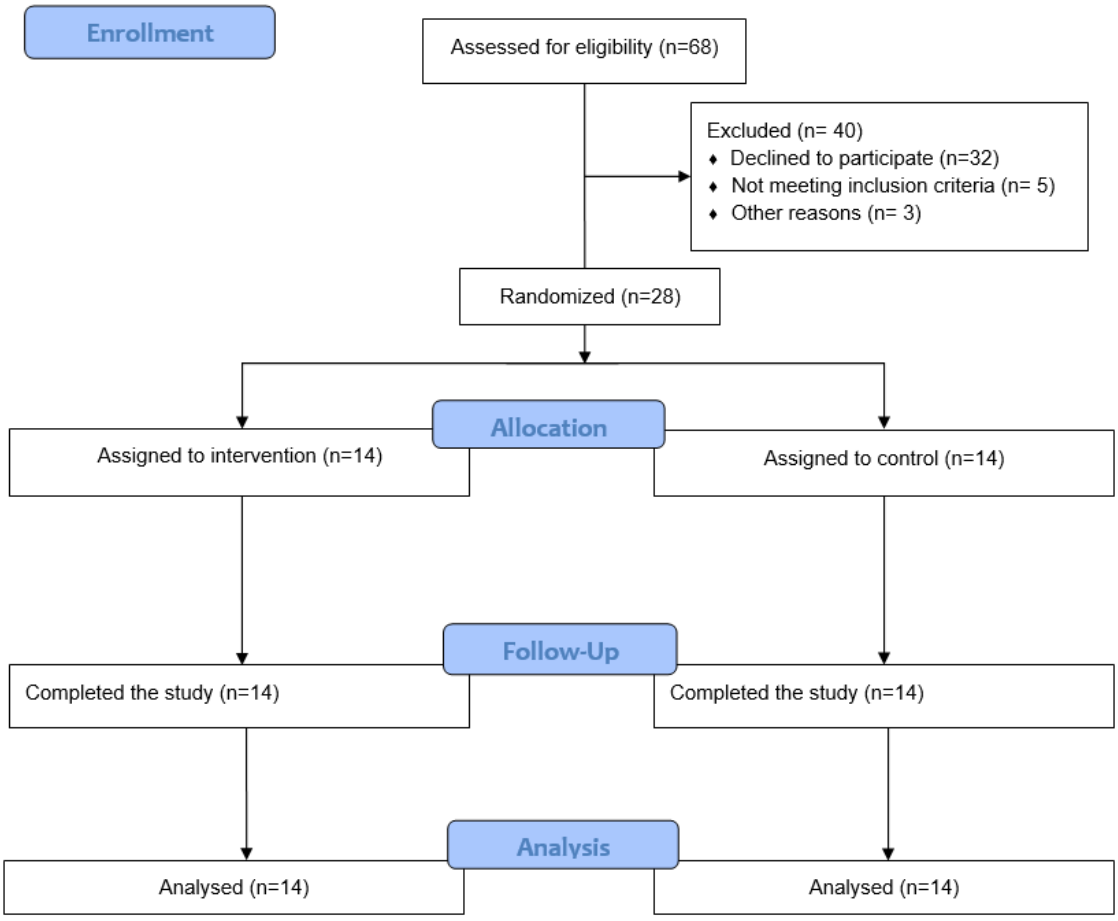


Table 19. Patients characteristics.

	Control (N=14)	STUDIA (N=14)
Age	26.0 (23.0 - 42.5)	39.5 (32.3 - 54.8)
Sex		
Women	8 (57.1)	6 (42.9)
Man	6 (42.9)	8 (57.1)
Timen in range	59.9 (20.8)	63.4 (23.7)
Time counting carbohydrates		
Less than a year	1 (7.1%)	2 (14.3)
More than a year	13 (92.9%)	12 (85.7)
Education		
Secondary	5 (35.7%)	3 (21.4%)
Post-Secondary	9 (64.3%)	11 (78.6%)
Insulin pump users	2 (14.28%)	1 (7.14%)
Glycated hemoglobin	7.29 (1.00)	7.27 (0.873)
Coefficient of variation	36.4 (32.8, 40.2)	33.6 (28.4, 36.8)
DTSQ	28.5 (26.3, 29.8)	28.5 (23.3, 31.5)

Data are mean (SD), n (%), n/N (%), or median (IQR). DTSQ: Diabetes Treatment Satisfaction Questionnaire

Table 20. Primary and secondary outcomes.

Outcome	Control (N=14)	STUDIA (N=14)	Estimated Adjusted Difference (95%CI)	P Value
Change in TIR	-3.71±12	7.93±11.3	6.95 (3.51 to 10.39)	**<0.001**
Change in TBR	1.93±2.89	-1.64±2.10	-1.10 (-2.20 to -0.20)	**0.022**
Change in TAR	1.43±13.3	-3.93±13.6	-3.21 (-7.67 to 1.25)	0.396
Change in CV	-1.09±3.4	0.0357±7.7	0.38 (-2.41 to 3.17)	0.787

Adjusted differences were estimated using an adjusted mixed-effects model. TIR: Time in range, TBR: Time below range, TAR: Time above range, CV: Coefficient of variation.

Figure 37. Change in time in range during the trial.

A generalized additive model with integrated smoothness due to its effectiveness allowing plotting patterns in the presence of without overplotting.

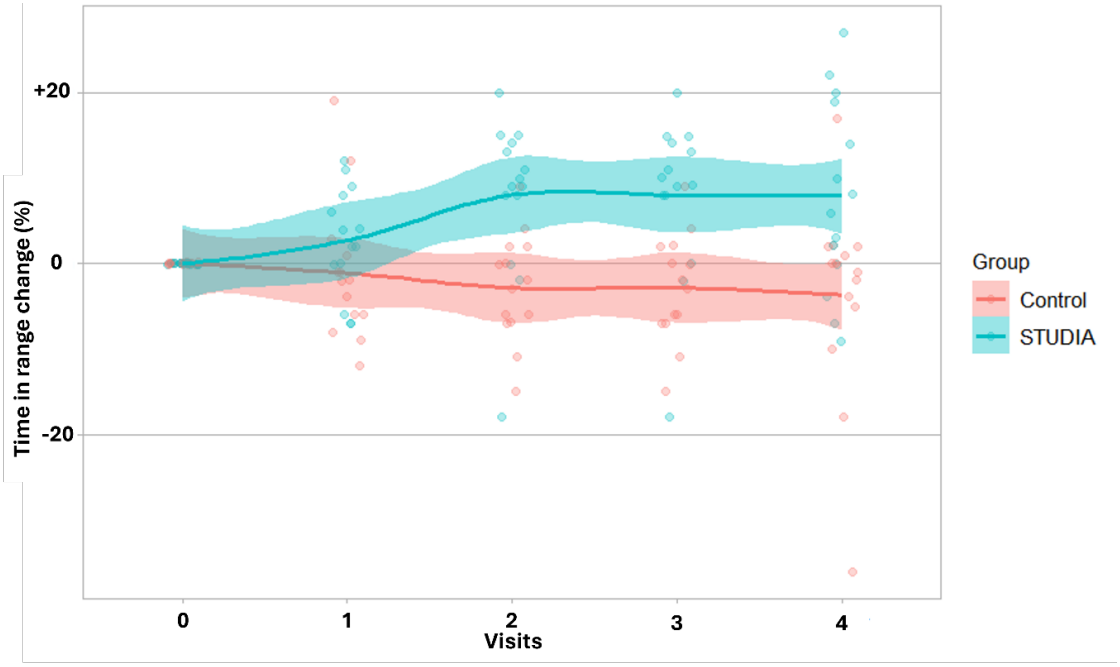
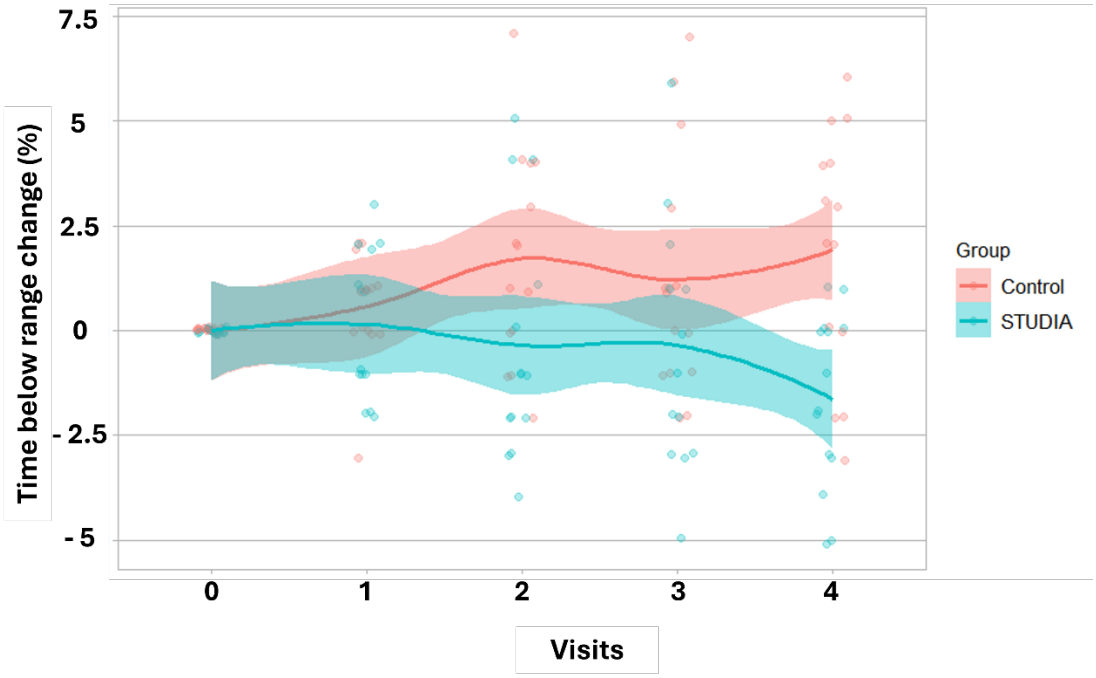


Figure 38. Change in time below range (hypoglycemia) during the trial.

A generalized additive model with integrated smoothness due to its effectiveness allowing plotting patterns in the presence of without overplotting.



Safety outcomes

A total of 20 hypoglycemia events were reported by eight participants, six from the control group. Fifteen of the hypoglycemia events were reported in the control group and five in the STUDIA group (Table 21). The STUDIA group's incidence rate of hypoglycemia events was 0.31 (95%CI 0.10 to 0.81). Only two grade 3 hypoglycemia events occur during the study, both in patients in the control group. No DKA episodes were reported during the trial.

Table 21. Safety outcomes.

Outcome	Control (N=14)	STUDIA (N=14)	Incidence rate (95%CI)	P Value
Any hypoglycemia			0.31 (0.10 to 0.81)	**0.025**
No of events	15	5	-	-
No of patients (%)	6 (42.8)	2 (14.3)	-	-
Grade 3 hypoglycemia			-	-
No of events	2	0	-	-
No of patients	2 (14.3)	0	-	-

STUDIA agreement with the CGM readings

A total of 4432 differences between both methods were evaluated; 72% (CI%, 70% to 73%) of the differences were lower than 50 mg/dL, and Figure 39 shows some simulations. The limits of agreement for a 50 mg/dL difference are presented in Figure 40. The mean relative difference between the model and the CGM was 6.4%. The Mean Absolute Relative Difference was 26.4%.

In the surveillance grid analysis, 95% of the difference between the simulation and the model falls within the no-risk or slight-risk category, Figure 41.

Figure 39. Limits of agreement within 50 mg/dL.

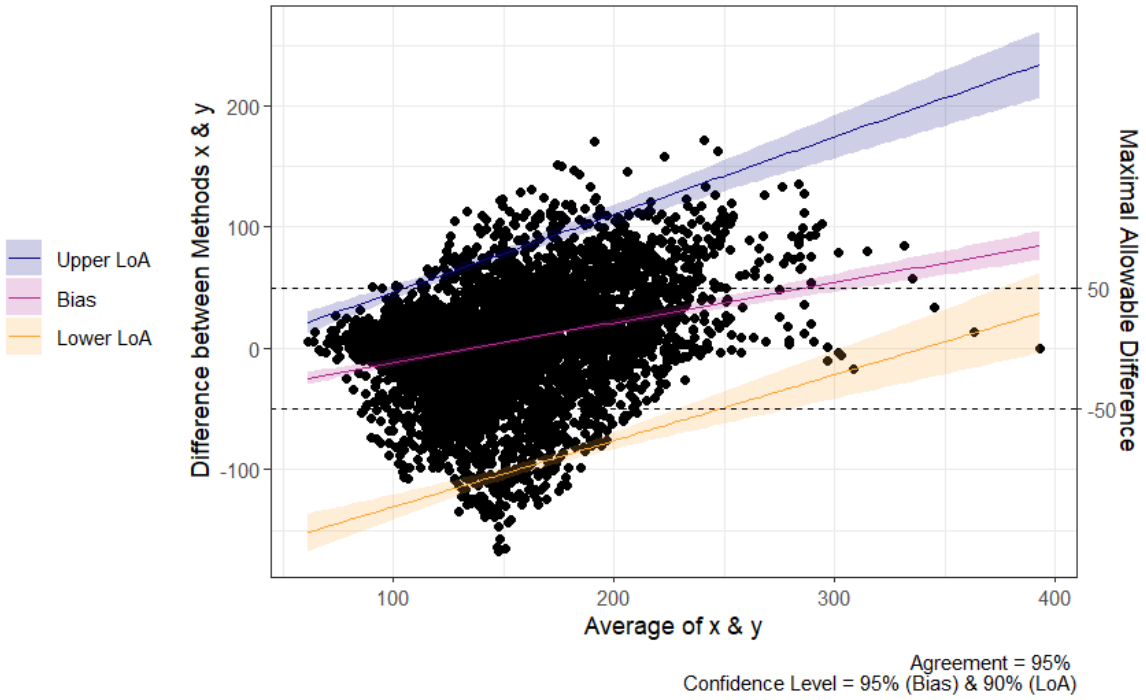


Figure 40. CGM vs. app glucose simulations.

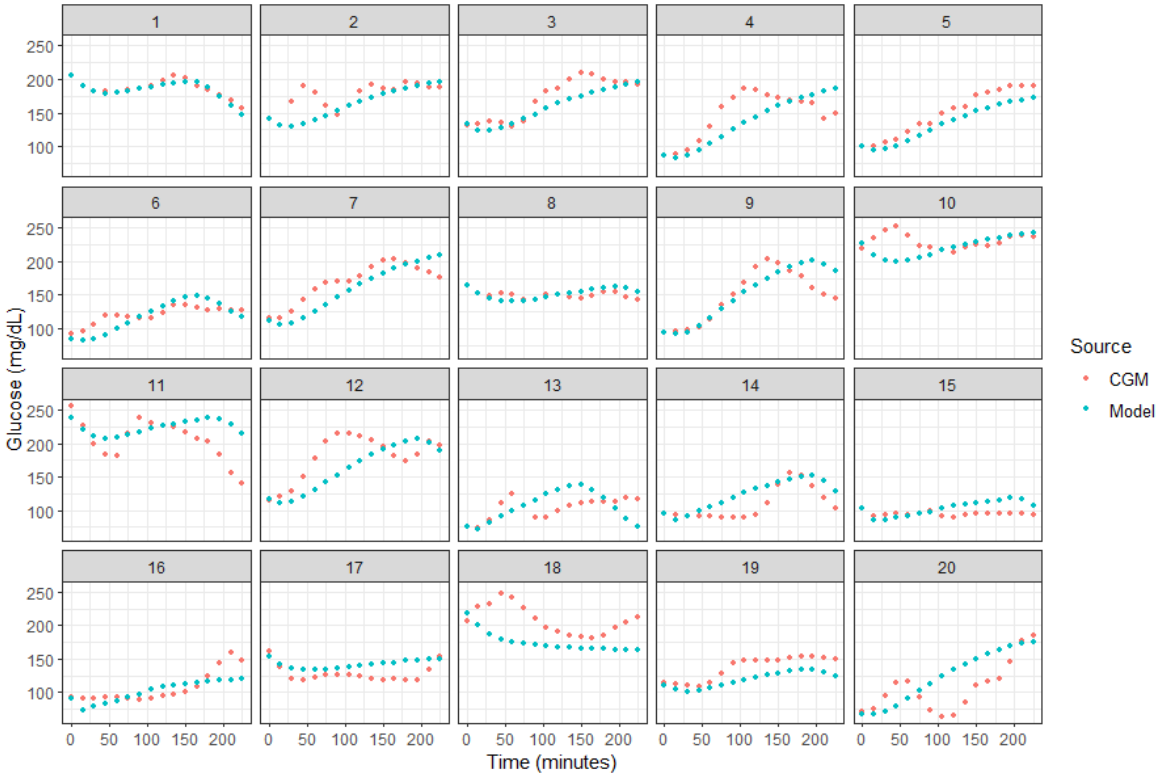
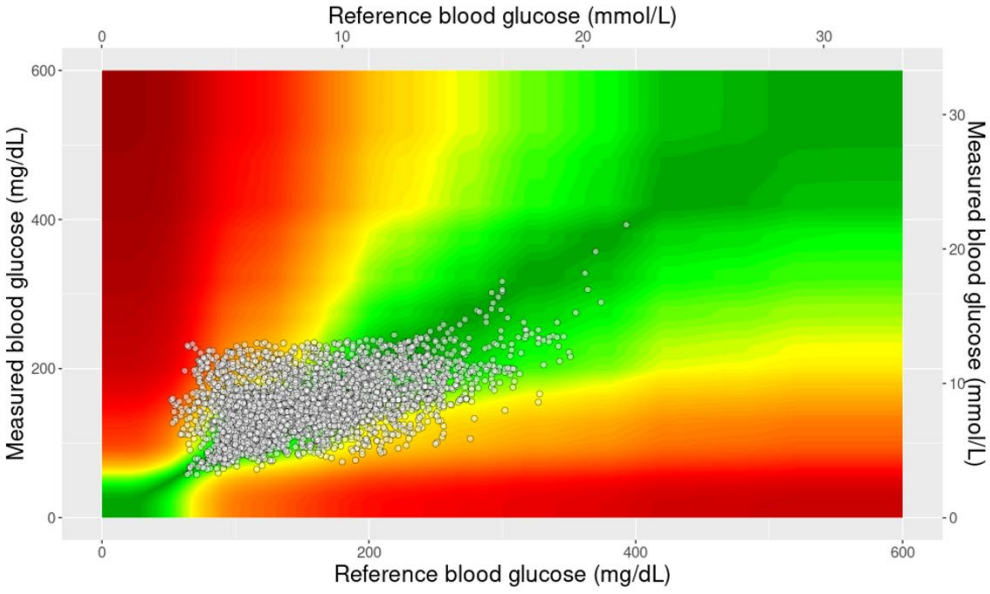


Figure 41. Surveillance Grid analysis.



1	0	None	2571	58%
2	1	Slight, Lower	1295	29.2%
3	2	Slight, Higher	343	7.7%
4	3	Moderate, Lower	170	3.8%
5	4	Moderate, Higher	46	1%
6	5	Severe, Lower	7	0.2%
7	6	Severe, Upper		NA
8	7	Extreme		NA

STUDIA usability and patients reported outcomes.

The median of the recommended simulations in the control group was 57.5 % (IQR 16.8 to 80.3), and 56.5% (IQR 26.3 to 75.0) in the intervention group. The mean computer systems usability questionnaire score in the control group was 101 (SD 6.9), and in the intervention group, it was 101 (SD 10.8). The DSTQ median change in the control group was 10.0 (IQR 9.25, 13.5), and in the STUDIA group, 11.5 (IQR 8.5, 14.8).

Discussion

In this randomized, controlled trial involving people with DM1 trained in carbohydrate counting, the aid of a novel simulation-based decision support system (STUDIA) acting as a persuasive tool that provides information on possible postprandial glucose changes, allows for adjustment of either the insulin dose or meal nutrient balance, lead to an increase on time in range of 7% and a 70% reduction in hypoglycemia perceived events.

STUDIA adds a forecast of the glucose impact of a meal, resulting in a much more conscious decision about food choices or a more precise insulin dose adjustment. In the long term, using STUDIA could lead to changes in HbA1c of around 0.7% (229). People with DM1 trained in carbohydrate counting to match carbohydrate intake with insulin dosage had better glucose control than those receiving traditional diabetes nutritional education, allowing for a less restricted diet (206). However, unpredictability and fluctuations in blood glucose levels remain an important issue (68). Focusing on carbohydrate content does not always lead to a freer diet due to the challenges in food content estimation and its possible effects on blood glucose (250).

STUDIA uses a highly detailed physiological model as an everyday simulator to aid carbohydrate counting, proving that highly detailed models can be used in routine clinical practice. Traditionally, this kind of models had been restricted to basic or preclinical research on glucose-insulin interactions, insulin secretion, insulin sensitivity, insulin clearance, and glucose absorption from meals, among other aspects of glucose homeostasis. A recent experience reported in a pilot study used a Web-Based Simulation

Tool to generate personalized models of glucose metabolism, but its use did not affect time in range (214).

The reduction in hypoglycemia and hypoglycemic events without an increase in time in hyperglycemia results from better-informed decisions based on the simulations. One of the significant contributions of CGM technology in treating diabetes is a decrease in time below range and hypoglycemia events. People who experience a mild hypoglycemia event are at greater risk of severe hypoglycemia events, hypoglycemia awareness, and reduced quality of life (251). A better-informed decision process regarding meal choices and insulin dose guided by systems like STUDIA may help to alleviate the burden of living with diabetes.

STUDIA makes predictions of a possible glucose trend given the amount of nutrients and insulin dose. Only the control group was analyzed to determine the difference between STUDIA and the CGM. Participants in the STUDIA group could see the glucose trend before a meal and may have changed the meal and insulin dose, changing the postprandial glucose trend. The prediction capability of the model is promising; with a single parameter adjustment based on a few retrospective meals at the beginning of the trial, the mean relative difference is low, and more than 70% of the predicted measurements fell within a 50mg/dL difference and the MARD although higher than the recommended standard is similar to that of some real-life reported experiences of patient using CGM (252).

The consistent results using a combination of dispersion metrics that had been extensively used to assess the accuracy of CGM systems (222, 253) denote the robustness of our results. However, relying only on dispersion metrics that treat measurement errors in low, average, and high glucose values the same limits the clinical risk assessment. We used a surveillance grid analysis to overcome this limitation. Although most of the difference between the prediction and the CGM measurement fell within the no-risk or slight-risk category, the proportions within the no-risk category are far from the recommended for traditional glucose measurement devices (249). However, STUDIA is not a measurement device but a prediction tool that provides 5-minute estimates for the upcoming four hours. It is not clear how patients may use this data to inform decisions. Some people may prefer to use the

highest or lowest point on a graph to decide, while others may find the glucose trend more valuable than the absolute value.

Finally, the usability evaluation on both groups was high; this was one of the goals during STUDIA development, and we believed that it was accomplished thanks to the simplicity of the interface and familiarity for CGM users of the glucose trend graphic with the everyday CGM system report. However, the number of simulations performed in the STUDIA group was only half the intended; the relatively low use continuous use of technology by people with diabetes is a well-known phenomenon (79), and efforts had to be made to increase adherence to interventions that positively impact on important outcomes such as STUDIA.

This study has some limitations. First, the nature of the intervention prevented a blind design. Also, although the length of the study was selected to detect differences in hypoglycemia, four weeks remains a short time for using a decision support system, and longer trials are necessary to evaluate the persistence of the use of the app. Another potential pitfall is the high within-subject glucose variability; a crossover design may have helped control this issue, but a proper washout period for an educational intervention is difficult to establish. Finally, the model's accuracy can be improved with other parameter identification methods, even for some people, as with a sensitive index and carbohydrate/insulin ratio that changes at different times within a day; maybe different parameters for the model are needed.

Conclusions

This clinical trial provides evidence that for people with DM1, knowing in advance how their glucose may change with a given meal, an insulin dose improves their glucose control and reduces hypoglycemia events. Also, a detailed physiological glucose model can be used daily for decision-making.

CONCLUSIONS AND FUTURE WORK

It has been estimated that people who have type 1 diabetes must decide their condition every five minutes. Most of these decisions are related to food or blood glucose levels. Carbohydrate counting is perhaps the most used education technique for people with diabetes to couple their diet with the insulin dose. Not only does it lead to better glucose control without increasing the risk of hypoglycemia, but it can also lead to a freer diet. Unlike other educational aspects of diabetes treatment, people with diabetes seem to continue using it throughout the years.

Mathematical modeling in diabetes research has many applications, including the possibility of answering questions about glucose homeostasis without experimentation. Most of the knowledge of glucose physiology has been obtained through modeling, mainly using the so-called physiological or maximal models. These models can be developed based solely on data (black box), using the knowledge and laws governing the phenomena of interest (white box), or with models in between (the so-called grey box). Phenomenological-based semi-physical Models belong to the latter category and harness the best of both worlds: direct interpretability of the structural parameters due to the phenomenological origin, but also using available data from the process on its structure, gaining versatility. These models have been primarily used in engineering due to their properties, making them especially attractive to model physiological processes. This thesis has proved that the phenomenological-based semi-physical modeling technique can answer questions about glucose homeostasis.

Physiological models have been used mainly in basic science research and are frequently thought too complex for practical use. The thesis challenges this idea by incorporating such a model on a mobile app for everyday use by people with diabetes. Using this technology leads to positive glucose control results and reduces the risk of hypoglycemia. Continuous use of this decision support system may help to alleviate the burden of the disease in people with type 1 diabetes.

Much work is left to be done. Although the prediction capabilities of the model in a real life-changing scenario are good, a better parameter identification process could lead to better results. Also, the model may benefit from dynamic on-line parameter adaptation to better capture the ever-changing insulin/food relation within the human body. Also, the decision support system could be coupled to existing solutions that automatized the carbohydrate counting process using pictures and can be used as an insulin dose optimizer or a personal diet recommendation system. Also, its use in people without diabetes deserves to be explored.

REFERENCES

1. Gingras V, Haidar A, Messier V, Legault L, Ladouceur M, Rabasa-Lhoret R. A Simplified Semiquantitative Meal Bolus Strategy Combined with Single- and Dual-Hormone Closed-Loop Delivery in Patients with Type 1 Diabetes: A Pilot Study. Diabetes technology & therapeutics. 2016;18(8):464-71.
2. Saeedi P, Petersohn I, Salpea P, Malanda B, Karuranga S, Unwin N, et al. Global and regional diabetes prevalence estimates for 2019 and projections for 2030 and 2045: Results from the International Diabetes Federation Diabetes Atlas, 9th edition. Diabetes research and clinical practice.
3. 9. Pharmacologic Approaches to Glycemic Treatment: Standards of Medical Care in Diabetes-2019. Diabetes care. 2019;42(Suppl 1):S90-s102.
4. Klein R. Hyperglycemia and microvascular and macrovascular disease in diabetes. Diabetes care. 1995;18(2):258-68.
5. Adler AI, Boyko EJ, Ahroni JH, Stensel V, Forsberg RC, Smith DG. Risk factors for diabetic peripheral sensory neuropathy. Results of the Seattle Prospective Diabetic Foot Study. Diabetes care. 1997;20(7):1162-7.
6. Turner RC, Millns H, Neil HA, Stratton IM, Manley SE, Matthews DR, Holman RR. Risk factors for coronary artery disease in non-insulin dependent diabetes mellitus: United Kingdom Prospective Diabetes Study (UKPDS: 23). BMJ (Clinical research ed). 1998;316(7134):823-8.
7. Lehto S, Ronnemaa T, Pyorala K, Laakso M. Predictors of stroke in middle-aged patients with non-insulin-dependent diabetes. Stroke. 1996;27(1):63-8.
8. Stratton IM, Adler AI, Neil HA, Matthews DR, Manley SE, Cull CA, et al. Association of glycaemia with macrovascular and microvascular complications of type 2 diabetes (UKPDS 35): prospective observational study. BMJ (Clinical research ed). 2000;321(7258):405-12.
9. Builes-Montaño CE, Chavarriaga A, Ballesteros L, Muñoz M, Medina S, Donado-Gomez JH, Ramirez-Rincón A. Characteristics of hyperglycemic crises in an adult population in a teaching hospital in Colombia. Journal of Diabetes & Metabolic Disorders. 2018;17(2):143-8.
10. Zhang P, Zhang X, Brown J, Vistisen D, Sicree R, Shaw J, Nichols G. Global healthcare expenditure on diabetes for 2010 and 2030. Diabetes research and clinical practice. 2010;87(3):293-301.
11. Gonzalez JC, Walker JH, Einarson TR. Cost-of-illness study of type 2 diabetes mellitus in Colombia. Rev Panam Salud Publica. 2009;26(1):55-63.
12. Estadística DNd. Defunciones no fetales 2019 2019 [Available from: https://www.dane.gov.co/index.php/estadisticas-por-tema/salud/nacimientos-y-defunciones/defunciones-no-fetales/defunciones-no-fetales-2019.
13. Agudelo-Botero M, Dávila-Cervantes CA. Carga de la mortalidad por diabetes mellitus en América Latina 2000-2011: los casos de Argentina, Chile, Colombia y México. Gaceta Sanitaria. 2015;29(3):172-7.
14. Nathan DM. The Diabetes Control and Complications Trial/Epidemiology of Diabetes Interventions and Complications Study at 30 Years: Overview. Diabetes care. 2014;37(1):9-16.
15. The Effect of Intensive Treatment of Diabetes on the Development and Progression of Long-Term Complications in Insulin-Dependent Diabetes Mellitus. New England Journal of Medicine. 1993;329(14):977-86.
16. Effect of intensive blood-glucose control with metformin on complications in overweight patients with type 2 diabetes (UKPDS 34). UK Prospective Diabetes Study (UKPDS) Group. Lancet. 1998;352(9131):854-65.

17. Holman RR, Paul SK, Bethel MA, Matthews DR, Neil HAW. 10-Year Follow-up of Intensive Glucose Control in Type 2 Diabetes. New England Journal of Medicine. 2008;359(15):1577-89.
18. 9. Pharmacologic Approaches to Glycemic Treatment: Standards of Care in Diabetes-2024. Diabetes care. 2024;47(Suppl 1):S158-s78.
19. Imran SA, Agarwal G, Bajaj HS, Ross S. Targets for Glycemic Control. Can J Diabetes. 2018;42 Suppl 1:S42-s6.
20. Food, Administration D. Guidance for industry: diabetes mellitus—evaluating cardiovascular risk in new antidiabetic therapies to treat type 2 diabetes. US Department of Health and Human Services. 2008.
21. Tricco AC, Ivers NM, Grimshaw JM, Moher D, Turner L, Galipeau J, et al. Effectiveness of quality improvement strategies on the management of diabetes: a systematic review and meta-analysis. Lancet. 2012;379(9833):2252-61.
22. Avery L, Flynn D, van Wersch A, Sniehotta FF, Trenell MI. Changing physical activity behavior in type 2 diabetes: a systematic review and meta-analysis of behavioral interventions. Diabetes care. 2012;35(12):2681-9.
23. Villegas Perrasse A, Abad SB, Faciolince S, Hernandez N, Maya C, Parra L, et al. Controlling diabetes mellitus and its complications in Medellin, Colombia, 2001-2003. Rev Panam Salud Publica. 2006;20(6):393-402.
24. Machado Alba JE, Moncada Escobar JC, Mesa Escobar G. Antidiabetic drugs prescription patterns among a group of patients in Colombia. Rev Panam Salud Publica. 2007;22(2):124-31.
25. Barengo NC, Camacho S, López PA, Camacho PA, García ÁA, Hincapié JA, et al. Patrones de prescripción de medicamentos para la diabetes mellitus tipo 2 en cinco departamentos de Colombia, en 2014. Revista Facultad Nacional de Salud Pública. 2018;36:58-65.
26. Davidson PC, Hebblewhite HR, Steed RD, Bode BW. Analysis of guidelines for basal-bolus insulin dosing: basal insulin, correction factor, and carbohydrate-to-insulin ratio. Endocrine practice : official journal of the American College of Endocrinology and the American Association of Clinical Endocrinologists. 2008;14(9):1095-101.
27. Evert AB, Boucher JL, Cypress M, Dunbar SA, Franz MJ, Mayer-Davis EJ, et al. Nutrition therapy recommendations for the management of adults with diabetes. Diabetes care. 2013;36(11):3821-42.
28. Gray GM, Ingelfinger FJ. Intestinal absorption of sucrose in man: interrelation of hydrolysis and monosaccharide product absorption. The Journal of clinical investigation. 1966;45(3):388-98.
29. Brener W, Hendrix TR, McHugh PR. Regulation of the gastric emptying of glucose. Gastroenterology. 1983;85(1):76-82.
30. Jenkins DJ, Cuff D, Wolever TM, Knowland D, Thompson L, Cohen Z, Prokipchuk E. Digestibility of carbohydrate foods in an ileostomate: relationship to dietary fiber, in vitro digestibility, and glycemic response. Am J Gastroenterol. 1987;82(8):709-17.
31. Swallow DM. Genetics of lactase persistence and lactose intolerance. Annu Rev Genet. 2003;37:197-219.
32. Elleri D, Allen JM, Harris J, Kumareswaran K, Nodale M, Leelarathna L, et al. Absorption patterns of meals containing complex carbohydrates in type 1 diabetes. Diabetologia. 2013;56(5):1108-17.
33. Bantle JP, Wylie-Rosett J, Albright AL, Apovian CM, Clark NG, Franz MJ, et al. Nutrition recommendations and interventions for diabetes: a position statement of the American Diabetes Association. Diabetes care. 2008;31 Suppl 1:S61-78.
34. Bell KJ, Barclay AW, Petocz P, Colagiuri S, Brand-Miller JC. Efficacy of carbohydrate counting in type 1 diabetes: a systematic review and meta-analysis. The lancet Diabetes & endocrinology. 2014;2(2):133-40.

35. Training in flexible, intensive insulin management to enable dietary freedom in people with type 1 diabetes: dose adjustment for normal eating (DAFNE) randomised controlled trial. BMJ (Clinical research ed). 2002;325(7367):746.
36. Gilbertson HR, Brand-Miller JC, Thorburn AW, Evans S, Chondros P, Werther GA. The effect of flexible low glycemic index dietary advice versus measured carbohydrate exchange diets on glycemic control in children with type 1 diabetes. Diabetes care. 2001;24(7):1137-43.
37. Kalergis M, Pacaud D, Strychar I, Meltzer S, Jones PJ, Yale JF. Optimizing insulin delivery: assessment of three strategies in intensive diabetes management. Diabetes, obesity & metabolism. 2000;2(5):299-305.
38. Laurenzi A, Bolla AM, Panigoni G, Doria V, Uccellatore A, Peretti E, et al. Effects of Carbohydrate Counting on Glucose Control and Quality of Life Over 24 Weeks in Adult Patients With Type 1 Diabetes on Continuous Subcutaneous Insulin Infusion: A randomized, prospective clinical trial (GIOCAR). Diabetes care. 342011. p. 823-7.
39. Scavone G, Manto A, Pitocco D, Gagliardi L, Caputo S, Mancini L, et al. Effect of carbohydrate counting and medical nutritional therapy on glycaemic control in Type 1 diabetic subjects: a pilot study. Diabetic medicine : a journal of the British Diabetic Association. 2010;27(4):477-9.
40. Schmidt S, Meldgaard M, Serifovski N, Storm C, Christensen TM, Gade-Rasmussen B, Norgaard K. Use of an automated bolus calculator in MDI-treated type 1 diabetes: the BolusCal Study, a randomized controlled pilot study. Diabetes care. 2012;35(5):984-90.
41. Trento M, Trinetta A, Kucich C, Grassi G, Passera P, Gennari S, et al. Carbohydrate counting improves coping ability and metabolic control in patients with Type 1 diabetes managed by Group Care. J Endocrinol Invest. 2011;34(2):101-5.
42. Fu S, Li L, Deng S, Zan L, Liu Z. Effectiveness of advanced carbohydrate counting in type 1 diabetes mellitus: a systematic review and meta-analysis. Sci Rep. 2016;6:37067.
43. Vaz EC, Porfirio GJM, Nunes HRC, Nunes-Nogueira VDS. Effectiveness and safety of carbohydrate counting in the management of adult patients with type 1 diabetes mellitus: a systematic review and meta-analysis. Arch Endocrinol Metab. 2018;62(3):337-45.
44. Souto DL, Zajdenverg L, Rodacki M, Rosado EL. Impact of advanced and basic carbohydrate counting methods on metabolic control in patients with type 1 diabetes. Nutrition. 2014;30(3):286-90.
45. James ML, Green L, Amiel SA, Choudhary P. Evaluation of the Effect of Carbohydrate Intake on Postprandial Glucose in Patients With Type 1 Diabetes Treated With Insulin Pumps. Journal of diabetes science and technology. 2016;10(6):1287-93.
46. Hissa AS, Albuquerque LL, Hissa MN. Evaluation of how satisfactory is carbohydrate counting in patients with diabetes. Arquivos brasileiros de endocrinologia e metabologia. 2004;48(3):394-7.
47. Meade LT, Rushton WE. Accuracy of Carbohydrate Counting in Adults. Clin Diabetes. 2016;34(3):142-7.
48. Kawamura T, Takamura C, Hirose M, Hashimoto T, Higashide T, Kashihara Y, et al. The factors affecting on estimation of carbohydrate content of meals in carbohydrate counting. Clin Pediatr Endocrinol. 2015;24(4):153-65.
49. Wolpert HA, Atakov-Castillo A, Smith SA, Steil GM. Dietary fat acutely increases glucose concentrations and insulin requirements in patients with type 1 diabetes: implications for carbohydrate-based bolus dose calculation and intensive diabetes management. Diabetes care. 2013;36(4):810-6.
50. Garcia-Lopez JM, Gonzalez-Rodriguez M, Pazos-Couselo M, Gude F, Prieto-Tenreiro A, Casanueva F. Should the amounts of fat and protein be taken into consideration to calculate the

lunch prandial insulin bolus? Results from a randomized crossover trial. Diabetes technology & therapeutics. 2013;15(2):166-71.
51. Bozzetto L, Giorgini M, Alderisio A, Costagliola L, Giacco A, Riccardi G, et al. Glycaemic load versus carbohydrate counting for insulin bolus calculation in patients with type 1 diabetes on insulin pump. Acta Diabetol. 2015;52(5):865-71.
52. Krebs JD, Arahill J, Cresswell P, Weatherall M, Parry-Strong A. The effect of additional mealtime insulin bolus using an insulin-to-protein ratio compared to usual carbohydrate counting on postprandial glucose in those with type 1 diabetes who usually follow a carbohydrate-restricted diet: A randomized cross-over trial. Diabetes, obesity & metabolism. 2018;20(10):2486-9.
53. Holt SH, Miller JC, Petocz P. An insulin index of foods: the insulin demand generated by 1000-kJ portions of common foods. The American journal of clinical nutrition. 1997;66(5):1264-76.
54. Bell KJ, Gray R, Munns D, Petocz P, Steil G, Howard G, et al. Clinical Application of the Food Insulin Index for Mealtime Insulin Dosing in Adults with Type 1 Diabetes: A Randomized Controlled Trial. Diabetes technology & therapeutics. 2016;18(4):218-25.
55. Zeigler BP, Praehofer H, Kim TG. Theory of modeling and simulation: Academic press; 2000.
56. Ajmera I, Swat M, Laibe C, Le Novere N, Chelliah V. The impact of mathematical modeling on the understanding of diabetes and related complications. CPT Pharmacometrics Syst Pharmacol. 2013;2:e54.
57. L L-P, E A-Z, J G-T, editors. Recent advances in mathematical models for the understanding and treatment of Type 1 Diabetes Mellitus. 2015 IEEE 2nd Colombian Conference on Automatic Control (CCAC); 2015 14-16 Oct. 2015.
58. Fritzen K, Heinemann L, Schnell O. Modeling of Diabetes and Its Clinical Impact. Journal of diabetes science and technology. 2018;12(5):976-84.
59. Man CD, Micheletto F, Lv D, Breton M, Kovatchev B, Cobelli C. The UVA/PADOVA Type 1 Diabetes Simulator: New Features. Journal of diabetes science and technology. 2014;8(1):26-34.
60. Cameron IT, Hangos K. Process modelling and model analysis: Elsevier; 2001.
61. Rees DA, Alcolado JC. Animal models of diabetes mellitus. Diabetic medicine : a journal of the British Diabetic Association. 2005;22(4):359-70.
62. McKnight LL, Lopez S, Shoveller AK, France J. Models for the Study of Whole-Body Glucose Kinetics: A Mathematical Synthesis. ISRN Biomathematics. 2013;2013:120974.
63. Bergman RN, Ider YZ, Bowden CR, Cobelli C. Quantitative estimation of insulin sensitivity. Am J Physiol. 1979;236(6):E667-77.
64. Bolie VW. Coefficients of normal blood glucose regulation. J Appl Physiol. 1961;16:783-8.
65. Cobelli C, Pacini G, Toffolo G, Sacca L. Estimation of insulin sensitivity and glucose clearance from minimal model: new insights from labeled IVGTT. American Journal of Physiology-Endocrinology and Metabolism. 1986;250(5):E591-E8.
66. Radziuk J, Norwich KH, Vranic M. Experimental validation of measurements of glucose turnover in nonsteady state. Am J Physiol. 1978;234(1):E84-93.
67. Caumo A, Cobelli C. Hepatic glucose production during the labeled IVGTT: estimation by deconvolution with a new minimal model. American Journal of Physiology-Endocrinology and Metabolism. 1993;264(5):E829-E41.
68. Cobelli C, Toffolo G, Ferrannini E. A model of glucose kinetics and their control by insulin, compartmental and noncompartmental approaches. Mathematical Biosciences. 1984;72(2):291-315.
69. Ghosh S, Maka S. A NARX modeling-based approach for evaluation of insulin sensitivity. Biomedical Signal Processing and Control. 2009;4(1):49-56.

70. Yates JWT, Watson EM. Estimating insulin sensitivity from glucose levels only: Use of a non-linear mixed effects approach and maximum a posteriori (MAP) estimation. Computer Methods and Programs in Biomedicine. 2013;109(2):134-43.
71. Basu R, Di Camillo B, Toffolo G, Basu A, Shah P, Vella A, et al. Use of a novel triple-tracer approach to assess postprandial glucose metabolism. Am J Physiol Endocrinol Metab. 2003;284(1):E55-69.
72. Lehmann ED, Deutsch T. A physiological model of glucose-insulin interaction in type 1 diabetes mellitus. Journal of Biomedical Engineering. 1992;14(3):235-42.
73. Horowitz M, Maddox A, Bochner M, Wishart J, Bratasiuk R, Collins P, Shearman D. Relationships between gastric emptying of solid and caloric liquid meals and alcohol absorption. Am J Physiol. 1989;257(2 Pt 1):G291-8.
74. Dalla Man C, Camilleri M, Cobelli C. A system model of oral glucose absorption: validation on gold standard data. IEEE Trans Biomed Eng. 2006;53(12 Pt 1):2472-8.
75. Dalla Man C, Rizza RA, Cobelli C. Meal simulation model of the glucose-insulin system. IEEE Trans Biomed Eng. 2007;54(10):1740-9.
76. Woldaregay AZ, Årsand E, Walderhaug S, Albers D, Mamykina L, Botsis T, Hartvigsen G. Data-driven modeling and prediction of blood glucose dynamics: Machine learning applications in type 1 diabetes. Artificial Intelligence in Medicine. 2019;98:109-34.
77. Alvarez H, Lamanna R, Vega P, Revollar S. Metodología para la Obtención de Modelos Semifísicos de Base Fenomenológica Aplicada a una Sulfitadora de Jugo de Caña de Azúcar. Revista Iberoamericana de Automática e Informática Industrial RIAI. 2009;6(3):10-20.
78. Lema-Perez L, Muñoz-Tamayo R, Garcia-Tirado J, Alvarez H. On Parameter Interpretability of Phenomenological-Based Semiphysical Models. bioRxiv. 2018:446583.
79. Builes-Montaño CE, Ortiz-Cano NA, Ramirez-Rincón A, Rojas-Henao NA. Efficacy and safety of carbohydrate counting versus other forms of dietary advice in patients with type 1 diabetes mellitus: a systematic review and meta-analysis of randomised clinical trials. J Hum Nutr Diet. 2022;35(6):1030-42.
80. Saeedi P, Petersohn I, Salpea P, Malanda B, Karuranga S, Unwin N, et al. Global and regional diabetes prevalence estimates for 2019 and projections for 2030 and 2045: Results from the International Diabetes Federation Diabetes Atlas, 9th edition. Diabetes research and clinical practice. 2019;157.
81. Gosmanov AR, Gosmanova EO, Kitabchi AE. Hyperglycemic crises: diabetic ketoacidosis (DKA), and hyperglycemic hyperosmolar state (HHS). Endotext [Internet]: MDText. com, Inc.; 2018.
82. Nathan DM, Genuth S, Lachin J, Cleary P, Crofford O, Davis M, et al. The effect of intensive treatment of diabetes on the development and progression of long-term complications in insulin-dependent diabetes mellitus. The New England journal of medicine. 1993;329(14):977-86.
83. Gillespie SJ, Kulkarni KD, Daly AE. Using carbohydrate counting in diabetes clinical practice. J Am Diet Assoc. 1998;98(8):897-905.
84. Higgins JP, Thomas J, Chandler J, Cumpston M, Li T, Page MJ, Welch VA. Cochrane handbook for systematic reviews of interventions: John Wiley & Sons; 2019.
85. Liberati A, Altman DG, Tetzlaff J, Mulrow C, Gøtzsche PC, Ioannidis JP, et al. The PRISMA statement for reporting systematic reviews and meta-analyses of studies that evaluate healthcare interventions: explanation and elaboration. BMJ (Clinical research ed). 2009;339:b2700.
86. Sterne JA, Savović J, Page MJ, Elbers RG, Blencowe NS, Boutron I, et al. RoB 2: a revised tool for assessing risk of bias in randomised trials. BMJ (Clinical research ed). 2019;366.

87. Guyatt GH, Oxman AD, Vist GE, Kunz R, Falck-Ytter Y, Alonso-Coello P, Schunemann HJ. GRADE: an emerging consensus on rating quality of evidence and strength of recommendations. BMJ (Clinical research ed). 2008;336(7650):924-6.
88. Egger M, Davey Smith G, Schneider M, Minder C. Bias in meta-analysis detected by a simple, graphical test. BMJ (Clinical research ed). 1997;315(7109):629-34.
89. Duval S, Tweedie R. Trim and fill: A simple funnel-plot-based method of testing and adjusting for publication bias in meta-analysis. Biometrics. 2000;56(2):455-63.
90. R Development Core Team. R: A language and environment for statistical computing. Vienna, Austria: R Foundation for Statistical Computing; 2021.
91. Harrer M, Cuijpers P, Furukawa TA, Ebert DD. Doing meta-analysis in R: A hands-on guide. PROTECT Lab Erlangen. 2019.
92. Enander R, Gundevall C, Strömgren A, Chaplin J, Hanas R. Carbohydrate counting with a bolus calculator improves post-prandial blood glucose levels in children and adolescents with type 1 diabetes using insulin pumps. Pediatric Diabetes. 2012;13(7):545-51.
93. Schmidt S, Meldgaard M, Serifovski N, Storm C, Christensen TM, Gade-Rasmussen B, Nørgaard K. Use of an automated bolus calculator in MDI-treated type 1 diabetes: the BolusCal Study, a randomized controlled pilot study. Diabetes care. 2012;35(5):984-90.
94. de Albuquerque IZ, Stringhini MLF, Marques RdMB, Mundim CA, Rodrigues MLD, Campos MRH. Carbohydrate counting, nutritional status and metabolic profil eof adolescents with type 1 diabetes mellitus. Scientia Medica. 2014;24(4):5.
95. Gökşen D, Atik Altınok Y, Özen S, Demir G, Darcan Ş. Effects of Carbohydrate Counting Method on Metabolic Control in Children with Type 1 Diabetes Mellitus. J Clin Res Pediatr Endocrinol. 2014;6(2):74-8.
96. Donzeau A, Bonnemaison E, Vautier V, Menut V, Houdon L, Bendelac N, et al. Effects of advanced carbohydrate counting on glucose control and quality of life in children with type 1 diabetes. Pediatr Diabetes. 2020.
97. Olkin I, Dahabreh IJ, Trikalinos TA. GOSH – a graphical display of study heterogeneity. Research Synthesis Methods. 2012;3(3):214-23.
98. Hartigan JA, Wong MA. AK-means clustering algorithm. Journal of the Royal Statistical Society: Series C (Applied Statistics). 1979;28(1):100-8.
99. Schubert E, Sander J, Ester M, Kriegel HP, Xu X. DBSCAN revisited, revisited: why and how you should (still) use DBSCAN. ACM Transactions on Database Systems (TODS). 2017;42(3):1-21.
100. Fraley C, Raftery AE. Model-based clustering, discriminant analysis, and density estimation. Journal of the American statistical Association. 2002;97(458):611-31.
101. Peters JL, Sutton AJ, Jones DR, Abrams KR, Rushton L. Contour-enhanced meta-analysis funnel plots help distinguish publication bias from other causes of asymmetry. J Clin Epidemiol. 2008;61(10):991-6.
102. Bao J, de Jong V, Atkinson F, Petocz P, Brand-Miller JC. Food insulin index: physiologic basis for predicting insulin demand evoked by composite meals. The American journal of clinical nutrition. 2009;90(4):986-92.
103. Wild D, von Maltzahn R, Brohan E, Christensen T, Clauson P, Gonder-Frederick L. A critical review of the literature on fear of hypoglycemia in diabetes: Implications for diabetes management and patient education. Patient Education and Counseling. 2007;68(1):10-5.
104. Rossi MC, Nicolucci A, Ozzello A, Gentile S, Aglialoro A, Chiambretti A, et al. Impact of severe and symptomatic hypoglycemia on quality of life and fear of hypoglycemia in type 1 and type 2 diabetes. Results of the Hypos-1 observational study. Nutrition, Metabolism and Cardiovascular Diseases. 2019;29(7):736-43.

105. Allen C, LeCaire T, Palta M, Daniels K, Meredith M, D'Alessio DJ. Risk Factors for Frequent and Severe Hypoglycemia in Type 1 Diabetes. Diabetes care. 2001;24(11):1878-81.
106. Defining and Reporting Hypoglycemia in Diabetes. A report from the American Diabetes Association Workgroup on Hypoglycemia. 2005;28(5):1245-9.
107. Lema-Perez L, Herrón-Bedoya A, Paredes-Ángel V, Hernández-Arango A, Builes-Montaño CE, Alvarez H. Estimation of glucose rate of appearance in portal vein circulation using a phenomenological-based model. PLoS One. 2023;18(5):e0285849.
108. Builes-Montaño CE, Lema-Perez L, Garcia-Tirado J, Alvarez H. Main glucose hepatic fluxes in healthy subjects predicted from a phenomenological-based model. Comput Biol Med. 2022;142:105232.
109. DeFronzo RA, Tobin JD, Andres R. Glucose clamp technique: a method for quantifying insulin secretion and resistance. American Journal of Physiology-Endocrinology and Metabolism. 1979;237(3):E214.
110. Segre G, Turco GL, Vercellone G. Modeling blood glucose and insulin kinetics in normal, diabetic and obese subjects. Diabetes. 1973;22(2):94-103.
111. Marchetti L, Reali F, Dauriz M, Brangani C, Boselli L, Ceradini G, et al. A Novel Insulin/Glucose Model after a Mixed-Meal Test in Patients with Type 1 Diabetes on Insulin Pump Therapy. Scientific Reports. 2016;6(1):36029.
112. Uluseker C, Simoni G, Marchetti L, Dauriz M, Matone A, Priami C. A closed-loop multi-level model of glucose homeostasis. PloS one. 2018;13(2):e0190627.
113. Manrique-Córdoba J, Romero-Ante J, Vivas A, Vicente J, Sabater-Navarro J. Modelado matemático de ingestas de alimento e infusión de insulina en un paciente con diabetes tipo 1 en lazo cerrado. Revista Iberoamericana de Automática e Informática industrial. 2020;17(2):156-68.
114. Lema-Perez L, Garcia-Tirado J, Builes-Montano C, Alvarez H. Phenomenological-Based model of human stomach and its role in glucose metabolism. J Theor Biol. 2019;460:88-100.
115. Blandón LA, Gallego MSC, Patino SIO, Pérez LL, editors. A Phenomenological-Based Model for the Small Intestine Role in Human Glucose Homeostasis. 2019 IEEE 4th Colombian Conference on Automatic Control (CCAC); 2019 15-18 Oct. 2019.
116. Lema-Perez L, Muñoz-Tamayo R, Garcia-Tirado J, Alvarez H. On parameter interpretability of phenomenological-based semiphysical models in biology. Informatics in Medicine Unlocked. 2019;15:100158.
117. Lamanna R, Vega P, Revollar S, Alvarez H. Diseno simultáneo de proceso y control de una torre sulfitadora de jugo de cana de azúcar. Revista Iberoamericana de Automática e Informática Industrial RIAI. 2009;6(3):32-43.
118. Hoyos E, López D, Alvarez H. A phenomenologically based material flow model for friction stir welding. Materials & Design. 2016;111:321-30.
119. Zimmerman M, Snow B. An Introduction to Nutrition: Independent; 2012.
120. Collins PJ, Houghton LA, Read NW, Horowitz M, Chatterton BE, Heddle R, Dent J. Role of the proximal and distal stomach in mixed solid and liquid meal emptying. Gut. 1991;32(6):615-9.
121. Gentilcore D, Chaikomin R, Jones KL, Russo A, Feinle-Bisset C, Wishart JM, et al. Effects of fat on gastric emptying of and the glycemic, insulin, and incretin responses to a carbohydrate meal in type 2 diabetes. J Clin Endocrinol Metab. 2006;91(6):2062-7.
122. Rayner CK, Hebbard GS, Horowitz M. Chapter 35 - Physiology of the Antral Pump and Gastric Emptying. In: Johnson LR, Ghishan FK, Kaunitz JD, Merchant JL, Said HM, Wood JD, editors. Physiology of the Gastrointestinal Tract (Fifth Edition). Boston: Academic Press; 2012. p. 959-76.
123. Jolliffe DM. Practical gastric physiology. Continuing Education in Anaesthesia Critical Care & Pain. 2009;9(6):173-7.

124. Holst JJ, Gribble F, Horowitz M, Rayner CK. Roles of the Gut in Glucose Homeostasis. Diabetes care. 2016;39(6):884-92.
125. Malagelada JR, Longstreth GF, Summerskill WH, Go VL. Measurement of gastric functions during digestion of ordinary solid meals in man. Gastroenterology. 1976;70(2):203-10.
126. Akhtar R, Sherratt MJ, Cruickshank JK, Derby B. Characterizing the elastic properties of tissues. Mater Today (Kidlington). 2011;14(3):96-105.
127. Marieb EN. Human Anatomy & Physiology: Benjamin Cummings; 2001.
128. Avvari RK. Effect of local longitudinal shortening on the transport of luminal contents through small intestine. Acta Mechanica Sinica. 2019;35(1):45-60.
129. Van Der Schoor SR, Reeds PJ, Stoll B, Henry JF, Rosenberger JR, Burrin DG, Van Goudoever JB. The high metabolic cost of a functional gut. Gastroenterology. 2002;123(6):1931-40.
130. Green DW, Southard MZ. Perry's chemical engineers' handbook: McGraw-Hill Education; 2019.
131. Bellini C, Glass P, Sitti M, Di Martino ES. Biaxial mechanical modeling of the small intestine. J Mech Behav Biomed Mater. 2011;4(8):1727-40.
132. Chagnon G, Ohayon J, Martiel J-L, Favier D. Hyperelasticity modeling for incompressible passive biological tissues. Biomechanics of living organs: Elsevier; 2017. p. 3-30.
133. Ma Y, Choi J, Hourlier-Fargette A, Xue Y, Chung HU, Lee JY, et al. Relation between blood pressure and pulse wave velocity for human arteries. Proc Natl Acad Sci U S A. 2018;115(44):11144-9.
134. Layer P, Gröger G. Fate of pancreatic enzymes in the human intestinal lumen in health and pancreatic insufficiency. Digestion. 1993;54 Suppl 2:10-4.
135. Wilborn CD, Willoughby DS. The role of dietary protein intake and resistance training on Myosin heavy chain expression. J Int Soc Sports Nutr. 2004;1(2):27-34.
136. Holtzer A, Lowey S. The molecular weight, size and shape of the myosin molecule. Journal of the American Chemical Society. 1959;81(6):1370-7.
137. Koepsell H. Glucose transporters in the small intestine in health and disease. Pflugers Arch. 2020;472(9):1207-48.
138. Kellett GL, Helliwell PA. The diffusive component of intestinal glucose absorption is mediated by the glucose-induced recruitment of GLUT2 to the brush-border membrane. Biochem J. 2000;350 Pt 1(Pt 1):155-62.
139. Kellett GL. The facilitated component of intestinal glucose absorption. J Physiol. 2001;531(Pt 3):585-95.
140. Dawson DJ, Burrows PC, Lobley RW, Holmes R. The kinetics of monosaccharide absorption by human jejunal biopsies: evidence for active and passive processes. Digestion. 1987;38(2):124-32.
141. Kandasamy P, Gyimesi G, Kanai Y, Hediger MA. Amino acid transporters revisited: New views in health and disease. Trends Biochem Sci. 2018;43(10):752-89.
142. Winne D. Formal kinetics of water and solute absorption with regard to intestinal blood flow. J Theor Biol. 1970;27(1):1-18.
143. Gisolfi CV, Summers RW, Schedl HP, Bleiler TL. Intestinal water absorption from select carbohydrate solutions in humans. J Appl Physiol (1985). 1992;73(5):2142-50.
144. Jackson AD, McLaughlin J. Digestion and absorption. Surgery (oxford). 2009;27(6):231-6.
145. Alvarez H, Peña M. Modelamiento de sistemas de inferencia borrosa tipo Takagi-Sugeno. Avances en Sistemas e Informatica. 2004;1(1):1-11.
146. Keller J, Layer P. Human pancreatic exocrine response to nutrients in health and disease. Gut. 2005;54(suppl 6):1-28.

147. Félétou M, Mittal RK, Kopp UC, Solaro RJ, Pittman RN, Korthuis RJ, et al. Colloquium Series on Integrated Systems Physiology: From Molecule to Function to Disease. 2011.
148. Howard PJ, Murphy GM, Dowling RH. Gall bladder emptying patterns in response to a normal meal in healthy subjects and patients with gall stones: ultrasound study. Gut. 1991;32(11):1406-11.
149. Al-Atabi M, Ooi RC, Luo XY, Chin SB, Bird NC. Computational analysis of the flow of bile in human cystic duct. Med Eng Phys. 2012;34(8):1177-83.
150. Olsen O, Schaffalitzky de Muckadell OB, Cantor P. Fat and pancreatic secretion. Scand J Gastroenterol. 1989;24(1):74-80.
151. Basu R, Schiavon M, Petterson XM, Hinshaw L, Slama M, Carter R, et al. A novel natural tracer method to measure complex carbohydrate metabolism. Am J Physiol Endocrinol Metab. 2019;317(3):E483-e93.
152. Dalla Man C, Caumo A, Basu R, Rizza R, Toffolo G, Cobelli C. Minimal model estimation of glucose absorption and insulin sensitivity from oral test: validation with a tracer method. Am J Physiol Endocrinol Metab. 2004;287(4):E637-43.
153. Ferrannini E, Bjorkman O, Reichard GA, Jr., Pilo A, Olsson M, Wahren J, DeFronzo RA. The disposal of an oral glucose load in healthy subjects. A quantitative study. Diabetes. 1985;34(6):580-8.
154. Hinsberger A, Sandhu BK. Digestion and absorption. Current Paediatrics. 2004;14(7):605-11.
155. Chung YC, Kim YS, Shadchehr A, Garrido A, Macgregor IL, Sleisenger MH. Protein digestion and absorption in human small intestine. Gastroenterology. 1979;76(6):1415-21.
156. Krajmalnik-Brown R, Ilhan ZE, Kang DW, DiBaise JK. Effects of gut microbes on nutrient absorption and energy regulation. Nutr Clin Pract. 2012;27(2):201-14.
157. Johansson C. Studies of gastrointestinal interactions. VII. Characteristics of the absorption pattern of sugar, fat and protein from composite meals in man. A quantitative study. Scand J Gastroenterol. 1975;10(1):33-42.
158. Jackson AD, McLaughlin J. Digestion and absorption. Surgery - Oxford International Edition. 2009;27(6):231-6.
159. Kong F, Singh RP. Disintegration of solid foods in human stomach. J Food Sci. 2008;73(5):R67-80.
160. Builes-Montaño CE, Lema-Pérez L, Monsalve-Arango LE, Naranjo-Cano MA, Sierra Duque CM, García-Tirado JF, Alvarez Zapata HD. STUDIA: An application to support carbohydrate counting by simulating glucose dynamics. Revista Colombiana de Endocrinología, Diabetes & Metabolismo. 2022;9(4).
161. Bergman RN, Piccinini F, Kabir M, Ader M. Novel aspects of the role of the liver in carbohydrate metabolism. Metabolism. 2019;99:119-25.
162. Sherwin RS. Role of liver in glucose homeostasis. Diabetes care. 1980;3(2):261-5.
163. Laurenti MC, Vella A, Adams JD, Schembri Wismayer DJ, Egan AM, Dalla Man C. Assessment of individual and standardized glucagon kinetics in healthy humans. American Journal of Physiology-Endocrinology and Metabolism. 2021;320(1):E71-E7.
164. Najjar SM, Perdomo G. Hepatic Insulin Clearance: Mechanism and Physiology. Physiology (Bethesda). 2019;34(3):198-215.
165. Duke L, Fereira de Moura A, Gorban de Lapertosa S, Lucy Hammond L, Jacobs E, Abha Kaundal A. IDF Diabetes Atlas. International Diabetes Federation, Brussels, Belgium; 2019.
166. Association AD. 7. Diabetes technology: standards of medical care in diabetes—2020. Diabetes care. 2020;43(Supplement_1):S77-S88.

167. Kaufman N. Digital therapeutics: leading the way to improved outcomes for people with diabetes. Diabetes Spectrum. 2019;32(4):301-3.
168. Kovatchev B. A century of diabetes technology: signals, models, and artificial pancreas control. Trends in Endocrinology & Metabolism. 2019;30(7):432-44.
169. Kovatchev BP, Breton M, Man CD, Cobelli C. In silico preclinical trials: a proof of concept in closed-loop control of type 1 diabetes. Journal of diabetes science and technology. 2009;3(1):44-55.
170. Cobelli C, Dalla Man C, Sparacino G, Magni L, De Nicolao G, Kovatchev BP. Diabetes: models, signals, and control. IEEE reviews in biomedical engineering. 2009;2:54-96.
171. Lema-Perez L, Builes-Montaño CE, Alvarez H. A phenomenological-based semi-physical model of the kidneys and its role in glucose metabolism. J Theor Biol. 2021;508:110489.
172. Radziuk J. Tracer methods and the metabolic disposal of a carbohydrate load in man. Diabetes Metab Rev. 1987;3(1):231-67.
173. Adkins A, Basu R, Persson M, Dicke B, Shah P, Vella A, et al. Higher insulin concentrations are required to suppress gluconeogenesis than glycogenolysis in nondiabetic humans. Diabetes. 2003;52(9):2213-20.
174. Han H-S, Kang G, Kim JS, Choi BH, Koo S-H. Regulation of glucose metabolism from a liver-centric perspective. Experimental & molecular medicine. 2016;48(3):e218-e.
175. Ahn KJ, Kim J, Yun M, Park JH, Lee JD. Enzymatic properties of the N- and C-terminal halves of human hexokinase II. BMB Rep. 2009;42(6):350-5.
176. Woerle HJ, Meyer C, Dostou JM, Gosmanov NR, Islam N, Popa E, et al. Pathways for glucose disposal after meal ingestion in humans. Am J Physiol Endocrinol Metab. 2003;284(4):E716-25.
177. McDevitt RM, Bott SJ, Harding M, Coward WA, Bluck LJ, Prentice AM. De novo lipogenesis during controlled overfeeding with sucrose or glucose in lean and obese women. The American journal of clinical nutrition. 2001;74(6):737-46.
178. Radziuk J, Pye S. Hepatic glucose uptake, gluconeogenesis and the regulation of glycogen synthesis. Diabetes/metabolism research and reviews. 2001;17(4):250-72.
179. Vandercammen A, Van Schaftingen E. Competitive inhibition of liver glucokinase by its regulatory protein. Eur J Biochem. 1991;200(2):545-51.
180. Iynedjian PB, Jotterand D, Nouspikel T, Asfari M, Pilot PR. Transcriptional induction of glucokinase gene by insulin in cultured liver cells and its repression by the glucagon-cAMP system. J Biol Chem. 1989;264(36):21824-9.
181. Brown KS, Kalinowski SS, Megill JR, Durham SK, Mookhtiar KA. Glucokinase regulatory protein may interact with glucokinase in the hepatocyte nucleus. Diabetes. 1997;46(2):179-86.
182. Argaud D, Zhang Q, Pan W, Maitra S, Pilkis SJ, Lange AJ. Regulation of rat liver glucose-6-phosphatase gene expression in different nutritional and hormonal states: gene structure and 5'-flanking sequence. Diabetes. 1996;45(11):1563-71.
183. Massillon D, Barzilai N, Chen W, Hu M, Rossetti L. Glucose regulates in vivo glucose-6-phosphatase gene expression in the liver of diabetic rats. J Biol Chem. 1996;271(17):9871-4.
184. Massillon D, Bollen M, De Wulf H, Overloop K, Vanstapel F, Van Hecke P, Stalmans W. Demonstration of a glycogen/glucose 1-phosphate cycle in hepatocytes from fasted rats. Selective inactivation of phosphorylase by 2-deoxy-2-fluoro-alpha-D-glucopyranosyl fluoride. J Biol Chem. 1995;270(33):19351-6.
185. Arbeláez-Gómez D, Benavides-López S, Giraldo-Agudelo MP, Guzmán-Álvarez JP, Ramirez-Mazo C, Gómez-Echavarría LM. A phenomenological-based model of the endometrial growth and shedding during the menstrual cycle. Journal of Theoretical Biology. 2022;532:110922.

186. Herron-Bedoya A, Walteros-Leon M, Lema-Perez L, Alvarez H. Phenomenological-based model of glucose transport from liver to abdominal subcutaneous adipose tissue. Journal of Theoretical Biology. 2021;530:110883.
187. Magnusson I, Rothman DL, Jucker B, Cline GW, Shulman RG, Shulman GI. Liver glycogen turnover in fed and fasted humans. Am J Physiol. 1994;266(5 Pt 1):E796-803.
188. Frevert U, Engelmann S, Zougbédé S, Stange J, Ng B, Matuschewski K, et al. Intravital observation of Plasmodium berghei sporozoite infection of the liver. PLoS Biol. 2005;3(6):e192.
189. Kenner T, Hinghofer-Szalkay H, Leopold H, Pogglitsch H. The relation between the density of blood and the arterial pressure in animal experiments and in patients during hemodialysis (author's transl). Zeitschrift fur Kardiologie. 1977;66(7):399-401.
190. Berndt N, Holzhütter HG. Dynamic Metabolic Zonation of the Hepatic Glucose Metabolism Is Accomplished by Sinusoidal Plasma Gradients of Nutrients and Hormones. Front Physiol. 2018;9:1786.
191. Alvarez H. Process Modeling for Analysis and Control. Dynamic Effects in Unitary Operations and Reactive Processes. In Press.
192. Ishida T, Field J. Hepatic handling of glucagon. Glucagon II: Springer; 1983. p. 361-88.
193. Raddatz D, Ramadori G. Carbohydrate metabolism and the liver: actual aspects from physiology and disease. Z Gastroenterol. 2007;45(1):51-62.
194. Sorensen JT. A physiologic model of glucose metabolism in man and its use to design and assess improved insulin therapies for diabetes: Massachusetts Institute of Technology; 1985.
195. Visentin R, Dalla Man C, Kovatchev B, Cobelli C. The University of Virginia/Padova Type 1 Diabetes Simulator Matches the Glucose Traces of a Clinical Trial. Diabetes technology & therapeutics. 2014;16(7):428-34.
196. Chalhoub E, Xie L, Balasubramanian V, Kim J, Belovich J. A distributed model of carbohydrate transport and metabolism in the liver during rest and high-intensity exercise. Annals of Biomedical Engineering. 2007;35:474-91.
197. Silber HE, Jauslin PM, Frey N, Karlsson MO. An integrated model for the glucose-insulin system. Basic & clinical pharmacology & toxicology. 2010;106(3):189-94.
198. El-Refai M, Bergman RN. Simulation study of control of hepatic glycogen synthesis by glucose and insulin. American Journal of Physiology-Legacy Content. 1976;231(5):1608-19.
199. Konig M, Bulik S, Holzhutter HG. Quantifying the contribution of the liver to glucose homeostasis: a detailed kinetic model of human hepatic glucose metabolism. PLoS Comput Biol. 2012;8(6):e1002577.
200. Koenig M, Holzhuetter H-G. Kinetic modeling of human hepatic glucose metabolism in type 2 diabetes mellitus predicts higher risk of hypoglycemic events in rigorous insulin therapy. Journal of Biological Chemistry. 2012;287(44):36978-89.
201. Hovorka R, Canonico V, Chassin LJ, Haueter U, Massi-Benedetti M, Federici MO, et al. Nonlinear model predictive control of glucose concentration in subjects with type 1 diabetes. Physiological measurement. 2004;25(4):905.
202. Panunzi S, Pompa M, Borri A, Piemonte V, De Gaetano A. A revised Sorensen model: Simulating glycemic and insulinemic response to oral and intra-venous glucose load. Plos one. 2020;15(8):e0237215.
203. Garcia-Tirado J, Colmegna P, Corbett JP, Ozaslan B, Breton MD. In Silico Analysis of an Exercise-Safe Artificial Pancreas With Multistage Model Predictive Control and Insulin Safety System. Journal of diabetes science and technology. 2019;13(6):1054-64.
204. Patek SD, Lv D, Ortiz EA, Hughes-Karvetski C, Kulkarni S, Zhang Q, Breton MD. Empirical representation of blood glucose variability in a compartmental model. Prediction Methods for Blood Glucose Concentration: Springer; 2016. p. 133-57.

205. Garcia-Tirado J, Brown SA, Laichuthai N, Colmegna P, Koravi CLK, Ozaslan B, et al. Anticipation of Historical Exercise Patterns by a Novel Artificial Pancreas System Reduces Hypoglycemia During and After Moderate-Intensity Physical Activity in People with Type 1 Diabetes. Diabetes technology & therapeutics. 2021;23(4):277-85.
206. Builes-Montaño CE, Ortiz-Cano NA, Ramirez-Rincón A, Rojas-Henao NA. Efficacy and safety of carbohydrate counting versus other forms of dietary advice in patients with type 1 diabetes mellitus: A systematic review and meta-analysis of randomized clinical trials. J Hum Nutr Diet. 2022.
207. Krebs JD, Parry Strong A, Cresswell P, Reynolds AN, Hanna A, Haeusler S. A randomised trial of the feasibility of a low carbohydrate diet vs standard carbohydrate counting in adults with type 1 diabetes taking body weight into account. Asia Pac J Clin Nutr. 2016;25(1):78-84.
208. Álvarez HD, Peña M. Modelamiento de Sistemas de Inferencia Borrosa Tipo Takagi-Sugeno. Rev Avances en Sistemas Informática. 2004;1(1):1-11.
209. Rizun N, Taranenko Y. Simulation models of human decision-making processes. Management Dynamics in the Knowledge Economy. 2014;2(2):241-64.
210. Pagé C, Bernier P-M, Trempe M. Using video simulations and virtual reality to improve decision-making skills in basketball. Journal of sports sciences. 2019;37(21):2403-10.
211. Benjamin P, Koola P, Akella K, Graul M, Painter M, editors. Using Simulation Based Training Methods for Improved Warfighter Decision Making. International Conference on Augmented Cognition; 2013: Springer.
212. LARKIN A, HANLEY KL, WARTERS M, LITTMAN GS. Virtual Simulation Improves Clinical Decision-Making in Managing Type 2 Diabetes. Diabetes. 2018;67(Supplement 1):688-P.
213. Sperl-Hillen J, O'Connor P, Ekstrom H, Rush W, Asche S, Fernandes O, et al. Using Simulation Technology to Teach Diabetes Care Management Skills to Resident Physicians. Journal of diabetes science and technology. 2013;7(5):1243-54.
214. Colmegna P, Bisio A, Mcfadden R, Wakeman CA, Oliveri MC, Nass R, Breton MD. 97-LB: Bringing Simulation Technologies to People with T1D: A Pilot Study. Diabetes. 2021;70(Supplement_1).
215. ElSayed NA, Aleppo G, Aroda VR, Bannuru RR, Brown FM, Bruemmer D, et al. 14. Children and Adolescents: Standards of Care in Diabetes-2023. Diabetes care. 2023;46(Suppl 1):S230-s53.
216. Bland JM, Altman DG. Measuring agreement in method comparison studies. Stat Methods Med Res. 1999;8(2):135-60.
217. Finn E, Schlichting L, Grau L, Douglas IS, Pereira RI. Real-world Accuracy of CGM in Inpatient Critical and Noncritical Care Settings at a Safety-Net Hospital. Diabetes care. 2023;46(10):1825-30.
218. Cengiz E, Tamborlane WV. A tale of two compartments: interstitial versus blood glucose monitoring. Diabetes technology & therapeutics. 2009;11 Suppl 1(Suppl 1):S11-6.
219. Pleus S, Schauer S, Baumstark A, Beil A, Jendrike N, Link M, et al. Differences in venous, capillary and interstitial glucose concentrations in individuals without diabetes after glucose load. Journal of Laboratory Medicine. 2023;47(3):97-104.
220. Parkes JL, Slatin SL, Pardo S, Ginsberg BH. A new consensus error grid to evaluate the clinical significance of inaccuracies in the measurement of blood glucose. Diabetes care. 2000;23(8):1143-8.
221. Bedini JL, Wallace JF, Pardo S, Petruschke T. Performance Evaluation of Three Blood Glucose Monitoring Systems Using ISO 15197: 2013 Accuracy Criteria, Consensus and Surveillance Error Grid Analyses, and Insulin Dosing Error Modeling in a Hospital Setting. Journal of diabetes science and technology. 2015;10(1):85-92.

222. Freckmann G, Pleus S, Grady M, Setford S, Levy B. Measures of Accuracy for Continuous Glucose Monitoring and Blood Glucose Monitoring Devices. Journal of diabetes science and technology. 2019;13(3):575-83.
223. Steineck IIK, Mahmoudi Z, Ranjan A, Schmidt S, Jørgensen JB, Nørgaard K. Comparison of Continuous Glucose Monitoring Accuracy Between Abdominal and Upper Arm Insertion Sites. Diabetes technology & therapeutics. 2019;21(5):295-302.
224. Bedini JL, Wallace JF, Petruschke T, Pardo S. A Multicenter Performance Evaluation of a Blood Glucose Monitoring System in 21 Leading Hospitals in Spain. Journal of diabetes science and technology. 2015;10(1):93-100.
225. Builes-Montaño CE, Lema-Perez L, Restrepo JC, Garcia-Tirado JF, Alvarez H, Ramirez-Rincón A, Zuleta JJ. Carbohydrate Count Aided by a Simulation of Postprandial Glucose Dynamics Generated by a Mathematical Model in People with Type 1 Diabetes Mellitus. A Study Protocol for a Clinical Trial. A Study Protocol for a Clinical Trial.
226. Bell KJ, Barclay AW, Petocz P, Colagiuri S, Brand-Miller JC. Efficacy of carbohydrate counting in type 1 diabetes: a systematic review and meta-analysis. The lancet Diabetes & endocrinology. 2014;2:133-40.
227. Bell KJ, Smart CE, Steil GM, Brand-Miller JC, King B, Wolpert HA. Impact of fat, protein, and glycemic index on postprandial glucose control in type 1 diabetes: implications for intensive diabetes management in the continuous glucose monitoring era. Diabetes care. 2015;38(6):1008-15.
228. Battelino T, Danne T, Bergenstal RM, Amiel SA, Beck R, Biester T, et al. Clinical Targets for Continuous Glucose Monitoring Data Interpretation: Recommendations From the International Consensus on Time in Range. Diabetes care. 2019;42(8):1593-603.
229. Vigersky RA, McMahon C. The Relationship of Hemoglobin A1C to Time-in-Range in Patients with Diabetes. Diabetes technology & therapeutics. 2019;21(2):81-5.
230. Beck RW, Bergenstal RM, Riddlesworth TD, Kollman C, Li Z, Brown AS, Close KL. Validation of Time in Range as an Outcome Measure for Diabetes Clinical Trials. Diabetes care. 2019;42(3):400-5.
231. Xing D, Kollman C, Beck RW, Tamborlane WV, Laffel L, Buckingham BA, et al. Optimal sampling intervals to assess long-term glycemic control using continuous glucose monitoring. Diabetes technology & therapeutics. 2011;13(3):351-8.
232. Riddlesworth TD, Beck RW, Gal RL, Connor CG, Bergenstal RM, Lee S, Willi SM. Optimal Sampling Duration for Continuous Glucose Monitoring to Determine Long-Term Glycemic Control. Diabetes technology & therapeutics. 2018;20(4):314-6.
233. Kitabchi AE, Umpierrez GE, Miles JM, Fisher JN. Hyperglycemic crises in adult patients with diabetes. Diabetes care. 2009;32(7):1335-43.
234. Group IHS. Glucose concentrations of less than 3.0 mmol/L (54 mg/dL) should be reported in clinical trials: a joint position statement of the American Diabetes Association and the European Association for the Study of Diabetes. Diabetes care. 2017;40(1):155-7.
235. Danne T, Nimri R, Battelino T, Bergenstal RM, Close KL, DeVries JH, et al. International consensus on use of continuous glucose monitoring. Diabetes care. 2017;40(12):1631-40.
236. Aguilar MIH, de la Garza González A, Miranda MPS, Villegas AAG. Adaptación al español del cuestionario de usabilidad de sistemas informáticos CSUQ/spanish language adaptation of the computer systems usability questionnaire CSUQ. RECI Revista Iberoamericana de las Ciencias Computacionales e Informática. 2015;4(8):84-99.
237. Gomis R, Herrera-Pombo JL, Calderón A, Rubio-Terrés C, Sarasa P. Validación del cuestionario “Diabetes treatment satisfaction questionnaire” (DTSQ) en la población española. PharmacoEconomics Spanish Research Articles. 2006;3(1):7-18.

238. Bradley C. Handbook of psychology and diabetes: a guide to psychological measurement in diabetes research and practice: Routledge; 2013.
239. Battelino T, Phillip M, Bratina N, Nimri R, Oskarsson P, Bolinder J. Effect of continuous glucose monitoring on hypoglycemia in type 1 diabetes. Diabetes care. 2011;34(4):795-800.
240. van Beers CA, DeVries JH, Kleijer SJ, Smits MM, Geelhoed-Duijvestijn PH, Kramer MH, et al. Continuous glucose monitoring for patients with type 1 diabetes and impaired awareness of hypoglycaemia (IN CONTROL): a randomised, open-label, crossover trial. The lancet Diabetes & endocrinology. 2016;4(11):893-902.
241. Saslow LR, Kim S, Daubenmier JJ, Moskowitz JT, Phinney SD, Goldman V, et al. A randomized pilot trial of a moderate carbohydrate diet compared to a very low carbohydrate diet in overweight or obese individuals with type 2 diabetes mellitus or prediabetes. PLoS One. 2014;9(4):e91027.
242. Sequeira PA, Montoya L, Ruelas V, Xing D, Chen V, Beck R, Peters AL. Continuous glucose monitoring pilot in low-income type 1 diabetes patients. Diabetes technology & therapeutics. 2013;15(10):855-8.
243. Hommel E, Schmidt S, Vistisen D, Neergaard K, Gribhild M, Almdal T, Nørgaard K. Effects of advanced carbohydrate counting guided by an automated bolus calculator in Type 1 diabetes mellitus (StenoABC): a 12-month, randomized clinical trial. Diabetic Medicine. 2016;34(5):708-15.
244. Wittes J. Sample size calculations for randomized controlled trials. Epidemiol Rev. 2002;24(1):39-53.
245. Bergenstal RM, Garg S, Weinzimer SA, Buckingham BA, Bode BW, Tamborlane WV, Kaufman FR. Safety of a hybrid closed-loop insulin delivery system in patients with type 1 diabetes. JAMA : the journal of the American Medical Association. 2016;316(13):1407-8.
246. Luo J, Qu Y. Analysis of hypoglycemic events using negative binomial models. Pharm Stat. 2013;12(4):233-42.
247. Jiang H, Ni X, Huster W, Heilmann C. A Comparison of Different Statistical Methods Analyzing Hypoglycemia Data Using Bootstrap Simulations. Journal of Biopharmaceutical Statistics. 2015;25(1):54-65.
248. Hershon KS, Hirsch BR, Odugbesan O. Importance of Postprandial Glucose in Relation to A1C and Cardiovascular Disease. Clin Diabetes. 2019;37(3):250-9.
249. Klonoff DC, Lias C, Vigersky R, Clarke W, Parkes JL, Sacks DB, et al. The surveillance error grid. Journal of diabetes science and technology. 2014;8(4):658-72.
250. Lawton J, Rankin D, Cooke DD, Clark M, Elliot J, Heller S. Dose Adjustment for Normal Eating: a qualitative longitudinal exploration of the food and eating practices of type 1 diabetes patients converted to flexible intensive insulin therapy in the UK. Diabetes research and clinical practice. 2011;91(1):87-93.
251. Beck RW, Bergenstal RM, Riddlesworth TD, Kollman C. The association of biochemical hypoglycemia with the subsequent risk of a severe hypoglycemic event: analysis of the DCCT data set. Diabetes technology & therapeutics. 2019;21(1):1-5.
252. Gómez AM, Marín Sánchez A, Muñoz OM, Colón Peña CA. Numerical and clinical precision of continuous glucose monitoring in Colombian patients treated with insulin infusion pump with automated suspension in hypoglycemia. Endocrinología y Nutrición (English Edition). 2015;62(10):485-92.
253. Freckmann G, Mende J, Pleus S, Waldenmaier D, Baumstark A, Jendrike N, Haug C. Mean Absolute Relative Difference of Blood Glucose Monitoring Systems and Relationship to ISO 15197. Journal of diabetes science and technology. 2022;16(5):1089-95.

SUPPLEMENTARY MATERIAL

Supplementary Table 1. Search strategy

Source	Strategy	Results	Date
MEDLINE (Pubmed)	(("diabetes mellitus, type 1"[MeSH Terms] OR "diabetes mellitus type 1"[Title/Abstract] OR "diabetes type 1"[Title/Abstract] OR "Type 1 Diabetes"[Title/Abstract]) AND ("carbohydrate counting"[Title/Abstract]))	193 records	October 10/2020
EMBASE	"carbohydrate counting" and "type 1 diabetes mellitus"	69 records	October 12/2020
Cochrane Central Register of Controlled Trials (CENTRAL)	#1type 1 diabetes mellitus#2carbohydrate counting#3#1 and #2	183 records	October 12/2020
ClinicalTrials.gov	carbohydrate counting | Interventional Studies | Type 1 Diabetes	52 records	October 12/2020
World Health Organization International Clinical Trials Registry Platform (ICTRP)	Due to heavy traffic generated by the COVID-19 outbreak, the ICTRP Search Portal is not responding from outside WHO temporarily		October 12/2020
Open Grey	"carbohydrate counting" and "type 1 diabetes mellitus" "carbohydrate counting" and "diabetes mellitus" "carbohydrate counting" and " diabetes mellitus type 1"	2 records	October 13/2020
Lens	"carbohydrate counting" and "type 1 diabetes mellitus"	98 records	October 13/2020
Directory of Open Access Journals (DOA)	"carbohydrate counting" and "type 1 diabetes mellitus"	8 records	October 13/2020
Biblioteca Virtual en Salud (BVS)	"carbohydrate counting" and "type 1 diabetes mellitus"	178 records	October 13/2020

Supplementary Table 2. Risk of bias domains criteria

Risk of bias arising from the randomization process

Was the allocation sequence random?

Was the allocation sequence concealed until participants were recruited and assigned to interventions?

Were there baseline imbalances that suggest a problem with the randomization process?

Risk of bias due to deviations from the intended interventions

Were participants aware of their assigned intervention during the trial?

Were caregivers and trial personnel aware of participants' assigned intervention during the trial? Were there deviations from the intended intervention beyond what would be expected in usual practice?

Were these deviations from intended intervention unbalanced between groups and likely to have affected the outcome?

Were any participants analyzed in a group different from the one to which they were assigned?

Was there potential for a substantial impact (on the estimated effect of the intervention) of analyzing participants in the wrong group?

Risk of bias due to missing outcome data

Were outcome data available for all, or nearly all, participants randomized?

Are the proportions of missing outcome data and reasons for missing outcome data similar across intervention groups?

Is there evidence that results were robust to the presence of missing outcome data?

Risk of bias in the measurement of the outcome

Were outcome assessors aware of the intervention received by study participants?

Was the assessment of the outcome likely to be influenced by knowledge of intervention received?

Risk of bias in selection of the reported result

Are the reported outcome data likely to have been selected, on the basis of the results, from multiple outcome measurements (e.g. scales, definitions, time points) within the outcome domain?

Are the reported outcome data likely to have been selected, on the basis of the results, from multiple analyses of the data?

Supplementary Table 3. Equations for the stomach and small intestine

Equations for the stomach

$$\frac{dN_I}{dt} = \dot{n}_2 - \dot{n}_8 + \sum_s (\sigma_{s,I} \cdot r_{s,I}) \tag{30}$$

$$\frac{dN_{s_I}}{dt} = x_{s_2}\ \dot{n}_2 - x_{s_8}\ \dot{n}_8 + \sigma_{s,I} \cdot r_{s,I} \tag{31}$$

$$\dot{W} = \frac{1}{\eta}\,(\dot{m}_I \cdot h_f) \tag{32}$$

$$\dot{m}_4 = \frac{\dot{r}_{G_{II}}}{w_{G_4}} \tag{33}$$

$$\dot{r}_{G_{II}} = \frac{1}{\Delta H_{r_{G_{II}}}} \dot{W} \tag{34}$$

$$\frac{dM_{III}}{dt} = 0 \Rightarrow M_{III} = Constant \tag{35}$$

$$\frac{dw_{G_7}}{dt} = \frac{1}{M_{III}}\left(w_{G_6}\ \dot{m}_6 - w_{G_4}\ \dot{m}_4 - w_{G_7}\ \dot{m}_7\right) \tag{36}$$

$$\dot{m}_{10,1} = \dot{m}_8 + \dot{m}_9 \tag{37}$$

$$w_{s_{10,1}} = \frac{w_{s_8}\dot{m}_8 + w_{s_9}\dot{m}_9}{\dot{m}_{10,1}} \tag{38}$$

$$\tag{39}$$

Equations for the small intestine

$$\frac{dM_{V,j}}{dt} = \dot{m}_{10,j} - \dot{m}_{11,j} - \dot{m}_{17,j} \tag{40}$$

$$\frac{dV_{V,j}}{dt} = \frac{1}{\rho_{V,j}}\left(\dot{m}_{10,j} - \dot{m}_{11,j} - \dot{m}_{17,j} - V_{V,j}\dot{\rho}_{V,j}\right) \tag{41}$$

$$\frac{dr_j}{dt} = \frac{1}{2\pi L_V r_j \rho_{V,j}}\left(\dot{m}_{10,j} - \dot{m}_{11,j} - \dot{m}_{17,j} - V_{V,j}\dot{\rho}_{V,j}\right) \tag{42}$$

$$\frac{d\rho_{V,j}}{dt} = \frac{1}{V_{V,j}}\left(\dot{m}_{10,j} - \dot{m}_{11,j} - \dot{m}_{17,j} - \rho_{V,j}\dot{V}_{V,j}\right) \tag{43}$$

$$\frac{dM_{s_{V,j}}}{dt} = w_{s_{10,j}}\dot{m}_{10,j} - \dot{n}_{s_{11,j}}\mathfrak{M}_s - w_{s_{17,j}}\dot{m}_{17,j} + V_{V,j}\mathfrak{M}_s\sum_i r_{s_{i,j}} \tag{44}$$

$$\frac{dC_{s_{V,j}}}{dt} = \frac{1}{\mathfrak{M}_s V_{V,j}}\left(w_{s_{10,j}}\dot{m}_{10,j} - \dot{n}_{s_{11,j}}\mathfrak{M}_s - w_{s_{17,j}}\dot{m}_{17,j} + V_{V,j}\mathfrak{M}_s\sum_i r_{s_{i,j}} - C_{s_{V,j}}\dot{V}_{V,j}\right) \tag{45}$$

$$\frac{dw_{s_{V,j}}}{dt} = \frac{1}{M_{V,j}}\left(w_{s_{10,j}}\dot{m}_{10,j} - \dot{n}_{s_{11,j}}\mathfrak{M}_s - w_{s_{17,j}}\dot{m}_{17,j} + V_{V,j}\mathfrak{M}_s\sum_i r_{s_{i,j}} - w_{s_{V,j}}\dot{M}_{V,j}\right) \tag{46}$$

$$\frac{dM_{VI,j}}{dt} = \dot{m}_{11,j} + \dot{m}_{14,j} - \dot{m}_{12,j} - \dot{m}_{13,j} - r_{s_{VI,j}} \tag{47}$$

$$\frac{dM_{s_{VI,j}}}{dt} = \dot{n}_{s_{11,j}}\mathfrak{M}_s + w_{s_{14,j}}\dot{m}_{14,j} - w_{s_{12,j}}\dot{m}_{12,j} - w_{s_{13,j}}\dot{m}_{13,j} - r_{s_{VI,j}} \tag{48}$$

$$\dot{m}_{16,j} = \dot{m}_{12,j} + \dot{m}_{15,j} - \dot{m}_{14,j} \tag{49}$$

$$\dot{m}_{16} = \sum_j \dot{m}_{16,j} \tag{50}$$

$$\dot{m}_{G_{16,j}} = \dot{m}_{G_{16,j}} - w_{G_{12,j}}\dot{m}_{12,j} + w_{G_{15,j}}\dot{m}_{15,j} - w_{G_{14,j}}\dot{m}_{14,j} \tag{51}$$

$$\dot{m}_{G_{16}} = \sum_j \dot{m}_{G_{16,j}} \tag{52}$$

$$w_{G_{16}} = \frac{\dot{m}_{G_{16}}}{\dot{m}_{16}} \tag{53}$$

$$\dot{m}_{17,j} = \dot{m}_{10,j+1} \tag{54}$$

$$w_{s_{17,j}} = w_{s_{10,j+1}} \tag{55}$$

$$\dot{m}_{10,j+1} = c_{v_j}\,\rho_{V,j}\sqrt{P_{V,j} - P_{V,j+1}} \tag{56}$$

$$\tag{57}$$

Supplementary Table 4. Constitutive and assessment equations for structural parameters of the model.

#	Description	Cons./Ass. Equation	Inst.	Ref.
1	Molar flow of gastric juices entering the stomach through the stomach walls.	$\dot{n}_2 = \frac{\dot{m}_2}{\mathfrak{M}_{GJ}}$	1	M
2	Molar flow of gastric mass leaving the stomach due to gastric emptying.	$\dot{n}_8 = \frac{\dot{m}_8}{\mathfrak{M}_I}$	1	M
3	Rate of reaction for the substance s: Lip, Pro, GL, GP.	$r_{s,I} = \begin{cases} k_{0_{Lip_I}} \cdot C_{Lip_I}^{n_I} \cdot C_{GL_I}^{m_I} \cdot e^{\frac{-Ea_{Lip_I}}{R \cdot T}} & \text{if } s = Lip \\ k_{0_{Pro_I}} \cdot C_{Pro_I}^{n_I} \cdot C_{GP_I}^{m_I} \cdot e^{\frac{-Ea_{Pro_I}}{R \cdot T}} & \text{if } s = Pro \\ k_{0_{GL_I}} \cdot C_{GL_I}^{m_I} \cdot e^{\frac{-Ea_{GL_I}}{R \cdot T}} & \text{if } s = GL \\ k_{0_{GP_I}} \cdot C_{GP_I}^{m_I} \cdot e^{\frac{-Ea_{GP_I}}{R \cdot T}} & \text{if } s = GP \end{cases}$	4	[1]
4	Molar fraction of substance s in the stream containing gastric juices.	$x_{s_2} = \begin{cases} 1 & \text{if } s = GJ \\ 0 & \text{if } s \neq GJ \end{cases}$	1	A
5	Molar fraction of each substance s (CHO, Lip, Pro, G, FA, AA, W, Fib, Gly, GL, GP, GJ) in the stomach emptying into the duodenum.	$x_{s_8} = \frac{N_{s_I}}{N_I}$	12	[1]
6	Efficiency of the stomach wall to perform mechanical work.	$\eta = 0.5$	1	A
7	Mass flow of gastric mass that churns within the stomach.	$\dot{m}_I = \dot{V}_I \cdot \rho_I$	1	M
8	Friction losses experienced by the mass flow when circulating in the piping circuit (stomach).	$h_f = \sum_s \frac{K_{sc} \cdot v_{sc}^2}{2}$	1	[2]
9	Mass fraction of glucose in the stream containing the required reactants	$w_{G_4} = 0.484$	1	M
10	Specific molar heat of reaction of glucose combustion.	$\Delta \bar{H}_{r_{G_{II}}} = 2813\, kJ \cdot mol^{-1}$	1	[3]
11	Mass fraction of glucose that supplies the stomach wall through the artery.	$w_{G_6} = \frac{C_{G_6}}{\rho_b}$	1	M
12	Mass flow of blood supplying the stomach through the artery.	$\dot{m}_6 = \dot{V}_6 \cdot \rho_b$	1	[1]
13	Mass flow of blood from the stomach wall that drains through the vein.	$\dot{m}_7 = \dot{m}_6$	1	M
14	Mass flow resulting from mixing ingested food emptied from the stomach.	$\dot{m}_8 = \begin{cases} \text{if } V_I(t) > 0.35 V_I(0): \\ \dot{m}_{8(t-1)} + \frac{1}{\tau_{ini}} \left(\dot{m}_{8req} - \dot{m}_{8(t-1)} \right) t_s \\ \text{if } V_I(t) \leq 0.35 V_I(0): \\ \dot{m}_{8(t-1)} + \frac{1}{\tau_{end}} \left(\dot{m}_{8req} - \dot{m}_{8(t-1)} \right) t_s \end{cases}$	1	A
15	Mass flow of bile and pancreatic juice entering the duodenum.	$\dot{m}_9 = \rho_9 \cdot SP \left(\dot{V}_{bile,basal} + 3\dot{V}_{PJ,basal} \right)$	1	A

Abbreviations. A: Assumed, I: Identified, M: From the model.

(This table continues on the next page)

(It comes from the Table 5 above)

#	Description	Cons./Ass. Equation	Inst.	Ref.
16	Mass fraction of component s (CHO, Pro, Lip, G, AA, FA, W, F, GL, GP, GJ, Gly) of ingested food that are emptied into the duodenum.	$w_{s_8} = x_{s_1} \cdot \frac{1}{\mathfrak{M}_l} \cdot \mathfrak{M}_s$	12	M
17	Mass fraction of s (PA, PP, PL) in pancreatic juices and bile emptied into the duodenum.	$w_{s_9} = \frac{C_{s_9} \mathfrak{M}_s}{\rho_9}$	3	M
18	Mass flow of gastric mass entering a tank (portion j of the intestine).	$\dot{m}_{10,j} = \sum_s \dot{m}_{s_{10,j}}$	1	M
19	Mass absorption rate through each portion j of the intestinal wall.	$\dot{m}_{11,j} = \sum_s \dot{n}_{s_{11,j}} \cdot \mathfrak{M}_s$	1	M
20	Length of an elastic tank.	$L_V = \frac{L}{n}$	1	A
21	Mass fraction of s (CHO, G, Pro, AA, Lip, FA, W, F, GJ, GL, GP, Gly, CHO*, Pro*, PA, PP, PL, PA-In, PP-In, PL-In) in the stream 10 entering the j-th tank.	$w_{s_{10,j}} = \frac{\dot{m}_{s_{10,j}}}{\dot{m}_{10,j}}$	20	1
22	Term for the molar rate of absorption of s (G, AA, FA, W) in the j-th tank (z : Duo, Je, Ile).	$\dot{n}_{s_{11,j}} = \begin{cases} \left(K_{d_{G,z}} + \frac{v_{max_{G,z}} C_{G_{V,j}}}{K_{M_G} + C_{G_{V,j}}}\right) M_{VI,dry} \text{ if } s = G \\ \left(\frac{v_{max_{AA,z}} C_{AA_{V,j}}}{K_{M_{AA}} + C_{AA_{V,j}}}\right) L_V \text{ if } s = AA \\ A_M K_{FA,z} \left(C_{FA_{V,j}} - C^*_{FA_{VI}}\right) \text{ if } s = FA \\ L_V \left(K_{W,z} \dot{m}_{10,1} + 2.67e-7\right) \text{ if } s = W \end{cases}$	4	4 5 A A
23	Molar rate of reaction of the component s (CHO, G, W, PA, AA, Pro, PP, FA, Lip, Gly, PL, PA-In, PL-In, PP-In) in the reaction i taking place in the small intestine.	$r_{s_{i,j}} =$ See Table 3	16	
24	Mass flow of absorbed components passing into the blood in capillaries.	$\dot{m}_{12,j} = \sum_s \dot{n}_{s_{11,j}} \cdot \mathfrak{M}_s$ for $s : W, G, AA$	1	M
25	Mass flow of components drained by the lymph.	$\dot{m}_{13,j} = \sum_s \dot{n}_{s_{11,j}} \cdot \mathfrak{M}_s$ for $s : FA, Gly$	1	M
26	Mass flow of glucose for cell uptake of the small intestine wall.	$\dot{m}_{14,j} = \begin{cases} 0 & \text{if } M_{G_{V,j}} \neq 0 \\ 1.8e-8 & \text{if } M_{G_{V,j}} = 0 \end{cases}$	1	A I
27	Mass flow of blood supplying the small intestine.	$\dot{m}_{15,j} = \rho_b \cdot \dot{V}_{15}$	1	M
28	Rate of consumption of s (available in the intestinal lumen) by each portion j of the small intestine wall.	$r_{G_{VI,j}} = \begin{cases} 0.1\, \mathfrak{M}_G\, \dot{n}_{G_{11,j}} & if\ M_{G_{V,j}} \neq 0 \\ 1.8e-8 & if\ M_{G_{V,j}} = 0 \end{cases}$	1	6
29	Mass fractions of s (G, AA, W) that are absorbed through stream 12.	$w_{s_{12,j}} = \frac{\dot{m}_{11,j}}{\dot{m}_{12,j}}$	3	M
30	Mass fractions of s (FA, Gly) that are exchanged with the interstitium through stream 13.	$w_{s_{13,j}} = \frac{\dot{m}_{11,j}}{\dot{m}_{13,j}}$	2	M
31	Mass fractions of s (G) in the stream 14.	$w_{s_{14,j}} = \begin{cases} 0 \text{ for } s \neq G \\ 1 \text{ for } s = G \end{cases}$	1	M
32	Mass fraction of glucose via arterial blood irrigating the small intestine.	$w_{G_{15,j}} =$ Data from the literature	1	7
33	Hydrodynamic pressure on gastric mass flow entering the portion j.	$P_{V,j} =$ See Eq 29	1	8
34	Valve flow coefficient.	$c_{v_j} = f_{z_j}\, C_v$	1	9

Abbreviations. A: Assumed, I: Identified, M: From the model.

Supplementary Table 5. Constitutive equations for functional parameters of the gastrointestinal model.

#	Description	Cons./Ass. Equation	Inst.	Ref.
1	Mass flow of gastric juices entering the stomach through the stomach wall.	$\dot{m}_2 = \dot{V}_2 \cdot \rho_{GJ}$	1	M
2	Molecular mass of the gastric mixture contained in the stomach.	$\mathfrak{M}_I = \sum_s x_{s_I} \cdot \mathfrak{M}_s$	1	M
3	Molar-volumetric concentration of component s (Lip, Pro, GL, GP), after the addition of gastric juices but before the enzymatic reactions and emptying.	$C_{s_I} = \frac{N_{s_I}}{V_{I_{sw}}}$	4	M
4	Volumetric flow of gastric mass within the stomach.	$\dot{V}_I = v_{0_{I_C}} \cdot A_{flow_{I_C}}$	1	M
5	Density of gastric mass in the stomach.	$\rho_I = \sum_s \frac{1}{w_{s_I}/\rho_s}$	1	[1]
6	Friction factor for each section of the pipe circuit representing the stomach. Total number of sections: 12	$K_{sc} = \begin{cases} K_{straight} = f_{Darcy}\frac{L_{straight_{sc}}}{D_{sc}} \\ K_{expan} = [1 - \frac{SD}{HD}^2]^2 \\ K_{cont} = 0.5[1 - \frac{SD}{HD}^2]^2 \\ K_{180^\circ_{Elbow}} = \frac{1000}{Re_{sc}} + 0.6(1 + \frac{1}{ID}) \end{cases}$	12	[10]
7	Velocity of the gastric mass in each section of the pipe circuit representing the stomach.	$v_{sc} = \frac{\dot{V}_I}{A_{flow_{I_{sc}}}}$	12	M
8	Characteristic time of gastric emptying start.	$\tau_{int} = 0.5 \cdot t_{lag}$	1	A
9	Mass flow out of the stomach required for the flow to be isocaloric.	$\dot{m}_{S_{req}} = \frac{\dot{E}_{s_{sto}}}{c_{meal} w_{s_{meal}}}$	1	M
10	Molar fraction of component s (Lip, AG, Pro, AA, CHO, G, F, W, GJ, GL, GP, Gly) in the stomach.	$x_{s_I} = \frac{N_{s_I}}{N_I}$	12	M
11	Mass flow of component s (CHO, G, Pro, AA, Lip, FA, PA, PP, PL, GP, GL, W, Gly, AP-In, PP-In, PL-In, F, GJ) entering each portion j of the small intestine.	$\dot{m}_{s_{10,j}} = \dot{m}_{17,J} \cdot w_{s_{V,j}}$	18	M
12	Length of the small intestine.	$L = \sum_z L_z$	1	M
13	Dry mass of a portion j of intestinal wall.	$M_{VI,dry} = \rho_{VI,dry} \cdot V_{VI}$	1	M
14	Concentration of s (PA, PP, PL) in bile and pancreatic juice flow.	$C_{s_0} = \begin{cases} \left(\frac{SP}{SP_{max}}\right)\left(\frac{Act_{PA_0}}{Act_{PA_0}\mathfrak{M}_{PA}}\right) & \text{if } s: PA \\ C_{PA_0}\left(\frac{Z_{P\to A}}{Act_{PP_0}\mathfrak{M}_{PP}}\right) & \text{if } s: PP \\ C_{PA_0}\left(\frac{Z_{L\to A}}{Act_{PL_0}\mathfrak{M}_{PL}}\right) & \text{if } s: PL \end{cases}$	3	M
15	Pancreatic amylase activity.	$Act_{AP_0} = 0.101 + \frac{0.05059\, C_{PA_{V,1}}}{C_{PA_{V,1}} + 0.5321}$	1	[11]
16	Effective area for the mass transfer of fatty acids in the enterocytes.	$A_M = 2 \cdot \pi \cdot \bar{r} \cdot L_V \cdot F_{fold}$	1	A
17	Fung material constant C for the small intestine wall of tank j.	$C_j = -12.0\, L_j^4 + 165.9\, L_j^3 - 782.1\, L_j^2 + 1317\, L_j + 1256$	1	[12]

Abbreviations. A: Assumed, I: Identified, M: From the model.

(This table continues on the next page)

(It comes from the Table 6 above)

#	Description	Cons./Ass. Equation	Inst.	Ref.
18	Fung material constant a_1 for the small intestine wall of tank j.	$a_{1_j} = -1.61\,L_j^3 + 16.8\,L_j^2 - 44.7\,L_j + 72.70$	1	12
19	Fung material constant a_2 for the small intestine wall of tank j.	$a_{2_j} = 1.5\,L_j^3 - 17.4\,L_j^2 + 51.5\,L_j + 29.02$	1	12
20	Cross-area of the tank j.	$A_{V,j} = \pi r_j^2$	1	M
21	Cross-area of the tank j when deflated.	$A_{0_{V,j}} = \pi r_{0_j}^2$	1	M
22	Cross area of the intestinal wall of tank j.	$A_{wall_{V,j}} = \pi\left(r_{0_j} + h_{0_j}\right) - A_{0_{V,j}}$	1	M
23	Volumetric flow of gastric juices entering the stomach.	$\dot{V}_2 = \frac{k_{V_2}}{t_{lag}} \cdot V_I$	1	M
24	Total volume in the stomach, before emptying, including gastric juices.	$V_{I_{av}} = V_I + (\dot{V}_2 \cdot t_s)$	1	A
25	Cross area of each section sc.	$A_{flow_{Ic}} = FC_A\, A_{0_{flow_{I_{sc}}}}$	12	A
26	Mass fraction of component s in the stomach.	$w_{s_I} = \frac{M_{s_I}}{M_I}$	11	M
27	Darcy factor.	$f_{Darcy} = \frac{64}{Re_{sc}}$	1	1
28	Reynolds number for straight and elbow sections (sc=1, 3, 5, 6, 10, 12).	$Re_{sc} = \frac{\rho_I \cdot v_{sc} \cdot D_{sc}}{\mu_I}$	6	M
29	Cross sectional area of the fitting at the distal extreme (in the case of contractions and expansions, the smallest SD diameter is considered).	$A_{0_{flow_{I_{sc}}}} = \pi \frac{D_{sc}^2}{4}$	12	M
30	Specific energy content of the ingested food mass.	$e_{meal} = \frac{E_{meal}}{\sum_s M_{s_I}}$	1	M
31	Mass fraction of caloric food ingested (s: Lip, FA, Pro, AA, CHO, G).	$w_{s_{meal}} = \sum_s w_{s_I}$	1	M
32	Volume of a portion j of intestinal wall.	$V_{VI} = 2\pi r_{0_j} h_{0_j} L_V$	1	M
33	Gastric emptying mass flow of component s (CHO, G, Pro, AA, Lip, FA, W, F, GJ, GL, GP, PA, PP, PL, Gly, PA-In, PP-In, PL-In).	$\dot{m}_{s_{10,1}} = \dot{n}_8 \cdot x_{s_I} \cdot \mathfrak{M}_s + w_{s_9} \cdot \dot{m}_9$	18	M
34	Valve displacement following the inherent valve characteristic.	$f_{x_j} = \frac{P_{V,j} - P_{V,j+1}}{P_{cont}}$	1	A
35	Equivalent mean contraction pressure	$\bar{P}_{cont} = DC \cdot P_{cont}$	1	M
36	Duty cycle.	$DC = \frac{\tau}{t_{pw}}$	1	M
37	Volume of gastric mass present in the stomach.	$V_I = \sum_s \frac{N_{s_I} \cdot \mathfrak{M}_s}{\rho_s}$	1	M
38	Correction factor for the area of each stomach section.	$FC_A = \frac{V_I}{A_{0_{flow_{I_{sc}}}} \cdot L_{I_{sc}}}$	12	A
39	Total mass in the stomach.	$M_I = \sum_s M_{s_I}$	1	M
40	Viscosity of the gastric mass.	$\mu_I = 0.001 \cdot (\mu_{I_{MP}} + \mu_{I_{limit}})$	1	13
41	Energy content of the initial food.	$E_{meal} = (M_{Lip_I} + M_{FA_I}) \cdot E_{Lip} + (M_{Pro_I} + M_{AA_I}) \cdot E_{Pro} + (M_{CHO_I} + M_{G_I}) \cdot E_{CHO}$	1	M

Abbreviations. A: Assumed, I: Identified, M: From the model.

(This table continues on the next page)

(It comes from the Table 6 above)

#	Description	Cons./Ass. Equation	Inst.	Ref.
42	Basal radius of the small intestine.	$r_{0_j} = -0.081\,L_j^2 + 0.15\,L_j + 6.21$	1	[14]
43	Thickness of the intestinal wall.	$h_{0_j} = -0.0015\,L_j^3 + 0.014\,L_j^2 - 0.032\,L_j + 1.53$	1	[14]
44	Polynomial correlation for a mix meal.	$\mu_{I_{MP}} = -4346.483214 \cdot FVM^4 + 5855.694121 \cdot FVM^3 - 1767.803009 \cdot FVM^2 + 295.563994 \cdot FVM - 10.04508874$	1	[13]
45	Length traveled by gastric mass in the tank j.	$L_j = j \cdot L_V$	1	M
46	Modified Viscosity Factor.	$FVM = FD^{2.97}$	1	see [15]
47	Dilution factor.	$FD = -6.007024928 \times 10^{-8} \cdot t_{Sim}^3 + 7.018107705 \times 10^{-6} \cdot t_{Sim}^2 - 0.002301353528 \cdot t_{Sim} + 0.6412266547$	1	[16, 17, 18]

Abbreviations. A: Assumed, I: Identified, M: From the model.

Supplementary Table 6. Assessment equations and constants of the gastrointestinal model.

Symbol	Description	Value	Inst.	Ref.
$\sigma_{s,I}$	Stoichiometric coefficient of component s: Lip, FA, W, Gly, Pro, AA, GL, GP, in the reactions of digestion that takes place in the stomach.	$\sigma_{(Lip,Pro),I} = -1$ $\sigma_{(LG,PG),I} = -1$ $\sigma_{FA,I} = 3$ $\sigma_{W,I} = -3$ $\sigma_{Gly,I} = 1$ $\sigma_{AA,I} = 153$	8	M
$\mathfrak{M}_s$	Molar mass of the component s (Lip, Pro, CHO, FA, AA, G, Fib, W, GJ, GL, GP, Gly, PA, PP, PL, PA-In, PP-In, PL-In).	-	18	[19]
$k_{0_{s_I}}$	Rate constant due to the frequency of molecular collisions in the correct orientation for component s (Lip, Pro, GL, GP) in the stomach.	See Table 4 in [15]	4	I
$E_{a_{s_I}}$	Activation energy for reaction of component s (Lip, Pro, GL, GP) in the stomach.	See Table 4 in [15]	4	I
n_I	Exponent for the concentration of lipids and proteins in their degradation reactions in the stomach.	1	1	
m_I	Exponent for the concentration of lipases and proteases in their degradation reactions in the stomach.	1	1	
C_{G_c}	Glucose concentration in the arterial blood supplying the stomach.	$0.9\,kg \cdot m^{-3}$	1	A
ρ_b	Blood density.	$1060\,kg \cdot m^{-3}$	1	[20]
$\dot{V}_6$	Volumetric flow of arterial blood supplying the stomach	$0.00001\,m^3 \cdot s^{-1}$	1	
τ_{end}	Characteristic time for the end of gastric emptying.	$1200s$	1	A
t_s	Sampling time.	$1s$	1	A
$\dot{V}_{bile,basal}$	Basal bile volume flow.	$8.33 \times 10^{-9}\,m^3 \cdot s^{-1}$	1	[21,22]
$\dot{V}_{PJ,basal}$	Basal pancreatic juice volume flow.	$4.17 \times 10^{-9}\,m^3 \cdot s^{-1}$	1	[23]
ρ_9	Density of bile and pancreatic juice.	$1000\,kg \cdot m^{-3}$	1	A
SP	Basal percentage of bile and pancreatic juice secretion	*Determined by the fuzzy model [24].	1	[25]
SP_{max}	Maximum basal secretion percentage.	500%	1	A
$\widetilde{Act}_{Ez_0}$	Specific activity of pancreatic enzymes (Ez): pancreatic amylase (PA), pancreatic protease considered here trypsin as equivalent (PP), and pancreatic lipase (PL).	$\widetilde{Act}_{PA,PL_0} = 1.2 \times 10^{-2}\,kU \cdot mg^{-1}$ $\widetilde{Act}_{PP_0} = 7.73 \times 10^{-3}\,kU \cdot mg^{-1}$	3	[25,26]
$Z_{P \to A}$	Ratio of protease to amylase.	0.54	1	[25]
$Z_{L \to A}$	Ratio of lipase to amylase	3.5	1	[25]
L_z	Length of each part of small intestine (z: Duodenum, jejunum, and ileum).	$Duo = 0.2\,m$ $Je = 2.3\,m$ $Ile = 2.7\,m$	3	[27]
$K_{d_{Cl,z}}$	Mass transfer constant of passive glucose absorption in each section of small intestine (z: duodenum, jejunum, and ileum).	$Duo = 1.955 \times 10^{-5}\,m^3 \cdot kg^{-1} \cdot s^{-1}$ $Je = 4.301 \times 10^{-6}\,m^3 \cdot kg^{-1} \cdot s^{-1}$ $Ile = 1.251 \times 10^{-8}\,m^3 \cdot kg^{-1} \cdot s^{-1}$	3	[4]

Abbreviations. A: Assumed, I: Identified, M: From the model.

(This table continues on the next page)

(It comes from the Table 7 above)

Symbol	Description	Value	Inst.	Ref.
$v_{max_{G,z}}$	Maximum velocity of saturable glucose absorption in each section z of intestine (z: Duodenum, jejunum, and ileum).	$Duo = 1.667 \times 10^{-10}\, m^3 \cdot kg^{-1} \cdot s^{-1}$ $Je = 3.667 \times 10^{-11}\, m^3 \cdot kg^{-1} \cdot s^{-1}$ $Ile = 1.067 \times 10^{-13}\, m^3 \cdot kg^{-1} \cdot s^{-1}$	3	[4]
K_{M_G}	Michaelis constant of glucose absorption.	$2.06 \times 10^{-3}\, kmol \cdot m^{-3}$	1	[4]
$v_{max_{AA,z}}$	Maximum velocity of saturable amino acid absorption in each section z of intestine (z: Duodenum, jejunum, and ileum).	$Duo = 1.222 \times 10^{-6}\, kmol \cdot kg^{-1} \cdot s^{-1}$ $Je = 1.000 \times 10^{-8}\, kmol \cdot kg^{-1} \cdot s^{-1}$ $Ile = 1.889 \times 10^{-9}\, kmol \cdot kg^{-1} \cdot s^{-1}$	3	[5]
$K_{M_{AA}}$	Michaelis constant of amino acid absorption.	$3.60 \times 10^{-2}\, kmol \cdot m^{-3}$	1	I
$K_{FA,z}$	Fatty acid mass transfer coefficient.	$Duo = 1.945 \times 10^{-7}\, m \cdot s^{-1}$ $Je = 2.123 \times 10^{-8}\, m \cdot s^{-1}$ $Ile = 2.805 \times 10^{-9}\, m \cdot s^{-1}$	3	[5]
$C^*_{FA_{VI}}$	Fatty acid equilibrium concentration.	$1 \times 10^{-4}\, kmol \cdot m^{-3}$	1	A
$K_{W,z}$	Water mass transfer coefficient.	$Duo = 1.05 \times 10^{-3}\, kmol \cdot kg^{-1} \cdot m^{-1}$ $Je = 2.32 \times 10^{-4}\, kmol \cdot kg^{-1} \cdot m^{-1}$ $Ile = 1.31 \times 10^{-3}\, kmol \cdot kg^{-1} \cdot m^{-1}$	3	I
$\sigma_{s,1-6}$	Stoichiometric coefficient of s (W, CHO, PA, Pro, PP, Lip, PL) in the reactions of digestion that takes place in the small intestine[a].	-1	7	M
$\sigma_{s,1-6}$	Stoichiometric coefficient of s (G, CHO*, PA-In, AA, Pro*, PP-In, Gly, PL-In) in the reactions of digestion that takes place in the small intestine[b].	1	8	M
$\sigma_{s,5}$	Stoichiometric coefficient of water and fatty acids in reaction 5 taking place in the small intestine to digest fat.	$s : W = -3$ $s : FA = 3$	1	M
$k_{0_{1,z}}$	Pre-exponential factor of carbohydrate digestion in each section z (duodenum, jejunum, ileum) of intestine.	$k_{0_{1,Duo}} = 8.31 \times 10^{9}\, s^{-1}$ $k_{0_{1,Je}} = 6.89 \times 10^{8}\, s^{-1}$ $k_{0_{1,Ile}} = 5.54 \times 10^{7}\, s^{-1}$	3	I
E_{a_1}	Activation energy of carbohydrate digestion in the intestine.	$5.749 \times 10^{7}\, J \cdot kmol^{-1}$	1	[28]
$k_{0_{2,z}}$	Pre-exponential factor of pancreatic amylase inactivation in each section z (duodenum, jejunum, ileum) of intestine.	$k_{0_{2,Duo}} = 2.88 \times 10^{-3}\, s^{-1}$ $k_{0_{2,Je}} = 4.80 \times 10^{-4}\, s^{-1}$ $k_{0_{2,Ile}} = 4.80 \times 10^{-4}\, s^{-1}$	3	[25]
E_{a_2}	Activation energy of pancreatic amylase inactivation in the intestine.	$2.54 \times 10^{7}\, J \cdot kmol^{-1}$	1	[29]
$k_{deg_{2,z}}$	Denaturation rate constants of pancreatic amylase inactivation.	$k_{deg_{2,Duo}} = 2.01 \times 10^{-4}\, s^{-1}$ $k_{deg_{2,Je}} = 3.34 \times 10^{-5}\, s^{-1}$ $k_{deg_{2,Ile}} = 3.34 \times 10^{-5}\, s^{-1}$	3	I

[a] In the reaction 5, the stoichiometric coefficient for water (W) is −3.

[b] In the reaction 5, the stoichiometric coefficient for fatty acids (FA) is 3.

Abbreviations. A: Assumed, I: Identified, M: From the model.

(This table continues on the next page)

(It comes from the Table ? above)

Symbol	Description	Value	Inst.	Ref.
$\dot{E}_{g_{Exo}}$	Energy flow out of the stomach.	$3\,kcal \cdot m^{-1}$	1	[32]
$\rho_{VI,dry}$	Density of dry small intestine.	$1400\,kg \cdot m^{-3}$	1	[33]
$\bar{r}$	Mean overall small intestine radius.	$0.02\,m$	1	[32]
F_{fold}	Small intestine fold change.	7.22	1	[34]
$k_{\dot{V}_2}$	Constant of proportionality for the addition of gastric juices.	2	1	A
C_v	Maximum valve flow coefficient with a pressure drop of 60°.	$1 \times 10^{-9}\,m^3 \cdot s^{-1} \cdot Pa^{-0.5}$	1	I
P_{cont}	Pressure exerted by periodic small intestine wall contractions on the chyme flow for the postprandial state.	$2666\,Pa$	1	[35]
τ	Duration of muscle contraction during an average peristaltic wave.	$3.1\,s$	1	[35, 36]
t_{pw}	Period of occurrence of an average peristaltic wave.	$25s$	1	[35, 36]
$L_{I_{sc}}$	Length of each section sc of the pipe circuit.	$L_{I_1} = 2.3\,cm$ $L_{I_5} = 2.2\,cm$ $L_{I_9} = 3.2\,cm$ $L_{I_2} = 3.2\,cm$ $L_{I_6} = 3.6\,cm$ $L_{I_{10}} = 3.3\,cm$ $L_{I_3} = 2.2\,cm$ $L_{I_7} = 1.4\,cm$ $L_{I_{11}} = 3.1\,cm$ $L_{I_4} = 1.6\,cm$ $L_{I_8} = 2.7\,cm$ $L_{I_{12}} = 4.9\,cm$	12	[15]
$\mu_{I_{limit}}$	Lower limit of the viscosity of the mixture.	10P	1	
E_s	Energy content of macronutrients (s: Lip, Pro, CHO).	$9.19,\quad 5.5,\quad 4.1\,kcal \cdot g^{-1}$	3	[37]
M_{s_I}	Grams of food ingested (s: Lip, Pro, CHO, FA, AA, G).	$M_{Lip} = 27g$ $M_{Pro} = 35g$ $M_{CHO} = 52g$ $M_{FA,AA,G} = 0g$ $M_W = 457.29g$ $M_F = 5g$	8	A
ρ_s	Density of component s in the stomach: Lip, Pro, CHO, G, Fib, W, GJ, AA, FA, Gly, GL, GP.	$-\,kg \cdot m^{-3}$	12	
n	Number of tanks in which the intestine is partitioned.	52	1	A
t_{Stm}	Simulation time.	10h	1	M

Abbreviations. A: Assumed, I: Identified, M: From the model.

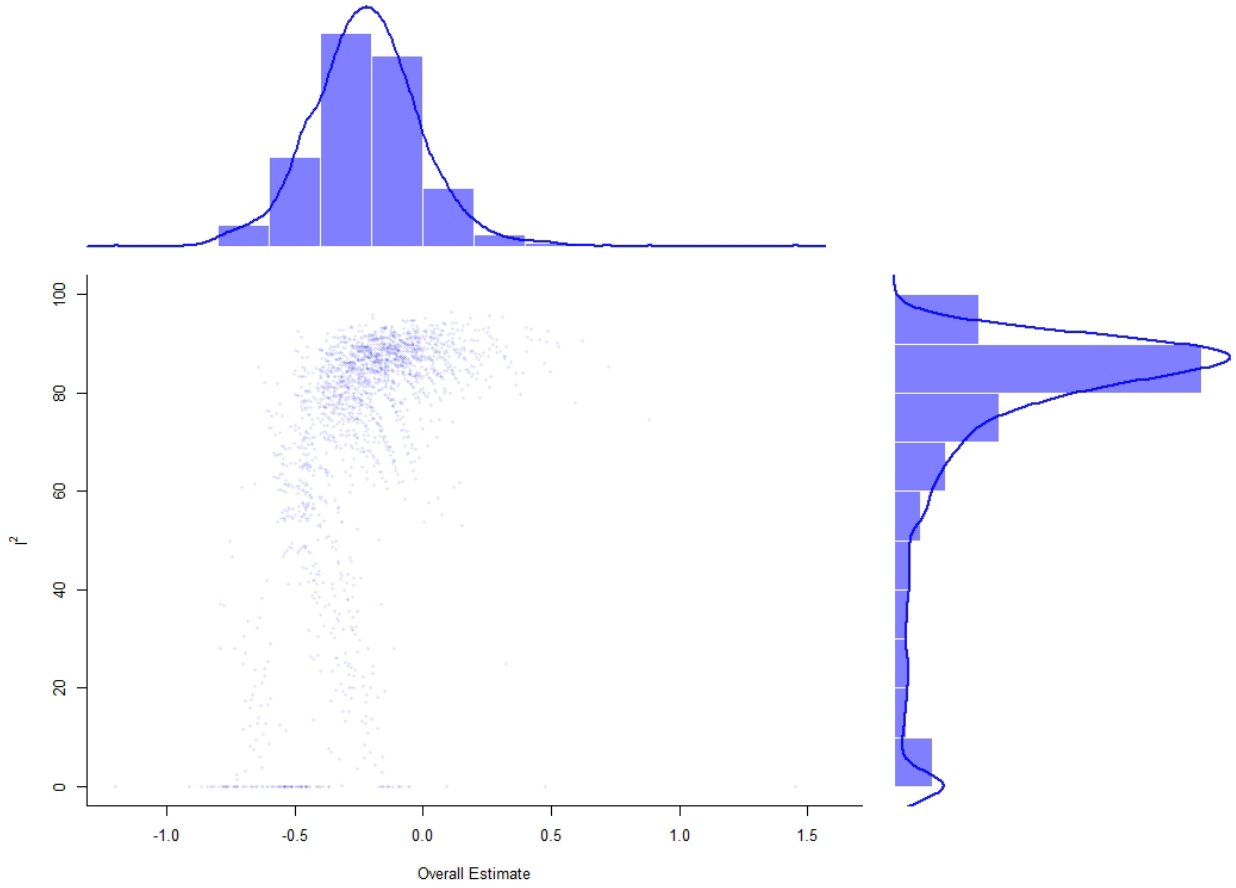
Supplementary Table 7. Diagnostic criteria for Diabetic Ketoacidosis (DKA) hyperglycemic hyperosmolar state (HHS).

	DKA			HHS
	Mild	**Moderate**	**Severe**	
Plasma glucose	>250 mg/dL	>250 mg/dL	>250 mg/dL	> 600 mg/dL
Arterial pH	7.25–7.30	7.00 to <7.24	<7.00	>7.30
Serum bicarbonate (mEq/l)	15–18	10 to <15	<10	>18
Urine ketone	Positive	Positive	Positive	Small
Serum ketone	Positive	Positive	Positive	Small
Effective serum osmolality*	Variable	Variable	Variable	>320 mOsm/kg
Anion gap‡	>10	>12	>12	Variable
Mental status	Alert	Alert/drowsy	Stupor/coma	Stupor/coma

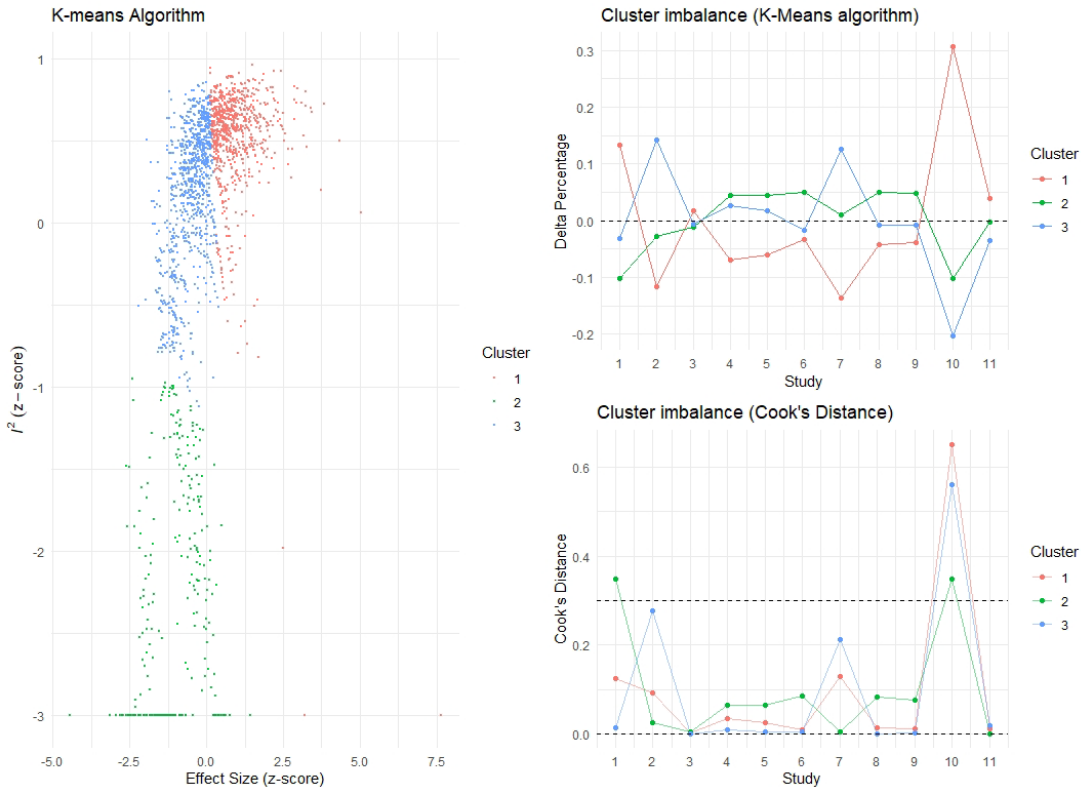
†Effective serum osmolality: 2[measured Na^+ (mEq/l)] + glucose (mg/dl)/18.

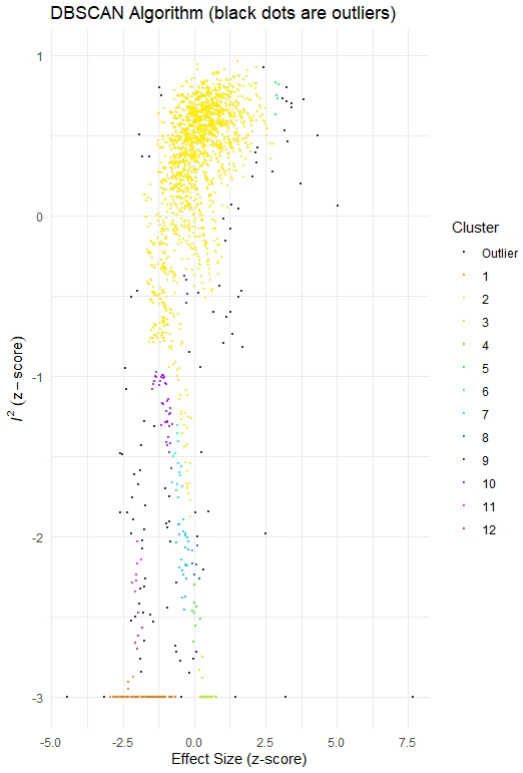
‡Anion gap: (Na^+) − [(Cl^- + HCO_3^- (mEq/l)].

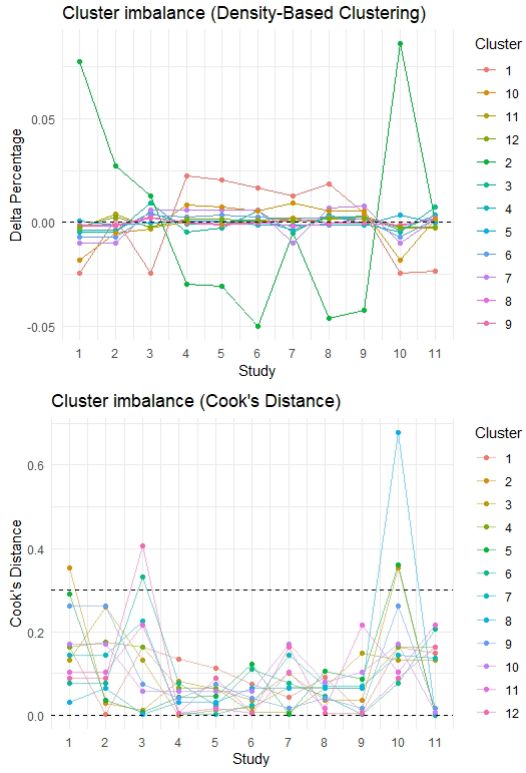
Supplementary Figure 1. Graphic Display of Heterogeneity (GOSH) plot



Supplementary Figure 2. Clustering algorithms k-means, density reachability and connectivity clustering (DBSCAN), and Gaussian Mixture Models

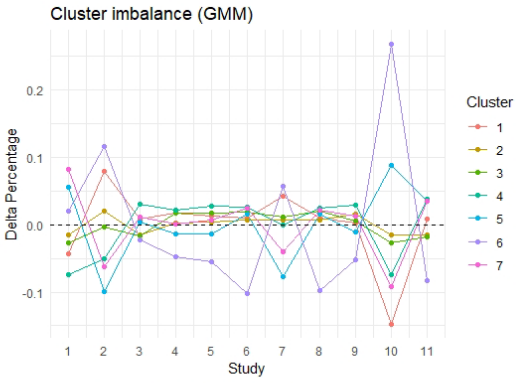


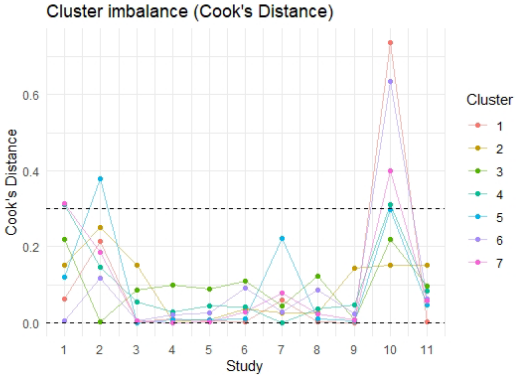

DBSCAN Algorithm (black dots are outliers)
I^2 (z – score)
Effect Size (z-score)
Cluster
Outlier
1
2
3
4
5
6
7
8
9
10
11
12

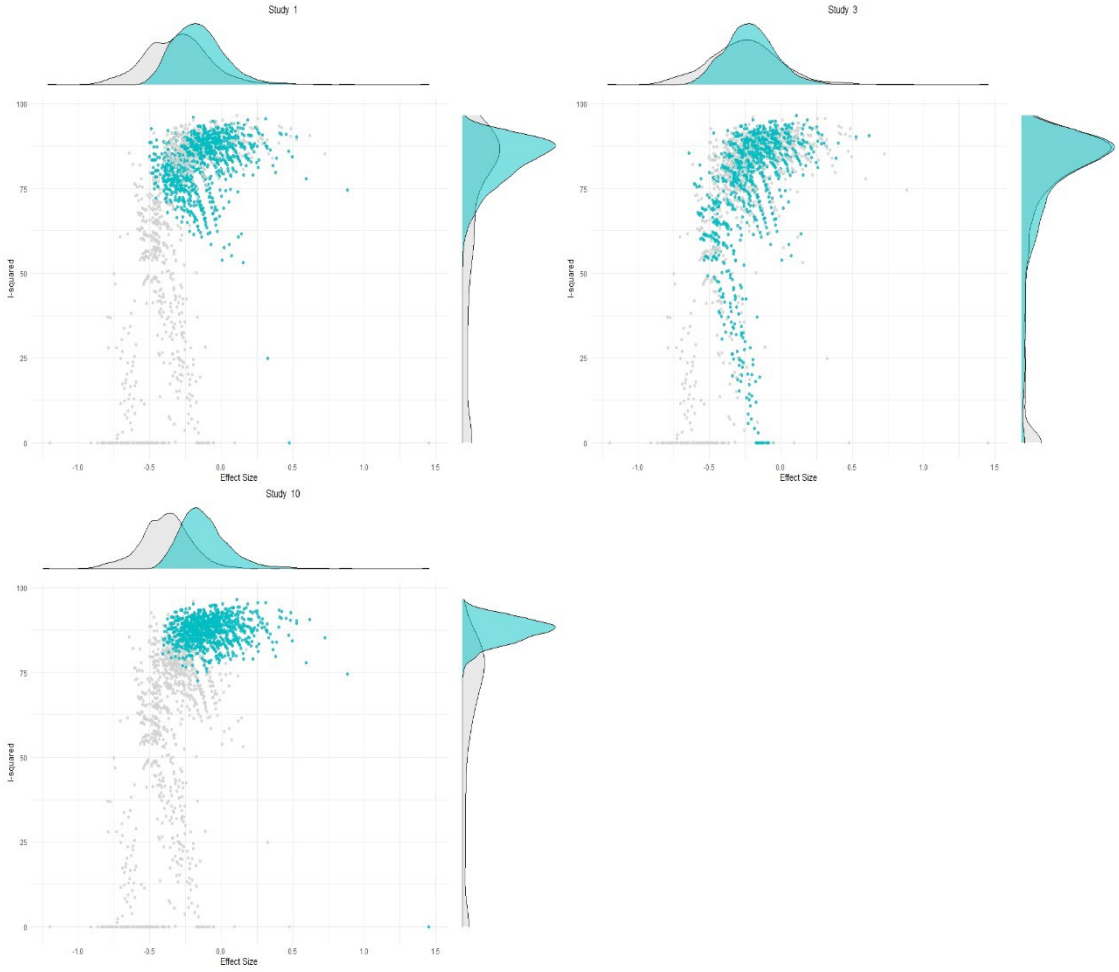

Cluster imbalance (Density-Based Clustering)
Delta Percentage
Study
Cluster
1
10
11
12
2
3
4
5
6
7
8
9

Cluster imbalance (Cook's Distance)
Cook's Distance
Study
Cluster
1
2
3
4
5
6
7
8
9
10
11
12

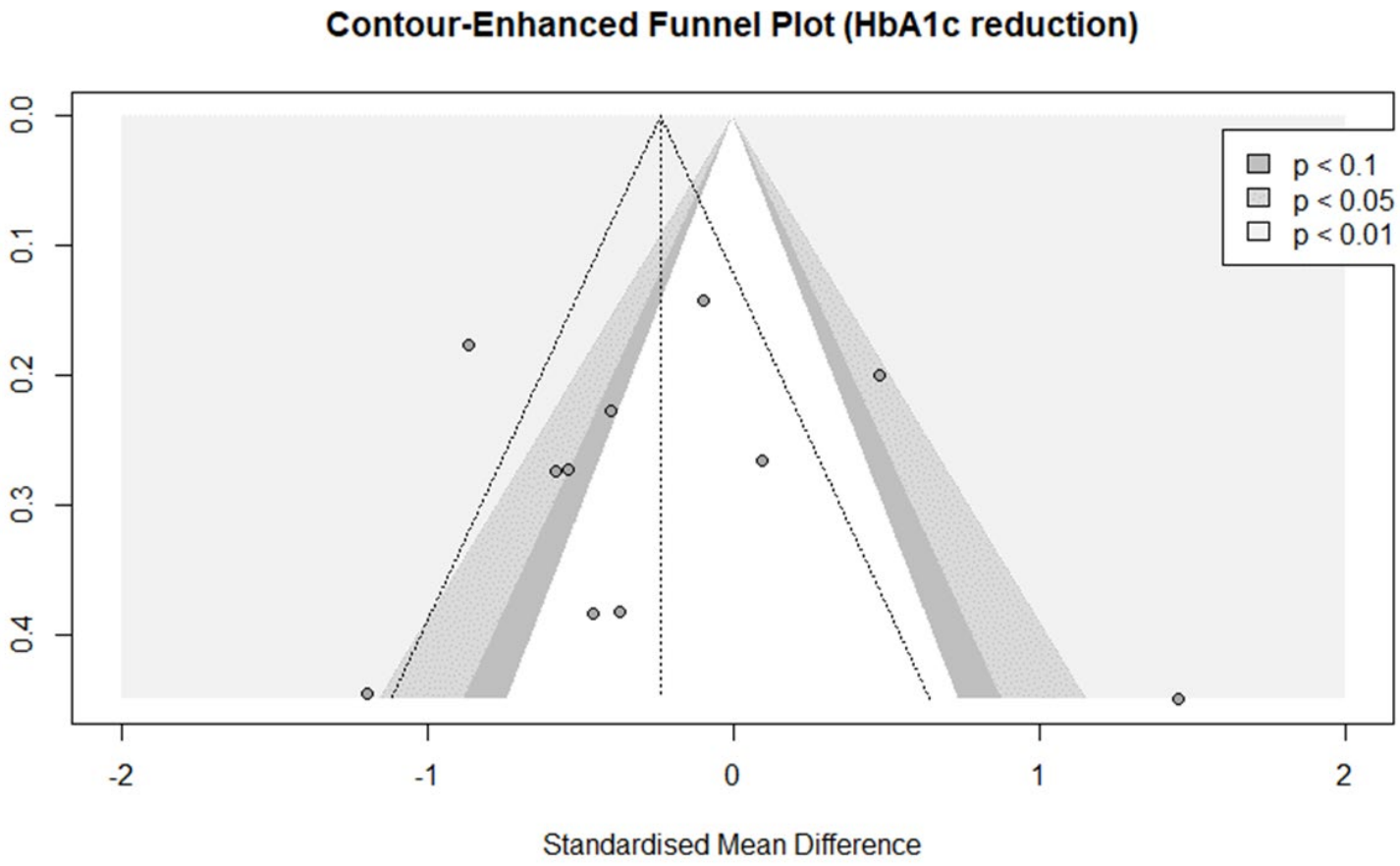

Gaussian Mixture Model
I^2 (z – score)
Effect Size (z-score)
Cluster
1
2
3
4
5
6
7


Cluster imbalance (GMM)
Delta Percentage
Study
Cluster
1
2
3
4
5
6
7


Cluster imbalance (Cook's Distance)
Cook's Distance
Study
Cluster
1
2
3
4
5
6
7


Study 1
Study 3
Study 10
I-squared
Effect Size

Supplementary Figure 3. Contour-enhanced funnel plot



Other Supplementary material 1. Informant consent format

Título del proyecto: Eficacia del Conteo de Carbohidratos Apoyado por una Simulación de la Dinámica de la Glucosa Postprandial Generada por un Modelo Semifísico de Base Fenomenológica en personas con Diabetes Mellitus Tipo 1. Ensayo Clínico Controlado de Asignación Aleatoria y Grupos Paralelos.

Es probable que el presente formulario de consentimiento contenga palabras o conceptos que usted no entienda. Por favor, pídale al médico investigador o a los asistentes del estudio que le expliquen todas las palabras, conceptos o información que no comprenda con claridad. Igualmente, puede realizar todas las preguntas que considere sean necesarias para tomar la decisión, tómese el tiempo necesario para pensar y, si es del caso, consulte a familiares, amigos o personas allegadas que le ayuden a comprender mejor las razones para aceptar su inclusión en la investigación.

Identificación de los investigadores.

Carlos Esteban Builes-Montaño, MD. (CEBM). Departamento de Medicina Interna, Sección de Endocrinología, Universidad de Antioquia. Departamento de Medicina Interna y Especialidades, Hospital Pablo Tobón Uribe. cbuiles@hptu.org.co. 4459000.

Juan Carlos Restrepo Gutierrez, MD, MSc, PhD. (JCRG), Departamento de Medicina Interna, Sección de hepatología, Universidad de Antioquia. Unidad de Trasplante Hepático, Hospital Pablo Tobón Uribe. jcrestrepo@hptu.org.co. 4459000

John Jairo Zuleta Tobón. MD, MSc. (JJZT). Departamento de Ginecología y Obstetricia, Facultad de Medicina Universidad de Antioquia y Unidad de Investigaciones y Docencia, Hospital Pablo Tobón Uribe. jzuleta@hptu.org.co. 4459753

Alex Humberto Ramírez -Rincón, MD (AHRR). Clínica Integral de Diabetes, Universidad Pontificia Bolivariana.

Sitio donde se llevará a cabo el estudio: Hospital Pablo Tobon Uribe

Entidad que respalda la investigación: Hospital Pablo Tobon Uribe y Universidad de Antioquia

Entidad que patrocina la investigación: Ninguna

Información para los participantes

Usted está siendo invitado a participar en un estudio de investigación en el cual se comparará la técnica del conteo de carbohidratos en la cual ya usted ha sido entrenado con esta misma técnica, pero acompañada de una simulación de cómo se pudiera cambiar el azúcar en la sangre después de una comida de acuerdo con la información de los alimentos que usted ingiere.

El propósito de esta investigación es evaluar si contar con la información que proporciona esta simulación mejora los niveles de azúcar en sangre después de comer.

La importancia de esta investigación radica en que la técnica del conteo de carbohidratos es actualmente la forma más recomendada para calcular la dosis de la insulina que se aplican las personas con diabetes con cada comida. Sin embargo, esta técnica requiere de una curva de aprendizaje y para algunas personas puede ser abrumadora. Con esta investigación pretendemos evaluar si la simulación pudiera ser una herramienta útil para ayudar a las personas con el proceso del conteo de carbohidratos.

Usted ha sido seleccionado para participar en esta investigación porque tiene diabetes mellitus tipo 1 desde hace más de un año, utiliza insulina con las comidas, ha sido entrenado en conteo de carbohidratos y es usuario de un sistema de monitoreo continuo de glucosa continuo o intermitente.

Esta investigación está siendo ejecutada por el Hospital Pablo Tobón Uribe, se espera reclutar 58 participantes y que su participación en esta investigación sea de 4 semanas.

Procedimientos del estudio.

Después de aceptar participar en la investigación a usted recibirá un nuevo entrenamiento en el cual se incluirá la manera de estimar cuanta grasa y proteína proporcionan los alimentos, así como detectar y tratar los episodios de hipoglucemia (niveles bajos de azúcar en sangre).

Una vez terminados estos entrenamientos usted será asignado a uno de los dos grupos de la investigación. La decisión sobre el grupo en el cual será incluido usted, se hará por azar, es decir, ni usted ni su médico podrán decidir en cual grupo quedará usted. Esto se hace para que los resultados de esta investigación sí sean creíbles. Después de hacer esto, tanto usted como su médico ya sabrán en qué grupo quedará, pero se solicita su mayor colaboración para seguir participando independiente de en cuál grupo quede. Esto es indispensable para hacer una evaluación justa de la intervención. Un grupo continuara utilizando la técnica de conteo de carbohidratos de manera usual para determinar la dosis de insulina ayudado por una aplicación que ha sido desarrollada para realizar el cálculo basado en el contenido de nutrientes que usted le informe. El otro grupo también realizará el conteo de los nutrientes para estimar la dosis de insulina, pero además la aplicación le mostrará una proyección de los niveles de azúcar en las siguientes cuatro horas. Durante las 4 semanas de la investigación usted contara con un monitor continuo de glucosa el cual permitirá hacer mediciones de los niveles de sangre intersticial cada 5 minutos, usted deberá escanear el dispositivo mínimo cada 8 horas, pero puede hacerlo con la frecuencia que desee. Adicionalmente los participantes del grupo de la simulación deberán responder dos preguntas relacionadas a su comportamiento después de conocer los datos de la simulación. En las 4 semanas de la investigación se realizarán cuatro seguimientos, uno cada semana que podrán ser virtuales o presenciales y en la

cual se obtendrán datos del sistema de monitoreo de glucosa y será interrogado por eventos como hipoglucemia y hospitalizaciones. En la última visita se le practicarán una encuesta para conocer como su experiencia utilizando la aplicación.

Los datos obtenidos tanto de identificación como del monitoreo de la glucosa y sus respuestas a los cuestionarios serán almacenados en una base de datos a la cual tendrán acceso restringidos sólo algunos miembros del equipo encargado de la investigación. A usted se le asignara un código que permitirá que quienes manipulan los datos no puedan conocer su verdadera identidad en ningún momento. Los datos de monitoreo de la glucosa pudieran ser utilizado en futuras investigaciones, pero estas deben ser aprobadas por el comité de ética del Hospital Pablo Tobón Uribe. Usted tiene derecho a retirar su consentimiento para esto en cualquier momento

Riesgos: El principal riesgo que se prevé durante la investigación son los episodios de hipoglucemia, este es un riesgo que tienen todas las personas que usan insulina. Usted recibirá un entrenamiento en como detectar y tratar estos episodios, si usted llegase a necesitar soporte médico para el tratamiento de estos episodios podrá acudir a su sitio usual de consulta dentro del sistema de salud y adicionalmente usted o un familiar pueden comunicarse con el investigador principal al teléfono que aparece al final o con su médico para hacer el enfoque inicial, recomendarle a donde acudir y prestar el apoyo que esté al alcance. Este experimento cuenta con el amparo de una póliza de responsabilidad civil.

Si durante la investigación usted debe ser hospitalizado es posible que se tenga que detener su participación en la investigación.

Participación en la investigación: Su participación en esta investigación es completamente voluntaria, si decidiera negarse a participar en ella esto no acarrearía ninguna consecuencia con respecto al tratamiento de su enfermedad o la relación con sus médicos. En cualquier momento durante la investigación usted puede decidir retirarse y esto no comprometerá su relación con sus médicos ni el tratamiento de la enfermedad.

Tratamiento de datos personales: Toda la información personal que se obtenga de los participantes durante la investigación será tratada de acuerdo con lo estipulado en la ley 1581 de 2012 de protección de datos personales. A esta información sólo tendrá acceso personal involucrado a la investigación que para su labor requiera de la misma o las personas encargadas de la elaboración y curadoría de la base de datos. Las variables clínicas serán consignadas en otra base de datos en la cual cada participante será identificado mediante un código, el acceso a la identidad del código lo tendrán sólo las personas encargadas del tratamiento de la base de datos general y se encontrara encriptada y protegida por una contraseña de conocimiento restringido. Por ninguna razón diferentes a las estipuladas en la ley esta información se hará pública. Los resultados de esta investigación se publicarán, pero sus datos se presentan agrupados con los de los otros participantes, y no habrá ninguna información que pudiera permitir identificarlo a usted.

Gastos del participante durante la investigación: Usted no debe incurrir en ningún gasto durante la investigación, el costo de desplazamiento para las visitas será cubierto por el estudio. Los medicamentos para el tratamiento de la diabetes mellitus deben ser suministrados por su aseguradora como lo viene recibiendo tradicionalmente y los dispositivos de medición de la glucosa (monitoreo continuo de glucosa) será suministrado por el estudio.

Beneficios para el participante: Como la simulación es una estrategia en estudio, es imposible asegurar que usted pueda obtener algún beneficio particular por su participación en este estudio. El hecho de conocer si esta estrategia es mejor que las existentes, pudiera tener beneficios a futuro para usted o para otras personas, pero eso primero se debe probar en esta investigación. Para todos los participantes en este estudio, queden en el grupo de simulación o el de control, los principales beneficios que se prevén por participar en la investigación son los siguientes:

- Recibir reentrenamiento en la técnica del conteo de carbohidratos y realizarlo con la ayuda de una aplicación.
- Recibir entrenamiento en detección y tratamiento de los episodios de hipoglucemia.
- Se espera que los participantes en el grupo de la intervención presenten una mejoría en el tiempo que sus niveles de azúcar en sangre se mantienen entre 70 y 180 mg/dL después de las comidas principales

Obligaciones: Como participante usted se compromete a:

1. Asistir a los entrenamientos mencionados.
2. Utilizar durante las 4 semanas el monitor continuo de glucosa e informar cualquier mal funcionamiento de este.
3. Escanear el dispositivo de monitoreo continuo de glucosa cada 8 horas como mínimo.
4. Informar al equipo o monitor asignado eventos de hipoglucemia, enfermedad, hospitalización o cualquier otro evento inusual.
5. Asistir a las visitas asignadas.
6. A registrar en la aplicación los datos solicitados correspondiente a los nutrientes de las tres comidas principales del día y las preguntas que se hacen con cada una de ellas.

Los investigadores se comprometen a:

1. Llevar a cabo los seguimientos del participante durante la investigación, estos son las evaluaciones semanales.
2. Solucionar problemas que surjan con la técnica de conteo de carbohidratos o los dispositivos.
3. En caso de ser necesario, facilitar la conexión del participante con los servicios médicos que se requieran para la atención de un episodio de hipoglucemia.
4. Guardar la confidencialidad con los datos y situaciones que pudiera llegar a conocer del participante.

5. Aclarar la situación de la investigación y del investigador frente a las entidades de salud y las instancias legales pertinentes.
6. Informar al participante sobre cualquier hallazgo de la investigación que pueda significar problemas o beneficios para él.

Resultados esperados: Al final de la investigación se espera comparar los datos obtenidos mediante el monitoreo continuo de glucosa de ambos grupos y determinar si la intervención mejora el tiempo que se pasa en el rango de azúcar en la sangre establecido. Estos datos permitirán establecer si la simulación es una herramienta útil para ayudar a las personas con el conteo de carbohidratos.

En caso de probarse eficaz se planean futuros estudios para evaluar la efectividad de esta técnica en el diseño de herramientas para el soporte a la toma de decisiones en personas con diabetes mellitus y apoyar el desarrollo de dispositivos como el páncreas artificial.

Personas para contactar para información

Carlos Esteban Builes-Montaño, MD. (CEBM). Departamento de Medicina Interna, Sección de Endocrinología, Universidad de Antioquia. Departamento de Medicina Interna y Especialidades, Hospital Pablo Tobón Uribe, correo electrónico cbuiles@hptu.org.co, teléfono 3053385136.

Presidente del Comité de Investigación y Ética en Investigación del Hospital Pablo Tobón Uribe: presbítero Jaime Alberto López Monsalve, teléfono 4459000, extensión 8905.

Aceptación de la participación

Si toda la información está clara, todas sus preguntas han sido resueltas de manera satisfactoria y usted desea participar en la investigación firme este documento con su número de identificación, su huella dactilar, la fecha y la hora.

Manifiesto que no he recibido presiones verbales, escritas y/o mímicas para participar en el estudio; que dicha decisión la tomó en pleno uso de mis facultades mentales, sin encontrarme bajo efectos de medicamentos, drogas o bebidas alcohólicas, consciente y libremente.

_____ _____

Nombre del participante Firma del participante

_____	_____
Identificación del participante	Fecha de la firma
_____	_____
Nombre de quien toma el consentimiento	Firma de quien toma el consentimiento
_____	_____
Identificación de quien toma el consentimiento	Fecha de la firma
_____	_____
Nombre del testigo	Firma del testigo
_____	_____
Identificación del testigo	Fecha de la firma
_____	
Relación con el participante	
_____	_____
Nombre del testigo	Firma del testigo
_____	_____
Identificación del testigo	Fecha de la firma
_____	
Relación con el participante	